

Volume 234

David M. Whitacre *Editor*

# Reviews of Environmental Contamination and Toxicology

 Springer

Reviews of  
Environmental Contamination  
and Toxicology

VOLUME 234

For further volumes:

<http://www.springer.com/series/398>



# Reviews of Environmental Contamination and Toxicology

Editor  
David M. Whitacre

## Editorial Board

Maria Fernanda, Cavieres, Valparaiso, Chile • Charles P. Gerba, Tucson, Arizona, USA  
John Giesy, Saskatoon, Saskatchewan, Canada • O. Hutzinger, Bayreuth, Germany  
James B. Knaak, Getzville, New York, USA  
James T. Stevens, Winston-Salem, North Carolina, USA  
Ronald S. Tjeerdema, Davis, California, USA • Pim de Voogt, Amsterdam, The Netherlands  
George W. Ware, Tucson, Arizona, USA

Founding Editor  
Francis A. Gunther

VOLUME 234

 Springer

## Coordinating Board of Editors

DR. DAVID M. WHITACRE, *Editor*  
*Reviews of Environmental Contamination and Toxicology*

5115 Bunch Road  
Summerfield, North Carolina 27358, USA  
(336) 634-2131 (PHONE and FAX)  
E-mail: dmwhitacre@triad.rr.com

DR. ERIN R. BENNETT, *Editor*  
*Bulletin of Environmental Contamination and Toxicology*  
*Great Lakes Institute for Environmental Research*

University of Windsor  
Windsor, Ontario, Canada  
E-mail: ebennett@uwindsor.ca

PETER S. ROSS, *Editor*  
*Archives of Environmental Contamination and Toxicology*

Fisheries and Oceans Canada  
Institute of Ocean Sciences Sidney  
British Columbia, Canada  
E-mail: peter.s.ross@dfo-mpo.gc.ca

Additional material to this book can be downloaded from <http://extras.springer.com>

ISSN 0179-5953                      ISSN 2197-6554 (electronic)  
ISBN 978-3-319-10637-3            ISBN 978-3-319-10638-0 (eBook)  
DOI 10.1007/978-3-319-10638-0  
Springer Cham Heidelberg New York Dordrecht London

© Springer International Publishing Switzerland 2015

This work is subject to copyright. All rights are reserved by the Publisher, whether the whole or part of the material is concerned, specifically the rights of translation, reprinting, reuse of illustrations, recitation, broadcasting, reproduction on microfilms or in any other physical way, and transmission or information storage and retrieval, electronic adaptation, computer software, or by similar or dissimilar methodology now known or hereafter developed. Exempted from this legal reservation are brief excerpts in connection with reviews or scholarly analysis or material supplied specifically for the purpose of being entered and executed on a computer system, for exclusive use by the purchaser of the work. Duplication of this publication or parts thereof is permitted only under the provisions of the Copyright Law of the Publisher's location, in its current version, and permission for use must always be obtained from Springer. Permissions for use may be obtained through RightsLink at the Copyright Clearance Center. Violations are liable to prosecution under the respective Copyright Law.

The use of general descriptive names, registered names, trademarks, service marks, etc. in this publication does not imply, even in the absence of a specific statement, that such names are exempt from the relevant protective laws and regulations and therefore free for general use.

While the advice and information in this book are believed to be true and accurate at the date of publication, neither the authors nor the editors nor the publisher can accept any legal responsibility for any errors or omissions that may be made. The publisher makes no warranty, express or implied, with respect to the material contained herein.

Printed on acid-free paper

Springer is part of Springer Science+Business Media ([www.springer.com](http://www.springer.com))

# Foreword

International concern in scientific, industrial, and governmental communities over traces of xenobiotics in foods and in both abiotic and biotic environments has justified the present triumvirate of specialized publications in this field: comprehensive reviews, rapidly published research papers and progress reports, and archival documentations. These three international publications are integrated and scheduled to provide the coherency essential for nonduplicative and current progress in a field as dynamic and complex as environmental contamination and toxicology. This series is reserved exclusively for the diversified literature on “toxic” chemicals in our food, our feeds, our homes, recreational and working surroundings, our domestic animals, our wildlife, and ourselves. Tremendous efforts worldwide have been mobilized to evaluate the nature, presence, magnitude, fate, and toxicology of the chemicals loosed upon the Earth. Among the sequelae of this broad new emphasis is an undeniable need for an articulated set of authoritative publications, where one can find the latest important world literature produced by these emerging areas of science together with documentation of pertinent ancillary legislation.

Research directors and legislative or administrative advisers do not have the time to scan the escalating number of technical publications that may contain articles important to current responsibility. Rather, these individuals need the background provided by detailed reviews and the assurance that the latest information is made available to them, all with minimal literature searching. Similarly, the scientist assigned or attracted to a new problem is required to glean all literature pertinent to the task, to publish new developments or important new experimental details quickly, to inform others of findings that might alter their own efforts, and eventually to publish all his/her supporting data and conclusions for archival purposes.

In the fields of environmental contamination and toxicology, the sum of these concerns and responsibilities is decisively addressed by the uniform, encompassing, and timely publication format of the Springer triumvirate:

*Reviews of Environmental Contamination and Toxicology* [Vol. 1 through 97 (1962–1986) as Residue Reviews] for detailed review articles concerned with

any aspects of chemical contaminants, including pesticides, in the total environment with toxicological considerations and consequences.

*Bulletin of Environmental Contamination and Toxicology* (Vol. 1 in 1966) for rapid publication of short reports of significant advances and discoveries in the fields of air, soil, water, and food contamination and pollution as well as methodology and other disciplines concerned with the introduction, presence, and effects of toxicants in the total environment.

*Archives of Environmental Contamination and Toxicology* (Vol. 1 in 1973) for important complete articles emphasizing and describing original experimental or theoretical research work pertaining to the scientific aspects of chemical contaminants in the environment.

Manuscripts for Reviews and the Archives are in identical formats and are peer reviewed by scientists in the field for adequacy and value; manuscripts for the Bulletin are also reviewed, but are published by photo-offset from camera-ready copy to provide the latest results with minimum delay. The individual editors of these three publications comprise the joint Coordinating Board of Editors with referral within the board of manuscripts submitted to one publication but deemed by major emphasis or length more suitable for one of the others.

Coordinating Board of Editors

# Preface

The role of *Reviews* is to publish detailed scientific review articles on all aspects of environmental contamination and associated toxicological consequences. Such articles facilitate the often complex task of accessing and interpreting cogent scientific data within the confines of one or more closely related research fields.

In the nearly 50 years since *Reviews of Environmental Contamination and Toxicology* (formerly *Residue Reviews*) was first published, the number, scope, and complexity of environmental pollution incidents have grown unabated. During this entire period, the emphasis has been on publishing articles that address the presence and toxicity of environmental contaminants. New research is published each year on a myriad of environmental pollution issues facing people worldwide. This fact, and the routine discovery and reporting of new environmental contamination cases, creates an increasingly important function for *Reviews*.

The staggering volume of scientific literature demands remedy by which data can be synthesized and made available to readers in an abridged form. *Reviews* addresses this need and provides detailed reviews worldwide to key scientists and science or policy administrators, whether employed by government, universities, or the private sector.

There is a panoply of environmental issues and concerns on which many scientists have focused their research in past years. The scope of this list is quite broad, encompassing environmental events globally that affect marine and terrestrial ecosystems; biotic and abiotic environments; impacts on plants, humans, and wildlife; and pollutants, both chemical and radioactive; as well as the ravages of environmental disease in virtually all environmental media (soil, water, air). New or enhanced safety and environmental concerns have emerged in the last decade to be added to incidents covered by the media, studied by scientists, and addressed by governmental and private institutions. Among these are events so striking that they are creating a paradigm shift. Two in particular are at the center of everincreasing media as well as scientific attention: bioterrorism and global warming. Unfortunately, these very worrisome issues are now superimposed on the already extensive list of ongoing environmental challenges.



The ultimate role of publishing scientific research is to enhance understanding of the environment in ways that allow the public to be better informed. The term “informed public” as used by Thomas Jefferson in the age of enlightenment conveyed the thought of soundness and good judgment. In the modern sense, being “well informed” has the narrower meaning of having access to sufficient information. Because the public still gets most of its information on science and technology from TV news and reports, the role for scientists as interpreters and brokers of scientific information to the public will grow rather than diminish. Environmentalism is the newest global political force, resulting in the emergence of multinational consortia to control pollution and the evolution of the environmental ethic. Will the new politics of the twenty-first century involve a consortium of technologists and environmentalists, or a progressive confrontation? These matters are of genuine concern to governmental agencies and legislative bodies around the world.

For those who make the decisions about how our planet is managed, there is an ongoing need for continual surveillance and intelligent controls to avoid endangering the environment, public health, and wildlife. Ensuring safety-in-use of the many chemicals involved in our highly industrialized culture is a dynamic challenge, for the old, established materials are continually being displaced by newly developed molecules more acceptable to federal and state regulatory agencies, public health officials, and environmentalists.

*Reviews* publishes synoptic articles designed to treat the presence, fate, and, if possible, the safety of xenobiotics in any segment of the environment. These reviews can be either general or specific, but properly lie in the domains of analytical chemistry and its methodology, biochemistry, human and animal medicine, legislation, pharmacology, physiology, toxicology, and regulation. Certain affairs in food technology concerned specifically with pesticide and other food-additive problems may also be appropriate.

Because manuscripts are published in the order in which they are received in final form, it may seem that some important aspects have been neglected at times. However, these apparent omissions are recognized, and pertinent manuscripts are likely in preparation or planned. The field is so very large and the interests in it are so varied that the editor and the editorial board earnestly solicit authors and suggestions of underrepresented topics to make this international book series yet more useful and worthwhile.

Justification for the preparation of any review for this book series is that it deals with some aspect of the many real problems arising from the presence of foreign chemicals in our surroundings. Thus, manuscripts may encompass case studies from any country. Food additives, including pesticides, or their metabolites that may persist into human food and animal feeds are within this scope. Additionally, chemical contamination in any manner of air, water, soil, or plant or animal life is within these objectives and their purview.

Manuscripts are often contributed by invitation. However, nominations for new topics or topics in areas that are rapidly advancing are welcome. Preliminary communication with the editor is recommended before volunteered review manuscripts are submitted.

Summerfield, NC, USA

David M. Whitacre



# Contents

<b>Release, Transport and Toxicity of Engineered Nanoparticles.....</b>	<b>1</b>
Deepika Soni, Pravin K. Naoghare, Sivanesan Saravanadevi, and Ram Avatar Pandey	
<b>Source Characterization of Polycyclic Aromatic Hydrocarbons by Using Their Molecular Indices: An Overview of Possibilities .....</b>	<b>49</b>
Efsthios Stogiannidis and Remi Laane	
<b>Respiratory and Cardiovascular Effects of Metals in Ambient Particulate Matter: A Critical Review.....</b>	<b>135</b>
Deborah L. Gray, Lance A. Wallace, Marielle C. Brinkman, Stephanie S. Buehler, and Chris La Londe	
<b>Index.....</b>	<b>205</b>

# Release, Transport and Toxicity of Engineered Nanoparticles

Deepika Soni, Pravin K. Naoghare, Sivanesan Saravanadevi,  
and Ram Avatar Pandey

## Contents

1	Introduction .....	2
2	Engineered Nanoparticles and Their Applications .....	6
3	Release Pathways of Engineered Nanoparticles in the Environment.....	9
4	Fate and Transport of Engineered Nanoparticles in the Environment .....	12
4.1	Air.....	12
4.2	Water .....	14
4.3	Soil .....	15
5	Toxicity of the ENPs .....	16
5.1	Microbes.....	16
5.2	Animals.....	24
5.3	Plants .....	29
5.4	Toxicity to Different Cell Lines.....	32

---

D. Soni

Environmental Biotechnology Division, National Environmental Engineering Research Institute [CSIR-NEERI], Nehru Marg, Nagpur 440020, India

Environmental Health Division, National Environmental Engineering Research Institute [CSIR-NEERI], Nehru Marg, Nagpur 440020, India

P.K. Naoghare • S. Saravanadevi (✉)

Environmental Health Division, National Environmental Engineering Research Institute [CSIR-NEERI], Nehru Marg, Nagpur 440020, India

R.A. Pandey (✉)

Environmental Biotechnology Division, National Environmental Engineering Research Institute [CSIR-NEERI], Nehru Marg, Nagpur 440020, India

e-mail: [ra\\_pandey@neeri.res.in](mailto:ra_pandey@neeri.res.in)

© Springer International Publishing Switzerland 2015

D.M. Whitacre (ed.), *Reviews of Environmental Contamination and Toxicology*

*Volume 234*, Reviews of Environmental Contamination and Toxicology 234,

DOI 10.1007/978-3-319-10638-0\_1

6	Possible Mechanisms by Which Nanoparticles Induce Toxicity.....	35
6.1	Generation of ROS .....	35
6.2	Interaction with Proteins .....	36
6.3	DNA Damage.....	37
7	Summary .....	38
	References.....	39

## 1 Introduction

Nanotechnology is associated with the design and application of nanoscale particles (viz., 1–100 nm) that possess properties that are quite different from their bulk counterparts. The Royal Society and Royal Academy of Engineering offer the following definition for this term: “Nanotechnologies are the design, characterization, production and application of structures, devices, and systems by controlling shape and size at nanometer scale” (Royal Society and Royal Academy of Engineering 2004).

Different types of engineered nanoparticles (ENPs) are presently synthesized and utilized for multiple applications. These include particles that are made of carbon, metal and metal-oxide and quantum dots (QDs) (see Table 1 for a list of abbreviations and acronyms). ENPs have specific physico-chemical properties that are utilized for applications that have social and economic benefit. Metal nanoparticles are used in medicine and have great antibacterial potential (Chopra 2007). ZnO and TiO<sub>2</sub> nanoparticles have light-scattering potential and are used to protect against harmful UV light (Rodríguez and Fernández-García 2007). ENPs have also proved to be potential drug delivery agents (Alivisatos 2004; Gibson et al. 2007; Huber 2005; Tsai et al. 2007). ENPs are efficient scrubbers of gaseous pollutant like carbon dioxide (CO<sub>2</sub>), nitrogen oxides (NO<sub>x</sub>), and sulphur oxides (SO<sub>x</sub>) (Schmitz and Baird 2002). Moreover, ENPs are used for applications in environmental remediation (Zhang 2003).

Scientists and economists have predicted that ENP-based processes and technology will increasingly be used in nanotechnology research and development (Guzman et al. 2006). It has been estimated that the value of nanotechnology products will reach \$1 trillion by 2015 and will employ about two million workers (Nel et al. 2006; Roco and Bainbridge 2005).

The increased growth of nano-based products for multiple applications will ultimately be the source of their expanded release to air, water and soil (Nowack and Bucheli 2007). Nanomaterial wastes are released into the environment from operating or disposing of nanodevices and during nanomaterial manufacturing processes. Such releases may be dangerous because of the small size of the particles involved, i.e., such particles can float into the air, be chemically transformed, and can affect water quality and/or accumulate in soils. Moreover, ENPs can be easily transported to animal and plant cells, either directly or indirectly, and cause unknown effects. The dearth of information on environmental transport and safety has raised concerns among the public and among scientific authorities. There is a desire to know much more about the fate and behavior of ENPs in the environment and in biological systems. Nanotechnology is still in its infancy, and it is critical that action be taken to evaluate the potential adverse effects that ENPs may have on organisms and

**Table 1** Abbreviations and acronyms used in this paper

Abbreviations	Acronyms
8-OHdG	8-hydroxyl deoxyguanosine
A549 cells	Human lung cell line
AB	Alamar blue
AFM	Atomic Force Microscopy
Ag	Silver
AK	Adenylate kinase
Al	Aluminium
Al <sub>13</sub> or Al <sub>30</sub>	polynuclear complexes of aluminium
Al <sub>2</sub> O <sub>3</sub>	Aluminium oxide
AP-	As prepared
ATP	Adenosine Triphosphate
ATM	Ataxia Telangiectasia Mutant
Au	Gold
BaO	Barium oxide
BEAS-2B	Human bronchial epithelial cell lines
BRL 3A	Rat liver cell lines
BSA	Bovine Serum Albumin
C-18-4	Mouse spermatogonial stem cells
Ca	Calcium
CaCl <sub>2</sub>	Calcium chloride
CaO	Calcium oxide
CAT	Catalase
Cd	Cadmium
CdSe	Cadmium selenide
CdSe/ZnS	Cadmium selenide/zinc sulphide
CdTe	Cadmium telluride
CeO <sub>2</sub>	Cerium oxide
CHO-K1	Chinese Hamster Ovary
CNTs	Carbon nanotubes
CO	Carbon monoxide
CO <sub>2</sub>	Carbon dioxide
Cu <sub>4</sub> S <sub>6</sub>	Complex of sulfides
CYP1A	Cytochrome P450 1A
CYP2D6*2	Cytochrome P450 2D6
D	Particle diffusivity
daf-12	dauer formation protein
DEB	Dynamic Energy Budget
DOC	Dissolved Organic Carbon
DWNTs	Double walled nanotubes
EDS	Electron Dispersive X-ray analysis
EDTA	Ethylene diamine tetra acetic acid
ENPs	Engineered nanoparticles
ETC	Electron Transport Chain

(continued)

**Table 1** (continued)

Abbreviations	Acronyms
Fe	Iron
Fe <sub>2</sub> O <sub>3</sub> and Fe <sub>3</sub> O <sub>4</sub>	Iron oxide
Fe <sub>3</sub> O <sub>4</sub>	Magnetite
FeO	Wustite or Iron (II) oxide
FPW	Filtered Pond Water
FTIR	Fourier Transform Infrared
GSH	Total glutathione
GSH-px	Glutathione peroxidase
GST	Glutathione S transferase
GSTM1	Glutathione-S-transferase M1
H[AuCl <sub>4</sub> ]	Chloroauric acid
H <sub>2</sub> O <sub>2</sub>	Hydrogen peroxide
HDF	Human dermal fibroblast
HepG2	Human liver carcinoma
HSP 70	Heat shock protein 70
IL-8	Interleukin-8
InP	Indium phosphide
KCl	Potassium chloride
KNO <sub>3</sub>	Potassium nitrate
LC <sub>50</sub>	Lethal concentration
LDH	Lactate dehydrogenase
LED	Light emitting diodes
LTC	Low Temperature Carbonization
M	Mass of the particle
MAP	Monoammonium phosphate
MBC	Minimum bactericidal concentration
MDA	Malonyldialdehyde
MgO	Magnesium oxide
MIC	Minimum inhibitory concentration
MNP	Magnetic nanoparticles
MRI	Magnetic resonance imaging
MT	Metallothionein
MTT	3-(4, 5-Dimethylthiazol-2-yl)-2, 5-diphenyltetrazolium bromide
MWNT	Multi walled nanotubes
NO	Nitrous oxide
NOM	Natural organic matter
NO <sub>x</sub>	Nitrogen oxides
NQO1	NAD(P)H quinine oxidoreductase 1
NR	Neutral red
nZVI	Nano zero valent iron
O <sub>2</sub> <sup>-</sup>	Superoxide radical
PAHs	Poly aromatic hydrocarbons

(continued)



**Table 1** (continued)

Abbreviations	Acronyms
PbSe	Lead selenide
PC 12 M	Rat pheochromocytoma cell line
pHzpc	pH at zero point charge
PPY	Proteose peptone yeast extract medium
PVP	Poly vinyl pyrolidone
QDs	Quantum dots
RAW-264.7	Human macrophage cell lines
RBEC	Rat brain endothelial cell
ROS	Reactive oxygen species
SDS	Sodium dodecyl sulphate
Se	Selenium
SEM	Scanning electron microscope
SH	Sulfhydryls
SiO <sub>2</sub>	Silicon dioxide
SO <sub>2</sub>	Sulphur dioxide
SOD	Superoxide dismutase
Sod-3	Superoxide dismutase-3
SO <sub>x</sub>	Sulphur oxides
SWNT	Single walled nanotubes
T	Time
T	Translational energy of a gas molecule
TEM	Transmission electron microscope
TGA	Thermogravimetric Analysis
THP-1	Human monocytic cell line
TiO <sub>2</sub>	Titanium dioxide
TNF- $\alpha$	Tumor necrosis factor
U	Velocity
UV-B	Ultraviolet light
X	Direction coordinate
XAS	X-ray absorption spectroscopy
ZnO	Zinc oxide
ZrO <sub>2</sub>	Zirconium oxide
$\alpha$ -Fe <sub>2</sub> O <sub>3</sub>	Hematite
$\gamma$ -Fe <sub>2</sub> O <sub>3</sub>	Maghemite
$\gamma$ -H2AX	Histone H2AX
Z	Friction coefficient
K	Boltzmann constant

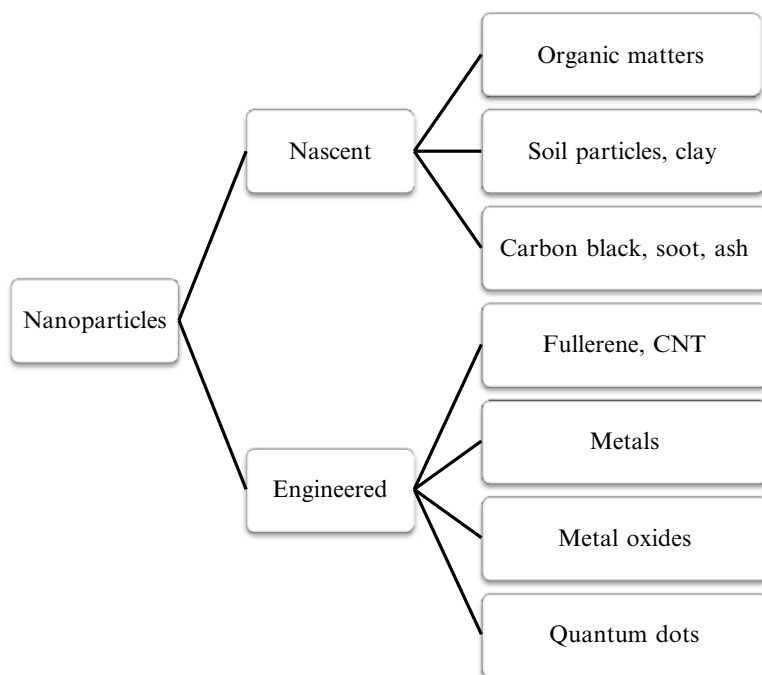
on the environment (Nel et al. 2006; Colvin 2002). Although reports have been published on the potential safety of ENPs, few details on their transport, fate and toxicity are currently available.

In this review, we address the release and transport of ENPs to the environment and summarize the deleterious effects they have been observed to induce on different organisms. Several important issues that impinge on the environmental behavior and safety of ENPs are addressed. These include the mobility of ENPs in different environmental media (e.g., air, water and soil), their toxicity on different organisms, and the possible pathways by which the ENPs may produce their toxicity.

## 2 Engineered Nanoparticles and Their Applications

Since time immemorial, organisms and the environment have been exposed to natural nanoparticles like volcanic dust, ash, combustion by-products (e.g., carbon black, soot), organic matter like humic and fulvic acids, proteins, peptides and colloidal inorganic species present in natural water and in soil systems (Fig. 1) (Buffle 2006). In contrast to nascent and incidental nanoparticles, ENPs are produced by processing materials at the nano scale.

ENPs are composed of carbon, metal and metal-oxides, semiconductors (quantum dots (QDs) and polymers (dendrimers)). Carbon-based nanoparticles include buckminsterfullerene, a  $C_{60}$  molecule that resembles the stitching pattern evident on



**Fig. 1** An outline of nanoparticle types that can be released to the environment

a soccer ball and has 60 carbon atoms arranged as 12 pentagons and 20 hexagons. Other fullerene nanoparticles also exist (e.g., C<sub>70</sub>, C<sub>74</sub>, C<sub>76</sub>, C<sub>78</sub>, etc.). Fullerenes are hydrophobic and have application as organic photovoltaics, antioxidants, catalysts, polymers, in water purification, bio-hazard protective agents, and in various medical and pharmaceutical applications (Yadav and Kumar 2008). Carbon nanotubes (CNTs) are also important. CNTs include single- and multi-walled nanotubes (SWNTs and MWNTs) that are cylindrical in shape. CNTs possess excellent tensile strength and elasticity and show different metallic and kinetic properties that vary by their size. For example, high tensile strength carbon nanotubes (CNTs) have applications in the electronic and polymer industries (Koehler et al. 2008; Wu et al. 2004; Table 2). Moreover, the energy sector and the consumer goods industries are doing research with this unique material (Koehler et al. 2008). CNTs promise to have interesting future applications by being integrated into polymers (Chang et al. 2005) and into lithium ion secondary batteries (Ouellette 2003). The demand for carbon-based nanoparticles in the market, especially in the electronics and polymer sectors, is enormous and is estimated to reach \$1.096 billion by 2015 (Garland 2009).

Metal nanoparticles are made by manipulating heavy metals like gold, silver, iron and platinum. Such ENPs possess specific properties that are based on their shape, size and dissolution medium. Different routes have been used to synthesize these nanoparticles; recently, green synthesis methods have been utilized to make silver and iron nanoparticles (Ramteke et al. 2010, 2012; Sahu et al. 2012; Shankar et al. 2003). Metal nanoparticles have many uses and new ones are routinely being discovered. For example, colloidal gold is used to treat rheumatoid arthritis in an animal model (Tsai et al. 2007), is used as a drug carrier (Gibson et al. 2007) and as an agent for detecting tumors (Qian et al. 2008). Colloidal gold has also been used as a contrast agent for biological probes like antibodies, nucleic acids, glycans and receptors (Horisberger and Rosset 1977) (Table 2). Silver nanoparticles are used in medicine (Table 2) as a disinfectant, antiseptic, in surgical masks, and in wound dressings that have anti-bacterial activity (Chopra 2007). Many textiles, keyboards, cosmetics, water purifier appliances, plastics and biomedical devices are now known to contain silver nanoparticles that provide protection against microorganisms (Li et al. 2010).

Iron nanoparticles are utilized in magnetic recording media and tapes, as a catalyst in Fischer-Tropsch synthesis, in drug-delivery applications, in magnetic resonance imaging (MRI) and in treating hyperthermia (Huber 2005). Iron nanoparticles have been used to remediate industrial sites that were contaminated with chlorinated organic compounds (Zhang 2003) (Table 2). Platinum nanoparticles exhibit antioxidant properties, but what applications they are to be put to is as yet undeciphered. Although no applications have yet emerged, it is interesting to note that platinum NPs have antioxidant activity that increases roundworm longevity (Kim et al. 2008; Table 2). The total market for nanoparticles in biotechnology, drug discovery and development was valued at \$17.5 billion in 2011. The value is predicted to reach approximately \$53.5 billion in 2017 (BCC Research 2012).

The commercially important metal oxide nanomaterials include TiO<sub>2</sub>, ZnO, Fe<sub>2</sub>O<sub>3</sub>, Fe<sub>3</sub>O<sub>4</sub>, SiO<sub>2</sub>, MgO and Al<sub>2</sub>O<sub>3</sub>. These nanomaterials increasingly have applications as catalytic devices, sensors, uses in environmental remediation and in

**Table 2** A summary of the major applications for engineered nanoparticles

Nanoparticle	Applications	Reference
Carbon -based nanoparticle		
a. Fullerene	a. Organic photovoltaics, antioxidants, catalysts, polymers, water purification and biohazard protective agents	a. Yadav and Kumar (2008)
b. CNT (SWNT and MWNT)	b. Electronics and polymer industry, batteries	b. Koehler et al. (2008)
Metal nanoparticles		
a. Gold	a. Medical field and biological probe	a. Gibson et al. (2007), Horisberger and Rosset (1977), Qian et al. (2008), Tsai et al. (2007)
b. Silver	b. As disinfectant in medical field, cosmetics, water purifiers, plastic wares, textiles.	b. Chopra (2007), Li et al. (2010)
c. Iron	c. Magnetic recording media, magnetic tapes, catalysts, drug delivery, remediation of contaminated sites.	c. Huber (2005), Zhang (2003)
d. Platinum	d. Antioxidant	d. Kim et al. (2008)
Metal oxide nanoparticles		
a. Magnesium oxide	a. As scrubber for air pollutant gases (CO <sub>2</sub> , NO <sub>x</sub> , SO <sub>x</sub> ), sensors and catalysts	a. Rodríguez and Fernández-García (2007)
b. TiO <sub>2</sub>	b. Photo catalyst, in photovoltaic devices, cosmetics, paintings, electronic devices and sensors.	b. Foller (1978)
c. ZnO	c. UV blocker in sunscreens, sensors, non linear optical systems	c. Forzatti (2000), Wang (2004)
d. Iron oxide	d. Ferrofluids, rotary shaft sealing, loudspeakers, computer hard drives and in magnetic resonant imaging.	d. Raj and Moskowitz (1990)
Quantum dots	Biomedical imaging, targeting specific cell membrane receptors, cellular biomolecules such as peroxisomes and DNA and electronic industries	Alivisatos (2004), Chan et al. (2002), Colton et al. (2004), Dubertret et al. (2002), Lidke et al. (2004), Wu et al. (2004)

different commercial products like cosmetics, sunscreens, textiles, paints, varnishes and household appliances (Rodríguez and Fernández-García 2007). In Table 2, we summarize the major applications to which metal oxide nanoparticles have been put. Some metal oxide nanoparticles like MgO, TiO<sub>2</sub>, CaO and BaO are used as scrubber material for gaseous pollutants (e.g., CO<sub>2</sub>, NO<sub>x</sub>, SO<sub>x</sub>) in the chemical industry and as a catalyst support (Foller 1978; Forzatti 2000; Schmitz and Baird 2002). ZnO nanoparticles exhibit multiple novel nanostructures like nanorings, nanohelics, nanosprings, which are not observed in other types of oxide nanoparticles (Wu et al. 2007) (Table 2). Wang (2004) suggested future applications for ZnO

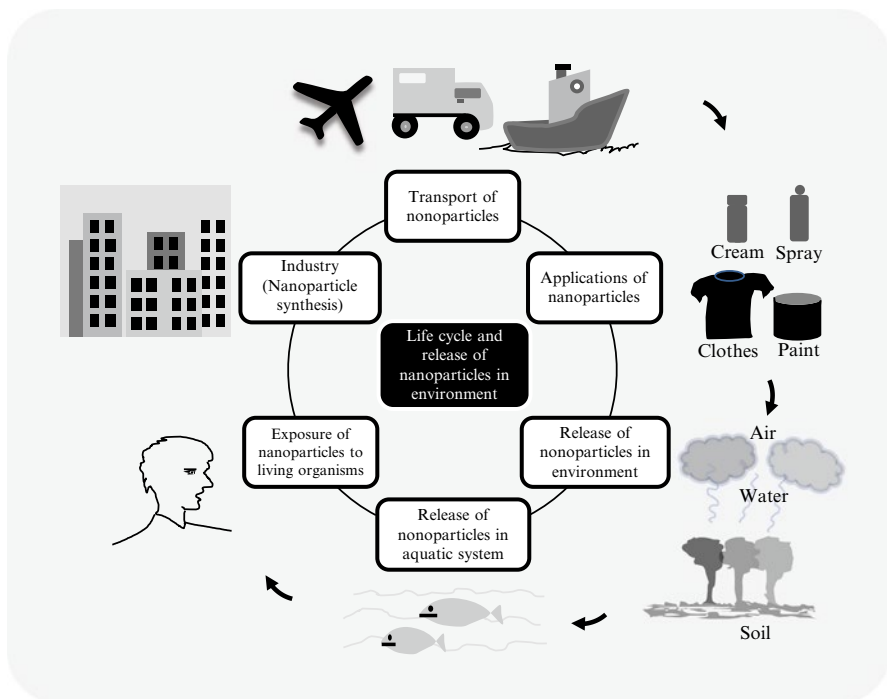
in gas sensors, solar cells and non-linear optical systems. Iron oxide nanoparticles like FeO (Iron oxide), Fe<sub>3</sub>O<sub>4</sub> (Magnetite),  $\alpha$ -Fe<sub>2</sub>O<sub>3</sub> (Hematite) and  $\gamma$ -Fe<sub>2</sub>O<sub>3</sub> (Maghemite) occur naturally. These are found in bacteria, insects, weathered soils, rocks, natural atmosphere and polluted aerosols (Cornell and Schwertmann 1996). Magnetite and maghemite minerals are used in different sectors owing to their magnetic properties as ferrofluids (Raj and Moskowitz 1990) (Table 2). Fe<sub>3</sub>O<sub>4</sub> nanoparticles have received regulatory approval as an antibacterial agent and can be applied to limit bacterial growth (Ramteke et al. 2010).

Nanomaterials made of fluorescent semiconductor nanocrystals (~2–100 nm) have electronic properties between those of bulk semiconductors and discrete molecules, and are referred to as Quantum dots (QDs) (Brus 2007). Such nanomaterials include CdTe (cadmium telluride), CdSe/ZnS (cadmium selenide/zinc sulphide), CdSe (cadmium selenide), PbSe (lead selenide) and InP (indium phosphide). These QDs materials have certain sought-after properties that include a narrow emission band, wide excitation wavelength and photo stability. These properties qualify QDs as a candidate for applications in biomedical imaging, specific cell membrane receptor targeting (Alivisatos 2004; Chan et al. 2002; Lidke et al. 2004), and use with cellular biomolecules such as peroxisomes (Colton et al. 2004) and DNA (Dubertret et al. 2002) (Table 2). QDs are used currently in the manufacture of advanced flat panel LED displays, and are expected to be used for ultrahigh-density data storage and quantum information processing (Wu et al. 2004). Hence, it is clear that the ENPs are rapidly gaining wider application in consumer products and in the industrial sector. As a consequence of their growing popularity, production and application, environmental releases of ENPs will increase.

### 3 Release Pathways of Engineered Nanoparticles in the Environment

As for other metal or organic pollutants, nanoparticles are either intentionally or accidentally released, and come from either point or non-point sources (Fig. 2). Point or stationary sources include production facilities and wastewater treatment plants. Treatment plants are major potential sources of release for nanoparticles. As occurs with other inorganic or organic pollutants that are concentrated for treatment in water treatment plants, nanoparticles may interact with organic and inorganic matter to form complexes, or new compounds (Pandey and Kumar 1990). Thus, nanoparticles may be retained and interact with other environmental constituents after passing through treatment procedures. Gottschalk et al. (2009) predicted significant environmental concentrations of nano- TiO<sub>2</sub>, ZnO, CNT, Ag and fullerene in USs, European and Swiss treated plant effluents. The concentrations of such released nanoparticles tend to be in the ng/L range. Moreover, these authors expect potential risks to aquatic organisms from release of Ag, TiO<sub>2</sub> and ZnO nanoparticles (Gottschalk et al. 2009).

Nonpoint source releases may occur from leaching or “wear” of nanomaterial-containing products like paints, varnishes, cosmetics, and cleaning agents that are



**Fig. 2** Schematic diagram depicting the engineered nanoparticle life cycle, including use, release, transport, and ultimate environmental exposures

disposed of or released to soil or surface water (Biswas and Wu 2005). Accidental release may occur during the production or transportation of nanomaterial-containing products. Some nanomaterials are intentionally released into the environment, e.g., for remediation of ground- and waste-water (Nowack and Bucheli 2007). It is becoming necessary that both scientists and regulators do more to understand the different routes by which nanoparticles are released to the different environmental compartments, i.e., air, water and soil.

Nanomaterials are released to air mainly via use of aerosol products, vehicle emissions of gases containing nanoparticles, manufacturing and production discharges, consumer product aerosols, and release of industrial soot and smoke. It has been reported that vehicle exhaust produces aerosol concentration ranges from  $10^4$  to  $10^6$  particles per  $\text{cm}^3$ , with most nanoparticles in the size ranges below 50 nm diameter (Biswas and Wu 2005).

In Table 3 we summarize literature studies that were undertaken to evaluate nanoparticle releases to the atmosphere.

Nanoparticles that are released to aquatic systems may result from land run-off, and industrial and household wastewater effluents; moreover, a major source is metal-based nanoparticle use for water remediation (e.g., zero-valent iron nanoparticles) (Defra 2007; Vaseashta et al. 2007). Kaegi et al. (2008) has shown that  $\text{TiO}_2$  nanoparticles present in building paints (whitening pigments) are shed and then released to

**Table 3** A summary of studies in which the release of nanoparticles to the atmosphere has been addressed

Study done	Results obtained	Reference
Release from the handling of surface coatings	No significant released concentration of <100 nm was detected	Vorbau et al. (2009)
Release of CNTs during the disposal of lithium-ion secondary batteries and synthetic textiles, in landfills or dumpsites or by lower temperature incineration.	Observed release as dust particles of CNT.	Koehler et al. (2008)
Release from gas-stoves, electric stoves and electric toasters	High concentrations of particles with average diameter of 5 nm were found from gas and electric stove, which quickly coagulate.	Wallace et al. (2008)
62 printers tested for nanoparticles release	40% emission of PM-2.5 with particle size range of 7–500 nm	He et al. (2007)
Indoor and outdoor environment nanoparticles coming from soot of candle, wood or other cooking species and diesel soot, soot from fires.	Most includes aggregates of carbonaceous and MWNT, silica and concentric fullerene.	Murr and Garza (2009)
1999–2001 study conducted in Madrid and Mexico city for the presence of polycyclic aromatic hydrocarbons on the surface and the total active surface area of nanoparticles present on the road.	Observe reduction in both measurements.	Siegmann et al. (2008)
PM10 and PM2.5 mass concentration study at 31 sites in Europe	Increased concentrations observed during morning hours, relating to increased traffic.	Dingenen et al. (2004)
Urban and suburban aerosol levels looking at the effects of seasonal variation, wind speed, traffic density and temperature	90% of nanoparticles are found in urban areas and 70–80% in suburban areas	Hussein et al. (2005)
Study in southwest Detroit to establish ultrafine number concentrations and size distribution.	Major sources of ultrafines were concluded to be from fossil fuel combustion and atmospheric gas-to-particle conversion of precursor gases	Young and Keeler (2004)
21 days study at two major road sides of El Paso, USA	Mean average particle concentrations noted to be 13,600 and 14,600 cm <sup>-3</sup>	Noble et al. (2003)

surface water via atmospheric precipitation. Nanoclusters and polynuclear complexes of aluminium (Al<sub>13</sub> or Al<sub>30</sub>) (Casey et al. 2001; Furrer et al. 2002) and sulfides (Cu<sub>4</sub>S<sub>6</sub>) (Luther and Rickard 2005) were reported to exist in natural water. Infiltration is the major source of ground water recharge and is through which nanomaterials enter ground water (Greg 2004).

Nanomaterials are applied to remediate soil and water pollutants (Waychunas et al. 2005; Yue and Economy 2005). In the near future, it is expected that wastes from the nano-industry that are treated by municipalities and cities will be released in plant effluents (Blaise et al. 2008).

## 4 Fate and Transport of Engineered Nanoparticles in the Environment

After ENPs are released to the environment, they may remain as they are, or their makeup and character may be altered by the action of the environment. Their surface characteristics, structure and reactivity may be altered during transport into or within the environment. Moreover, the physico-chemical characteristics (e.g., pH, ionic strength, presence of organic matter) of various environmental media may affect the transport of ENPs. Below we describe the studies that have been conducted to discover how ENPs move and are affected by environmental media.

### 4.1 Air

Madler and Friedlander (2007) described how nanoparticles are transported in air (Table 4). They compared the transport of these very small entities (ENPs) as being similar to how fluids are transported. In the absence of external forces, Brownian diffusion is the main transport mechanism by which nanoparticles move in gaseous atmospheres. Madler and Friedlander (2007) derived an equation of particle diffusivity ( $D$ ) that is given as follows:

$$D = \frac{\overline{x^2}}{2t} = \frac{\overline{u^2 t}}{\beta t} = \frac{\overline{u^2 m}}{\zeta} = \frac{\kappa T}{\zeta}$$

Where  $D$  is particle diffusivity,  $x$  is direction coordinate,  $t$  is time,  $u$  is velocity,  $m$  is mass of the particle,  $\zeta$  is the friction coefficient,  $\kappa$  is Boltzmann constant and  $T$  is the translational energy of a gas molecule. As described by this equation, particle transport is related to the frictional coefficient that depends on drag force and velocity between particle and fluid. However, this relation may not be accurate for determining particle diffusivity through air.

**Table 4** Factors that facilitate the transport of ENPs in ecosystems

Ecosystem	Behavior of nanoparticles	Reference
Air (Abiotic interaction)	a. Diffusion	a. Friedlander (2000), Madler and Friedlander (2007)
	b. Brownian coagulation	b. Lall and Friedlander (2006)
	c. Agglomeration	c. Bandyopadhyaya et al. (2004)
Water	a. Aggregation	a. Guzman et al. (2006)
	b. Interaction with natural organic matter	b. Ghosh et al. (2008)
	c. Adsorption	c. Keller et al. (2010)
Soil	a. Depend on charge	a. Darlington et al. (2009)
	b. Aggregation	b. Solovitch et al. (2010)
	c. Interaction with organic molecules	c. Jaisi and Elimelech (2009)
	d. Degradation and surface modification	d. Navarro et al. (2011)



Brownian diffusion leads to dispersion of particles into the air. Dispersion may also occur from mechanical mixing during industrial processes, interfacial instability between immiscible layers of solvents and differences in molecular structures of particles. A velocity-based model describes the spreading of a solute in time and space. The convection-dispersion equation (CDE) for dispersion of non-reactive solute can be given as:

$$\frac{\partial C}{\partial t} = K \frac{\partial^2 C}{\partial x^2} - v \frac{\partial C}{\partial x}$$

Where C is the concentration of solute, t is time, x is distance, K is the diffusion-dispersion coefficient and v is the mean velocity. This equation predicts that the K and v do not vary in space or with direction. K and v are related to the mean and variance of the normal distribution of distances traversed by the solute (Perfect and Sukop 2001).

Another ENP transport mechanism in air is via agglomeration. Herein, individual particles agglomerate through Brownian motion and collide, leading to increased size. The small size of nanoparticles makes them unstable and thus assists their collision with each other. Repeated collisions form particle agglomerates (Bandyopadhyaya et al. 2004). Nanoparticle agglomerates may collide with the molecules of surrounding gas (Lall and Friedlander 2006) (Table 4). Friedlander (2000) suggested that Brownian movement was responsible for the highest collision rates of nanoparticles and was more influential than other transport mechanisms such as turbulent flow (Table 4). Friedlander described the fractal nature of ENPs agglomerates mathematically as:

$$N_p = K_f \left( \frac{R_g}{d_p / 2} \right)^{D_f}$$

Where,  $N_p$  is the number of primary particles that forms agglomerates,  $d_p$  is diameter of particles,  $K_f$  is fractal prefactor,  $R_g$  is radius of gyration (mean root square of the distances between the spherules and the centre of mass of the agglomerate) and  $D_f$  is fractal dimension. The above mentioned equation can be used to estimate the number of ENPs undergoing agglomeration.

The physico-chemical characteristics of ENPs affect their fate as does how they are transported in air. Lowry et al. (2012) reported the possible mechanisms by which nanoparticles behave and are transformed in the environment Aitken et al. (2004) reported that particles having diameters  $\leq 100$  nm remain suspended in air for longer times and are capable of diffusing. Particle size bears an inverse relationship with diffusion rate, whereas gravitational settling is directly proportional. ENPs have been classified by their sizes and behavior, when present in the atmosphere. Small particles ( $< 80$  nm) tend to be short lived and to agglomerate. Large particles ( $> 2,000$  nm) are coarse and are subjected to gravitational settling or sedimentation. Particles of intermediate size ( $> 80$  nm and  $< 2,000$  nm) persist for longer periods in the atmosphere ([http://www.epa.gov/osa/pdfs/nanotech\\_epa\\_nanotechnology\\_whitepaper\\_0207.pdf](http://www.epa.gov/osa/pdfs/nanotech_epa_nanotechnology_whitepaper_0207.pdf)).

Considerable research work is underway to better describe what the fate is of ENPs in the atmosphere. The current emphasis is on defining how ENPs interact, and are retained, adsorbed or absorbed by other suspended particles or by living organisms.

## 4.2 Water

Information on transport, distribution and fate of ENPs in aquatic ecosystems is limited, and derives mainly from insights given by colloid chemistry and colloid movement in aqueous systems. Hydrophobic colloids are insoluble in water. Such colloids are stabilized by their electro-kinetic properties, which depend on their electrical charge. The magnitude of charge is responsible for the stability and is referred to as the zeta potential as defined by the equation:

$$\zeta = \frac{4\pi\delta q}{D}$$

Where  $\zeta$  is zeta potential,  $q$  is charge on the particle,  $\delta$  is thickness of the zone of influence of the charge on the particle, and  $D$  is dielectric charge. The zeta potential is a repelling force that protects cells from coalesces due to intermolecular or inter-particle forces (i.e., Van der Waal's forces). This happens when attractive forces overcome repulsive ones (Sawyer and Mc Carty 1967). Guzman et al. (2006) described how ENPs are transported in an aqueous system by using  $\text{TiO}_2$  as model nanoparticle. They concluded that when medium pH approaches zero point charge (pHzpc), the repulsion/zeta potential between nanoparticles having a similar surface potential decreases and they tend to agglomerate (Guzman et al. 2006) (Table 4). Agglomerated nanoparticles have less mobility and induce sedimentation.

The presence of Natural Organic Matter (NOM) influences the transport of ENPs in the environment. Humic and fulvic acids and polysaccharides contribute to the NOM content of aqueous systems. NOM provides a surface for adsorption of nanoparticles (Table 4). Such adsorption changes the surface charge and charge density of ENPs, and can affect their water transport (Ghosh et al. 2008; Guzman et al. 2006; Hyung et al. 2007). Keller et al. (2010) studied the electrophoretic mobility of nanoparticles (viz.,  $\text{TiO}_2$ ,  $\text{ZnO}$  and  $\text{CeO}_2$ ) in water bodies like ground-water, lakes, rivers and sea water. The transport of these nanoparticles depended on particle size and was dominated by the presence of NOM and ionic strength of the transport medium, whereas it was shown to be independent of pH (Table 4).

ENPs in the aquatic environment can aggregate, dissolve, adsorb, or interact with NOM, which may impart a colloidal-like stabilization (Batley and McLaughlin 2010). However, the fate of nanoparticles in aqueous systems is not well understood, and will be better elucidated only after much additional and intense investigation (Moore 2006; Wiesner et al. 2006). How ENPs behave in the environment depends on the following factors: type, characteristics (size and surface properties) and process used to make the nanoparticle, and the physico-chemical properties of the water (pH, ionic strength and dissolved organic carbon content), in which the

ENPs reside (Guzman et al. 2006; Benn and Westerhoff 2008). In turn, these factors just mentioned, determine the fate of ENPs in water, as does the interactions the ENPs have with co-existing natural/anthropogenic chemicals and the action of natural biotic/abiotic processes like photolysis and hydrolysis (Klaine et al. 2008). Such interactions and transformations of the ENPs remain poorly understood. However, some researchers have evaluated the aqueous behavior of ENPs. For example, the interaction of NOM with fullerene and CNTs caused disaggregation of their aggregates and increased stability (Kennedy et al. 2008). Similarly, NOM may influence the characteristics of metal and metal oxide nanoparticles (nano-Ag, nano-Cu, fullerene and iron oxide nanoparticle) at different pHs or at different ionic strengths (Baalousha et al. 2008; Diegoli et al. 2008; Gao et al. 2009). Zhang et al. (2008) reported rapid aggregation of metal oxide nanoparticles from electric double layer compression that facilitated sedimentation. Before sedimentation the ENPs in the water interacted with aquatic organisms. However, as stated before, much more work is needed to better understand the fate of ENPs in the aqueous environment.

### 4.3 Soil

Similar to aerosol nanoparticles, ENPs aggregate and are deposited in porous structures of soil ecosystems. Such aggregation and deposition is assessed by the high diffusivity of aerosol nanoparticles. Size, surface characteristics and matrix constituents are major factor that affect transport and fate of ENPs in soil (Darlington et al. 2009) (Table 4). Guzman et al. (2006) described three mechanisms for how particles are transported in porous media: particle interception with media, gravitational sedimentation and diffusion. The deposition of colloids in porous media is given by the equation:

$$\frac{\delta C}{\delta t} + \bar{v} \cdot \Delta C = D \Delta^2 C - KC$$

Where C is the particle concentration, t is time,  $\bar{v}$  is the fluid velocity, D is diffusion coefficient of the particles, and k is the deposition rate coefficient (Guzman et al. 2006). The above equation can be used to determine how many of the ENPs involved are undergoing diffusion. Lecoanet and Wiesner (2004) assessed the mobility of three types of fullerenes (viz., fullerol, nC<sub>60</sub> and SWCNTs), TiO<sub>2</sub> and SiO<sub>2</sub> at two different flow rates (Table 4). The highest mobility was observed for fullerol and surfactant-modified SWCNTs in an unfractured sand aquifer (10–14 m), whereas the lowest mobility was observed for nC<sub>60</sub> (100 times lower than for fullerol). Similarly the transport of different ENPs (viz., CNTs, AgNPs, TiO<sub>2</sub>, ZnO, SWNTs, and QDs) has been studied by using saturated soil or sand columns (Tian et al. 2010; Jaisi and Elimelech 2009; Milani et al. 2010; Solovitch et al. 2010; Navarro et al. 2011) (Table 4). The results for different nanoparticles have shown either aggregation or surfactant-induced transportation through the column.

The fate of ENPs in soil is similar to its fate in other systems, in that behavior in the medium depends on the physico-chemical characteristics of both the nanoparticles and the soil. The fate of nanoparticles in the soil system is affected by the transformation mechanisms. For example, metallic ENPs have a higher surface area that favors easy sorption to soil particles, which renders them immobile. Alternately, nanomaterials easily insert themselves into smaller spaces of soil particles or travel larger distances before becoming trapped in the soil matrix. Soil microorganisms are capable of absorbing and degrading the released nanoparticles (Wiesner et al. 2006). Rice University's Centre of Biological and Environmental Nanotechnology Studies deduced that nanoparticles tend to bind to contaminating substances like cadmium and petrochemicals already present in the environment. This means that nanoparticles act as a carrier of pollutants to ground water resources (Colvin 2002). The nanomaterials (ZVI) that are used in pollutant remediation must travel through soil; as they move through the soil it is likely that they interact with various soil constituents in (Greg 2004; Zhang 2003). Another confounding factor when studying the fate of ENPs in soil is that natural nanoparticles are also present that could distort test results of the ENPs targeted for study. Clearly, much more work is needed to elucidate the transport mechanisms for ENPs in the environment.

## 5 Toxicity of the ENPs

As yet, few studies have been performed that adequately address how toxic the ENPs may be. We summarize below, and in Table 5 and Fig. 3 the results of the few studies that have been performed to test the toxicity of the ENPs. The organisms tested to date include microbes, such as bacteria, protozoans, invertebrates, and nematodes, earthworms, fish and mammals.

### 5.1 Microbes

#### 5.1.1 Bacteria

*Escherichia coli* and *Bacillus subtilis* have been used as model organisms to test the toxicity of pristine nano C<sub>60</sub>. Results indicate that the minimum inhibitory concentration (MIC) of nano C<sub>60</sub> for *E. coli* is much less (0.5–1.0 mg/L) than for *B. subtilis* (1.5–3.0 mg/L). Minimum bactericidal concentration (MBC) values for *E. coli* and *B. subtilis* ranged from 1.5 to 3 mg/L and 2–4 mg/L, respectively (Table 5). Comparing the toxicity of nano forms with other bulk materials like carboxy fullerene and benzene have shown that the nano-C<sub>60</sub> toxicity is slightly higher. Bacteria also appear to associate with nano-C<sub>60</sub>, and repeated washing could not remove it from bacterial cells (Lyon et al. 2005).

**Table 5** A summary of the toxic effects that ENPs have produced on different organisms

Nanoparticle studied	Concentration used	Organism studied	Observed effects	References
<b>Bacteria</b>				
Nano C <sub>60</sub>	0.5–3.0 mg/L (MIC) and 1.5–4.0 mg/L (MBC)	<i>Escherichia coli</i> and <i>Bacillus subtilis</i>	MIC and MBC	Lyon et al. (2005)
C <sub>60</sub>	0.5 and 0.01 mg/L	<i>Pseudomonas putida</i> and <i>Bacillus subtilis</i>	Decreased unsaturated fatty acid and increase in cyclopropane fatty acid	Fang et al. (2007)
nC <sub>60</sub>	1 and 1,000 µg/g	Total microbial biomass	Less impact on bacterial community	Tong et al. (2007)
SWNTs (0.75–1.2)	1–50 µg/L	<i>Escherichia coli</i> K12	Loss in viability which increases with time	Kang et al. (2007)
Silver nanoparticles	10 and 50 µg/mL	<i>Escherichia coli</i>	Inhibition in growth, leakage of reducing sugars and proteins, depression of activity of membranous enzymes	Li et al. (2010)
Nanosilver (15–21 nm)	10 mg/L	<i>Escherichia coli</i>	Aggregation and penetration after 1 h of exposure	Choi et al. (2010)
TiO <sub>2</sub> (20 and 10 nm)	5 mg/L	Planktons and biofilms	Cell membrane damage	Battin et al. (2009)
Nano TiO <sub>2</sub> , SiO <sub>2</sub> And ZnO	TiO <sub>2</sub> —1,000 mg/L–5,000 mg/L SiO <sub>2</sub> —> 5,000 mg/L ZnO—10 and 1,000 mg/L	<i>Bacillus subtilis</i> and <i>Escherichia coli</i>	Antibacterial activity increases in order SiO <sub>2</sub> < TiO <sub>2</sub> < ZnO	Adams et al. (2006)
ZnO (1.4–14 nm)	10 <sup>-3</sup> –3.0 × 10 <sup>-3</sup> M	<i>Escherichia coli</i>	Inhibition in bacterial growth, cellular internalization and increased membrane permeability	Brayner et al. (2006)
CeO <sub>2</sub> (7 nm)	0–730 mg/L	<i>Escherichia coli</i>	Cytotoxicity was observed when nanoparticles contact with the bacterial cell	Thill et al. (2006)
Quantum dots (CdSe)	10 mg/L–1 g/L at moderate acidic and alkaline pH	<i>Escherichia coli</i> and <i>Bacillus subtilis</i>	Reduced growth with intact surface coating whereas no growth with weathered surface coatings	Mahendra et al. (2008)

(continued)

**Table 5** (continued)

Nanoparticle studied	Concentration used	Organism studied	Observed effects	References
<b>Algae</b>				
SiO <sub>2</sub> (Water algae)	–	<i>Scenedesmus obliquus</i>	Decreased chlorophyll content	Wei et al. (2010)
Ag	–	<i>Ochromonas danica</i>	Np internalization and accumulation	Miao et al. (2010)
CeO <sub>2</sub>	a. 0.27–6.3 mg/L	a. <i>Anabaena</i> CPB4337	Acute toxicity, membrane disruption and cell damage	Palomares et al. (2011)
	b. 2.4–29.6 mg/L	b. <i>Pseudokirchneriella subcapitata</i>		
TiO <sub>2</sub> (25 and 100 nm)	40 mg/L (25 nm)	a. <i>Desmodesmus subspicatus</i>	Inhibited growth	Hund-Rinke and Simon (2006)
		b. <i>Pseudokirchneriella subcapitata</i>		
<b>Protozoa</b>				
MWNT	0.1–200 µg/mL	<i>Stylonychia mytilus</i> (protozoan)	Dose dependent growth inhibition, macronucleus and cell membrane damage	Zhu et al. (2006b)
MWNTs	–	<i>Tetrahymena pyriformis</i>	Growth inhibition in filtered pond water	Zhu et al. (2006a)
<b>Invertebrates</b>				
SWNTs	–	<i>Amphiascus tenuiremis</i> (copepod)	Size and concentration dependent lifecycle mortality and delayed development	Templeton et al. (2006)
TiO <sub>2</sub>	20 mg/L	<i>Daphnia magna</i> and <i>Thamnocephalus platyurus</i>	Acute toxicity	Baun et al. (2008)
		<i>Daphnia magna</i> and <i>Thamnocephalus platyurus</i> and <i>Tetrahymena thermophila</i>		
ZnO and CuO	90–224 mg/L (CuO) 1.1–16 mg/L (ZnO)	<i>Daphnia magna</i> and <i>Vibrio fischeri</i>	Acute toxicity	Blinova et al. (2010)
TiO <sub>2</sub> , Al, ALEX, L-ALEX and Boron	107.88 mg/L (TiO <sub>2</sub> ), 7.483 mg/L (L-ALEX)	<i>Daphnia magna</i> and <i>Vibrio fischeri</i>	Acute toxicity	Strigul et al. (2009)
C <sub>60</sub> and TiO <sub>2</sub>	–	<i>Daphnia magna</i>	Acute toxicity	Lovern and Klaper (2006)
CdTe quantum dots	1.6–8 mg/L	<i>Elitiptio complanata</i>	Immuno competence, oxidative stress	Gagne et al. (2008)

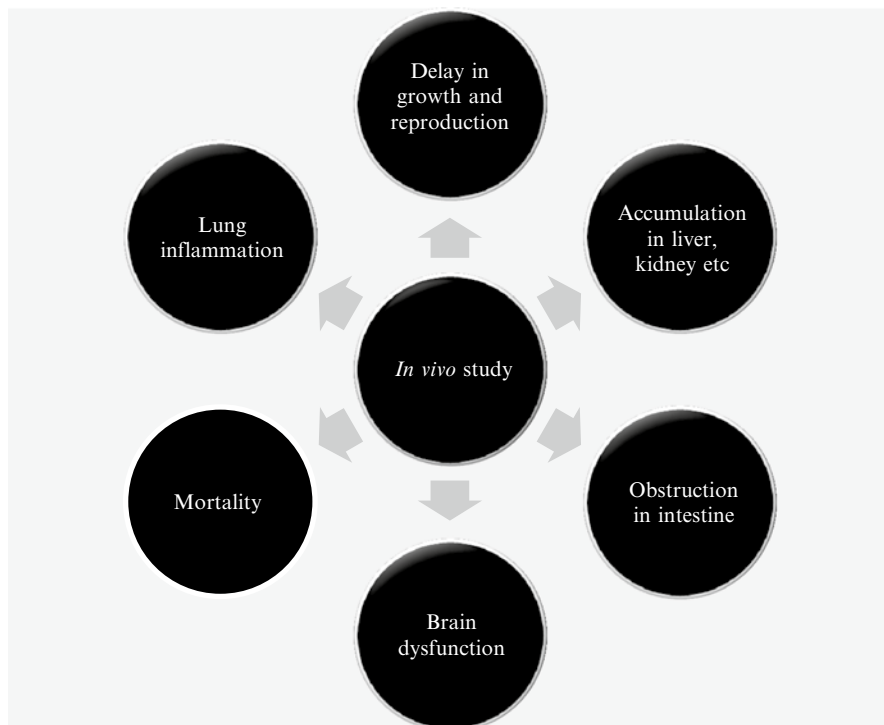
Ag	–	<i>Caenorhabditis elegans</i> (Wild and mutant)	Growth inhibition and NP internalization	Meyer et al. (2010)
Ag	0.05, 0.1, and 0.5 mg/L	<i>Caenorhabditis elegans</i>	Decreased reproductive potential, oxidative stress	Roh et al. (2009)
C <sub>60</sub>	0, 15.4 and 154 mg/kg soil	<i>Lumbricus rubellus</i>	Dose response effects, mortality, growth reduction with increasing dose.	Van der Ploeg et al. (2011)
DWNTs (10–30 nm) and C <sub>60</sub> (11 nm)	0, 50, 100, 300 and 495 mg/kg (DWNTs) 0 and 1,000 mg/kg C <sub>60</sub>	<i>Eisenia veneta</i>	Reproduction toxicity was observed but no effect on hatchability, growth and mortality	Scott-Fordsmand et al. (2008)
Cobalt and silver	–	<i>Eisenia fetida</i>	Accumulation of cobalt in blood and digestive tract, and excretion of silver	Courtis et al. (2012)
Ag, Cu, Ni, Al <sub>2</sub> O <sub>3</sub> , SiO <sub>2</sub> , TiO <sub>2</sub> , and ZrO <sub>2</sub>	1,000 mg/kg	<i>Eisenia fetida</i>	Survival rate was decreased with metal salts, sever reproductive toxicity was observed for Ag NP, AgNO <sub>3</sub> , and Cu NP	Heckmann et al. (2011)
ZnO	0, 50, 100, 200, 500, 1,000 mg/kg	<i>Eisenia fetida</i>	Accumulation in organelle and cytosol and membrane and tissue retention	Li et al. (2011)
ZnO	250 and 750 mg/kg	<i>Eisenia veneta</i>	Reduced toxic effects compared to bulk	Hooper et al. (2011)
TiO <sub>2</sub> and ZnO	0.1, 0.5, 1 and 5 g/kg	<i>Eisenia fetida</i>	Accumulation of ZnO, Changes in biochemical activity of CAT, MDA and cellulose. DNA damage	Hu et al. (2010)
Fish				
C <sub>60</sub>	0.5 mg/L	Largemouth bass	Lipid peroxidation in brain and depleted GSH levels	Oberdorster (2004)
C <sub>60</sub>	0.04–1.0 mg/L	Juvenile carp	No mortality	Zhu et al. (2008)
SWNTs	0.1, 0.25 and 0.5 mg/L	Rainbow trout	Gill pathology, oxidative stress	Smith et al. (2007)
TiO <sub>2</sub>	0.1, 0.5 and 1.0 mg/L	Rainbow trout	Oedema and thickening of lamellae in gills	Federici et al. (2007)

(continued)

**Table 5** (continued)

Nanoparticle studied	Concentration used	Organism studied	Observed effects	References
Ag	1.03 mg/L	Japanese medaka	Acute toxicity, Oedema and abnormalities in heart, fins, brain, spine and eyes, developmental, histopathological abnormalities	Wu et al. (2010)
Ag	–	Zebrafish embryo	Abnormal phenotypic appearance, distribution in heart, brain, yolk and blood	Asharani et al. (2008)
Ag	–	Japanese medaka	Cellular and DNA damage, oxidative stress and carcinogenicity	Chae et al. (2009)
Ag	1 µg/L	Japanese medaka (Male)	Oxidative and inflammatory stress	Pham et al. (2012)
Fluorescent Latex NP	10 mg/L	See through medaka	Accumulation in gills and intestine and other organs	Kashiwada (2006)
<b>Mammals</b>				
Fullerenol and quartz	0.02, 0.2, 20 and 200 µg/mouse	Mice	Lung inflammation caused by neutrophils	Roursguard et al. (2008)
Carbon nanotubes (SWNTs and MWNTs), TiO <sub>2</sub> , Cadmium particle and metal oxide (TiO <sub>2</sub> )	0.1–12.5 mg/kg (nanotubes), 0.5–10 mg/L (TiO <sub>2</sub> ), 70 µg/L (cadmium), 1–5 mg (Metal oxide)	Rats	Lung damage, pulmonary inflammation, activation of histocompatibility complex, alveolar inflammation	Handy and Shaw (2007)
		Mice		
		Guinea pig hamsters		
Carbon nanotubes	0.1 or 0.5 mg	mice	Lung inflammation, necrosis	Lam et al. (2004)
Polyalkylsulphonated C <sub>60</sub>	–	Rats	Accumulation in liver, kidney and spleen	Chen et al. (1998)
14-C labeled C <sub>60</sub>	–	Sprague-Dawley Rats (Female)	Long term accumulation in liver	Bullard-Dillard et al. (1996)
MWNTs	0.5, 2 or 5 mg	Sprague-Dawley rats	Pulmonary lesions and TNF-α production	Muller et al. (2005)
SWNTs	1–5 mg/kg	Rats	Transient inflammation and cellular injury	Warheit et al. (2004)
ZnO	5 g/kg	Adult mice	Obstruction in intestine, severe symptoms	Wang et al. (2006)
ZnO	6 mg/m <sup>3</sup>	Guinea pig	Decreased lung function	Comner et al. (1985)





**Fig. 3** Toxic endpoints in *in vivo* studies that have been observed for ENPs in different organisms

Physiological adaptation studies revealed decreased levels of unsaturated fatty acids and increased levels of cyclopropane fatty acids in *P. putida* in presence of nC<sub>60</sub> (Table 5). Fourier transform infrared spectroscopy (FTIR) data showed a slight increase in phase transition temperature ( $T_m$ ) and membrane fluidity of bacterial cells. These changes could be due to the conformational alterations of acyl chains at growth inhibiting concentrations (0.5 mg/L) of nC<sub>60</sub>. Increase in the levels of iso- and aniso-branched fatty acids was observed in *B. subtilis* at a lower concentration (0.01 mg/L) of nC<sub>60</sub> (Fang et al. 2007). These alterations could result from the interaction of nC<sub>60</sub> with lipid fractions of bacterial cell membrane and other cellular constituents to produce lipid peroxidation. Toxicity studies (for 180 days) of nC<sub>60</sub> on soil microbial community has revealed that nC<sub>60</sub> has less impact on the bacterial community in natural soils (Table 5) (Tong et al. 2007).

*E. coli* K12 cells appear to interact with SWNTs in saline solution (Kang et al. 2007). A substantial loss in viability of treated cells ( $79.9 \pm 9.8\%$ ) was observed within 60 min, compared to controls ( $7.6 \pm 2.1\%$ ) (Table 5). These results imply that direct contact between the cell and nanoparticles is needed for inactivation of *E. coli* cells. Moreover, the average percentage of viability loss increases with time. The authors of this study concluded that the SWNTs exhibit strong antibacterial activity and causes irrecoverable damage to bacterial cells (Kang et al. 2007).

Complete inhibition of *E. coli* growth was observed at 10 µg/mL Ag NPs (Li et al. 2010). Ag NPs resulted in leakage of reducing sugars and proteins, and led to inactivation of membrane-bound enzymes, suggesting that they had the ability to destroy membrane permeability (Table 5). This resulted from the potential of Ag<sup>+</sup> ions to disturb the proton gradient across the cell membrane, ultimately causing cell death. Moreover, AgNPs also interact with free sulphur-, oxygen- and nitrogen-containing compounds, leading to loss of their function. At a concentration of 50 µg/mL AgNPs, many pits and gaps were observed in bacterial cells as seen through TEM (Transmission electron microscope) and SEM (Scanning electron microscope) analyses. The conclusions were that AgNPs may damage the structure of bacterial cell membranes and suppress the activity of membranous enzymes (Li et al. 2010).

Choi et al. (2010) conducted a differential toxicity study to determine the effects of nanosilver (15–21 nm) on planktonic and biofilm cultures by using *E. coli*. Silver nanoparticle aggregation and penetration was observed after 1 h of exposure at two bactericidal concentrations (viz., 38 and 10 mg/L) (Table 5) (Choi et al. 2010). Similarly, Battin et al. (2009) performed a surface water study of TiO<sub>2</sub> nanoparticles (20 and 10 nm) with a exposure concentration of 5 mg/L. The aim of the study was to evaluate toxicity on planktonic and biofilms of the natural microbial community. Cell membrane damage was observed as a major toxic effect (Table 5). Moreover, toxic effects resulted from both individual nanoparticles and from their aggregates (Battin et al. 2009).

Adams et al. (2006) reported an antibacterial effect of nano TiO<sub>2</sub>, SiO<sub>2</sub> and ZnO water suspensions against *B. subtilis* and *E. coli*. They observed that the antibacterial effects were highest for SiO<sub>2</sub> and lowest for ZnO (SiO<sub>2</sub> < TiO<sub>2</sub> < ZnO) (Table 5). *B. subtilis* was more susceptible to the above-mentioned nanoparticles than was *E. coli*. TiO<sub>2</sub> showed a toxicity range of 1,000–5,000 mg/L. This wide response may have resulted from particle size and light-dependent reactive oxygen species (ROS) generation by these TiO<sub>2</sub> nanoparticles. Bulk SiO<sub>2</sub> is not toxic, whereas nano SiO<sub>2</sub> showed toxicity at concentrations higher than that of TiO<sub>2</sub> and ZnO. The ZnO nanoparticle resulted in 99% growth inhibition of *B. subtilis* at a 10 mg/L concentration; on the other hand, only 48% growth reduction was observed in *E. coli* cells at a 1,000 mg/L concentration. SiO<sub>2</sub> and ZnO showed similar antibacterial effects, either in light or dark conditions, indicating that light is insignificant in increasing the toxicity of these nanoparticles. Testing under dark conditions may have had some unexplained effects on toxicity (Adams et al. 2006).

Gram negative triple membrane disorganization was observed with ZnO (1.4–14 nm) nanoparticles in *E. coli* (Brayner et al. 2006). The interaction of this organism with ZnO nanoparticles revealed 100% inhibition of bacterial growth at a concentration of 10<sup>-2</sup>–3.0 × 10<sup>-3</sup> M. An increase in bacterial colonies was seen at lower concentrations (1.5 × 10<sup>-3</sup> and 10<sup>-3</sup> M) of ZnO nanoparticles. These results are presumed to result from metabolic utilization of Zn<sup>2+</sup> ions as an oligoelement. Cellular internalization and increased membrane permeability has also been observed through transmission electron microscopy (Table 5). In this study, the authors concluded that lower concentrations of ZnO nanoparticles do not cause harm to bacterial cells (Brayner et al. 2006).

CeO<sub>2</sub> nanoparticles (7 nm) were used to elicit *E. coli* cytotoxicity in the concentration range of 0–730 mg/L. Results obtained via sorption isotherms, TEM microscopy and XAS (X-Ray absorption spectroscopy) revealed that the nanoparticles were embedded in the bacterial membrane, and their presence produced further oxidative stress (Table 5) (Thill et al. 2006).

Antibacterial activity of QDs on *B. subtilis*, *E. coli* and *P. aeruginosa* was observed only after the organisms were weathered in acidic (pH 2) or alkaline (pH 12) environments (Mahendra et al. 2008). Such weathering results in release of free cadmium (Cd) and selenium (Se) ions due to degradation of surface coatings (Table 5). However, under moderate alkaline and acidic conditions, QDs are not bactericidal, even at concentrations from 10 mg/L to 1 g/L. QDs effects have been analyzed using UV-visible spectrophotometry and viable plate counts. The toxicity was reduced in the presence of humic acid, protein and other organic ligands that limit the bioavailability of metal ions (Mahendra et al. 2008).

It is worthy to note that the studies described above were conducted on different bacterial species, different types of ENPs, and under varying conditions (e.g., medium composition, differential interaction time, dose and reaction medium). These differential test conditions greatly influenced how the nanoparticles and bacteria interacted. For instance, the hydrophobic carbon-based nanoparticles attacked DNA, lipid fractions of cell membranes and other lipid components of the cell. But, in the natural soil systems, carbon-based NPs do not elicit toxicity. This may be because there is a physical interaction of the carbon-based nanoparticles with soil particles, to render them non-available for biological interaction. On the other hand metal oxide nanoparticles have been shown to induce ROS and oxidative stress-mediated toxicity by adsorbing to cell membranes or being absorbed through cell membranes. Once on or in the cell, such NPs can traverse ion channels and replace cations at their sites of action. Also, NPs interact with compounds containing free thiols, carboxylates, phosphates, hydroxyls, nitrates and amines present in the cellular constituents. Therefore, more effort must be expended in future research to better understand the nature of ENP properties like size, shape, chemical and catalytic activity and agglomeration behavior.

### 5.1.2 Algae

SiO<sub>2</sub> NPs having diameters of 10–20 nm were found to be toxic to water algae, *Scenedesmus obliquus* (Table 5). *S. obliquus* exposed to SiO<sub>2</sub> NPs at moderate to high concentrations for 96 h displayed decreased chlorophyll content. The authors assumed that the toxicity of these NPs to algal cells resulted from sorption through cell surfaces (Wei et al. 2010). In another study, Miao et al. (2010) noted that nanosilver was internalized and accumulated in the freshwater alga *Ochromonas danica*, and such uptake was the causative toxic mechanism (Table 5).

Palomares et al. (2011) studied the toxicity of CeO<sub>2</sub> nanoparticles on a self-luminescent cyanobacterial recombinant strain of *Anabaena* (CPB4337) and on the green alga *Pseudokirchneriella subcapitata*. Results indicated that these NPs caused

membrane disruption and heavy cellular damage (Table 5), which may have resulted from direct contact between the NPs and organismal cells (Palomares et al. 2011). A similar interaction was observed for *Desmodesmus subspicatus* with photoactive TiO<sub>2</sub> NPs (25 nm) and the effects were confirmed by illumination measurements. In particular, the main effects were growth reduction, which was enhanced with increased levels of TiO<sub>2</sub> NPs (Hund-Rinke and Simon 2006).

The dearth of information on the effects of ENPs on both bacteria and algae makes clear the need for new research to strengthen knowledge in this domain.

### 5.1.3 Protozoa

Toxicity testing on the living unicellular protozoan *Stylonychia mytilus* revealed that exposure to MWNTs resulted in uptake by the protozoa. Absorbed MWNTs were subsequently passed on after cell division and were ultimately excreted from the cell (Zhu et al. 2006b). A dose-dependent growth inhibition was observed as MWNT exposure concentrations increased. It was observed by using fluorescence and electron microscopy that the MWNTs caused damage to the macronucleus and external membranes of cells. Moreover, MWNTs remained exclusively localized in cell mitochondria (Table 5). Zhu et al. (2006b) proposed that the deleterious effects on the micronucleus, macronucleus and the cell membrane may be attributed to mitochondrial damage.

Zhu et al. (2006a) performed a similar study with the unicellular protozoan *Tetrahymena pyriformis*, and in contrast to previous results, showed a growth stimulation from exposure to MWNTs-peptone conjugates in a proteose peptone yeast extract medium (PPY). However, growth inhibition from exposure to MWNTs was observed in presence of filtered pond water. Furthermore, measurements of MDA (malondialdehyde) levels, and SOD (superoxide dismutase) activity demonstrated that MWNTs may be toxic or nontoxic depending on the medium used to cultivate *Tetrahymena pyriformis*.

## 5.2 Animals

### 5.2.1 Invertebrates

#### Crustacea

Templeton et al. (2006) performed a chronic life cycle bioassay with the estuarine copepod *Amphiascus tenuiremis* with SWNTs. No significant effects on mortality, development and reproduction was observed across exposures (<0.05) with purified SWNTs (Table 5). However, an AP-SWNT (As prepared) complex significantly increased the life cycle mortality and reduced the fertilization rate. The results of this study suggested increased life cycle mortality and delayed copepod development at various sizes and concentrations of AP-SWNT (Templeton et al. 2006).

Acute toxic effects have been observed in *Daphnia magna* and *Thamnocephalus platyurus* after being treated with nano TiO<sub>2</sub>. Of the total *D. magna* cells exposed to a 20 mg/L concentration, 60% showed toxic effects, whereas marginal toxic effects were observed in *T. platyurus* after exposure to nano TiO<sub>2</sub> (Table 5) (Baun et al. 2008).

*D. magna*, *T. platyurus* and *Tetrahymena thermophila* were tested for toxic responses to metal oxide nanoparticles (ZnO and CuO), in both natural and artificial waters (Blinova et al. 2010; Table 5). In natural waters, the toxicity to crustaceans to nano CuO (90–224 mg/L) was tenfold lower (based on LC<sub>50</sub> values) than for the bulk CuO counterpart. LC<sub>50</sub> values for ZnO nano forms were lower than those of CuO nano- and bulk-particles. However, in natural water, the toxicity was dependent on dissolved organic carbon (DOC) content (Blinova et al. 2010).

The acute toxicity of TiO<sub>2</sub> (6 nm), Al (100 nm), ALEX (aluminum explosive) nanoparticles coated with Al<sub>2</sub>O<sub>3</sub>, L-ALEX-NPs coated with carboxylate groups, and boron nanoparticles (10–20 nm) was tested on *Daphnia magna* and *Vibrio fischeri* (Strigul et al. 2009). TiO<sub>2</sub> and L-ALEX displayed low toxicity to *D. magna*. The LD<sub>50</sub> (48 h) values for TiO<sub>2</sub> and L-ALEX NPs in *D. magna* were 107.88 mg/L and 7.483 mg/L, respectively. This study proved that nano-aluminium is more toxic than its bulk counterparts (Table 5). Concentrations of boron nanoparticles (56 and 66 mg/L) were toxic to *V. fischeri* (Strigul et al. 2009). Boron, however, was slightly more toxic acutely to *D. magna*; LD<sub>50</sub> 24-, and 48-h LD<sub>50</sub> values were 19.5 mg/L and 6.7 mg/L, respectively (Table 5). The authors of this study concluded that boron nanoparticles are toxic to aquatic organisms (Strigul et al. 2009). Lovern and Klaper (2006) conducted an acute toxicity test for 48 h with C<sub>60</sub> and TiO<sub>2</sub> nanoparticles on *D. magna*. Results were that a concentration-dependent increase in mortality was observed (Table 5). However, fullerene (C<sub>60</sub>) showed greater toxicity at a lower concentration (Lovern and Klaper 2006).

## Mollusca

The CdTe QDs elicited sub lethal effects in the freshwater mussel *Elliptio complanata*, after 24 h of exposure (Gagne et al. 2008). Effects on hemocytes and immunocompetence were observed in the range of 1.6–8 mg/L for these CdTe QDs. Also noted by the authors were oxidative stress in gills and digestive glands (Table 5). A significant reduction in DNA strand breaks was observed in the concentration range of 4 and 8 mg/L (Gagne et al. 2008).

## Nematodes

*Caenorhabditis elegans* is the nematode most commonly used for toxicity testing of nanoparticles. Wang et al. (2009) evaluated the toxicity of both nano and bulk forms of ZnO, Al<sub>2</sub>O<sub>3</sub> and TiO<sub>2</sub> in *C. elegans*. Results were that LC<sub>50</sub> values for ZnO nano and bulk forms were the same (2.3 mg/L). However, LC<sub>50</sub> values for Al<sub>2</sub>O<sub>3</sub> and TiO<sub>2</sub> bulk forms were twice that of the nano forms, meaning they were only half as toxic

(Table 5). ENPs have a positive zeta potential, whereas nematodes have an even distribution of net negative charges on their membranes. Net negative charges on the surface of the nematodes attract ENPs. The bulk and nano ENP forms can affect the growth and reproduction capability of nematodes (Wang et al. 2009). Growth inhibition in both wild type and mutant nematode species are known to occur from exposure to and internalization of AgNPs (Table 5) (Meyer et al. 2010). AgNPs also decrease the reproduction potential and increase expression of Sod-3 in *C. elegans* through a oxidative pathway (Table 5) (Roh et al. 2009).

## Earthworms

Exposure tests were performed on earthworms (*Lumbricus rubellus*) with  $C_{60}$  at concentrations of 0, 15.4 and 154 mg/kg in soil, with the goal of measuring mortality, growth and reproduction effects. Dose-dependent effects were observed in both adult and juvenile growth after 4 weeks of exposure (Table 5). Juveniles were more sensitive to  $C_{60}$  than were adults (Van der Ploeg et al. 2011). Earthworms (*Eisenia veneta*) were given food spiked with double-walled nanotubes (DWNTs) (outer diameter 10–30 nm) and  $C_{60}$  fullerene (11 nm) at levels of viz., 0, 50, 100, 300 and 495 mg/kg (Scott-Fordsmand et al. 2008). The earthworms were kept in 500 g of soil for 28 days at 20 °C. No significant growth effect resulted from exposure to the lower concentrations; however a 20% reduction in growth occurred at the highest concentration of  $C_{60}$  (Table 5). Cocoon production and reproduction was severely impaired at concentrations above 37 mg DWNT/kg. No effects were observed on earthworm hatchability for any dose (Scott-Fordsmand et al. 2008).

Recently, Courtis et al. (2012) studied the bioavailability of cobalt (CoNPs) and AgNPs in earthworms (*Eisenia fetida*). It was observed that these NPs were taken up by the tested earthworms, and was excreted and bio-distributed. After 4 weeks of exposure significant amount of Co ions (88%) and CoNPs (69%) were found in the blood samples of earthworm, whereas Ag ions and AgNPs were found to be 2.3% and 0.4%, respectively (Table 5). The authors of this study concluded that most absorbed silver was excreted from the earthworms, whereas 32% of the cobalt taken up remained in blood and the digestive tract (Courtis et al. 2012).

A limit test design was used by Heckmann et al. (2011) to assess the toxicity in earthworms (*Eisenia fetida*) of three pure metal-based nanoparticles (Ag, Cu and Ni), four metal oxide nanoparticles ( $Al_2O_3$ ,  $SiO_2$ ,  $TiO_2$ , and  $ZrO_2$ ) and their bulk counterparts (i.e., metal and metal oxides) (Table 5). All treatments carried out were at a soil level of 1,000 mg/kg and tests were conducted for 28 days at 20 °C. The AgNPs,  $AgNO_3$ , CuNPs,  $TiO_2$  NPs and their metal salts all induced reproductive toxicity (Heckmann et al. 2011).

Li et al. studied the effect of DOM on earthworm (*Eisenia fetida*) toxicity for several salts of ZnO NPs (0, 50, 100, 200, 500 and 1,000 mg/kg). Tests were conducted in agar and on filter paper spiked with a soil extract and the intended amount of the nanoparticles. Accumulation of nanoparticle in organelles and in cytosol of earthworms was observed after feeding with the agar medium that had been impregnated

with the nanoparticles (Table 5). Increased SOD activity and average CAT (catalase) levels and GSH-px (Glutathione peroxidase) activities occurred in worms treated with the NPs (Li et al. 2011).

Earthworms (*E. veneta*) were chronically exposed to ZnO nanoparticles at concentrations of 250 and 750 mg/kg of soil. The ZnO nanoparticles were less toxic than their bulk counterparts (Hooper et al. 2011). Effects of different concentrations (0.1, 0.5, 1.0 or 5.0 g/kg) of TiO<sub>2</sub> and ZnO NPs on earthworms (*E. fetida*) were studied for 7 days. Biochemical activities of three biomolecules (viz., SOD, CAT, and cellulase) and the content of MDA were assayed after the acute toxicity studies and DNA damage was assessed (Table 5). No significant change in the SOD activity was observed, whereas CAT activity decreased with the increasing NP concentrations. MDA activity increase at lower doses of NPs but a sudden decrease was observed at the highest NP dose (5 g/kg). DNA damage occurred at higher doses (i.e., 1 and 5 g/kg). Of the two nanoparticles studied, ZnO accumulated in the earthworms and caused cellular and organelle damage (Hu et al. 2010).

### 5.2.2 Fish

Oberdorster (2004) studied the sub-lethal oxidative effects of C<sub>60</sub> at a concentration of 0.5 mg/L on largemouth bass. Lipid peroxidation occurred from this treatment in brain after 48 h of exposure. Marginal depletion in GSH levels of gills was also observed, and was attributed to bactericidal action on C<sub>60</sub> (Table 5) (Oberdorster 2004).

Zhu et al. (2008) performed a 32-day study on juvenile carp (*Carassius auratus*) with C<sub>60</sub> suspensions (0.04–1.0 mg/L). No mortality occurred. However, a significant reduction in mean total length was observed after C<sub>60</sub> exposure at 0.2 mg/L; moreover, reduced body weight occurred at 1.0 mg/L (Table 5) (Zhu et al. 2008).

Smith et al. (2007) used a system approach to understand the toxicity of SWNTs in rainbow trout. A dose-dependent rise in gill pathology (edema, altered mucocytes, hyperplasia), ventilation rate and mucus secretion was observed, with SWNT precipitation occurring in gill mucus (Table 5). Levels of Cu and Zn in brain and gill were altered from SWNT exposure, and occurred partly from a solvent effect. A significant decrease in thiobarbituric acid reactive substance (TBARS) in gills, brain and liver occurred, whereas an increase in total glutathione levels in gills (28%) and liver (18%) was observed from SWNT exposure. Apoptotic bodies and abnormal nuclear division were observed in liver cells (Smith et al. 2007). Similarly TiO<sub>2</sub> nanoparticles elicited a respiratory response from the fish and caused sublethal effects (Table 5) (Federici et al. 2007).

Effects of AgNPs on different developmental stages of Japanese medaka (*Oryzias latipes*) were studied (Table 5). The 48-h LC<sub>50</sub> value for Japanese medaka was 1.03 mg/L. Other abnormalities observed from exposure were edema and abnormalities in the heart, fins, brain, spine and eyes (Wu et al. 2010). The authors of this study concluded that the AgNPs were toxic to aquatic organisms. Asharani et al. (2008) reported the results of a similar study, in which starch and bovine serum albumin (BSA) capped AgNPs were tested in zebrafish embryos (*Denio rerio*).

The result was a dose-dependent toxicity of AgNPs in zebra fish embryos (Table 5). Nanoparticles were distributed in heart, brain, yolk and blood of embryos as evidenced by TEM and electron dispersive X-ray analysis (EDS). Phenotypic studies also revealed abnormal body axes, twisted notochord and slow blood flow.

In addition to acute toxicity studies, other studies have been performed to investigate the health and environmental impacts of NPs, by studying the changes in expression levels of stress-related genes. One such study was conducted on Japanese medaka to evaluate the toxicity of silver nanoparticle AgNPs. Heat shock protein-70 (HSP 70), p53, cytochrome P450 1A (CYP1A) and transferring gene were selected as stress markers. The mRNA concentrations were measured in liver extracts. In addition to cellular and DNA damage, AgNPs caused oxidative stress and carcinogenicity (Table 5) (Chae et al. 2009). This study was extended to evaluate two additional biomarkers (metallothionein (MT), and glutathione S-transferase (GST) gene) at an AgNP concentration of 1 µg/L in livers of exposed fish. The results indicated that AgNPs are potential inducers of metal detoxification, and oxidative/inflammatory stress (Pham et al. 2012).

Fluorescent latex nanoparticles are absorbed into the chorion of see-through medaka (*Oryzias latipes*) eggs and accumulate in the gills and intestine (Table 5). Nanoparticles have also been found in the brain, testis, liver and blood of medaka (*Oryzias latipes*). This study indicated that nanoparticles have the potential to penetrate the blood-brain barrier (Kashiwada 2006).

### 5.2.3 Mammals

The toxicity of nanoparticles has been investigated in rats, mice and guinea pigs. Roursguard et al. (2008) instilled fullerol NPs (dose levels per mouse: 0.02, 0.2, 20 and 200 µg) and quartz (50 µg) intratracheally in mice and monitored responses (Table 5). The result was a dose-dependent neutrophil-induced lung inflammation in the treated mice. Quartz induced more inflammation than did the fullerol nanoparticles; in fact, inflammation in the presence of nanoparticles was minimal.

Handy and Shaw (2007) performed respiratory studies in rats with carbon nanotubes (doses: 0.1–12.5 mg/kg), ultrafine TiO<sub>2</sub> NPs (doses: 0.5, 2.0, 10 mg/L), ultrafine cadmium particles (70 µg/L), and metal oxide particles (1–5 mg) (Table 5). Results indicated significant lung damage, inflammation and fibrotic responses when exposed to intra-tracheal doses of above-mentioned NPs (Handy and Shaw 2007; Lam et al. 2004).

Intraperitoneal injection of polyalkyl sulphonated C<sub>60</sub> produced toxicity due to accumulation of the nanoparticles in liver, spleen and kidney of rats (Chen et al. 1998).

Bullard-Dillard et al. (1996) studied the behavior and potential metabolism of <sup>14</sup>C-labelled C<sub>60</sub> in female Sprague-Dawley rats. <sup>14</sup>C<sub>60</sub> was cleared within 1 min from blood and the majority of NPs were accumulated in the liver (90–95%). Results of this study suggested that C<sub>60</sub> or its derivative may lead to long term accumulation in liver (Table 5).



Muller et al. (2005) studied the effect of intratracheally administered MWNTs (doses: 0.5, 2, or 5 mg) in Sprague-Dawley rats. The MWNTs persisted in the lung and caused inflammation and fibrosis. Further, NPs persisted in lung tissues have been examined biochemically and histologically after a period of 60 days. Results indicated that both inflammatory and fibrotic reactions were induced by the treatments Muller et al. (2005) (Table 5). Warheit et al. (2004) conducted a similar study with SWNTs in rats at 1–5 mg/kg, and found that the SWNTs produced transient inflammation and cell injury.

Gastrointestinal dosing (at 5 g/kg body wt) in mice (Wang et al. 2006), with either nano-zinc oxide or larger particles resulted in more severe symptoms being produced by the nano-treated group. The symptoms included lethargy, vomiting, diarrhea, and deaths from intestinal obstruction by aggregated nano-zinc oxide (Table 5) (Wang et al. 2006). A significant decrease in lung function was observed by Conner et al. (1985) in guinea pigs that had inhaled 6 mg/m<sup>3</sup> of nano zinc oxide particles (50 nm), along with 1 ppm of sulphur dioxide for 3 h daily for six consecutive days.

The effects of ENPs on human beings have yet to be studied. It is presumed that some insight to how ENPs affect humans may eventually be gleaned from occupational exposures or exposures to certain pollutants that have a NP character. Xia et al. (2009) predicted that reactive oxygen species (ROS) and oxidative stress may be generated by inhalation of ultrafine particles and may lead to respiratory and cardiovascular inflammation. For instance, occupational exposure of miners in central India to manganese during mining operations revealed a genetic polymorphism in cytochrome P450 2D6 (CYP2D6\*2), glutathione-S-transferase M1 (GSTM1) and NAD (P) H quinone oxidoreductase 1 (NQO1) genes (Vinayagamoorthy et al. 2010).

### 5.3 Plants

The toxicity of nanoparticles to terrestrial plants has been studied at different concentrations and under different conditions. In Table 6, we summarise the effects that ENPs have had on different plant species.

Khodavskaya et al. (2009) tested CNTs in tomato seeds at levels of 10–40 µg/mL and discovered that the seed coat was penetrated by the NPs, producing an increased germination rate. Wang et al. (2011) reported the effects of treating ryegrass (*Lolium perenne*) and pumpkin (*Cucurbita mixta* cv. white cushaw) with magnetite nanoparticles (Fe<sub>3</sub>O<sub>4</sub>) at levels of 30, 100 and 500 mg/L. These NPs induced more oxidative stress than did their bulk counterparts. This result was confirmed by measuring the activities of SOD, catalase and lipid peroxidation (Table 6).

Yang and Watts (2005) assayed the phytotoxicity of aluminium NPs (with or without phenanthrene) during seed germination, root elongation and formation of leaves in five plant species (corn, cucumber, soya bean, cabbage and carrot). Exposure of aluminium NPs at a 2 mg/mL concentration after 24 h resulted in stunted root growth.

Table 6 The toxicity of ENPs to plants

Nanoparticles studied	Concentration	Plant studied	Results	References
CNTs	10–40 µg/mL	Tomato seeds	Seed penetration and increased germination rate	Khodavskaya et al. (2009)
Fe <sub>3</sub> O <sub>4</sub>	30, 100 and 500 mg/L	<i>Lolium perenne</i> and <i>Cucurbita mixta</i>	Oxidative stress	Wang et al. (2011)
Aluminium	2 mg/mL	Corn	Stunted root growth	Yang and Watts (2005)
		Cucumber		
		Soya bean		
		Cabbage		
		carrot		
nZVI and Ag	0–5,000 and 0–100 mg/L	Ryegrass	nZVI beneficial at lower concentration, no clear effects with silver	El-Temshah and Joner (2012)
		Barley		
Ag	0–40 mg/L (Agar) 0–2,000 mg/kg (Soil)	<i>Phaseolus radiatus</i> , <i>Sorghum bicolor</i>	Root and shoot growth decreases in agar medium whereas in soil medium less toxicity was observed	Lee et al. (2012)
		Radish		
MWNTs	20, 200, 2,000 mg/L	Rapeseed	Inhibition in seed germination, difference in root growth pattern in different plant	Lin and Xing (2007)
Aluminium		Rye grass		
		Lettuce		
		Corn		
Zinc oxide		cucumber		
		Ryegrass	Reduced biomass, vacuolated epidermal or cortical cells	
ZnO	10, 20, 50, 100, 200, 1,000 mg/L			Lin and Xing (2008)
CuO	335 and 570 mg/L	<i>Triticum aestivum</i> (wheat) and <i>Phaseolus radiatus</i> (Mung)	Aggregation in plant cell	Lee et al. (2008)
Al <sub>2</sub> O <sub>3</sub> , SiO <sub>2</sub> , Fe <sub>3</sub> O <sub>4</sub> and ZnO	400, 2,000 and 4,000 mg/L	<i>Arabidopsis thaliana</i> (Mouse ear cross)	Toxicity follow the pattern ZnO > nFe <sub>3</sub> O <sub>4</sub> > nSiO <sub>2</sub> , while Al <sub>2</sub> O <sub>3</sub> does not show toxicity	Lee et al. (2010)
MWNTs	1,000 mg/L	<i>Cucurbita pepo</i> (Zucchini)	No effect on seed germination, stunted root growth	Stampoulis et al. (2009)
Silver				
Copper				
ZnO				
silicon				

EI-Temshah and Joner (2012) studied the toxicity of nano zero-valent iron (nZVI) and AgNPs to ryegrass, barley and flax using seed germination tests (0–5,000 mg/L of nZVI and 0–100 mg/L of Ag) (Table 6). They reported that nZVI could be helpful in remediation processes; lower concentrations of nZVI did not elicit toxicity.

Lee et al. (2012) reported that growth and germination rates of two edible plants (*Phaseolus radiatus* and *Sorghum bicolor*) was decreased in a dose-dependant manner, with increasing concentrations of silver nanoparticles; the test was performed in both an agar medium and in a soil at the respective concentration ranges of 0–40 mg/L and 0–2,000 mg/kg. Brown tips and necrosis was observed in roots of both plants in agar medium. Higher concentration of citrate-capped silver NPs per kg of soil showed 20% inhibition of seed germination of both plants. EC<sub>50</sub> values of 13 mg/L and 26 mg/L were reported for *Phaseolus radiatus* and *Sorghum bicolor*, respectively (Table 6).

Lin and Xing (2007) studied the toxicity of five types of NPs, viz., multi walled carbon nanotubes, aluminium, alumina, zinc and zinc oxide (20, 200 and 2,000 mg/L) to six different plant species (i.e., radish, rape, rye-grass, lettuce, corn and cucumber). Exposure to nanoscale zinc resulted in the inhibition of seed germination in ryegrass, whereas the exposure to ZnO NPs resulted in the inhibition of seed germination in corn plants (Table 6). The pattern of root growth differed from plant to plant and depended on the type of nanoparticle exposure.

Lin and Xing (2008) studied root uptake, cell internalization and phytotoxicity in ryegrass (*Lolium perenne*), in the presence of ZnO NPs at varying concentrations (10, 20, 50, 100, 200 and, 1,000 mg/L). ZnO NPs exposure reduced biomass and collapsed/vacuolated epidermal or cortical cells of ryegrass (Table 6). In addition, the ZnO NPs were not only attached to the root surface, but were also found in the apoplast and protoplast of the root endodermis and stele.

Lee et al. (2008) reported the toxicity of insoluble copper oxide (CuO) NPs to wheat (*Triticum aestivum*) and mung bean (*Phaseolus radiatus*). These NPs showed aggregation inside the plant cells (Table 6). The authors reported EC<sub>50</sub> values of CuO NPs to be 335 mg/L and 570 mg/L, respectively in mung bean and wheat. They concluded that wheat might be more tolerant to CuO NPs than mung bean.

Lee et al. (2010) reported the effects of four metal oxide NPs, viz. nAl<sub>2</sub>O<sub>3</sub>, nSiO<sub>2</sub>, nFe<sub>3</sub>O<sub>4</sub> and ZnO at three different concentrations (400, 2,000 and 4,000 mg/L) on seed germination, root elongation and leaf formation of mouse-ear cress (*Arabidopsis thaliana*). ZnO NPs were more toxic than nFe<sub>3</sub>O<sub>4</sub> and nSiO<sub>2</sub> NPs. However, nAl<sub>2</sub>O<sub>3</sub> NPs did not show any toxicity (Table 6). Nano forms showed more toxic effects than their corresponding macro forms at the same concentration.

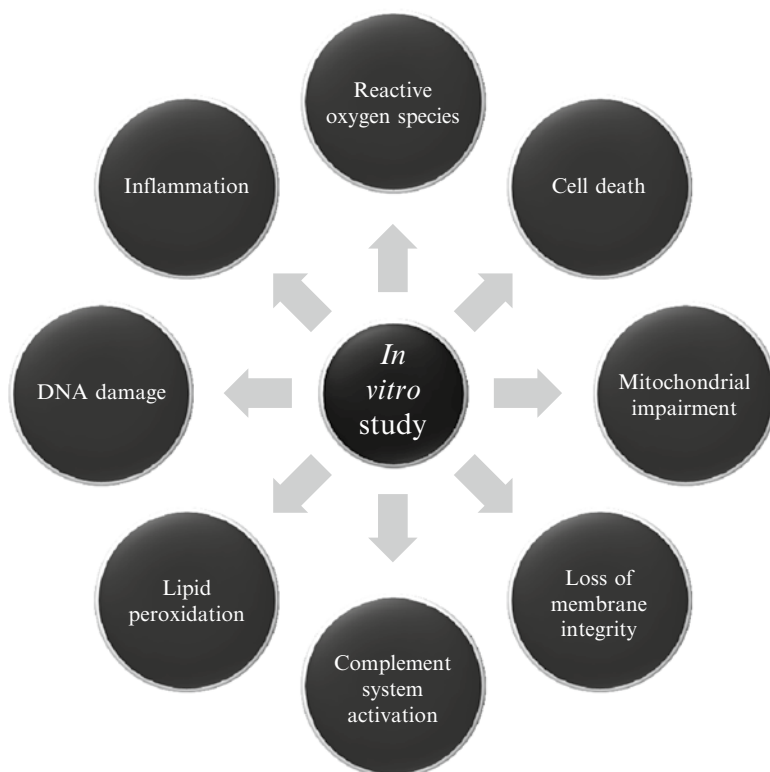
Stampoulis et al. (2009) reported the toxicity of five nanomaterials (MWNTs, Ag, Cu, ZnO, and Si) versus their bulk counterparts on seed germination, root elongation and plant biomass of zucchini (*Cucurbita pepo*) (Table 6). NPs at the concentration of 1,000 mg/L did not show toxicity on seed germination, but exposure to the CuNPs (1,000 mg/L) reduced root length of zucchini by 77%, while Ag and MWNTs NPs reduced root length by 60% and 75%, respectively.

## 5.4 Toxicity to Different Cell Lines

*In vitro* experiments are comparatively fast, simple and easy to use in analyzing the effects of ENPs on individual cell lines. The results of several studies were reported on different cell lines that enhanced the understanding of ENP toxic effects (Fig. 4) Table 7.

Colvin (2002) and Sayes et al. (2004) suggested that fullerene NPs can cause cytotoxicity due to their lipophilic nature. However, modifying the fullerene surface either with aliphatic or hydroxyl group reduced cytotoxicity to human dermal fibroblasts (HDF) and human liver carcinoma (HepG2) cells. Thus, surface characteristics can change the cytotoxic effect of NPs.

Yang et al. (2009) studied the cytotoxicity, genotoxicity and oxidative stress induced by carbon black (CB), SWNTs, SiO<sub>2</sub> and ZnO NPs on mouse embryo fibroblasts. These NPs differ in their particle size, shape and chemical nature and also in concentration. ZnO NPs were found to be more cytotoxic than SiO<sub>2</sub> and carbon nanotubes (Table 7). Shape-dependent genotoxicity was also observed. In a similar study, Mahmoudi et al. (2010) reported gas vesicle formation in mouse fibroblasts when the cells were exposed to coated and non-coated super paramagnetic iron oxide NPs (Mahmoudi et al. 2010) (Table 7).



**Fig. 4** Toxic effects noted and endpoints studied for ENPs in various cell types

**Table 7** The *in vitro* toxicity of ENPs in different cell lines

Nanoparticle	Concentration	Cell line	Results	References
Fullerene	0.24–2,400 ppb	Human dermal fibroblast and human liver carcinoma	Oxidative damage and cell death	Colvin (2002), Sayes et al. (2004)
Carbon black SWNTs	5, 10, 20, 50 and 100 µg/mL	Mouse embryo fibroblast	Cytotoxicity was observed in order ZnO > SWNTs > SiO <sub>2</sub>	Yang et al. (2009)
SiO <sub>2</sub>				
ZnO				
Superparamagnetic iron oxide	>14.5, 29 and 58 mg/mL	Mouse fibroblasts	Gas vesicle formation	Mahmoudi et al. (2010)
SWNTs	800 g/mL	A549 cell line (human)	Loss of cell membrane integrity, inflammation, low toxicity	Davoren et al. (2007)
CuO, TiO <sub>2</sub> , ZnO, CuZnFe <sub>2</sub> O <sub>4</sub> , Fe <sub>3</sub> O <sub>4</sub> , Fe <sub>2</sub> O <sub>3</sub> and MWNTs	0–80 µg/mL	Human lung epithelial	DNA damage and oxidative lesion	Karlsson et al. (2008)
CuO	–	Human lung epithelial	Reduced cellular viability, glutathione production	Ahamed et al. (2010)
PVP coated Ag	0–7.5 µg/ml	Human monocytic	Reactive oxygen species generation	Foldbjerg et al. (2009)
Ag	0–250 µg/mL	Rat liver	Toxicity in order Ag > MoO <sub>3</sub> > Fe <sub>2</sub> O <sub>3</sub> :Al: TiO <sub>2</sub> , abnormal and irregular cell shape and cell shrinkage	Hussain et al. (2005)
MoO <sub>3</sub>				
Al				
Fe <sub>2</sub> O <sub>3</sub>				
TiO <sub>2</sub>				
TiO <sub>2</sub>	2 µg/mL	Lung tumor	Altered cell morphology and internalization and cell death	Magrez et al. (2009)
CeO <sub>2</sub>	–	Human bronchial epithelial cell and macrophage	Antioxidant, cytoprotective (CeO <sub>2</sub> ) ROS production (ZnO)	Xia et al. (2008)
ZnO				
Magnetic nanoparticle	150 µM and 1.5, 15 mM	Rat Pheochromocytoma	Decreased cell viability and neuritis extension	Pisanic et al. (2007)
TiO <sub>2</sub>	–	Isolated porcine skin	No penetration	Wu et al. (2009)
C <sub>60</sub> and 14 C labeled ammonium salt derived C <sub>60</sub>	2 µM	Human keratinocytes	Accumulation in cell and growth inhibition	Bullard-Dillard et al. (1996)
Ag and Au	17.4 and 19 mg/L	Rainbow trout hepatocytes	Cytotoxicity and membrane disruption	Farkas et al. (2010)
Citrate and PVP coated silver	0.1–10 mg/L	Rainbow trout primary gill cell	Cellular absorption and increased glutathione production	Farkas et al. (2011)

Davoren et al. (2007) performed assays and reported SWNTS cytotoxicity in human lung epithelial (A549) cells using Alamar blue (AB), Neutral red (NR) and 3-(4, 5-Dimethylthiazol-2-yl)-2, 5-diphenyltetrazolium bromide (MTT). SWNTS were less toxic to A549 cells. TEM studies revealed no intracellular accumulation of SWNTS in the cells.

Karlsson et al. (2008) studied the comparative toxicity of metal oxide NPs, viz., CuO, TiO<sub>2</sub>, ZnO, CuZnFe<sub>2</sub>O<sub>4</sub>, Fe<sub>3</sub>O<sub>4</sub>, Fe<sub>2</sub>O<sub>3</sub> and MWNTs on A549 cells. All NPs, except Fe<sub>3</sub>O<sub>4</sub> and Fe<sub>2</sub>O<sub>3</sub>, induced DNA damage in the A549 cells. CuO was found to be the most toxic agent among all tested NPs (Table 7). Similar results for CuO NPs were reported by Ahamed et al. (2010). All these NPs were found to induce cytotoxicity through loss of membrane integrity and inflammation.

Foldbjerg et al. (2009) studied the effects of PVP-coated AgNPs (69 ± 3 nm) at varying concentrations (0.1–7.5 µg/mL) on a human monocytic cell line (THP-1). Induction in apoptosis/necrosis was studied using a flowcytometric annexin V/propidium iodide (PI) assay. Analysis using fluorogenic and 2',7'-dichlorofluorescein probes revealed a drastic increase in reactive oxygen species after 6 h (Table 7).

Hussain et al. (2005) performed *in vitro* studies to understand the toxic effects of silver (15, 100 nm), molybdenum (MoO<sub>3</sub>; 30, 150 nm), aluminium (Al; 30, 103 nm), iron oxide (Fe<sub>2</sub>O<sub>3</sub>; 30, 47 nm), and titanium dioxide (TiO<sub>2</sub>; 40 nm) NPs on a rat liver cell line (BRL 3A). In addition, micro molecules of cadmium oxide (CdO; 1 µm), manganese oxide (MnO<sub>2</sub>; 1–2 µm), and tungsten (W; 27 µm) were studied to elucidate their toxic effects on this same BRL 3A cell line. AgNPs at 5–50 µg/mL concentrations induced mitochondrial disruption, whereas all other NPs showed toxicity at higher concentrations (100–250 µg/mL) (Table 7). Microscopic analysis revealed abnormal/irregular cell shapes and cell shrinkage at higher concentrations of NPs. In addition, AgNPs were found to induce ROS generation in the BRL 3A cell line.

By using an *in vitro* MTT assay, combined with direct cell counting and cytopathology, Magrez et al. (2009) reported a strong dose-dependent effect on cell proliferation and cell viability of lung tumor cells after exposure to TiO<sub>2</sub> nanofilaments (2 µg/mL). In contrast, Xia et al. (2008) reported antioxidant and cryoprotective activities of CeO<sub>2</sub> NPs on human bronchial epithelial cell lines (BEAS-2B) and macrophages (RAW-264) (Table 7).

Pisanic et al. (2007) reported a dose-dependent cytotoxicity of magnetic NPs (MNPs) to a rat pheochromocytoma cell line (PC 12 M). Decreased cellular viability and neuritis extension was observed after exposure to increasing concentrations of MNPs. Wu et al. (2009) reported that TiO<sub>2</sub> NPs were unable to penetrate the isolated porcine skin before 24 h. A long-term study on hairless mice revealed the presence of TiO<sub>2</sub> nanoparticle in almost every organ, including the liver and brain (Table 7) (Wu et al. 2009).

Bullard-Dillard et al. (1996) studied the uptake of C<sub>60</sub> and <sup>14</sup>C-labelled ammonium-salt-derivatized-C<sub>60</sub> by human keratinocyte cells. Both the NPs were readily taken up by cells. However, the uptake rate of the derivatized C<sub>60</sub> was slower than for non-derivatized C<sub>60</sub> (Table 7). Exposure of human keratinocyte cells to an aqueous suspension of C60 fullerene with a <sup>14</sup>C-labeled core for 8 days resulted in a 50% growth inhibition.

Farkas et al. (2010) studied the toxic effects of silver and gold NPs ( $\text{HAuCl}_4$  and  $\text{AgNO}_3$ ) and their bulk counterparts on rainbow trout hepatocytes (Table 7). Silver and gold NPs showed agglomeration in media of higher ionic strength and in the presence of dissolved organic carbon (DOC). The AgNPs caused cytotoxicity and membrane disruption through ROS generation. However, gold NPs did not show cytotoxicity, even at a threefold concentration. In a similar study, Farkas et al. (2011) evaluated effects on primary gill cells of rainbow trout (*Oncorhynchus mykiss*). They assessed the cytotoxicity of citrate and PVP-coated AgNPs to primary gill cells of rainbow trout at varying concentrations (0.1–10 mg/L) by using membrane integrity and oxidative stress measurements. Compared to the PVP-coated AgNPs, the citrate capped AgNPs were more easily absorbed into cells, resulting in increased expression levels of glutathione.

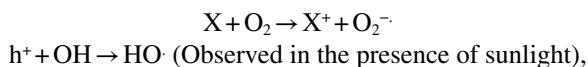
## 6 Possible Mechanisms by Which Nanoparticles Induce Toxicity

Nanoparticles are toxic to living organisms more because of their aggregation behavior than their solubility. In addition, the shape and size of NPs also affect their interactions with the cell surface and cytosolic components. NP-induced toxicity is mainly mediated through the generation of ROS in cells.

### 6.1 Generation of ROS

Different ENPs may have different mechanisms of generating ROS. Size, shape and physico-chemical properties of the ENPs can influence the mechanism of ROS generation. Three exogenous ROS generation mechanisms have been postulated for the ENPs:

- 1) Interaction of ENPs with water, oxygen or  $\text{H}_2\text{O}_2$  in the reaction medium. This interaction facilitates the generation of oxygen free radicals and HO· radical in presence of sunlight due to surface oxidation:



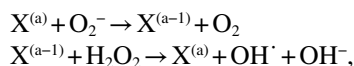
Where, X is ENP and  $h^+$  is electron holes.

- 2) Activation of inflammatory cells, like macrophages and neutrophils that can phagocytose ENPs and generate ROS.
- 3) Cleavage of C-H bonds through a multistep reaction, followed by oxidative damage of macromolecules like lipids and nucleic acids (Fenoglio et al. 2009).

ENPs can generate ROS in cellular components (membranes, proteins, lipids and DNA) in several ways that include: intrinsic sources, such as mitochondrial respiratory

chain dysfunction, microsomes, peroxisomes and inflammatory reactions within the cell. Interference of ENPs with the intrinsic sources forms the superoxide anion ( $O_2^{\cdot-}$ ). Superoxide radical can be further converted to either hydrogen peroxide ( $H_2O_2$ ) or hydroxyl ( $OH^{\cdot}$ ) radicals. Ng et al. (2010) and Li et al. (2009) showed that the presence of intracellular metal ions can facilitate a Fenton-like reaction by interacting with the superoxide and peroxide radicals. This forms  $OH^{\cdot}$  radicals that are extremely toxic to cells.

The following are possible reactions of metal ions with the  $H_2O_2$  and  $O_2^{\cdot-}$ :



Where, X=Fe, Zn, Cr, Cd and other metal ions.

ENPs ultimately cause toxicity by inducing oxidative stress. He et al. (2011) observed that carbon nanotubes can cause mitochondrial damage by inducing pro-inflammatory and fibrotic signals.

Huang et al. (2010) found that metal and metal oxide NPs can induce oxidative stress through Fenton reactions, when these NPs interact with the extracellular or intracellular components of cells. Asharani et al. (2009) reported that AgNPs generate free radicals in the form of  $Ag^+$  ions within the cell.  $Ag^+$  ions are generated after the AgNPs interact with intracellular  $H_2O_2$ . Similar reaction mechanisms have been proposed for other metal NPs like cobalt and nickel (Asharani et al. 2009) and follow the pattern:



Choi et al. (2008) studied the interaction of mitochondrial enzymes with oxidized Ag and found that they generated ROS.

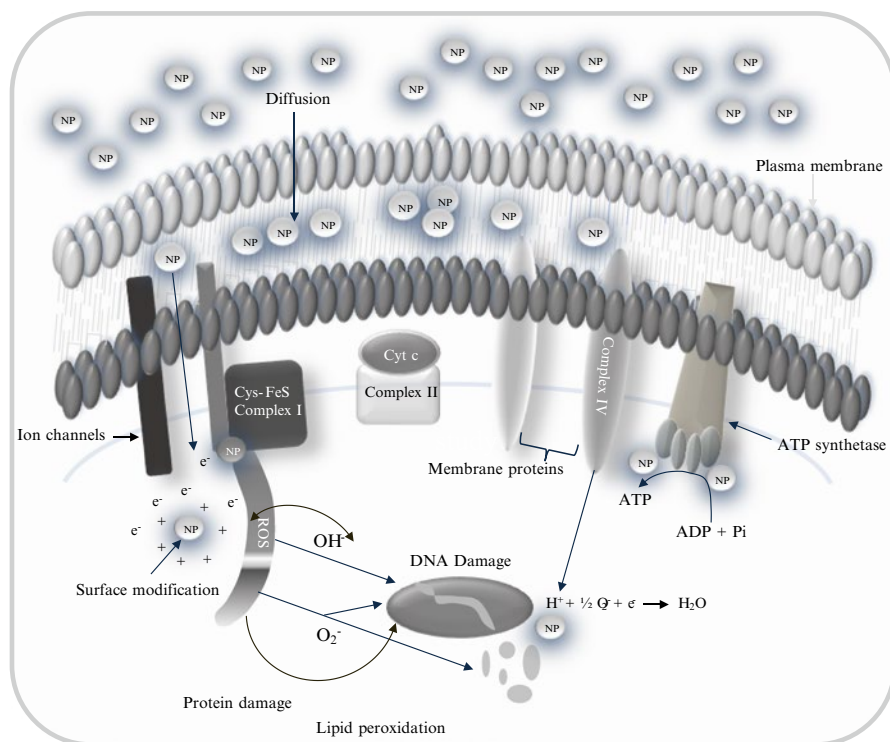
Cells normally have inbuilt mechanisms to overcome oxidative stress. However, excess stress may damage the mitochondria, cause lipid peroxidation, disrupt ion channels, interrupt  $Ca^{2+}$  homeostasis, curtail oxidation of sulfhydryls, damage DNA and cause cell death (Fig. 5).

## 6.2 Interaction with Proteins

The physico-chemical properties of NPs influence how they interact with proteins. Kim et al. (2007) reported that multireceptor sites on rat brain epithelial cells (RBEC) facilitate the interaction of NPs with apolipoproteins in ways that allow the NPs to enter the cells. Lynch and Dawson (2008) suggested that the interaction of NPs with proteins could form a "protein corona", which promotes cell internalization of NPs.

Aggarwal et al. (2009) found that NP-protein interactions alter the 3D confirmation of proteins, leading to impairment of protein activity. Halliwell and Gutteridge (1999) reported that metal NPs interact with sulfhydryl (-SH) groups present on proteins. Such interactions could oxidize GSH, and inhibit antioxidant pathways.





**Fig. 5** Schematic diagram presenting the possible effects of nanoparticle interactions with membrane proteins and cellular organelles that: (1) generate reactive oxygen species, (2) cause lipid peroxidation, and/or (3) protein and DNA damage

Holt and Bard (2005) found that AgNPs inhibits the electron transport chain (ETC) and adenosine triphosphate (ATP) synthesis. Moreover, they reported that intracellular Ag ions interact with thiol-containing proteins and induce phosphate efflux from the cell membrane, which inhibits respiratory and transport proteins. This phenomenon was observed to occur in *in vitro* studies. *In vivo* studies are needed to verify these results.

### 6.3 DNA Damage

Ng et al. (2010) studied how different NPs interact with DNA. Results of their study show that fullerene, carbon nanotubes, metal and metal oxide nanoparticles and quantum dots cause DNA damage. The NPs interact directly with the DNA molecule. The authors concluded that these interactions could induce DNA mutations (single or double strand breaks), chromosomal aberrations, oxidative damage, DNA repair inhibition and DNA methylation. Ahamed et al. (2008) suggested that the

ENPs may induce cytotoxicity by arresting the cell cycle and the mitotic phases. In contrast, exposures to ENPs may cause upregulation of the p53 tumor suppressor gene and to DNA repair proteins. Wan et al. (2012) showed that ENPs can induce DNA damage and cell death via up-regulation of phosphorylated p53, histone H2AX ( $\gamma$ -H2AX) and via an ataxia telangiectasia mutant (ATM).

## 7 Summary

Recent developments in nanotechnology have facilitated the synthesis of novel engineered nanoparticles (ENPs) that possess new and different physicochemical properties. These ENPs have been extensively used in various commercial sectors to achieve both social and economic benefits. However, the increasing production and consumption of ENPs by many different industries has raised concerns about their possible release and accumulation in the environment. Released ENPs may either remain suspended in the atmosphere for several years or may accumulate and eventually be modified into other substances. Settled nanoparticles can be easily washed away during rains, and therefore may easily enter the food chain via water and soil. Thus, ENPs can contaminate air, water and soil and can subsequently pose adverse risks to the health of different organisms.

Studies to date indicate that ENP transport to and within the ecosystem depend on their chemical and physical properties (*viz.*, size, shape and solubility). Therefore, the ENPs display variable behavior in the environment because of their individual properties that affect their tendency for adsorption, absorption, diffusional and colloidal interaction. The transport of ENPs also influences their fate and chemical transformation in ecosystems. The adsorption, absorption and colloidal interaction of ENPs affect their capacity to be degraded or transformed, whereas the tendency of ENPs to agglomerate fosters their sedimentation. How widely ENPs are transported and their environmental fate influence how toxic they may become to environmental organisms. One barrier to fully understanding how ENPs are transformed in the environment and how best to characterize their toxicity, is related to the nature of their ultrafine structure. Experiments with different animals, plants, and cell lines have revealed that ENPs induce toxicity via several cellular pathways that is linked to the size, shape, surface area, agglomeration state, and surface charge of the ENP involved. Future research is needed to elucidate the mechanisms by which nanoparticles act to induce their toxic effects after they reach various ecosystems. Moreover, work is needed to develop a holistic approach for better understanding the effects that ENPs produce at the cellular and genetic level.

**Acknowledgement** Authors are thankful to CSIR-NEERI and Department of Science and Technology, Government of India for providing opportunity and funds to work in this area.

## References

- Adams LK, Lyon DY, Alvarez PJJ (2006) Comparative eco-toxicity of nanoscale TiO<sub>2</sub>, SiO<sub>2</sub>, and ZnO water suspensions. *Water Res* 40(19):3527–3532
- Aggarwal P, Hall JB, McLeland CB, Dobrovolskaia MA, McNeil SE (2009) Nanoparticles interaction with plasma proteins as it relates to particle biodistribution, biocompatibility and therapeutic efficacy. *Adv Drug Del Rev* 61:428–437
- Ahamed M, Siddiqui MA, Akhtar MJ, Ahmad I, Pat AB, Alhadlaq HA (2010) Genotoxic potential of copper oxide nanoparticles in human lung epithelial cells. *Biochem Biophys Res Commun* 396:578–583
- Ahamed M, Karns M, Goodson M, Rowe J, Hussain SM, Schlager JJ, Hong Y (2008) DNA damage response to different surface chemistry of silver nanoparticles in mammalian cells. *Toxicol Appl Pharm* 233(3):404–410
- Aitken RJ, Creely KS, Tran CL (2004) Nanoparticles: an occupational hygiene review. Research Report 274. Prepared by the Institute of Occupational Medicine for the Health and Safety Executive, North Riccarton, Edinburgh, England
- Alivisatos P (2004) The use of nanocrystals in biological detection. *Nat Biotechnol* 22:47–52
- Asharani PV, Wu YL, Gong Z, Vallyaveettil S (2008) Toxicity of silver nanoparticles in zebrafish models. *Nanotechnology* 19:1–8
- Asharani PV, Mun GLK, Hande MP, Vallyaveettil S (2009) Cytotoxicity and genotoxicity of silver nanoparticles in human cells. *ACS Nano* 3(2):279–290
- Baalousha M, Manciulea A, Cumberland S, Kendall K, Lead JR (2008) Aggregation and surface properties of iron nanoparticles: influence of pH and natural organic matter. *Environ Toxicol Chem* 27:1875–1882
- Bandyopadhyaya R, Lall AA, Friedlander SK (2004) Aerosol dynamics and the synthesis of fine solid particles. *Powder Tech* 139(3):193–199
- Batley GE, McLaughlin MJ (2010) Fate of manufactured nanomaterials in the Australian environment. CSIRO niche manufacturing flagship report
- Battin TJ, Kammer FVD, Weilharter A, Ottofuelling S, Hofmann T (2009) Nanostructured TiO<sub>2</sub>: transport, behavior and effects on aquatic microbial communities under environmental conditions. *Environ Sci Technol* 43:8098–8104
- Baun A, Hartmann NB, Grieger K, Kusk KO (2008) Ecotoxicity of engineered nanoparticles to aquatic invertebrates: a brief review and recommendations for future toxicity testing. *Ecotoxicology* 17:387–395
- BCC Research (2012) Market research reports and technical publications. Product catalog. Available from: [http://C:/Users/pk\\_naoghare/Downloads/2012\\_BCC\\_Catalog%20\(1\).pdf](http://C:/Users/pk_naoghare/Downloads/2012_BCC_Catalog%20(1).pdf)
- Benn TM, Westerhoff P (2008) Nanoparticle silver released into water from commercially available sock fabrics. *Environ Sci Technol* 42(11):4133–4139
- Biswas P, Wu CY (2005) Critical review: nanoparticles and the environment. *J Air Waste Manage Assoc* 55:708–746
- Blaise C, Gagne F, Féraud JF, Eullaffroy P (2008) Ecotoxicity of selected nano-materials to aquatic organisms. *Environ Toxicol* 23:591–598
- Blinova I, Ivask A, Heinlaan M, Mortimer M, Kahru A (2010) Ecotoxicity of nanoparticles of CuO and ZnO in natural water. *Environ Pollu* 158:41–47
- Brayner R, Iliou RF, Brivois N, Djediat S, Benedetti MF, Fievey F (2006) Toxicological impact studies based on *Escherichia coli* bacteria in ultrafine ZnO nanoparticles colloidal medium. *Nano Lett* 6:866–870
- Brus LE (2007) Chemistry and physics of semiconductor nanocrystals. Accessed on 7 July 2009
- Buffe J (2006) The key role of environmental colloids/nanoparticles for the sustainability of life. *Environ Chem* 3:155–158
- Bullard-Dillard R, Creek KE, Scrivens WA, Tour JM (1996) Tissue sites of uptake of <sup>14</sup>C labelled C<sub>60</sub>. *Bioorg Chem* 24(4):376–385

- Casey WH, Phillips BL, Furrer G (2001) Aqueous aluminum polynuclear complexes and nanoclusters: a review. *Rev Mineral Geochem* 44(1):167–190
- Chae YJ, Pham CH, Lee J, Bae E, Yi J, Gu MB (2009) Evaluation of toxic impact of silver nanoparticles on Japanese medaka (*Oryzias latipes*). *Aquat Toxicol* 94(4):320–327
- Chan WCW, Maxwell DJ, Gao X, Bailey RE, Han M, Nie S (2002) Luminescent quantum dots for multiplexed biological detection and imaging. *Curr Opin Biotechnol* 13(1):40–46
- Chang T, Jensen L, Kisliuk A, Pipes R, Pyrz R, Sokolov A (2005) Microscopic mechanism of reinforcement in single-wall carbon nanotube/polypropylene nanocomposite. *Polymer* 46:439–444
- Chen HH, Yu C, Ueng TH, Chen S, Chen BJ, Huang KJ, Chiang LY (1998) Acute and subacute toxicity study of water-soluble poly alkyl sulfonated C<sub>60</sub> in rats. *Toxicol Pathol* 26(1):143–151
- Choi O, Deng K, Kim N, Ross L, Surampalli R, Hu Z (2008) The inhibitory effects of silver nanoparticles, silver ions, and silver chloride colloids on microbial growth. *Water Res* 42:3066–3074
- Choi O, Yu CY, Fernandez E, Hu Z (2010) Interactions of nanosilver with *Escherichia coli* cells in planktonic and biofilm cultures. *Water Res* 44(20):6095–6103
- Chopra I (2007) The increasing use of silver-based products as antimicrobial agents: a useful development or a cause for concern? *J Antimicrob Chemother* 59(4):587–590
- Colton HM, Falls JG, Ni H, Kwanyuen P, Creech D, McNeil E, Casey WM, Hamilton G, Cariello NF (2004) Visualization and quantitation of peroxisomes using fluorescent nanocrystals: treatment of rats and monkeys with fibrates and detection in the liver. *Toxicol Sci* 80(1):183–192
- Conner MW, Lam HF, Rogers AE, Fitzgerald S, Amdur MO (1985) Lung injury in guinea pigs caused by multiple exposures to submicron zinc oxide mixed with sulfur dioxide in a humidified furnace. *J Toxicol Environ Health* 16(1):101–114
- Cornell RM, Schwertmann U (1996) Iron oxides structure, properties, reactions, occurrence and uses. Wiley-VCH GmbH & Co. KGaA, Weinheim
- Courtis C, Hertel-Aas T, Lapied E, Joner EJ, Oughton DH (2012) Bioavailability of cobalt and silver nanoparticles to the earthworm *Eisenia fetida*. *Nanotoxicology* 6(2):186–195
- Colvin VL (2002) Responsible nanotechnology: looking beyond the good news. *Nat Biotechnol* 21:1166–1170
- Darlington TK, Neigh AM, Spencer MT, Nguyen OT, Oldenburg SJ (2009) Nanoparticle characteristics affecting environmental fate and transport through soil. *Environ Toxicol Chem* 28(6):1191–1199
- Davoren M, Herzog E, Casey A, Cottineau B, Chambers G (2007) *In vitro* toxicity evaluation of single walled carbon nanotubes on human A549 lung cells. *Toxicol In Vitro* 21:438–448
- Defra (2007) Characterising the potential risks posed by engineered nanoparticles: a second UK government research report. Department for Environment, Food and Rural Affairs, London, p 90. Available from: <http://www.defra.gov.uk/environment/nanotech/research/reports/index.htm>. Accessed on 12 March 2008
- Diegoli S, Manciulea AL, Begum S, Jones IP, Lead JR, Preece JA (2008) Interaction between manufactured gold nanoparticles and naturally occurring organic macromolecules. *Sci Tot Environ* 402(1):51–61
- Dingenen RV, Raes F, Putand J, Baltensperger U, Charron A, Facchini M, Decesari S, Fuzzi S, Gehrig R, Hansson H, Harrison RM, Hüglin C, Jones AM, Laj P, Lorbeer G, Maenhaut W, Palmgren F, Querol X, Rodriguez S, Schneider J, ten Brink H, Tunved P, Törseth K, Wehner B, Weingartner E, Wiedensohler A, Wahlin P (2004) A European aerosol phenomenology – 1: physical characteristics of particulate matter at Kerbside, urban, rural and background sites in Europe. *Atmos Environ* 38:2561–2577
- Dubertret B, Skourides P, Norris DJ, Noireaux V, Brivanlou AH, Libchaber A (2002) *In vivo* imaging of quantum dots encapsulated in phospholipid micelles. *Science* 298(5599):1759–1762
- EI-Temshah YS, Joner EJ (2012) Impact of Fe and Ag nanoparticles on seed germination and differences in bioavailability during exposure in aqueous suspension and soil. *Environ Toxicol* 27(1):42–49
- Fang J, Lyon DY, Wiesner MR, Dong J, Alvarez PJJ (2007) Effect of a fullerene water suspension on bacterial phospholipids and membrane phase behaviour. *Environ Sci Technol* 41:2636–2642

- Farkas J, Christian P, Urrea JAG, Roos N, Hasselov M, Tollefsen KE, Thomas KV (2010) Effects of silver and gold nanoparticles on rainbow trout (*Oncorhynchus mykiss*) hepatocytes. *Aquat Toxicol* 96(1):44–52
- Farkas J, Christian P, Gallego-Urrea JA, Roos N, Hasselov M, Tollefsen KE, Thomas KV (2011) Uptake and effects of manufactured silver nanoparticles in rainbow trout (*Oncorhynchus mykiss*) gill cells. *Aquat Toxicol* 101(1):117–125
- Federici G, Shaw BJ, Handy RD (2007) Toxicity of titanium dioxide nanoparticles to rainbow trout (*Oncorhynchus mykiss*): gill injury, oxidative stress, and other physiological effects. *Aquat Toxicol* 84:415–430
- Fenoglio I, Greco G, Livraghi S, Fubini B (2009) Non–UV-Induced radical reactions at the surface of TiO<sub>2</sub> nanoparticles that may trigger toxic responses. *Chem Eur J* 15:4614–4621
- Foldbjerg R, Olesen P, Hougaard M, Dang DA, Hoffmann HJ, Autrup H (2009) PVP-coated silver nanoparticles and silver ions induce reactive oxygen species, apoptosis and necrosis in THP-1 monocytes. *Toxicol Lett* 190:156–162
- Foller AM (1978) Magnesium oxide and its applications. Vollhardt, Berlin
- Forzatti P (2000) Environmental catalysis for stationary applications. *Catal Today* 62:51–65
- Friedlander SK (2000) Smoke, dust, and haze: fundamentals of aerosol dynamics, 2nd edn. Oxford University Press, New York, NY
- Furrer G, Phillips BL, Ulrich KU, Pothig R, Casey WH (2002) The origin of aluminum flocs in polluted streams. *Science* 297:2245–2247
- Gagne F, Auclair J, Turcotte P, Fournier M, Gagnon C, Sauve S, Blaise C (2008) Ecotoxicity of CdTe quantum dots to freshwater mussels: impacts on immune system, oxidative stress and genotoxicity. *Aquat Toxicol* 86:333–340
- Gao J, Youn S, Hovsepian A, Vernica LL, Wang Y, Bitton G, Bonzongo JJ (2009) Dispersion and toxicity of selected manufactured nanomaterials in natural river water samples: effects of water chemical composition. *Environ Sci Technol* 43(9):3322–3328
- Garland A (2009) The global market for Carbon nanotubes to 2015: a realistic market assessment. Nanoposts. Available from: <http://www.nanoposts.com/index.php?mod+nanotubes>. Accessed on 16 October 2009
- Ghosh S, Mashayekhi H, Pan B, Bhowmik P, Xing B (2008) Colloidal behavior of aluminum oxide nanoparticles as affected by pH and natural organic matter. *Langmuir* 24:12385–12391
- Gibson JD, Khanal BP, Zubarev ER (2007) Paclitaxel-functionalized gold nanoparticles. *J Am Chem Soc* 129(37):11653–11661
- Gottschalk F, Sonderer T, Scholz RW, Nowack B (2009) Modeled environmental concentrations of engineered nanomaterials (TiO<sub>2</sub>, ZnO, Ag, CNT, Fullerenes) for different regions. *Environ Sci Technol* 43:9216–9222
- Greg W (2004) Demonstration of in situ dehalogenation of DNAPL through injection of emulsified Zero Valent Iron at Launch complex 34 in Cape Canaveral Air force station, FL, Battelle conference on Nanotechnology applications for remediation: cost effective and rapid technologies removal of contaminants from soil, ground water and aqueous environment, September 10, 2004
- Guzman KAD, Finnegan MP, Banfield JF (2006) Influence of surface potential on aggregation and transport of titania particles. *Environ Sci Technol* 40:7688–7693
- Handy RD, Shaw BJ (2007) Toxic effects of nanoparticles and nanomaterials: implications for public health, risk assessment and the public perception of nanotechnology. *Health Risk Soc* 9:125–144
- Halliwell B, Gutteridge JMC (1999) Free radicals in biology and medicine. Oxford Univ. Press, Oxford
- He C, Morawska L, Taplin L (2007) Particle emission characteristics of office printers. *Environ Sci Technol* 41(17):6039–6045
- He X, Young S, Schwegler-Berry D, Chisholm WP, Fernback JE, Ma Q (2011) Multiwalled carbon nanotubes induce fibrogenic response by stimulating reactive oxygen species production, activating NF- $\kappa$ B signaling, and promoting fibroblast-to-myofibroblast transformation. *Chem Res Toxicol* 24:2237–2248

- Heckmann LH, Hovgaard MB, Sutherland DS, Autrup H, Besenbacher F, Scott-Fordsmand JJ (2011) Limit test toxicity screening of selected inorganic nanoparticles to the earthworm *Eisenia fetida*. *Ecotoxicology* 20:226–233
- Holt KB, Bard AJ (2005) Interaction of Silver (I) Ions with the respiratory chain of *Escherichia coli*: an electrochemical and scanning electrochemical microscopy study of the antimicrobial mechanism of micromolar Ag. *Biochemistry* 44:13214–13223
- Hooper HL, Jurkschat K, Morgan AJ, Bailey J, Lawlor AJ, Spurgeon DJ, Svendsen C (2011) Comparative chronic toxicity of nanoparticulate and ionic zinc to the earthworm *Eisenia veneta* in soil matrix. *Environ Int* 37:1111–1117
- Horisberger M, Rosset J (1977) Colloidal gold, a useful marker for transmission and scanning electron microscopy. *J Histochem Cytochem* 25(4):295–305  
<http://www.epa.gov/osa/pdfs/nanotech/epa-nanotechnology-whitepaper-0207.pdf>
- Hu CW, Li M, Cui YB, Li DS, Chen J, Yang LY (2010) Toxicological effects of TiO<sub>2</sub> and ZnO nanoparticles in soil on earthworm *Eisenia fetida*. *Soil Biol Biochem* 42:586–591
- Huang Y, Wu C, Aronstam RS (2010) Toxicity of transition metal oxide nanoparticles: recent insights from *in vitro* studies. *Materials* 3:4842–4859
- Huber DL (2005) Synthesis, properties and applications of iron nanoparticles. *Small* 1(5):482–501
- Hund-Rinke K, Simon M (2006) Ecotoxic effect of photocatalytic active nanoparticles (TiO<sub>2</sub>) on algae and daphnids. *Environ Sci Pollu Res Int* 13:225–232
- Hussain SM, Hess KL, Gearhart JM, Geiss KT, Schlager JJ (2005) In vitro toxicity of nanoparticles in BRL 3A rat liver cells. *Toxicol In Vitro* 19(7):975–983
- Hussein T, Hameri K, Aalto PP, Paatero P, Kulmala M (2005) Modal structure and spatial-temporal variation of urban and suburban aerosols in Helsinki-Finland. *Atmos Environ* 39:1655–1668
- Hyung H, Fortner JD, Hughes JB, Kim JH (2007) Natural organic matter stabilizes carbon nanotubes in aqueous phase. *Environ Sci Tech* 41:179–184
- Jaisi D, Elimelech M (2009) Single-walled carbon nanotubes exhibit limited transport in soil columns. *Environ Sci Technol* 43:9161–9166
- Kaegi R, Ulrich A, Sinnet B, Vonbank R, Wichser A, Zuleeg S, Simmler H, Brunner S, Vonmont H, Burkhardt M, Boller M (2008) Synthetic TiO<sub>2</sub> nanoparticle emission from exterior facades into the aquatic environment. *Environ Pollu* 156:233–239
- Kang S, Pinault M, Pfefferle LD, Elimelech M (2007) Single-Walled carbon nanotubes exhibit strong antimicrobial activity. *Langmuir* 23:8670–8673
- Karlsson HL, Cronholm P, Gustafsson J, Moller L (2008) Copper oxide nanoparticles are highly toxic: a comparison between metal oxide nanoparticles and carbon nanotubes. *Chem Res Toxicol* 21(9):1726–1732
- Kashiwada S (2006) Distribution of nanoparticles in the See-through medaka (*Oryzias latipes*). *Environ Health Perspect* 114:1697–1702
- Keller AA, Wang H, Zhou D, Lenihan HS, Cherr G, Cardinale BJ, Miller R, Ji Z (2010) Stability and aggregation of metal oxide nanoparticles in natural aqueous matrices. *Environ Sci Technol* 44(6):1962–1967
- Kennedy A, Hull MS, Steevens JA, Dontsova KM, Chappell MA, Gunter JC, Weiss CA (2008) Factors influencing the partitioning and toxicity of nanotubes in the aquatic environment. *Environ Toxicol Chem* 27:1932–1941
- Khodavskaya M, Dervishi E, Mahmood M, Xu Y, Li Z, Watanabe F, Biris AS (2009) Carbon nanotubes are able to penetrate plant seed coat and dramatically affect seed germination and plant growth. *ACS Nano* 3(10):3221–3227
- Kim HR, Gil S, Andrieux K, Nicolas V, Appel M, Chacun H, Desmaele D, Taran F, Georin D, Couvreur P (2007) Low-density lipoprotein receptor-mediated endocytosis of PEGylated nanoparticles in rat brain endothelial cells. *Cell Mol Life Sci* 64(3):356–364
- Kim J, Takahashi M, Shimizu T, Shirasawa T, Kajita M, Kanayama A, Miyamoto Y (2008) Effects of a potent antioxidant, platinum nanoparticle, on the lifespan of *Caenorhabditis elegans*. *Mech Ageing Dev* 129(6):322–331
- Klaine SJ, Alvarez PJJ, Batley GE, Fernandes TF, Handy RD, Lyon DY, Mahendra S, McLaughlin MJ, Lead JR (2008) Nanomaterials in the environment: behavior, fate, bioavailability, and effects. *Environ Toxicol Chem* 27(9):1825–1851

- Koehler A, Som C, Helland A, Gottschalk F (2008) Studying the potential release of carbon nanotubes throughout the application life cycle. *J Cleaner Prod* 16:927–937
- Lall AA, Friedlander SK (2006) On-line measurement of ultrafine aggregate surface area and volume distributions by electrical mobility analysis: I. Theoretical Analysis. *J Aerosol Sci* 37(3):260–271
- Lam CW, James JT, McCluskey R, Hunter RL (2004) Pulmonary toxicity of single-wall carbon nanotubes in mice 7 and 90 days after intratracheal instillation. *Toxicol Sci* 77:126–134
- Lecoanet HF, Wiesner MR (2004) Velocity effects on fullerene and oxide nanoparticle deposition in porous media. *Environ Sci Technol* 38:4377–4382
- Lee WM, An YJ, Yoon H, Kweon HS (2008) Toxicity and bioavailability of copper nanoparticles to the terrestrial plants mung bean (*Phaseolus radiatus*) and wheat (*Triticum aestivum*): plant agar test for water-insoluble nanoparticles. *Environ Toxicol Chem* 27(9):1915–1921
- Lee CH, Mahendra S, Zodrow K, Li D, Tsai YC, Braam J, Alvarez PJJ (2010) Developmental phytotoxicity of metal oxide nanoparticles to *Arabidopsis thaliana*. *Environ Toxicol Chem* 29(3):669–675
- Lee WM, Kwak JI, An YJ (2012) Effect of silver nanoparticles in crop plants *Phaseolus radiatus* and *Sorghum bicolor*: media effect on phytotoxicity. *Chemosphere* 86:491–499
- Li KG, Chen JT, Bai SS, Wen X, Song SY, Yu Q, Li J, Wang YQ (2009) Intracellular oxidative stress and cadmium ions release induce cytotoxicity of unmodified cadmium sulfide quantum dots. *Toxicol In Vitro* 23:1007–1013
- Li LZ, Zhou DM, Peijnenburg WJGM, Gestel CAMV, Jin SY, Wang YJ, Wang P (2011) Toxicity of zinc oxide nanoparticles in the earthworm, *Eisenia fetida* and subcellular fractionation of Zn. *Environ Int* 37(6):1098–1104
- Li WR, Xie XB, Shi QS, Zeng HY, Yang YSO, Chen YB (2010) Antibacterial activity and mechanism of silver nanoparticles on *Escherichia coli*. *Appl Microbiol Biotechnol* 85:1115–1122
- Lidke DS, Nagy P, Heintzmann R, Arndt-Jovin DJ, Post JN, Grecco HE, Jares-Erijman EA, Jovin TM (2004) Quantum dot ligands provide new insights into erbB/HER receptor-mediated signal transduction. *Nat Biotechnol* 22(2):198–203
- Lin D, Xing B (2007) Phytotoxicity of nanoparticles: inhibition of seed germination and root growth. *Environ Pollu* 150(2):243–250
- Lin D, Xing B (2008) Root uptake and phytotoxicity of ZnO nanoparticles. *Environ Sci Technol* 42:5580–5585
- Lovern SB, Klaper R (2006) *Daphnia magna* mortality when exposed to titanium dioxide and fullerene (C<sub>60</sub>) nanoparticles. *Environ Toxicol Chem* 25:1132–1137
- Lowry GV, Gregory KB, Apte SC, Lead JR (2012) Transformations of nanomaterials in the environment. *Environ Sci Technol* 46:6893–6899
- Luther GW, Rickard DT (2005) Metal sulfide cluster complexes and their biogeochemical importance in the environment. *J Nanopart Res* 7:389–407
- Lynch I, Dawson KA (2008) Protein-nanoparticle interactions. *Nano Today* 3:40–47
- Lyon DY, Fortner JD, Sayes CM, Colvin VL, Hughes JB (2005) Bacterial cell association and antimicrobial activity of a C<sub>60</sub> water suspension. *Environ Toxicol Chem* 24:2757–2762
- Madler L, Friedlander SK (2007) Transport of nanoparticles in gases: overview and recent advances. *Aerosol Qual Res* 7(3):304–342
- Magrez A, Horvath L, Smajda R, Salicio V, Pasquier N, Forro L, Schwaller B (2009) Cellular toxicity of TiO<sub>2</sub> based nanofilaments. *ACS Nano* 3(8):2274–2280
- Mahendra S, Zhu H, Colvin VL, Alvarez PJ (2008) Quantum dot weathering results in microbial toxicity. *Environ Sci Technol* 42:9424–9430
- Mahmoudi M, Simchi A, Imani M, Shokrgozar MA, Milani AS, Hafeli UO, Pieter S (2010) A new approach for the in vitro identification of the cytotoxicity of superparamagnetic iron oxide nanoparticles. *Colloids Surf B Biointerfaces* 75(1):300–309
- Meyer JN, Lord CA, Yang XY, Turner EA, Badireddy AR, Marinakos SM, Chilkoti A, Wiesner MR, Auffan M (2010) Intracellular uptake and associated toxicity of silver nanoparticles in *Caenorhabditis elegans*. *Aquat Toxicol* 100(2):140–150
- Miao AJ, Luo Z, Chen CS, Chin WC, Santschi PH, Quigg A (2010) Intracellular uptake: a possible mechanism for silver engineered nanoparticle toxicity to a freshwater alga *Ochromonas danica*. *PLoS One* 5(12):e15196

- Milani N, MJ McLaughlin, GM Hettiarachchi, DG Beak, JK Kirby, SP Stacey (2010) Fate of nanoparticulate zinc oxide fertilisers in soil: solubility, diffusion and solid phase speciation. In: Gilkes RJ, Prakongkep N (eds) Soil solutions for a changing world: 19th World Congress of Soil Science, Brisbane, QLD, Australia. 1–6 Aug. 2010. IUSS, pp 172–174
- Moore MN (2006) Do nanoparticles present ecotoxicological risks for the health of the aquatic environment? *Environ Int* 32(8):967–976
- Muller J, Huaux F, Moreau N, Mission P, Heilier JF, Delos M, Arras M, Fonseca A, Nagy JB, Lison D (2005) Respiratory toxicity of multi-walled carbon nanotubes. *Toxicol Appl Pharma* 207:221–231
- Murr LE, Garza KM (2009) Natural and anthropogenic environmental nanoparticles: their microstructural characterization and respiratory health implications. *Atmos Environ* 43(17):2683–2692
- Navarro DA, Banerjee S, Watson DF, Aga DS (2011) Differences in soil mobility and degradability between water-dispersible CdSe and CdSe/ZnS quantum dots. *Environ Sci Technol* 45:6343–6349
- Nel A, Xia T, Madler L, Li N (2006) Toxic potential of materials at the nanolevel. *Science* 311:622–627
- Ng CT, Li JJ, Bay BH, Yung LYL (2010) Current studies into the genotoxic effects of nanomaterials. *J Nucleic Acids* 2010, Article ID 947859, 12 p
- Noble CA, Mukerjee S, Gonzales M, Rodes CE, Lawless PA, Natarajan S, Myers EA, Norris GA, Smith L, Ozkaynak H, Neas LM (2003) Continuous measurement of fine and ultrafine particulate matter, criteria pollutants and meteorological conditions in urban El Paso, Texas. *Atmos Environ* 37:827–840
- Nowack B, Bucheli TD (2007) Occurrence, behavior and effects of nanoparticles in the environment. *Environ Pollu* 150:5–22
- Oberdorster E (2004) Manufactured nanomaterials (Fullerenes, C<sub>60</sub>) induce oxidative stress in the brain of juvenile largemouth bass. *Environ Health Perspect* 112:1058–1062
- Ouellette J (2003) Building the nano future with carbon tubes. *Ind Phys* 8:18–21
- Palomares IR, Boltes K, Pinas FF, Leganes F, Calvo EG, Santiago J, Rosal R (2011) Physicochemical characterization and ecotoxicological assessment of CeO<sub>2</sub> nanoparticles using two aquatic microorganisms. *Toxicol Sci* 119(1):135–145
- Pandey RA, Kumar A (1990) Heavy metals in coal carbonization wastewater and their complexation - some observations. *Water Air Soil Pollu* 50:31–38
- Pham CH, Yi J, Gu MB (2012) Biomarker gene response in male Medaka (*Oryzias latipes*) chronically exposed to silver nanoparticle. *Ecotoxicol Environ Saf* 78:239–245
- Perfect E, Sukop MC (2001) Models relating solute dispersion to pore space geometry in saturated media: a review. Physical and chemical processes of water and solute transport/retention in soil, vol 56. Soil Science Society of America, Madison, WI, pp 77–146
- Pisanic TR II, Blackwell JD, Shubayev VI, Finones RR, Jin S (2007) Nanotoxicity of iron oxide nanoparticle internalization in growing neurons. *Biomaterials* 28:2572–2581
- Qian X, Peng XH, Ansari DO, Yin-Goen Q, Chen GZ, Shin DM, Yang L, Young AN, Wang MD, Nie S (2008) *In vivo* tumor targeting and spectroscopic detection with surface-enhanced Raman nanoparticle tags. *Nat Biotechnol* 26(1):83–90
- Raj K, Moskowitz R (1990) Commercial applications of ferrofluids. *Magn Magn Mater* 85(1–3):233–245
- Ramteke C, Chakrabarti T, Sarangi BK, Pandey RA (2012) Synthesis of silver nanoparticles from the aqueous extract of leaves of *Ocimum sanctum* for enhanced antibacterial activity. *J Chem* 2013:1–7
- Ramteke C, Sarangi BK, Chakrabarti T, Mudliar S, Satpute D, Pandey RA (2010) Synthesis and broad spectrum antibacterial activity of magnetite ferrofluid. *Curr Nano* 6(6):587–591
- Roco MC, Bainbridge WS (2005) Societal implications of nanoscience and nanotechnology: maximizing human benefit. *J Nanopart Res* 7:1–13
- Rodríguez JA, Fernández-García M (2007) Synthesis, properties and applications of oxide nanoparticles. John Wiley & Sons, Totowa, NJ, pp 335–351



- Roh JY, Sim SJ, Yi J, Park K, Chung KH, Ryu DY, Choi J (2009) Ecotoxicity of silver nanoparticles on the soil nematode *Caenorhabditis elegans* using functional ecotoxicogenomics. *Environ Sci Technol* 43(10):3933–3940
- Roursguard M, Poulsen SS, Kopley CL, Hammer M, Nielsen GD, Larsen ST (2008) Polyhydroxylated C<sub>60</sub> fullerene (fullerenol) attenuates neutrophilic lung inflammation in mice. *Bas Clin Pharmacol Toxicol* 103(4):386–388
- Royal Society and Royal Academy of Engineering (2004) Nanoscience and nanotechnologies: opportunities and uncertainties. RS policy document 19/04. London, p 113. Available from: <http://www.nanotec.org.uk/finalReport.htm>. Accessed on 12 March 2008
- Sahu N, Soni D, Chandrashekhar B, Sarangi BK, Satpute D, Pandey RA (2012) Synthesis and characterization of silver nanoparticles using *Cynodon dactylon* leaves and assessment of their antibacterial activity. *Bioprocess Biosyst Eng* 36(7):999–1004
- Sawyer CN, Mc Carty PL (1967) Chemistry for Sanitary Engineers. 2nd edn. McGraw-Hill Series in Sanitary Science and Water Resources Engineering, McGraw-Hill, Toronto
- Sayes CM, Fortner LD, Guo W, Lyon D, Boyd AM, Ausman KD, Tao YJ, Sitharaman B, Wilson LJ, Hughes JB, West JL, Colvin VL (2004) The differential cytotoxicity of water soluble fullerenes. *Nano Lett* 4:1881–1887
- Schmitz PJ, Baird RJ (2002) NO and NO<sub>2</sub> adsorption on barium oxide: model study of the trapping stage of NO<sub>x</sub> conversion via lean NO<sub>x</sub> traps. *J Phys Chem B* 106:4172–4180
- Scott-Fordsmand JJ, Krogh PH, Schaefer M, Johansen A (2008) The toxicity testing of double walled nanotubes-contaminated food to *Eisenia veneta* earthworms. *Ecotoxicol Environ Saf* 71:616–619
- Shankar SS, Ahmed A, Shastry M (2003) Geranium leaf assisted biosynthesis of silver nanoparticles. *Biotechnol Prog* 19(6):1627–1631
- Siegmann P, Acevedo FJ, Siegmann K, Maldonado-Bascón S (2008) A probabilistic source attribution model for nanoparticles in air suspension applied on the main roads of Madrid and Mexico City. *Atmos Environ* 42:3937–3948
- Smith CJ, Shaw BJ, Handy RD (2007) Toxicity of single walled carbon nanotubes on rainbow trout, (*Oncorhynchus mykiss*): respiratory toxicity, organ pathologies, and other physiological effects. *Aquat Toxicol* 82:94–109
- Solovitch N, Labille J, Rose J, Chaurand P, Borschneck D, Wiesner MR, Bottero J (2010) Concurrent aggregation and deposition of TiO<sub>2</sub> nanoparticles in a sandy porous media. *Environ Sci Technol* 44:4897–4902
- Stampoulis D, Sinha SK, White JC (2009) Assay dependent phytotoxicity of nanoparticles to plants. *Environ Sci Technol* 43:9473–9479
- Strigul N, Vaccari L, Galdun C, Wazne M, Liu X, Christodoulatos C, Jasinkiewicz K (2009) Acute toxicity of boron, titanium dioxide, and aluminum nanoparticles to *Daphnia magna* and *Vibrio fischeri*. *Desalination* 248:771–782
- Templeton RC, Ferguson PL, Washburn KM, Scrivens WA, Chandler GT (2006) Life-cycle effects of single-walled carbon nanotubes (SWNTs) on an estuarine meiobenthic copepod. *Environ Sci Technol* 40:7387–7393
- Thill A, Zeyons O, Spalla O, Chauvat F, Rose J, Auffan M, Flank AM (2006) Cytotoxicity of CeO<sub>2</sub> nanoparticles for *Escherichia coli* physico-chemical insight of the cytotoxicity mechanism. *Environ Sci Technol* 40(19):6151–6156
- Tian Y, Gao B, Silvera-Batista C, Ziegler KJ (2010) Transport of engineered nanoparticles in saturated porous media. *J Nanopart Res* 12:2371–2380
- Tong Z, Bischoff M, Nies L, Applegate B, Turco RF (2007) Impact of fullerene (C<sub>60</sub>) on a soil microbial community. *Environ Sci Technol* 41:2985–2991
- Tsai CY, Shiao AL, Chen SY, Chen YH, Cheng PC, Chang MY, Chen DH, Chou CH, Wang CR, Wu CL (2007) Amelioration of collagen-induced arthritis in rats by nanogold. *Arthritis Rheum* 56(2):544–554

- Van der Ploeg MJC, Baveco JM, van der Hout A, Bakker R, Rietjens IMCM, van den Brink NW (2011) Effects of C<sub>60</sub> nanoparticle exposure on earthworms (*Lumbricus rubellus*) and implications for population dynamics. *Environ Pollu* 159:198–203
- Vaseashta A, Vaclavikova M, Vaseashta S, Gallios G, Roy P, Pummakarnchana O (2007) Nanostructures in environmental pollution detection, monitoring, and remediation. *Sci Tech Adv Mat* 8:47–59
- Vinayagamoorthy N, Krishnamurthi K, Devi SS, Naoghare PK, Biswas R, Biswas AR, Pramanik S, Shende AR, Chakrabarti T (2010) Genetic polymorphism of CYP2D6\*2 C T 2850, GSTM1, NQO1 genes and their correlation with biomarkers in manganese miners of Central India. *Chemosphere* 81:1286–1291
- Vorbau M, Hillemann L, Stintz M (2009) Method for the characterization of the abrasion induced nanoparticle release into air from surface coatings. *Aer Sci* 40:209–217
- Wallace L, Wang F, Howard-Reed C, Persily A (2008) Contribution of gas and electric stoves to residential ultrafine particle concentrations between 2 and 64 nm: size distributions and emissions and coagulation rates. *Environ Sci Technol* 42(23):8641–8647
- Wan R, Feng L, Mo Y, Chien S, Tollerud DJ, Zhang Q (2012) DNA damage caused by metal nanoparticles: involvement of oxidative stress and activation of ATM. *Chem Res Toxicol* 25:1402–1411
- Wang B, Feng WY, Wang TC, Jia G, Wang M, Shi JW, Zhang F, Zhao YL, Chai ZF (2006) Acute toxicity of nano- and micro-scale zinc powder in healthy adult mice. *Toxicol Lett* 161:115–123
- Wang H, Kou X, Pei Z, Xiao JQ, Shan X, Xing B (2011) Physiological effects of magnetite (Fe<sub>3</sub>O<sub>4</sub>) nanoparticles on perennial ryegrass (*Lolium perenne* L.) and pumpkin (*Cucurbita mixta*) plants. *Nanotoxicology* 5:30–42
- Wang H, Wick RL, Xing B (2009) Toxicity of nanoparticulate and bulk ZnO, Al<sub>2</sub>O<sub>3</sub> and TiO<sub>2</sub> to the nematode *Caenorhabditis elegans*. *Environ Pollu* 157:1171–1177
- Wang ZL (2004) Zinc oxide nanostructures: growth, properties and applications. *J Phys Condens Matter* 16:R829–R858
- Warheit DB, Laurence BR, Reed KL, Roach DH, Reynolds GAM, Webb TR (2004) Comparative pulmonary toxicity assessment of single-wall carbon nanotubes in rats. *Toxicol Sci* 77:117–125
- Waychunas GA, Kim CS, Banfield JF (2005) Nanoparticulate iron oxide minerals in soils and sediments: unique properties and contaminant scavenging mechanisms. *J Nanopart Res* 7:409–433
- Wei C, Zhang Y, Guo J, Han B, Yang X, Yuan J (2010) Effects of silica nanoparticles on growth and photosynthetic pigment contents of *Scenedesmus obliquus*. *J Environ Sci* 22(1):55–160
- Wiesner MR, Lowry GV, Alvarez P, Dionysiou D, Biswas P (2006) Assessing the risks of manufactured nanomaterials. *Environ Sci Technol* 40:4336–4345
- Wu J, Liu W, Xue C, Zhou S, Lan F, Bi L, Xu H, Yang X, Zeng FD (2009) Toxicity and penetration of TiO<sub>2</sub> nanoparticles in hairless mice and porcine skin after subchronic dermal exposure. *Toxicol Lett* 191:1–8
- Wu X, Jiang P, Ding Y, Cai W, Xie SS, Wang ZL (2007) Mismatch strain induced formation of ZnO/ZnS heterostructured rings. *Adv Mater* 19:2319–2323
- Wu Y, Li X, Steel D, Gammon D, Sham LJ (2004) Coherent optical control of semiconductor quantum dots for quantum information processing. *Phys E Low Dimen Sys Nanostruct* 25(2–3):242–248
- Wu Y, Zhou Q, Li H, Liua W, Wanga T, Jianga G (2010) Effects of silver nanoparticles on the development and histopathological biomarkers of Japanese medaka (*Oryzias latipes*) using the partial-life test. *Aquat Toxicol* 100(2):160–167
- Xia T, Kovochich M, Liang M, Madler L, Gilbert B, Shi H, Yeh JI, Zink JI, Nel AE (2008) Comparison of the mechanism of toxicity of zinc oxide and cerium oxide nanoparticles based on dissolution and oxidative stress properties. *ACS Nano* 2(10):2121–2134
- Xia T, Li N, Nel AE (2009) Potential health impact of nanoparticles. *Ann Rev Public health* 30:137–150
- Yadav BC, Kumar R (2008) Structure, properties and applications of fullerenes. *Int J Nanotech Appl* 2(1):15–24

- Yang H, Liu C, Yang D, Zhang H, Xi Z (2009) Comparative study of cytotoxicity, oxidative stress and genotoxicity induced by four typical nanomaterials: the role of particle size, shape and composition. *J Appl Toxicol* 29(1):69–78
- Yang L, Watts DJ (2005) Particle surface characteristics may play an important role in phytotoxicity of alumina nanoparticles. *Toxicol Lett* 158:122–132
- Young LH, Keeler GJ (2004) Characterization of ultrafine particle number and size distribution during a summer campaign in southwest detroit. *J Air Waste Manag Assoc* 54:1079–1090
- Yue ZR, Economy J (2005) Nanoparticle and nanoporous carbon adsorbents for removal of trace organic contaminants from water. *J Nanopart Res* 7:477–487
- Zhang WX (2003) Nanoscale iron particles for environmental remediation: an overview. *J Nanopart Res* 5:323–332
- Zhang Y, Chen Y, Westerhoff P, Hristovski K, Crittenden JC (2008) Stability of commercial metal oxide nanoparticles in water. *Wat Res* 42(8–9):2204–2212
- Zhu X, Zhu L, Lang Y, Chen Y (2008) Oxidative stress and growth inhibition in the freshwater fish *Carassius auratus* induced by chronic exposure to sublethal fullerene aggregates. *Environ Toxicol Chem* 27(9):1979–1985
- Zhu Y, Ran T, Li Y, Guo J, Li W (2006a) Dependence of the cytotoxicity of multi-walled carbon nanotubes on the culture medium. *Nanotechnology* 17:4668–4674
- Zhu Y, Zhao Q, Li Y, Cai X, Li W (2006b) The interaction and toxicity of Multi-walled carbon nanotubes with *Styloynchia mytilus*. *J Nanosci Nanotechnol* 6(5):1357–1364

# Source Characterization of Polycyclic Aromatic Hydrocarbons by Using Their Molecular Indices: An Overview of Possibilities

Efstathios Stogiannidis and Remi Laane

## Contents

1	Introduction .....	50
2	Source Profiles of PAHs .....	56
2.1	Petrogenic .....	56
2.2	Pyrogenic .....	65
2.3	Biogenic/Diagenetic .....	72
3	Factors Influencing PAH Distribution in Aquatic Systems .....	73
4	Analytical Approach for PAH Source Characterization .....	74
5	Molecular Indices .....	76
5.1	Practical Concepts .....	76
5.2	Sum of PAHs .....	81
5.3	Low Molecular Weight PAH Ratios .....	81
5.4	Four-Ringed PAHs .....	89
5.5	Sulfur PAH Indices .....	98
5.6	HMW Five- and Six-Ringed PAHs .....	101
5.7	Non Isomer Ratios .....	106
5.8	Assignment of PAHs to Sources .....	108

---

**Electronic Supplementary Material:** The online version of this chapter (doi:[10.1007/978-3-319-10638-0\\_2](https://doi.org/10.1007/978-3-319-10638-0_2)) contains supplementary material, which is available to authorized users.

E. Stogiannidis (✉)

Environmental Sciences, Institute for Biodiversity and Ecosystem Dynamics, Universiteit van Amsterdam, Science Park 904, 1098XH Amsterdam, The Netherlands

Galatades 58300, Greece

e-mail: [eystog@teemail.gr](mailto:eystog@teemail.gr)

R. Laane

Deltares, Postbox 177, 2600 MH Delft, The Netherlands

e-mail: [Remi.Laane@deltares.nl](mailto:Remi.Laane@deltares.nl)

© Springer International Publishing Switzerland 2015

D.M. Whitacre (ed.), *Reviews of Environmental Contamination and Toxicology*

Volume 234, Reviews of Environmental Contamination and Toxicology 234,

DOI 10.1007/978-3-319-10638-0\_2

6	Discussion and Conclusions.....	114
6.1	What Are the Most Important PAH Sources in the Aquatic Environment and Which PAH Indicators Can Be Used to Unequivocally Identify Them?.....	115
6.2	What Are the Inherent Uncertainties in These Indicators and How Does the Value of the Indicator Change After Undergoing Biogeochemical Processes (i.e., Photochemical Oxidation, Degradation, Volatilization, etc.) in the Aquatic Environment?.....	117
6.3	Can the Borneff-6, 16 EPA, and 10 VROM PAHs Be Used to Calculate the Proposed Indicator—and, if so, Which Uncertainties are Introduced by This Approach?.....	119
7	Summary.....	120
	Appendix.....	121
	References.....	121

## 1 Introduction

The Polycyclic Aromatic Hydrocarbons (PAHs or polyaromatic hydrocarbons) have been extensively studied to understand their distribution, fate and effects in the environment (Haftka 2009; Laane et al. 1999, 2006, 2013; Okuda et al. 2002; Page et al. 1999; Pavlova and Ivanova 2003; Stout et al. 2001a; Zhang et al. 2005). They are organic compounds consisting of conjoined aromatic rings without heteroatoms (Schwarzenbach et al. 2003). Sander and Wise (1997) list 660 parent PAH compounds (i.e., aromatic substances without alkyl groups and consisting solely of fused rings connected to each other), ranging from the monocyclic molecule of benzene (molecular weight=78) up to nine-ringed structures (MW<sup>1</sup> up to 478). PAHs containing one or more alkyl groups are called alkyl PAHs. Our study deals with the parent compounds (without alkyl groups and/or heteroatoms), the alkyl PAHs (denoted as PAH<sub>*n*</sub>, with *n* referring to the number of methyl groups; see footnotes in Table 1), and certain heterocyclic sulfur PAHs (dibenzothiophenes). The term PAHs includes all the above, unless explicitly specified. In Table 1, we present the nomenclature of PAHs used in this paper.

The PAHs have high molecular weight (HMW), low volatility (Ou et al. 2004), and are classified as semivolatile organic contaminants (Ollivon et al. 1999). They are hydrophobic and lipophilic (Pavlova and Ivanova 2003). Their hydrophilicity and mobility decrease as the number of rings increases (Iqbal et al. 2008). In Table 2, we present the physicochemical properties of several parent PAHs. Because of their hydrophobic characteristics, PAHs tend to rapidly adsorb to particulate organic matter in sediments or soots, rather than vaporizing or dissolving in water (Bertilsson and Widenfalk 2002).

Depending on their volatility, the PAHs may be transported far from their original source, ending up in various environmental compartments, although their main environmental sink is the organic fraction of soils and sediments (Agarwal 2009; Harris et al. 2011; Morillo et al. 2008a; Stark et al. 2003). PAHs emitted from the combustion of fossil fuels are transported into marine sediments by atmospheric

<sup>1</sup>MW: molecular weight.

**Table 1** PAH (poly aromatic hydrocarbon) abbreviations used in text, figures and tables

PAH	RN <sup>a</sup>	Abbreviation	PAH	RN	Abbreviation
Naphthalenes	2	<i>Nn</i> <sup>b</sup>	Biphenyl	2	B
Dibenzofuran	3	DF	Acenaphthylene	3	AY
Acenaphthene	3	AE	Fluorenes	3	<i>Fn</i> <sup>b</sup>
Phenanthrenes	3	<i>Pn</i> <sup>b</sup>	Anthracenes	3	<i>An</i> <sup>b</sup>
Phenanthrenes + anthracenes	3	<i>PA</i> <sup>b</sup>	Retene	3	RET
Dimethylphenanthrene	3	DMP	Dibenzothiophenes	3	<i>Dn</i> <sup>b</sup>
Naphthodibenzothiophenes	4	<i>NT</i> <sup>b</sup>	Pyrenes	4	<i>PY</i> <sup>b</sup>
Fluoranthenes	4	<i>FL</i> <sup>b</sup>	Pyrenes + fluoranthenes	4	<i>FP</i> <sup>b</sup>
Chrysenes	4	<i>Cn</i> <sup>b</sup>	Benz[ <i>a</i> ]anthracene	4	BaA
Chrysenes + Benz[ <i>a</i> ]anthracenes	4	<i>BC</i> <sup>b</sup>	Benzo[ <i>b</i> ]fluorene	4	BFu
Benzo[ <i>k</i> ]fluoranthene	5	BkF	Benzo[ <i>a</i> ]fluoranthene	5	BaF
Benzo[ <i>b</i> ]fluoranthene	5	BbF	Benzo[ <i>j</i> ]fluoranthene	5	BjF
Benzo[ <i>j+k</i> ]fluoranthenes	5	Bjk	Benzo[ <i>b+j+k</i> ] fluoranthenes	5	BF
Benzo[ <i>a</i> ]pyrene	5	BaP	Benzo[ <i>e</i> ]pyrene	5	BeP
Cyclopenta[ <i>cd</i> ]pyrene	5	CP	Benzo[ <i>b</i> ]chrysene	5	BbC
Perylene	5	PER	Benzo[ <i>ghi</i> ]perylene	6	ghi
Indeno[1,2,3- <i>cd</i> ]pyrene	6	IP	Dibenz[ <i>ah</i> ]anthracene	5	DA
Coronene	6	Cor	Dibenz[ <i>ac</i> ]anthracene	5	DcA

Parent PAH names written in the plural form denote parent and its alkylated PAHs together. In text, figures, or tables, when relevant, the position of alkylation is indicated by a number preceding the abbreviation (e.g., 1-P1 denotes 1-methylphenanthrene)

<sup>a</sup>Number of rings

<sup>b</sup>*n* refers to the alkylation level (e.g., *n*=0 for the parent PAH, and so C0 stands for the parent chrysene, C1 for methylchrysenes, 1-C1 for 1-methylchrysene and so on); in such a case, PAH names written in the plural form denote all the homologues of that certain alkylation level

fallout (dry or wet deposition), riverine inflows, or discharge from urban runoff (Compaan and Laane 1992; Fabbri et al. 2003; Ollivon et al. 1999).

PAHs can be of anthropogenic or natural origin (Bertilsson and Widenfalk 2002; Morillo et al. 2008a). Natural sources include oil seeps from crude oil deposits, forest fires, volcanoes and erosion of ancient sediment (e.g., Jiao et al. 2009; Zakaria et al. 2002). Some PAHs, such as perylene, are produced naturally in the environment from chemical or biological transformation of natural organic matter, or from biological processes (Venkatesan 1988).

Anthropogenic PAHs in the environment are formed either by thermal alteration of organic matter, or its incomplete combustion (e.g., Luo et al. 2008; Ou et al. 2004). Today, the major sources of PAHs in the biosphere are human utilization of petroleum products and incomplete combustion of fossil fuels, biofuels or other forms of organic matter, which far exceed natural sources (Kim et al. 2008; Morillo et al. 2008a; Yan et al. 2006; Zakaria et al. 2002). As a result, the PAH concentrations in sediments increase at points that are near emission sources, especially near

urban and industrial areas that often have multiple point sources of release (Boll et al. 2008; Elmquist et al. 2007).

PAHs are potentially toxic and mutagenic to many living organisms, such as marine plants and animals (Boehm et al. 2007; Guo et al. 2007; Swietlik et al. 2002). The lower molecular weight PAHs (LMW PAHs) are acutely toxic but non-carcinogenic to many aquatic organisms, whereas the high molecular weight PAHs (HMW PAHs) are strongly carcinogenic and mutagenic (Karlsson and Viklander 2008; Laane et al. 2006; Ou et al. 2004). Different PAH priority lists have been compiled by different environmental or statutory bodies, such as the U.S. Environmental Protection Agency (EPA), the Dutch ministry of housing, spatial planning and the environment (VROM) and the so called “Borneff-6” PAHs (e.g., European Commission 2001; Laane et al. 1999; Table 2).

PAH source characterization defensibly links the contaminants with their sources for the purpose of finding parties that are liable for the contamination. Source apportionment quantifies the amount of contamination contributed by each party involved, so that regulators can make accountability decisions (relating to, e.g., cleanup costs, mitigation, etc.). If a strategy for characterizing PAHs is to succeed, knowledge of the sources, chemistry and fate of each individual PAH is crucial, and the PAHs to be analyzed must be carefully selected (Peters et al. 2005).

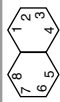
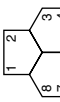

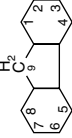
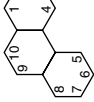
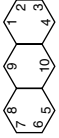
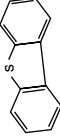
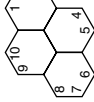
PAHs are classified according to the temperature at which they form, or their origin. An example is the threefold classification espoused by Boehm et al. (2007) and Mitra et al. (1999): i) pyrogenic PAHs, which originate from different pyrolysis substrates, such as fossil fuels and biomass, ii) petrogenic PAHs from petroleum-related sources, and iii) natural PAHs of biogenic or diagenetic origin.

In the history of determining the PAH contaminating source and the contaminants themselves, it was realized that petroleum and its products, as well as combustion byproducts, included quite complicated mixtures of PAHs (Farrington et al. 1977; Giger and Blumer 1974; Windsor and Hites 1979; Youngblood and Blumer 1975). However, it was observed that the distribution of PAHs varied among different PAH sources (Grimmer et al. 1981, 1983; Laflamme and Hites 1978; Youngblood and Blumer 1975). Since then, there has been an ongoing effort to find the proper molecular indices of a PAH distribution that would allow source characterization of contaminated areas.

Our approach on reviewing PAH molecular indices that are used for source characterization is twofold. Firstly, we review indices of a PAH distribution (ubiquitous PAH markers, PAH abundance, modes of distribution, etc.) which are characteristic for pyrogenic and petrogenic sources. The possible modifications that a PAH distribution undergoes on its way from source to receptor are also reported. Secondly, we review a selection of certain indices of a PAH distribution (PAH ratios and some of their combinations) in a quantitative way and evaluate their use in source characterization. Finally, we address the following questions in this review:

- What are the most important PAH sources in the aquatic environment, and which PAH indicators can be used to unequivocally identify them?

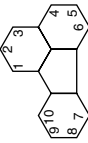
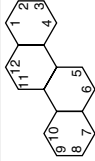
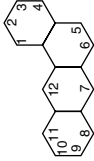
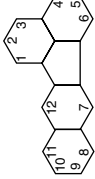
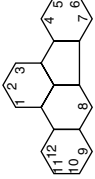
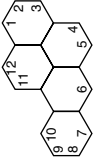
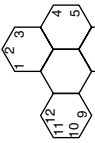
Table 2 The physicochemical properties of selected parent PAHs

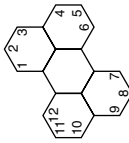
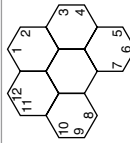
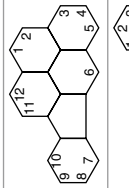
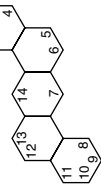
PAH	Priority list <sup>a</sup>	Structure	MW	RN	S (mg/l)	P (Pa)	K <sub>ow</sub>	bp (°C)
Naphthalene	E, U, V		128	2	32	11	3.37	218 <sup>b</sup>
Acenaphthylene	U		152	3	3.9	9.0×10 <sup>-1</sup>	4.1	280
Acenaphthene	U		152	3	3.9	3.0×10 <sup>-2</sup>	3.9	279
Fluorene	B, U		166	3	1.9 <sup>c</sup>	9.0×10 <sup>-2</sup>	4.18	295
Phenanthrene	U, V		178	3	1.1 <sup>c</sup>	2.0×10 <sup>-2</sup>	4.57	340
Anthracene	E, U, V		178	3	0.05 <sup>c</sup>	1.0×10 <sup>-3</sup>	4.54	342
Dibenzothiophene			184	3	1.0 <sup>b</sup>		4.49	333 <sup>d</sup>
Pyrene	U		202	4	0.13 <sup>c</sup>	6.0×10 <sup>-4</sup>	5.18	393

(continued)



Table 2 (continued)

PAH	Priority list <sup>a</sup>	Structure	MW	RN	S (mg/l)	P (Pa)	K <sub>ow</sub>	bp (°C)
Fluoranthene	E, U, V		202	4	0.26	$1.2 \times 10^{-3}$	5.22	375
Chrysene	C, U, V		228	4	0.002	$1.4 \times 10^{-6}$	5.86	448
Benzo[ <i>a</i> ]anthracene	C, U, V		228	4	0.009–0.014	$2.8 \times 10^{-5}$	5.6	400
Benzo[ <i>k</i> ]fluoranthene	B, C, E, U, V		252	5	0.0007–0.008	$5.2 \times 10^{-8}$	6	480
Benzo[ <i>b</i> ]fluoranthene	B, C, E, U		252	5	0.0014	$6.7 \times 10^{-5}$	5.8	481
Benzo[ <i>a</i> ]pyrene	B, C, E, U, V		252	5	0.003 <sup>c</sup>	$7 \times 10^{-7}$	6.0	496
Benzo[ <i>e</i> ]pyrene			252	5	0.005 <sup>c</sup>	$7.3 \times 10^{-6,c}$	6.44, 7.4	311 <sup>b</sup>

Perylene		252	5	0.0004	$1.8 \times 10^{-8}$	6.40	503 <sup>f</sup>
Benzo[ghi]perylene		276	6	0.00026	$1.4 \times 10^{-8,e}$	7.1	550 <sup>e</sup>
Indeno[1,2,3-cd]pyrene		276	6	0.00019 <sup>f</sup>	$1.3 \times 10^{-8}$	6.6	536
Dibenz[ah]anthracene		278	5	0.0005	$3.7 \times 10^{-8}$	6.5	524

Double (or conjugated) bonds are not explicitly indicated, but aliphatic carbons are designated by associated hydrogen atoms. *MW* = molecular weight, *RV* = ring number, *S* = aqueous solubility (25 °C), *P* = vapor pressure (25 °C), *K<sub>ow</sub>* = the logarithm of the octanol-water partition coefficient, *bp* = boiling point. Images and molecular weights are taken from Sander and Wise (1997). Unless otherwise specified, all solubility and *K<sub>ow</sub>* data are from Irwin et al. (1997) and all vapor pressure and bp data are from Hailwood et al. (2001)

<sup>a</sup>Priority PAH pollutant lists that enlist the specific PAH: *B* Borneff6, *C* considered carcinogenic (Stout and Emsbo-Mattingly 2008), *E* European priority pollutant as defined by the European Commission (2001), *U* U.S. EPA 16, *V* VROM 10

<sup>b</sup>Lide (2004)

<sup>c</sup>Hafika (2009)

<sup>d</sup>Dean (1999)

<sup>e</sup>Irwin et al. (1997)

<sup>f</sup>Mackay et al. (2006)

- What are the inherent uncertainties in these indicators and how does the value of the indicator change after undergoing biogeochemical processes (i.e., photochemical oxidation, degradation, volatilization, etc.) in the aquatic environment?
- Can the Borneff-6, 16 EPA, and 10 VROM PAHs be used to calculate the proposed indicator—and, if so, which uncertainties are introduced by utilizing this approach?

## 2 Source Profiles of PAHs

If source inventories are lacking or incomplete, the first task is to clarify whether the known or unknown sources of PAHs are petrogenic, pyrogenic or natural. This is usually accomplished by observing PAH fingerprints that show the relative PAH abundances (Douglas et al. 2007a). For example, the relative distribution of PAHs in each homologous family is used to differentiate compositional changes during the degradation of oil spills (Wang et al. 1999a). Characteristic PAH fingerprints of petrogenic and pyrogenic sources from the literature are shown in Figs. S1–S32 (Supporting Material).

Once released to the environment, the PAHs are prone to a wide variety of degradation processes, including evaporation, dissolution, dispersion, emulsification, adsorption on suspended materials, microbial degradation (biotic or biodegradation), photo-oxidation, and interaction among the contaminants and sediments (Gogou et al. 2000; Kim et al. 2009; Page et al. 1996; Wang et al. 2004). Degradation substantively changes the physicochemical properties and relative abundances of even the highest MW PAHs, and such changes must be considered when identifying and quantifying PAH sources (Page et al. 1996; Wang et al. 2004).

### 2.1 Petrogenic

Petrogenic substances (petrogenics) are defined as the substances that originate from petroleum, including crude oil, fuels, lubricants, and their derivatives (Saber et al. 2006). Petrogenic PAHs are introduced into the aquatic environment through accidental oil spills, discharge from routine tanker operations, municipal and urban runoff, etc. (Zakaria et al. 2002). There have been no observations of widespread, and continuous (i.e., nationwide and non-accidental) input of petrogenic PAHs (Zakaria et al. 2002).

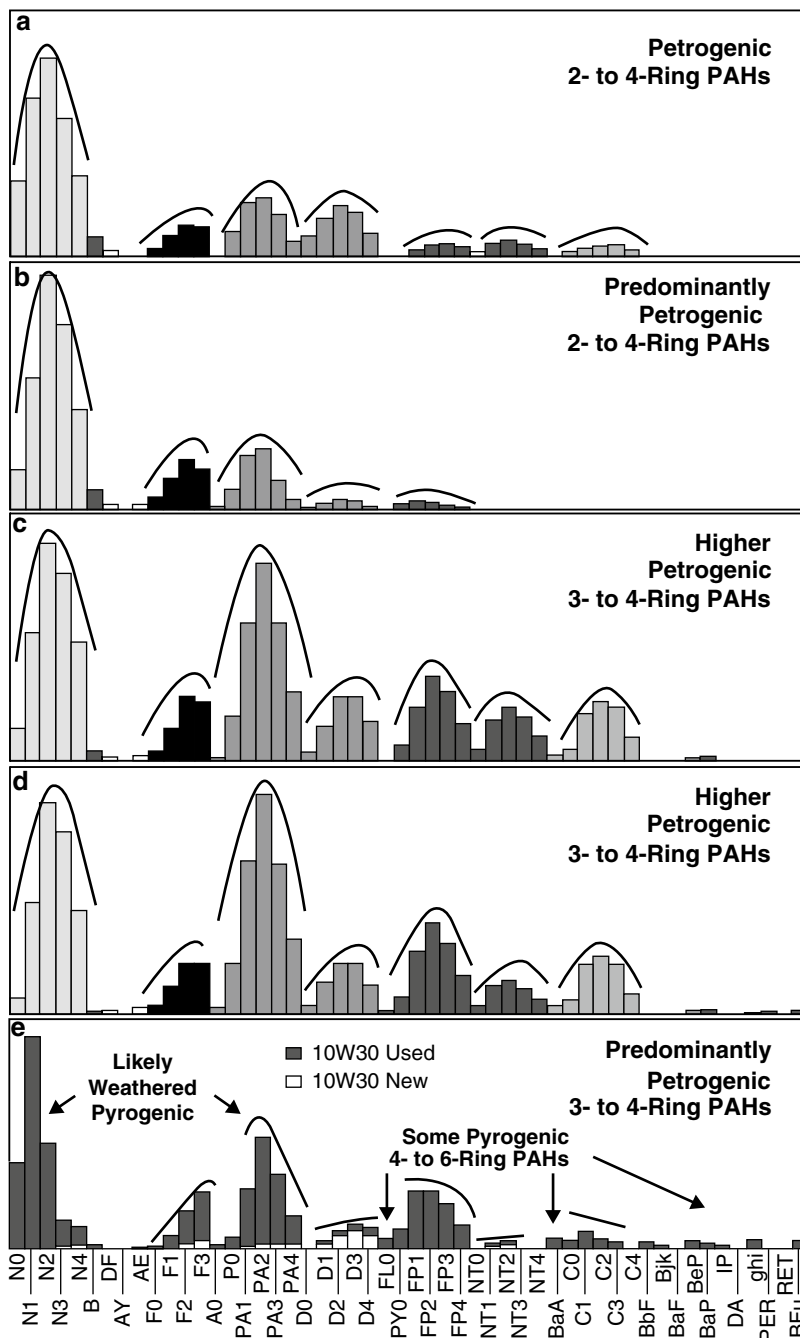
Petroleum is a complex mixture of different organic compounds formed during different geological ages and under different geological conditions. The different depositional environments during oil formation are reflected in different PAH distributions (e.g., dibenzothiophenes:  $D_n$ ) in crudes from different sources

(Page et al. 1996; Wang and Fingas 2003; Wang et al. 1999a, 2001). For example, many of the monomethyl PAH derivatives are preserved in petroleum because of their low formation temperatures (<150 °C) (Mitra et al. 1999). The proportion of thermally stable phenanthrene isomers increases as the crude matures (Stout et al. 2002). Furthermore, the dibenzothiophene abundance in source rock, i.e., the rock in which the oil matured, is a function of anoxia (leading to reduced sulfur), and therefore reflects the type of source rock facies (Peters et al. 2005; Stout et al. 2002).

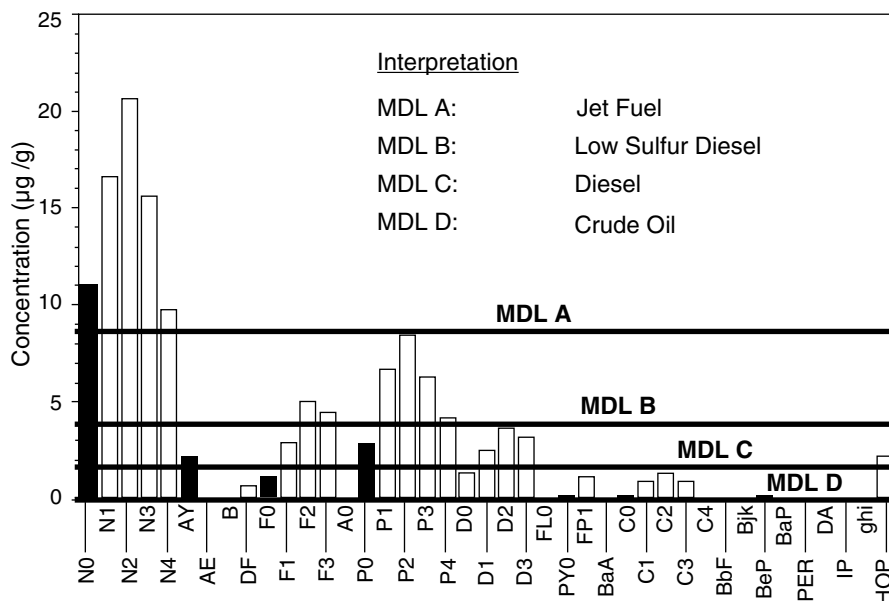
The main PAH components of a petroleum source include the EPA 16 parent PAHs and the petroleum-specific alkylated (PAH1-PAH4) homologues of selected PAHs: viz., alkylated naphthalene, phenanthrene, dibenzothiophene, fluorene, and chrysene series, which are also called “the alkylated five” or “*five target*” (Bertilsson and Widenfalk 2002; Wang et al. 1999a; Zeng and Vista 1997). These PAHs are source-specific (concentrations vary among different oils) and their abundance in sediment is taken to indicate petrogenic sources (Boll et al. 2008; De Luca et al. 2004; Stout and Wang 2007; Wang et al. 2001). For example, dibenzothiophenes, together with phenanthrenes, are widely used for PAH source apportionment because of their numerous isomers and their mild and similar degradabilities (absolute concentrations of the methyl-dibenzothiophenes increase during weathering) (Page et al. 1996; Stout and Wang 2007; Wang and Fingas 1995, 2003; Wang et al. 1999a, 2001).

Figure 1a–d show that petroleum products contain mainly two- to three-ringed PAHs and only the heavier ones (Fig. 1c, d) contain significant amounts of four-ringed PAHs. In all instances (except Fig. 1e), five- and six-ringed PAHs, and occasionally compounds such as acenaphthylene (AY), anthracene (A0) and fluoranthene (FLO) (e.g., Fig. 2; Fig. S3, Supporting Material), are undetectable in crude oil and its refined products (Stout et al. 2002). For instance, benz[*a*]anthracene (BaA), benzo[*a*]pyrene (BaP), benzo[*b*]fluoranthene (BbF), benzo[*k*]fluoranthene (BkF) and chrysene (C0) are minor constituents of petroleum products, if present at all (e.g., Irwin et al. 1997; Jiang et al. 2009; Shreadah et al. 2011; Wang et al. 2001). Figure 1e, given for comparison, shows a mixture of pyrogenic and petrogenic products, as is common in used lubricants.

In crude oil, the content of LMW PAHs (containing two or three fused aromatic rings), and especially their alkylated homologues far exceed the unsubstituted parent PAHs. The petroleum PAHs exhibit a characteristic bell-shaped pattern within their homologue series (Fig. 1a–d; Figs. S2–S5, Supporting Material): PAH3 or PAH2 alkylated PAHs predominate and amounts of PAH0-PAH2 and PAH4 homologues decrease (Douglas et al. 2007a; Stout 2007). Thus, much more information is contained in the alkylated homologue series of crude oil than in the parent PAHs, i.e., the abundance of alkylated PAHs, bell-shaped patterns and depletion of HMW PAHs (compare Figs. S1 vs. S2; Figs. S5 and S6 vs S9, Supporting Material). This information allows us to differentiate between petrogenic products and to distinguish them from pyrogenic forms, regardless of the oil formation environ-



**Fig. 1** Source profiles/fingerprints of characteristic petrogenic PAHs. (a) crude oil, (b) fuel oil #2, (c) fuel oil #4, (d) fuel oil #6, (e) new and used lubricating oils. See Table 1 for PAH abbreviations. Adapted from Douglas et al. (2007a), with permission, © Elsevier Academic Press



**Fig. 2** How the method detection limit (MDL) affects the interpretation of fingerprinting. Shown here is a comparison of fingerprints of crude and its refined products (crude fractions). EPA16 priority PAHs are shown in *black*. See Table 1 for PAH abbreviations, except for *HOP*: hopane. Adapted from Douglas et al. (2007a), with permission, © Elsevier Academic Press

ment or the degree of degradation to which they were subjected (Ou et al. 2004; Yan et al. 2005).

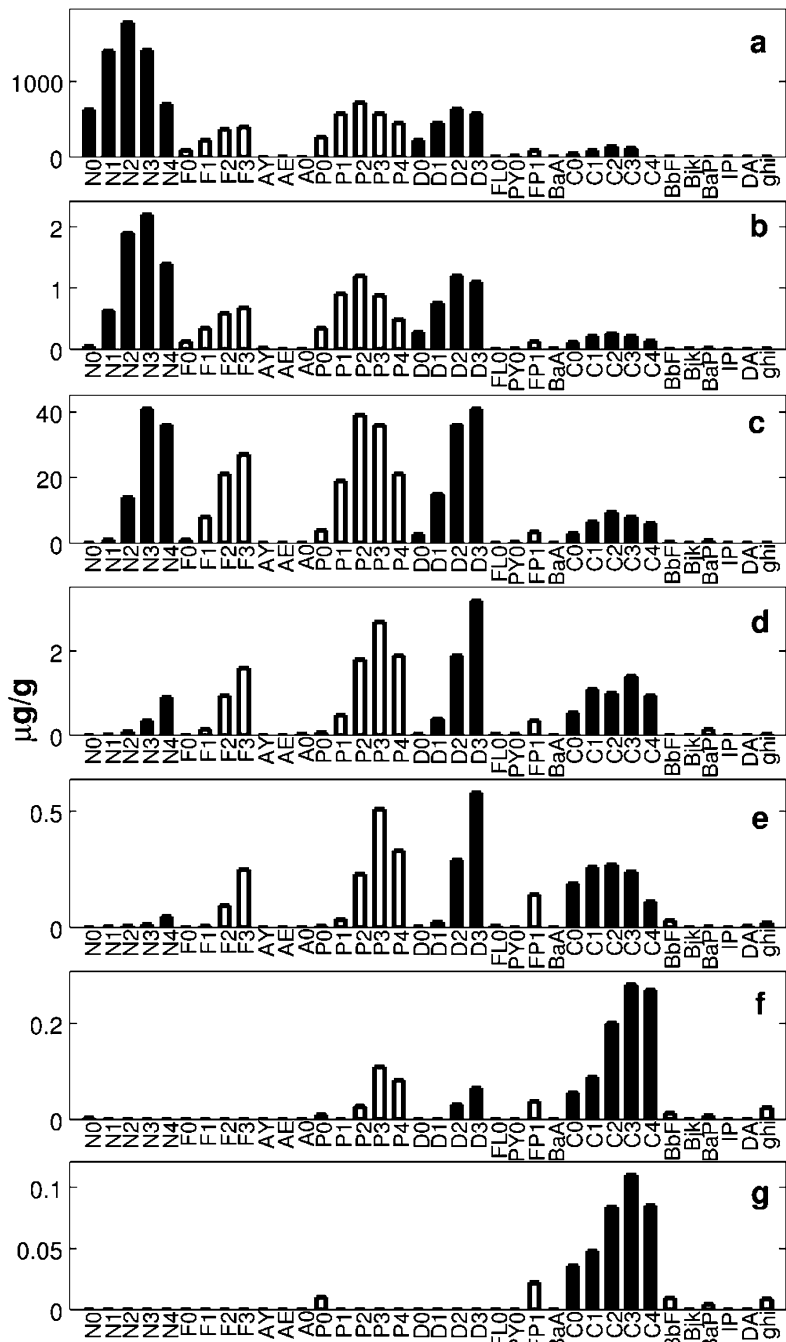
Distilling crude oil does not produce significant amounts of new PAHs in the crude fractions (Stout et al. 2001b). As a result, all refined petroleum products mainly contain PAHs that were present in the original crude oil. Nevertheless, fractionation among refined products (Fig. 2), and different crude oil feedstocks, make the PAH compositions of the refined crude products distinguishable (Stout et al. 2001b; Wang and Fingas 2003). Lighter products, such as jet fuel, tend to contain the more volatile LMW PAHs (e.g., phenanthrene). In crude and heavier fractions (higher distillation temperature), the higher MW PAHs become more abundant (Fig. 2; and note boiling points and vapor pressures of the PAHs in Table 2). For example, because methylphenanthrene isomers all boil in the same temperature range, they pass unchanged from the crude oil feedstock into a straight-run distillate (Stout and Wang 2007). Nevertheless, during the refining process, alkylated chrysenes are removed from diesel (Bence et al. 1996). Other heavily alkylated three- and four-ringed homologues are impoverished in fuel #2 PAH distributions (Figs. S3 vs. S5, Supporting Material). Similarly, the abundances and distributions of sulfur-bearing compounds, such as dibenzothiophenes, are altered during hydrodesulfurization processing of crude oil or middle distillate blending stocks (Page et al. 2006; Stout et al. 2006).

Oil degradation processes, including evaporation, dissolution, and microbial oxidation, are controlled by factors such as oil type, environmental conditions and microbiological activity (Short et al. 2007; Sicre et al. 1987; Wang et al. 1999a). The petrogenic PAHs degrade at much faster rates than pyrogenic ones, because the former are more bioavailable and associate less with carbon particles after their release, e.g., oil spills, discharges (Gogou et al. 2000; Zakaria et al. 2002). Figure 3 shows the PAH fingerprint of the spilled Exxon Valdez crude (EVC) at different states of degradation (Burns et al. 1997). The weathering largely resulted from evaporation and dissolution, which first impacted the more volatile and soluble LMW compounds (Hostettler et al. 2007; Table 2; Wang et al. 1999a).

Evaporation of the PAHs after their incorporation into sediments is not a significant process (Stout et al. 2001b), but the evaporation of PAHs before they associate with sediments or particles (e.g., oil spills) is the most important short-term (hours–days) weathering factor (Wang and Fingas 2003). The degree of loss from evaporation depends on the kind of petroleum product involved. Light products containing light PAHs evaporate readily, whereas heavier ones lose as little as 5–10% of their total volume (Philp 2007; Wang and Fingas 2003). Thereafter a PAH0 < PAH1 < PAH2 < PAH3 profile emerges for each alkylated PAH family (Iqbal et al. 2008; Stout 2007), starting from the LMW PAHs (Fig. 3c–g).

Dissolution depends mainly on the structure of the PAHs and decreases as the ring number and alkylation level of the PAHs increases, although exceptions exist (e.g., chrysene is less soluble than its methyl and dimethyl homologues) (Stout et al. 2001b). Furthermore, the linear PAHs are less soluble than their angular equivalents (anthracene is less soluble than phenanthrene) (Stout et al. 2001b; Wang and Fingas 2003). As dissolution proceeds, biodegradation may begin to affect the distribution of individual compounds. The biodegradation rate depends on the nature of the spill and environment ( $O_2$ , pH, microbial populations, etc.) into which the oil is spilled (Philp 2007; Stout et al. 2002); biodegradation is slower and less predictable than abiotic degradation. Biodegradation can even alter the distribution of PAHs within a homologue category, because individual isomers have different susceptibilities to microbial activity (Wang et al. 1998, 1999a, 2004). Utilizing a biodegradation index for oils has been proposed to assist in evaluating their potential for biodegradation in the lab (Christensen et al. 2004; Wang et al. 1998, 2004). It is generally accepted that PAH biodegradation decreases concomitantly with increasing PAH ring numbers and alkylation (Stout et al. 2001b).

Further degradation (Fig. 3c–g) leads to the enhancement of chrysenes relative to other PAH series, and to a significant decrease in the relative ratios of the sum of naphthalenes, phenanthrenes, dibenzothiophenes, and fluorenes, to chrysenes (most stable) (Wang et al. 1998). In Fig. 3, there are two distinct and apparent features of PAH degradation. The first is the more rapid depletion of the less alkylated homologues, together with faster degradation of the parent PAH. The second is the enhancement of the more alkylated homologues at certain degrees of degradation, not only relative to the less alkylated homologues, but also in absolute terms.



**Fig. 3** Weathering process of spilled Exxon Valdez crude (EVC) spill. (a) fresh EVC, (b) very lightly weathered EVC, (c) lightly weathered EVC, (d) moderately weathered EVC, (e) heavily weathered EVC, (f) very heavily weathered EVC, and, (g) extremely weathered EVC. See Table 1 for PAH abbreviations. Drawn using data from Burns et al. (1997)



The rate of petrogenic PAH degradation decreases with time and as the number of rings increases, i.e., naphthalenes > fluorenes > phenanthrenes  $\approx$  dibenzothiophenes  $\approx$  fluoranthenes/pyrenes > chrysenes (e.g., Hegazi and Andersson 2007; Page et al. 1996; Short et al. 2007). Hence, the relative ratios of phenanthrenes, dibenzothiophenes, fluorenes and naphthalenes remain very consistent as the weathering percentages increase, which makes them useful for source identification (Hegazi and Andersson 2007). Nevertheless, oil degradation is a very complex process and although different first-rate kinetic models have been developed, source apportionment of petroleum products is best dealt with case by case (Wang and Fingas 2003).

Crude oil contains significant amounts of PAHs: from 0.2% to more than 7% total PAHs (Zakaria et al. 2002). For certain crudes, only a small portion of the total PAHs are priority pollutant PAHs (Stout et al. 2007). The PAHs in crude oils decrease in concentration as their molecular weight increases (Stout 2007; Stout et al. 2001b). The HMW PAHs that may be non-detectable, or only present in minute quantities include acenaphthylene (AY), anthracene (A0), fluoranthene (FL0), pyrene (PY0), benzo[ghi]perylene (*ghi*), indeno[1,2,3-*cd*]pyrene (IP), benzo[*k*]fluoranthene (BkF), benzo[*b*]fluoranthene (BbF), perylene (PER), dibenz[*ah*]anthracene (DA), benzo[*e*]pyrene (BeP), benzo[*a*]pyrene (BaP) (Fig. 2 and Figs. S1–S4, Supporting Material). Many crude oils are dominated by alkyl naphthalenes (Figs. S2–S4, Supporting Material). Stout et al. (2007) observed variable environmental weathering for some crudes after their release. In most instances, weathering resulted in the loss of hydrocarbons that had boiling points below that of *n*-eicosane (including naphthalene and alkylated naphthalenes). Weathered crude tends to contain more PAHs than does unweathered crude (Stout et al. 2001b).

Diesel PAHs (Figs. S5–S7 and S9, Supporting Material) are largely composed of two- and three-ringed PAHs and their alkylated homologues (Douglas et al. 2007a; Wang et al. 2001). Diesels contain only extremely small amounts of anthracenes (A0) and HMW PAHs (four to six rings such as indeno[1,2,3-*cd*]pyrene, dibenz[*ah*]anthracene and benzo[*ghi*]perylene), because most of these are removed during refining (Wang et al. 2001). Of the *five target alkylated PAH series* of diesel, the most abundant (>55%) is alkylated naphthalene and the least abundant (<0.02%) is chrysene; thus, the absence of chrysene can be used to identify diesel or diesel soot (Wang et al. 1999a, 2001). Conversely, the presence of chrysenes or HMW PAHs possibly excludes diesel or its soot as a main PAH source (Burns et al. 1997).

Figures S8 and S10 (Supporting Material) show that naphthalene is abundant in jet B fuel (99% of total PAHs is naphthalenes), gasoline (97% of EPA priority PAHs) and diesel No.2 (86% naphthalenes, 5% phenanthrenic content and no chrysenes). In contrast, in the bunker C diesel mixture, the alkylphenanthrenes account for 35% of PAHs and chrysenes for 18% (Karlsson and Viklander 2008; Wang and Fingas 2003; Wang et al. 1999a). In the orimulsion oil (Fig. S11, Supporting Material), the phenanthrenic and dibenzothiophenic content is much higher (38% and 22% of total PAHs respectively) (Wang and Fingas 2003). PAHs having a MW greater than that of pyrene are hardly present in light distillates such as jet B fuel or gasoline, although in heavier products such as bunker C diesel and orimulsion oil they may be present in significant quantities (Figs. S5–S11, Supporting Material).

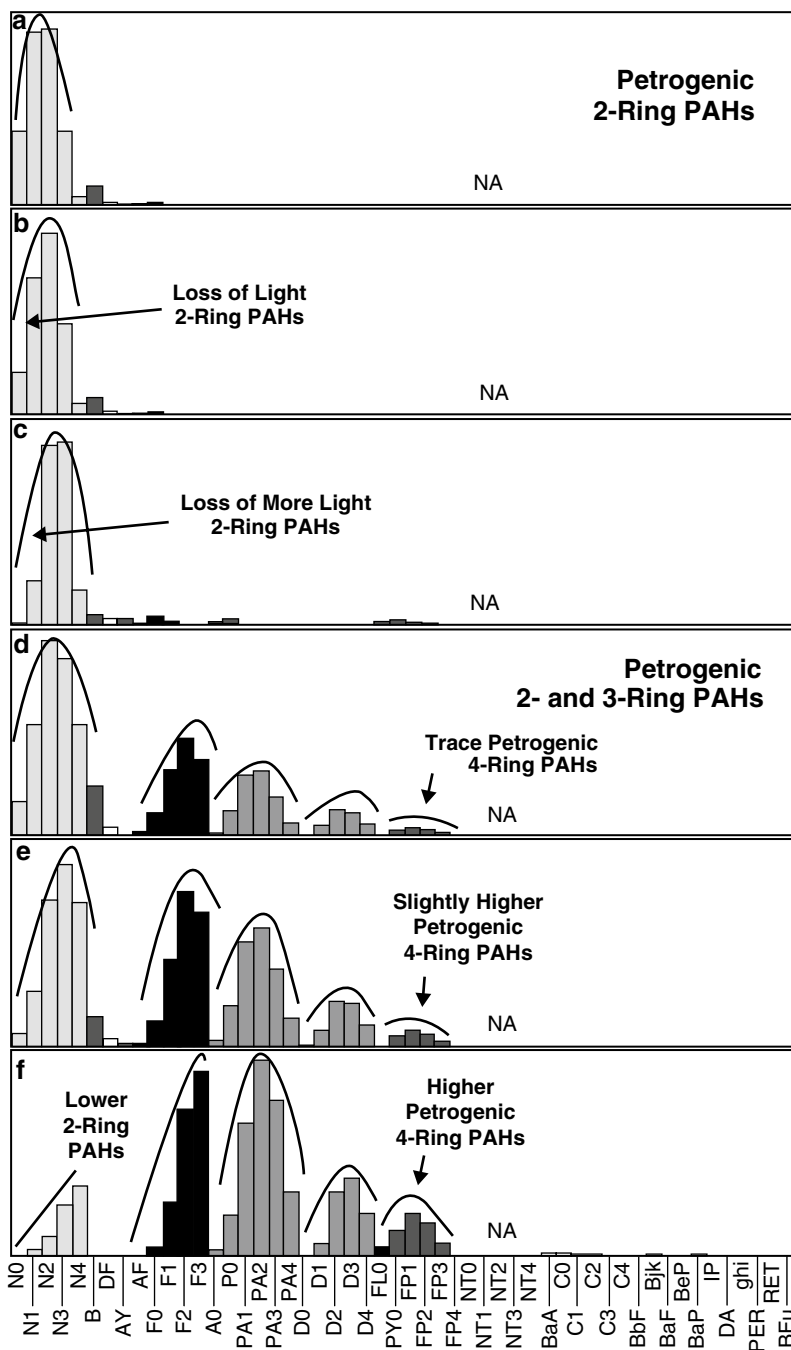
For this reason, it is suggested that highly alkylated PAHs (e.g., P4 or P3–phenanthrenes) be selected and used for identifying the source of PAHs in distilled oil products such as diesel and jet fuel samples (Wang et al. 1999a).

Some coal PAHs have been characterized, as occasionally has their contribution to sediment contamination (Achten and Hofmann 2009; Boehm et al. 2001; Dzou et al. 1995; Peters et al. 2005; Radke et al. 1982; Stout and Emsbo-Mattingly 2008). Lower rank coals (lignite and sub-bituminous coal) may contain significant amounts of perylene. Dibenzothiophenes may also be abundant in coals (Stark et al. 2003). Coal PAHs are generally not bioavailable and the concentrations at which they exist are below risk limits. However, they are of practical interest in forensic studies, and for understanding potential sources of PAHs (Stout and Emsbo-Mattingly 2008).

The PAH distribution patterns in coals seem to be a function of coal rank (Fig. S27, Supporting Material; Radke et al. 1982; Stout and Emsbo-Mattingly 2008). The higher the coal rank, the more dominant are the LMW compounds over the HMW ones (petrogenic characteristic). However, the homologous series of phenanthrenes (minus retene), fluoranthenes and chrysenes show a bell-shaped PAH profile in low rank coals (typical of petrogenic PAHs). In higher coal ranks, this bell-shaped profile shifts to a pyrogenic-like skewed pattern that is dominated by parent PAHs (Fig. S27, Supporting Material).

Leakage, spillage and dumping of fresh and used lubricating oils (Fig. 1e; Figs. S12–S15, Supporting Material) are major sources of PAHs in the aquatic environment of Malaysia (Zakaria et al. 2002). “Fresh” lubricants are severely depleted of HMW PAHs and contain small amounts of LMW PAHs, such as dibenzothiophenes (Denton 2006; Sicre et al. 1987; Wang et al. 2004; Zakaria et al. 2002). In contrast, the PAH content of used lubricating oil is three orders of magnitude higher than that of fresh lubricating oil. The “extra” PAHs are derived both from the accumulation of PAHs formed in the engine combustion chamber (Pyrogenic HMW compounds) and from the incorporation of petrogenic PAHs from unburned fuel (gasoline or diesel alkyl-homologues such as P1) into the lubricating oil (Boonyatumanond et al. 2007; Douglas et al. 2007a; Zakaria et al. 2002). For example, methylphenanthrenes are less abundant in diesel than in used lubricating oils (Boonyatumanond et al. 2007). Thus, lubricants used in fuel combustion chambers might be classified as a mixed source of PAHs that show an enhanced pyrogenic profile (Fig. 1e and Figs. S12–S15, Supporting Material).

A significant amount of liquid fuel used in vehicles or in other combustion processes may be unburned (up to 1.2%), and therefore may contain the initial petrogenic fingerprint (Fig. 4, Figs. S16, S17, Supporting Material) of the fuel as vapor (Bucheli et al. 2004; Lehnendorff and Schwark 2009; Simoneit 1985; Wang et al. 1999b; Williams et al. 1986; Zeng and Vista 1997). For example, automobile and boat engine exhausts contain both petroleum residues and incomplete combustion products (Zeng and Vista 1997). In Tokyo, Japan, alkyl PAHs and the street dust of heavily traveled roads contained a greater abundance of alkyldibenzothiophenes than the street dust from roads in residential areas (Takada et al. 1990). Diesel fuel contributes more alkylated, sulfur and three-ringed PAHs (petrogenic fingerprint) to the atmosphere than does gasoline (Hwang et al. 2003; Lehnendorff and Schwark 2009).



**Fig. 4** PAH profiles during combustion of fossil fuels. (a) kerosene, (b) kerosene combusted 50%, (c) kerosene combustion residue, (d) middle petroleum distillate (diesel), (e) diesel combusted 50%, (f) diesel combustion residue. NA: not analyzed. See Table 1 for PAH abbreviations. Adapted from Douglas et al. (2007a), with permission, © Elsevier Academic Press

## 2.2 Pyrogenic

Pyrogenic substances are defined as organic substances produced from oxygen-depleted, high-temperature combustion of fossil fuels and biomass (e.g., incomplete combustion, pyrolysis, cracking, and destructive distillation) (Saber et al. 2006). Pyrogenic PAHs are released in the form of exhaust and solid residues, and are largely prevalent in aquatic environments (De Luca et al. 2004; Zakaria et al. 2002). Only in a limited number of locations do petrogenic PAHs dominate over pyrogenic ones (Guo et al. 2007; He and Balasubramanian 2010; Wickramasinghe et al. 2011; Zakaria et al. 2002). The HMW PAHs of pyrolytic origin reach aquatic environments by direct atmospheric deposition or via contaminated soil (Budzinski et al. 1997; Morillo et al. 2008b). LMW pyrogenic PAHs are mainly introduced to aquatic environments by rain washout (Ollivon et al. 1999).

Hailwood et al. (2001) list the main industrial processes that produce significant amounts of PAHs. Power stations may contribute less than 5% to the PAH emissions of a large city (Masclat et al. 1987). It is the mobile PAH emission sources that have sharply increased in the environment during recent decades (Hwang et al. 2003). The main pyrogenic sources in urban waterways include fuel combustion products, and discharges from aluminum smelters and manufacturing gas plant (MGP) sites (Stout et al. 2001b). Sources such as municipal and industrial waste discharges, and runoff (e.g., from farms and farmland) contain a mixture of pyrogenic, petrogenic, and natural PAHs (Van Metre and Mahler 2010; Zeng and Vista 1997). The distribution of PAHs from such sources is similar to that in pyrogenic sources (Stout et al. 2001b).

In pyrogenic PAH patterns, unsubstituted compounds predominate over their alkylated homologues. As the alkylation level increases, the PAH homologues become less abundant (i.e., a skewed pattern), whereas the HMW four- to six-ringed PAHs are more abundant than LMW two- to three-ringed PAHs (e.g., Boll et al. 2008; Ou et al. 2004; Page et al. 2006; Stout 2007; Stout et al. 2004; Wang et al. 1999a). Furthermore, the abundance of alkyl PAHs relative to parent PAHs, and also the abundance of LMW PAHs relative to HMW ones in combustion products, decrease with increasing combustion temperature (Laflamme and Hites 1978; Sporstol et al. 1983; Takada et al. 1990; Tobiszewski and Namiesnik 2012; Zeng and Vista 1997). Some researchers (Budzinski et al. 1997; Sicre et al. 1987) have noted that catacondensed PAHs (wherein no more than two rings have a carbon atom in common) are abundant in pyrolytic PAHs.

Combusting two petrogenic products (Fig. 4—kerosene and diesel) in an open flame does not create a significant amount of important five-ringed PAHs (Douglas et al. 2007a). Open-flame combustion significantly alters the distribution of naphthalene (N0) and its homologues. Simultaneously, the relative abundance of phenanthrene, fluorene, pyrene and their alkylated homologues increases. Combustion in a closed system (such as diesel engines), however, characteristically creates the pyrogenic signature of LMW and HMW PAHs and their alkylated homologues (Douglas et al. 2007a).

Wang et al. (1999b) found that emissions, residues, and soots of combusted PAH-containing liquid fuels (e.g., diesel, crude) were likely to inherit the pyrogenic

bell-shaped distribution of volatilized LMW PAHs (2-4 rings). In such cases, the destruction efficiency of PAHs decreased as the MW increased. The newly diesel-combustion-generated PAHs (mainly HMW) were in the range of 0.5–1.5‰ of the destroyed/combusted PAHs (mainly LMW) (Fig. S16, Supporting Material; Wang et al. 1999b).

The most abundant pyrogenic PAHs are fluoranthene, pyrene, and, to a lesser extent, phenanthrene (Page et al. 1999). Predominance of P0, FL0 and PY0 indicates the pyrolytic origin of the contamination (Morillo et al. 2008a). Like phenanthrene, anthracene is also common to pyrogenic sources (De Luca et al. 2004; Gogou et al. 2000). In sediments, absence of IP has been interpreted as the absence of pyrogenic PAHs (De Luca et al. 2004). Moreover, it has been shown that the use of HMW PAHs (e.g., MW=252, benzo[*k*]fluoranthene, benzo[*b*]fluoranthene, benzo[*a*]pyrene, benzo[*e*]pyrene, benzo[*j*]fluoranthene, and perylene) is adequate to discriminate between different high-temperature processes, e.g., carbonization and coking in manufacturing gas plants, and combustion in motor vehicle engines (Boll et al. 2008; Costa and Sauer 2005; Costa et al. 2004; Ollivon et al. 1999; Stout and Graan 2010).

The HMW pyrogenic PAHs emitted at high temperatures as gases condense on particulates when cooled (Tobiszewski and Namiesnik 2012 and references therein). Accordingly, LMW pyrogenics are more abundant in the gaseous phase.

The pyrogenic PAHs (especially parent PAHs) associate with small soot-rich particles (Sicre et al. 1987; Yunker et al. 2002). As a result, pyrogenic PAHs are more often associated with sediments and become more resistant to microbial degradation than PAHs of petrogenic origin (De Luca et al. 2004). Nevertheless, weathering also causes pyrogenic products to increasingly be dominated by four- to six-ringed PAHs, producing a pattern very similar to what appears in urban runoff (see below), rendering it more difficult to identify the source (Stout et al. 2003).

The pyrogenic PAHs are subject to differential photodegradation (first order kinetics). The isomer pairs of phenanthrene-anthracene, fluoranthene-pyrene and indeno[1,2,3-*cd*]pyrene-benzo[*ghi*]perylene degrade photolytically at about the same rate in the atmosphere (Behymer and Hites 1988; Yunker et al. 2002). By contrast, BaP is photolyzed in the atmosphere at much faster rates than are its isomers (Behymer and Hites 1988; Gogou et al. 2000; Sicre et al. 1987; Yunker et al. 2002). On the other hand, Brenner et al. (2002) used BaP as a normalization constant to calculate PAH losses in a weathered creosote site. Despite not being listed as a priority pollutant (Table 2), benzo[*e*]pyrene (BeP) has been included in many studies (especially of iron and steel plant emissions) because of its chemical stability in the atmosphere and the additional information it can provide (Daisey et al. 1986; Ollivon et al. 1999; Soclo et al. 2000; Yang et al. 2002). PAH photodegradation also takes place in other environmental matrices (e.g., water), which preferentially protect certain isomers (Bertilsson and Widenfalk 2002; Tobiszewski and Namiesnik 2012).

Motor vehicles are a major source of potential carcinogenic HMW PAHs (such as benzo[*a*]pyrene, benz[*a*]anthracene, and benzo[*b*]fluoranthene), especially in highly populated areas (Dickhut et al. 2000; Simoneit 1985). Marr et al. (1999) reported unburned fuel, lubricating oil, and pyrosynthesis as possible sources for PAHs from

motor vehicle exhausts. Indeno[1,2,3-*cd*]pyrene (IP) and benzo[*ghi*]perylene (*ghi*) are indicators (e.g., correlate with the total PAHs) of combustion sources and are typical products of motor vehicle exhausts – although these HMW PAHs are not transported far from their source (Boll et al. 2008; Larsen and Baker 2003; Ollivon et al. 1999; Yunker et al. 2002). Ollivon et al. (1999) have suggested using benzo[*ghi*]perylene and pyrene as tracers of vehicle emissions in river waters. Benz[*a*]anthracene and chrysene are also considered to be automobile markers when other petroleum sources are excluded (Morillo et al. 2008b; Yunker et al. 2002). Similarly, particulate phase coronene in city centers may hypothetically be exclusively traffic-related (Larsen and Baker 2003), especially at locations far from main point sources of PAH emission (Bucheli et al. 2004 and references therein). Unlike the higher MW alkylated PAHs (i.e., alkyl-fluoranthenes, -benz[*a*]anthracenes, -chrysenes, -pyrenes), the alkylated LMW PAHs (i.e., alkyl phenanthrenes, alkyl anthracenes and alkyl naphthalenes) are usually present in higher proportions than their parent PAHs in diesel combustion soots and burn residues (Wang et al. 1999b). The bell-shaped profile of LMW PAHs in diesel combustion products accentuates the deviation from the classical pyrogenic fingerprint, which prevails in higher MW PAHs (Fig. S17, Supporting Material ; Sect. 2.1; Wang et al. 1999b; Yunker et al. 2002). Higher MW or sulfur PAHs such as coronene, BkF or benzo[*b*]naphtho[2,1-*d*]thiophene and dibenzothiophenes have been proposed as markers of diesel emissions (Dobbins et al. 2006; Larsen and Baker 2003; Marvin et al. 2000; Riddle et al. 2007; Wang et al. 1999b).

Compared with gasoline exhausts, diesel exhausts are said to be enriched in phenanthrene, fluoranthene, pyrene and chrysene (Larsen and Baker 2003; Masclat et al. 1986). Gasoline combustion produces patterns dominated by naphthalene and HMW PAHs, such as benzo[*a*]pyrene and dibenz[*ah*]anthracene (Larsen and Baker 2003; Marr et al. 1999; Miguel et al. 1998; Valle et al. 2007). Instead, cyclopenta[*cd*]pyrene and benzo[*ghi*]perylene have been proposed as markers for gasoline-fuel combustion (Dzepina et al. 2007; Larsen and Baker 2003).

Motorcycles contribute significant amounts of PAHs to atmospheric environments in some locations, such as Southeast Asia. In other parts of the world (e.g., U.S.A. and Canada), motorcycle contribution to air PAHs is insignificant compared to other traffic-related PAH emissions (Chien and Huang 2010; Oanh et al. 2013; Valle et al. 2007). Two-stroke motorcycle exhausts have been reported to contain higher amount of PAHs than four stroke or fuel injection motorcycles (Boonyatumanond et al. 2007). Different factors such as motorcycle speed, engine type and age affect the PAH patterns emitted (Chien and Huang 2010). Exhausts from motor vehicles are transported far from point sources and contribute to diffuse background levels.

The PAH concentrations decrease as the distance from traffic sources increases (Boll et al. 2008). The typical gray particle color of automobile emissions makes the particle-associated PAHs vulnerable to photodegradation (Dickhut et al. 2000 and references therein). Furthermore, automotive emissions of PAHs depend on the fuel and vehicle type and local traffic conditions (e.g., Geller et al. 2006; Lim et al. 2007; Riddle et al. 2007).

Biomass combustion occurs at relatively low temperatures and is a significant source of pyrogenic PAHs in nearshore subtidal sediments (Barra et al. 2007; Gogou et al. 2000; Oanh et al. 1999; Page et al. 1999; Tobiszewski and Namiesnik 2012). However, aerosol from wheat and rice straw burning is enriched in HMW PAHs (Ravindra et al. 2008 and references therein). Stark et al. (2003) identified three- to six-ringed parent PAH compounds as the major PAHs in fireplace soots (see also Figs. S18–S20, Supporting Material); alkylated three- and four-ringed compounds were less abundant. Stark et al. (2003) noted that when soots have high total PAH concentrations, they also contain larger amounts of three- and four-ringed parent compounds. In contrast, soots with lower total PAH concentrations show a relative increase in the amounts of five- and six-ringed PAHs.

Guillon et al. (2013) identified fluoranthene and pyrene as dominant parent PAH compounds in particulates from wood combustion, whereas the dominant parent HMW PAHs are benz[*a*]anthracene and chrysene, followed by benzo[*a*]pyrene. Cyclopenta[*a*]phenanthrene, phenylnaphthalene and either cyclopenta[*cd*]pyrene or benzo[*ghi*]fluoranthene are present in fireplace soots (O'Malley et al. 1997; Stark et al. 2003). Other HMW PAHs such as benzo[*ghi*]perylene are also produced by biomass combustion (Dzepina et al. 2007).

Under certain conditions (e.g., steady combustion and forest fires), and in contrast to HMW parent PAHs, alkylated naphthalenes, phenanthrenes, and even chrysenes may be ubiquitous biomass combustion products (Figs. S18–S20, Supporting Material; Wang and Fingas 2003). Furthermore, three-ringed alkyl PAHs such as 1-methylphenanthrene, 1,7-dimethylphenanthrene (also known as pimanthrene) and retene (1-methyl-7-isopropyl phenanthrene) are produced from abietic and pimic acid—both present in pine wood resin—and can be used as markers for softwood combustion (Benner et al. 1995; Bucheli et al. 2004; Gogou et al. 2000; Sicre et al. 1987; Yan et al. 2005; Yunker et al. 2002). The 2,6-dimethylphenanthrene isomer is present at comparable concentrations in emissions from fossil fuel and residential wood combustion (Benner et al. 1995).

The PAHs derived from coal combustion are a concern in some regions of the world (Chen et al. 2005). Fluoranthene, pyrene, phenanthrene and anthracene dominate in coal combustion profiles (Larsen and Baker 2003 and references therein). Chrysene and benzo[*k*]fluoranthene dominance has also been suggested as an indicator of coal combustion (Ravindra et al. 2008 and references therein). Dibenzothiophenes are also abundant in coal emission condensates (Marvin et al. 2000; Sicre et al. 1987) and industrial coal emissions, and escape from most modern SO<sub>x</sub> removal processes (Lehndorff and Schwark 2009).

Coal combustion patterns sometimes deviate from the general pyrogenic fingerprint of PAH homologues (i.e., maxima at the parent PAH), and can show maxima for the methyl or dimethyl homologues of phenanthrene and anthracene (Oros and Simoneit 2000; Yunker et al. 2002). Similarly, four-ringed methyl PAHs methylfluoranthene or methylpyrene may also show maxima in coal combustion PAH patterns (Oros and Simoneit 2000; Yunker et al. 2002). PAH emissions from coal burning depend not only on the coal rank, but also on the temperature of combustion.

Lower coal combustion temperatures (e.g., domestic stoves) yield more PAHs than do high-temperature processes, such as in coal power plants (Chen et al. 2005; Oros and Simoneit 2000). Therefore, in addition to coal content, the combustor is crucial when calculating coal PAH emissions.

Much attention has been paid to increased creosote PAH contamination in sediments, particularly in the U.S. (Brenner et al. 2002; Stout et al. 2001a, 2003). Coal tar, creosote and coal tar pitch contain very large quantities of pyrogenic PAHs (>10%). As a result, small amounts of these materials greatly influence the distribution of PAHs in sediments (Stout et al. 2001b). Two- and three-ringed PAHs are abundant in creosote. For example, parent PAHs, such as naphthalene (NO), acenaphthene (AE), fluorene (FO), phenanthrene (PO), fluoranthene (FLO) and pyrene (PYO) (see also Fig. S28a, Supporting Material), dominate over four- to six-ringed PAHs (Stout et al. 2001a and references therein).

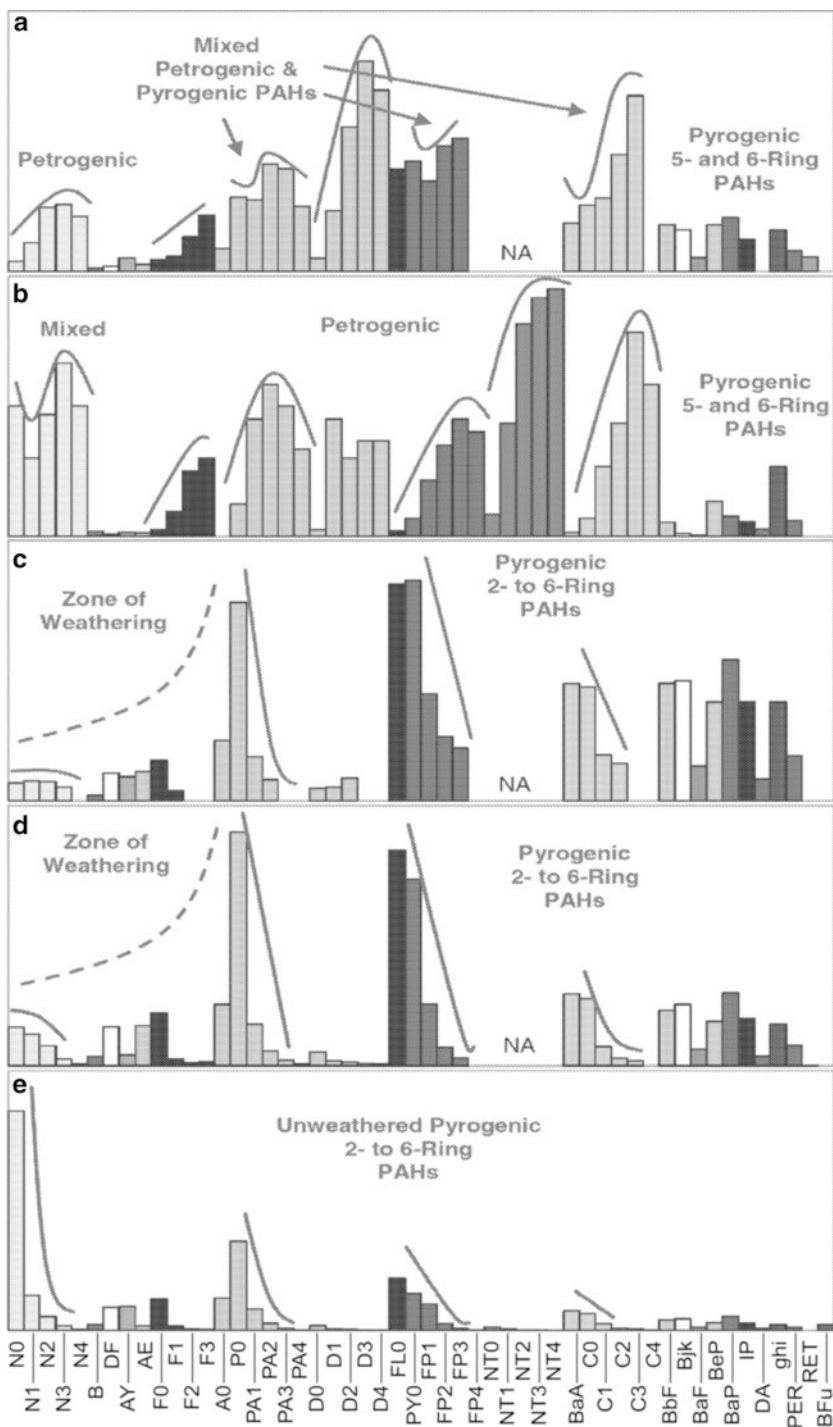
Creosote degradation (Fig. S28b–d, Supporting Material) results in the loss of LMW PAHs and a PAH signature dominated by four to six rings (increasing abundance of benz[*a*]anthracenes, chrysenes, benzofluoranthenes, benzopyrenes) (Brenner et al. 2002; Stout et al. 2003). This fingerprint is hardly distinguishable from the urban background, which contains mainly pyrolytic sources. Therefore, creosote is classified as a pyrogenic PAH source (Stout et al. 2001b).

Industrial activities such as coke and steel production have released large quantities of not only pyrogenic PAHs (Orecchio 2010; Saber et al. 2005), but also of LMW PAHs such as naphthalene (Fig. S31), and all of these PAHs eventually end up in soil or sediment (Karlsson and Viklander 2008; Morillo et al. 2008b). Distillation of tars (e.g., coal tar) alters the pyrogenic PAH composition (depending on the PAH boiling point), leading to mixtures enriched in LMW PAHs, as occurs with creosote (Neff et al. 2005). Coal tar PAHs are present in pavements and asphalt, and result from high-temperature baking of hard coal in a reducing atmosphere to produce coke and manufactured gas. These sources (i.e., those rich in PAHs such as benz[*a*]anthracene, chrysene, indeno[1,2,3-*cd*]pyrene and benzo[*ghi*]perylene), show a characteristic pyrogenic profile (Fig. 5e), and are likely to be washed out by rain and end up in sediments (Douglas et al. 2007a; Neff et al. 2005; Yunker et al. 2002).

PAH patterns in paving materials show distributions of both LMW PAHs (petrogenic) and HMW PAHs (pyrogenic) (Fig. 5). Such patterns reflect the blending that occurs with different types of heavy petroleum products (Fig. 1c, d), paving materials (Fig. 5a) and coal tar (Fig. 5e) (Douglas et al. 2007a). In general, PAHs heavier than fluoranthene or pyrene (and to a lesser extent anthracene, phenanthrene, and acenaphthene) are dominant in such materials, although coal tar pitch or tar residues may be enriched in naphthalenes, phenanthrenes, and possibly dibenzothiophenes (Figs. S29, S30; Supporting Material; Saber et al. 2006). The HMW PAH tar fingerprint is minimally changed, even after degradation (Uhler and Emsbo-Mattingly 2006), making it possible to use HMW PAHs to characterize coal tars (Costa et al. 2004).

Street dust is transported in sediments, rivers, wastewater treatment plants and estuaries via street runoff, which is an important source and pathway of how PAHs reach sediment, particularly in regions that have high and intense rainfall events





**Fig. 5** Mixed PAH profiles. **(a)** hot patch (paving material), **(b)** modern (2005) roadway paving, **(c, d)** older types of roadway paving, **(e)** coal tar oil. *NA*: not analyzed. See Table 1 for PAH abbreviations. Adapted from Douglas et al. (2007a), with permission, © Elsevier Academic Press

(Lorenzi et al. 2011; Ollivon et al. 1999; Takada et al. 1990). Street dust is a mixture of weathered material from street surfaces, automobile exhaust, asphalt, lubricating oils, gasoline, diesel fuel, tire particles, atmospheric fallout, and soil (Breault et al. 2005; Takada et al. 1990). Figures S21–S26 (Supporting Material) show different fingerprints of sources that contribute to street dust.

Depending on the local traffic conditions, asphalt and tire particles contribute variable PAH amounts to street dusts (Boonyatumanond et al. 2007; Takada et al. 1990; Zakaria et al. 2002). Ou et al. (2004) reported only a small amount of PAHs in asphalt (0.7%). It is known that tire particles can contribute significant quantities of phenanthrenes, pyrene, and benzo[*ghi*]perylene to street dust (Figs. S22 and S24, Supporting Material; Zakaria et al. 2002). Chen et al. (2006) reported that indeno[1,2,3-*cd*]pyrene, dibenz[*ah*]anthracene and benzo[*a*]pyrene are the most dominant PAHs (>90% of total) in tire powder. In other cases, PAHs in street dust result mainly from automobile exhaust, although domestic heating emissions contribute to PAH releases as well (Takada et al. 1990; Zakaria et al. 2002).

The primary components of street dust are reported to be parent PAHs ranging from phenanthrene (three aromatic rings) to benzo[*ghi*]perylene (six aromatic rings) and in particular, the three- and four-ringed PAHs (i.e., phenanthrene, fluoranthene, pyrene and benzo[*ghi*]perylene) (Ollivon et al. 1999; Stark et al. 2003). Lower (two-ringed) and higher MW PAHs may also be present, and so may a range of parent, methylated, and substituted compounds (such as biphenyls and dibenzothiophenes) (Stark et al. 2003). If lower MW PAHs (such as dimethylphenanthrenes present in tire wear particles) are mixed with street dust, they will selectively dissolve in runoff water and will reach sediment (Mandalakis et al. 2004; Takada et al. 1990). The impact of street dust PAHs on aquatic environments can be quantified by determining the PAH contents and profiles in runoff samples from street surfaces (Karlsson and Viklander 2008; Takada et al. 1990).

For decades, rainfall from storm events have washed PAHs from numerous non-point and point sources (e.g., urban dust/soot, used lubricants, petroleum products) into stormwater outfalls along urban waterways (Battelle Memorial Institute et al. 2003). This mix of point and non-point pollution sources usually dominates a whole area with a unique, or hardly varying fingerprint (Fig. S32a, b, Supporting Material), which is not representative of any specific PAH source, and is termed “background concentration” (Costa and Sauer 2005; Page et al. 1999; Stout et al. 2003, 2004). PAH background concentrations are highly variable and site-dependent, owing to the variable effects of dilution and transport processes in the aquatic environment (Battelle Memorial Institute et al. 2003).

“Anthropogenic background” sediment concentrations in both urban and remote locations have long exceeded the low concentrations of naturally occurring background PAHs (e.g., from forest fires, natural oil seeps, etc.) (Fig. S32a, b, Supporting Material; Page et al. 1996; Saber et al. 2005; Stout et al. 2003, 2006). Stout et al. (2004) suggested that sediments containing significantly more than 20 µg/g dry weight of any of the EPA 16 Priority Pollutant PAHs (or more than 30 µg/g of 43 parent and alkylated PAHs) is suspect for containing PAHs that are not entirely

attributable to urban background, unless site- or region-specific survey data support a different urban background concentration profile.

As with street dust, the most abundant of the 16 parent PAHs in storm water (and in urban background) are fluoranthene and pyrene, and to a lesser extent, phenanthrene and anthracene (Battelle Memorial Institute et al. 2003; Karlsson and Viklander 2008). Urban background is generally enriched in four- to six-ringed PAHs, and depleted in LMW PAHs (Battelle Memorial Institute et al. 2003). In urban runoff, the pyrogenic homologues of fluoranthene and chrysene, and to a lesser extent those of phenanthrene and anthracene exhibit the sloping pyrogenic pattern. Therefore, urban background reflects pyrogenic characteristics that are distinct from those of other pyrogenic sources. Nevertheless, weathering may alter a pyrogenic fingerprint (preferential elimination of LMW and parent PAHs over HMW and alkylated PAHs) to resemble that of urban background (Battelle Memorial Institute et al. 2003).

### 2.3 *Biogenic/Diagenetic*

Diagenetic PAHs are produced during the slow transformation of organic materials in lake sediments, whereas biogenic PAHs are produced by plants, algae/phytoplankton and microorganisms (Venkatesan 1988). Perylene (PER) is produced under several conditions: by diagenesis and biosynthesis from terrestrial precursors (e.g., perylenequinone pigment) or other organic matter; under anoxic conditions; and in soil and subtidal, marine and freshwater sediments (e.g., Boll et al. 2008; Guo et al. 2007; Venkatesan 1988; Zakaria et al. 2002). In the tropics, termite nests may act as a perylene source in soil (Barra et al. 2007; Mandalakis et al. 2004; Wilcke et al. 2002).

If perylene does not correlate with the total organic carbon, then the perylene is likely to have a natural origin (Luo et al. 2008). In such a case, perylene may not yield its source of organic matter, although it can be a useful tracer for water and for depositional conditions (Budzinski et al. 1997). For instance, assuming a biogenic perylene origin, Page et al. (1996) used perylene depth gradients to show lack of vertical mixing.

Other PAHs such as benzo[*b*]fluoranthene (BbF), phenanthrene (P0) and naphthalene (N0) can originate from vascular land plants or termite activity (Bakhtiari et al. 2009; Irwin et al. 1997; Tobiszewski and Namiesnik 2012). Benzo[*a*]pyrene can be biosynthesized by certain bacteria and plants (Peters et al. 2005). Retene (RET) can be produced from the anaerobic microbial degradation of dehydroabietic acid (present in tire particles in urban areas) in soils and sediments (Mandalakis et al. 2004).

Perylene or biogenic-diagenetic PAHs also potentially have anthropogenic sources. PER has been detected in trace amounts after pyrolytic processes (Luo et al. 2008), such as coal pyrolysis in municipal incinerator waste products and automotive emissions (Abrajano et al. 2003; Boll et al. 2008; Gogou et al. 2000).

Retene has other anthropogenic sources, such as fresh oil, diesel, exhaust emissions from heavy-duty diesel fuels, pulp/paper mill effluents, and emissions from coals (Mandalakis et al. 2004; Yan et al. 2005).

### 3 Factors Influencing PAH Distribution in Aquatic Systems

Sediments are sensitive indicators of natural and anthropogenic origin, such as PAH contamination (De Luca et al. 2004; Klamer et al. 1990). Variables such as OC, particle size and depositional environment are important for discovering and characterizing the source, transport and bioavailability of PAHs in sediment (e.g., Dickhut et al. 2000; Morillo et al. 2008b; Soclo et al. 2000; Wang and Fingas 2003).

In the different environmental matrices (atmosphere, water column, oil, sediments), easily degradable LMW PAHs (i.e., two- and three-ringed) are relatively soluble and predominate in the water phase, whereas the more recalcitrant and more lipophilic alkylated and/or HMW PAHs are more often associated with particulate matter, and thus are better protected from degradation (Budzinski et al. 1997; Cailleaud et al. 2007; De Luca et al. 2005; Karlsson and Viklander 2008; Page et al. 1996; Stout et al. 2001a, b). This fact has implications that need to be taken into consideration when dealing with PAH distributions:

- a. It is difficult to distinguish certain weathered pyrogenic sources (e.g., severely weathered coal tar) from urban background, which is also dominated by HMW four- to six-ringed PAHs (Battelle Memorial Institute et al. 2003).
- b. Lack of oxygen (that fosters biodegradation) in deeper sediment layers and also the physical-chemical association of PAHs with the sediment matrix can result in long-term PAH stability (Page et al. 1996, 1999; Short et al. 2007).
- c. Small molecules, such as three-ringed/LMW PAHs, are selectively depleted by physical mixing and tend to be enriched in the fine sand fraction, whereas the larger PAHs (six-ringed) are enriched in the fine silt fraction (Karlsson and Viklander 2008; Mitra et al. 1999). Partitioning of PAHs into different sediment fractions has been reported in the literature (Johnson-Restrepo et al. 2008; Magi et al. 2002; Micic et al. 2011). Sediment particle size affects the oxygenation of sediments, as well (Jeanneau et al. 2008).
- d. Climatic conditions may affect the distribution of PAHs in different environmental compartments, particularly in the atmosphere and consequently may determine what constitutes the final sink. For example, fluctuations in temperature directly affect the particle and vapor phase distributions of retene, a common softwood combustion marker (Benner et al. 1995; Gogou et al. 2000; Stout 2007; Yunker et al. 2002). Accordingly, retene's diagnostic reliability for softwood combustion in aqueous environments has been doubted (Bucheli et al. 2004; Gogou et al. 2000).
- e. The sorption and desorption of PAHs to the organic carbon (OC) content of sediments can be used to interpret the source of PAH contamination (Boehm et al. 2001, 2002; De Luca et al. 2004, 2005; Mitra et al. 1999; Morillo et al. 2008b; Zakaria et al. 2002).

## 4 Analytical Approach for PAH Source Characterization

It is often complicated to define the sources of PAH contamination in waterways and coastal areas that have limited water circulation, particularly where multiple point sources co-occur with persistent non-point sources (i.e., urban areas or areas that have high ambient background levels). In such situations, the potential contributions of all possible point or non-point sources should be considered (De Luca et al. 2004; O'Reilly et al. 2012, 2014; Stout et al. 2003).

The major approaches used in source identification are pattern recognition, spatial and temporal analysis (sources, historic records, etc.), source-specific diagnostic ratios of PAH analytes, and principal component analysis (PCA) or positive matrix factorization (Battelle Memorial Institute et al. 2003; Burns et al. 1997; Johnson et al. 2007; Stout and Graan 2010). If the types of sources and the relative abundances of contributing PAHs are known, then the most useful tools for distinguishing pyrogenic from petrogenic hydrocarbons are the PAH distributions (patterns, boiling ranges and fingerprints of alkylated and non-alkylated PAHs) and diagnostic ratios (Benner et al. 1995; Elmquist et al. 2007; Neff et al. 2005; Wang and Brown 2009).

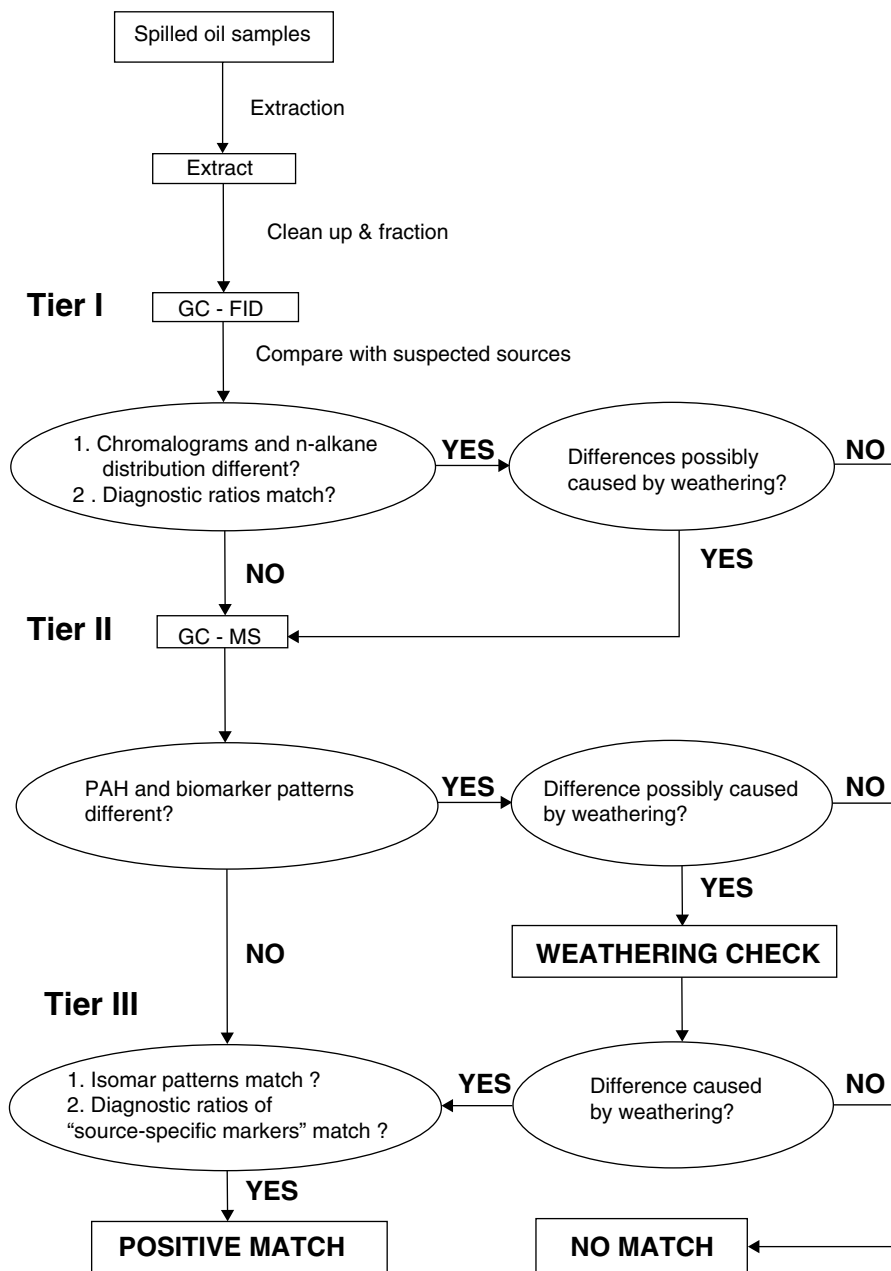
Successful inference and/or differentiation of sources depends on many factors, such as sampling plan design, sample collection, chemical analysis methods and knowledge of historical industrial processes (Johnson et al. 2007). Problems often exist in establishing unique organic “tracer” compounds for a given combustion source, and such problems include variability in the composition of emissions from the same types of source, degradation of the “tracer”, and general lack of source composition data for all but a few classes of compounds (Johnson et al. 2007).

There are three main steps (tiers) in characterizing the sources of PAHs (Fig. 6). First, inexpensive rapid screening techniques like gas chromatography (GC)—flame ionization detection (FID), are applied to identify trends, background concentrations, “hotspots”, and key samples (Page et al. 2006; Stout et al. 2003; Wang et al. 1999a). Second, if initial screening results allow defensible decision-making, advanced chemical fingerprinting (e.g., GC-MS,<sup>2</sup> GC-FID, use of diagnostic ratios, etc.) helps to reveal and identify distinct source “fingerprints” (Boehm et al. 1995; Page et al. 2006; Stout et al. 2003; Wang and Fingas 2003; Wang et al. 1999a).<sup>3</sup> Third, tier results are explored and explained by using statistical tools. In this review, we emphasize the use of molecular indices (PAH ratios) as the basis for characterizing PAH sources.

---

<sup>2</sup>Mass Spectrometry.

<sup>3</sup>For guidelines on how to perform a fingerprinting analysis of PAH sources (assessment of historic records, sampling considerations, climatic conditions, background pollution, quality assurance, etc.) see Christensen and Tomasi (2007), Christensen et al. (2004), Saber et al. (2006), Stout et al. (2001b, 2003), Wang et al. (1999a).



**Fig. 6** Oil spill identification protocol. If significant differences in hydrocarbon fingerprints and diagnostic ratios are found at any stage during the identification process, the conclusion will be that the samples are not from the suspected source. From Wang et al. (1999a) (modified decision chart of Nordtest Method 1991), with permission, © Elsevier Science BV

## 5 Molecular Indices

Comparing PAH concentrations in a contaminated area with the PAH content of potential/suspected sources can produce very useful results (e.g., Boehm et al. 1995; Wang et al. 2001; Yunker et al. 2002). To evaluate compositional differences in PAH profiles, the concentrations of PAHs are usually standardized into ratios that are both source-specific and refractory (De Luca et al. 2004; Kim et al. 2008). These indices are of interest, because during PAH formation the PAH distribution is temperature-dependent (De Luca et al. 2004, 2005; Yunker et al. 2002). The PAH distribution patterns are governed by the thermodynamics of low-temperature processes (e.g., the formation of petroleum), and the kinetic factors of high-temperature processes (e.g., combustion).

Different ratios may be attributable to differences between the sources (Hwang et al. 2003; Stout et al. 2004), such as the type of substrate and the available pathways and conditions of PAH formation (Yan et al. 2005). PAH ratios can also be used as tracers of PAH transformation during transport from the PAH source to deposition and burial (Mitra et al. 1999; Stout et al. 2002). Consequently, to optimize data analysis, one should use diagnostic ratios of PAH isomers, PAHs within a homologue category, or PAHs that have similar thermodynamic stabilities (Christensen et al. 2004). The use of PAH ratios minimizes confounding factors such as differences in volatility, water solubility and adsorption (Yunker et al. 2002). Therefore, such ratios may be used in two-component mixing models<sup>4</sup> for PAH sources in sediment (Page et al. 1996).

From a statistical point of view, by using diagnostic ratios the sample compositional information can be condensed into fewer variables that are less affected by analytical artifacts/errors (e.g., retention time shifts, changes in peak shapes, relative signal intensities, etc.; Christensen and Tomasi 2007). When degradation effects are factored in, a “multiple mixing model” can be developed that assists in establishing the range of contributions of different PAH sources (Gogou et al. 2000; Stout et al. 2003; Wang et al. 2001).

### 5.1 Practical Concepts

PAH ratios are expressed as the ratio of the thermodynamically most stable isomer (S) to the most unstable isomer (U) (e.g., S/U), or vice versa (e.g., Mitra et al. 1999; Stout 2007). Such ratios are sometimes called thermal parameters because they are

---

<sup>4</sup>A two component mixing model to estimate the “a” % contribution of the source A to the sample, where the ratio of the two isomers is “r<sub>s</sub>”, given the ratios of the isomer components in the sources A and B (r<sub>A</sub> and r<sub>B</sub> respectively), and only sources A and B contribute, would look like: 
$$a = \frac{(r_A + 1)(r_B - r_s)}{(r_s + 1)(r_B - r_A)}$$

a function of the formation temperature (e.g., Budzinski et al. 1997; Stout 2007; Yunker et al. 2002). For parent PAHs, combustion or anthropogenic input—or both—are often inferred from an increase in the proportion of the less stable, “kinetic” PAH isomer relative to the more stable, “thermodynamic” isomer, and the stability of the lighter PAH isomers has been calculated to support such interpretations (Budzinski et al. 1997; Yunker et al. 2002).

Some researchers prefer to limit the ratio to the range of 0–1 and thus report the

ratio as:  $\frac{S}{S+U} = \frac{S/U}{1+S/U} = \left(1 + \frac{1}{S/U}\right)^{-1}$ . In this paper, such ratios are usually

written in the form of “nominator/denominator”. For example, the formula FL0/

FL0+PY0 simplifies the form  $\frac{FL0}{FL0+PY0}$  (using the molar concentrations of these

compounds). The S/S+U form results in smaller relative standard deviations (RSD) than the S/U form does, but only the RSD of the S/U form is constant and independent of the numerical values of S and U (Hansen et al. 2007 and references therein). Therefore, the use of the S/U form is recommended.

PAH ratios that are used to indicate a characteristic molecular fingerprint of a substance are sometimes called source parameters (Stout 2007). For example, the ratios of dibenzothiophenes or benzonaphthothiophenes reflect the differences in the abundance of sulfurous aromatics in crudes (Boehm et al. 2001; Dzou et al. 1995; Grimmer et al. 1983; Stout 2007; Stout et al. 2006). Consequently, knowledge of the possible source fingerprints/PAH distributions is of critical importance when utilizing PAH ratios to identify sources (Johnson et al. 2007; O’Reilly et al. 2012, 2014). Finally, PAH ratios that vary according to the degree of weathering are used as weathering parameters/indicators (e.g., the ratio of the less stable compound to the significantly more stable compound).

PAH ratios are usually shown as one or more of the following plots:

- Double ratio plots. These are the most popular (e.g., Andersson et al. 2014; Budzinski et al. 1997; Yunker et al. 2002) and display the chart as areas separated according to PAH origin (e.g., pyrolytic, petrogenic, etc.).
- Time or depth plots of the ratio. Useful for studying temporal trends of PAH sources (effects of population, combustion practices, and new sources) (e.g., Guo et al. 2007; Mitra et al. 1999; Pereira et al. 1999). Occasionally, data such as  $^{137}\text{Cs}$ ,  $^{210}\text{Pb}$ , and  $\delta^{13}\text{C}_{\text{py}}$  are plotted against PAH ratios to elucidate the source profile over time (e.g., Elmquist et al. 2007; Stout et al. 2001b; Yan et al. 2005).
- Map plots and boxplots of PAH ratios. These are used to identify point sources and hotspots (Battelle Memorial Institute et al. 2003).
- Nordtest plot. Allows researchers to examine matches between the ratios for possible sources and sediment contamination.

The basis of selecting the proper diagnostic ratios should be based on the specificity and diversity of the ratio over a range of sources, the resistance of the ratio to weathering effects and the precision of the analytical method used (Christensen and Tomasi 2007; Christensen et al. 2004; Hansen et al. 2007 and references therein).

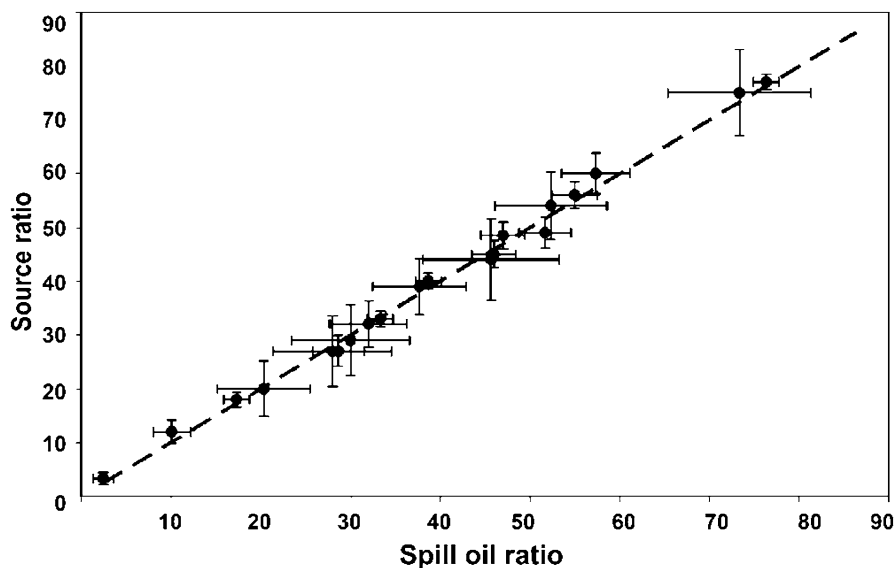


When the PAH ratios for sources are known, the ratios can be classified according to their diagnostic power (DP), so that the most suitable ones are selected for the study area (Christensen and Tomasi 2007; Christensen et al. 2004). Christensen and Tomasi (2007) evaluated the diagnostic power of 25 PAH ratios of oil spill samples. They reported high diagnostic power for ratios such as alkylated phenanthrenes to alkylated dibenzothiophenes, fluoranthene to pyrene, methylphenanthrenes to phenanthrenes and other less common ratios.

A standardized and simple means of comparing chemical fingerprints (Fig. 6—tier III) of different oil spills is the Nordtest (Douglas et al. 2007b; Stout et al. 2005). It entails plotting several diagnostic ratios (generally accepted, or calculated for the occasion) for the source and the sample, together with the 98% and 95% confidence intervals (Fig. 7) (Stout et al. 2005).

Douglas et al. (2007b) described the Nordtest method (limited to spilled oils and refined oil products in water) in more detail and showed how to establish new candidate ratios for discriminating between two known sources. They also recommended a list of 10 diagnostic ratios for identifying oil spills. Phenanthrenes and dibenzothiophenes are included on this list because they are common in all oils. The concentrations of methylfluoranthenes, methylpyrenes and benzofluorenes also vary among different oils and are included on the list (Douglas et al. 2007b).

Principal component analysis (PCA) (Davis 2002; Luo et al. 2008) is one of the most suitable tools for identifying potential sources of PAHs. PCA allows for greater resolution among different sources and for reduced variance than does the Nordtest



**Fig. 7** The Nordtest method. All ratios match the possible source (i.e., the ratios in the sample and source are within a 95% confidence interval). Adapted from Stout et al. (2005), with permission, © Taylor & Francis Inc

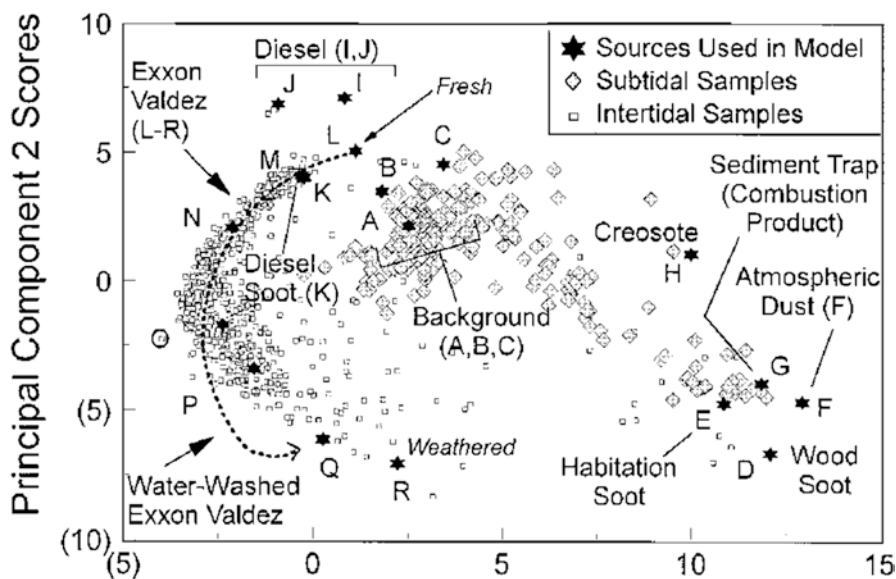


Fig. 8 PCA (principal component analysis) allocates sediment PAHs to the contributing sources by least-squares match of the PAH profile of the sample with the respective source. Adapted from Burns et al. (1997), with permission, © SETAC

method (De Luca et al. 2004; Douglas et al. 2007b; Neff et al. 2005). The first principal component accounts for the largest possible variance in the data, and each succeeding component explains as much of the remaining variability as possible (Davis 2002). If principal components can be given a meaningful explanation (i.e., pyrogenic, petrogenic or natural sources), by assigning certain compounds to a certain principal component, then it is possible to quantify the contribution of the different PAH sources (Luo et al. 2008). In a cross-plot of principal components, samples that have similar compositions will be close to each other (Fig. 8).

If there are doubts about the PAH source profiles, principal components can be used to indicate the possible sources (Burns et al. 1997). If more is known about the sources, PCA can be used to reveal the contributions of each source to the samples (Boehm et al. 2001). Because the concentrations of individual PAHs often differ by orders of magnitude in a given sample, they are usually normalized to the sum of the analytes (Boehm et al. 2001).

Burns et al. (1997) used PCA to determine the major contributions of 36 identified sources in Prince William Sound, Alaska. The sources that contributed most were then apportioned by a best-fit least square model to calculate a linear combination of contributing sources. Christensen et al. (2004) used externally normalized PAH ratios as the loading variables in PCA, providing an integrated methodology for oil spill identification similar to the tiered one presented in Fig. 6.

Basic guidelines for successful application of a PCA include adequate, good quality data (e.g., samples with higher PAH concentrations may have different origins), and the optimization of the sources and the number of principal components (Burns et al. 1997; Johnson et al. 2007; Luo et al. 2008). However, if the sources of the PAHs are strongly correlated, then other chemical compounds might have to be used.

The inherent disadvantages of the PCA method (Johnson et al. 2007) and growing interest in PAH source apportionment led to the adoption of a new analysis tool: positive matrix factorization (PMF). PMF (Comero et al. 2009) has been successfully used (sometimes in conjunction with PCA) to apportion PAH sources (Lang et al. 2013; Larsen and Baker 2003; Sofowote et al. 2008, 2011; Stout and Graan 2010). By combining multiple statistical techniques in source apportionment, Stout and Graan (2010) successfully determined the concentration of PAHs that originated from non-point sources (urban background).

An important difference between using only PAH ratios vs. a PCA/PMF approach is that ratios classify the sample into very few categories (e.g., pyrogenic, petrogenic, etc.), whereas PCA places the samples and the sources in a continuous multidimensional space. Similarities or differences among samples and sources are tracked and measured by PCA/PMF. Quantitative assessments are achieved by using the PCA/PMF approach (Luo et al. 2008) or by applying a mass balance model, in which several PAH ratios are simultaneously considered. Uncertainties in the PAH ratios may cause a sample to be misclassified, whereas employing a PCA/PMF method by itself does not misclassify the samples. Most importantly, application of a PAH ratio relies on the correlation of two variables, whereas PCA/PMF takes account of all available variables. Consequently, once they have been established through a PCA/PMF apportionment method (e.g., Luo et al. 2008; Nasher et al. 2013; Stout and Graan 2010; Stout et al. 2005), PAH ratios may prove to be a rapid and inexpensive way to infer sources and/or to develop a mixing model, albeit on a case by case basis.

The potential problem of using molecular ratios in source identification is the chemical and biological alterations of PAHs relative to each other (Galarneau 2008; Mansuy-Huault et al. 2009; O'Malley et al. 1994). It is possible to take the photodegradation effects on the ratio<sup>5</sup> into account, if the kinetics of photodegradation (half-lives, first order kinetics) and the color of the particles are known (Behymer and Hites 1988; Dickhut et al. 2000; Tobiszewski and Namiesnik 2012). Therefore, the association of PAHs with particles (e.g., soot, fly ash etc.) is fundamental to understanding how photodegradation affects PAH ratios. Similarly, it is possible to

---

<sup>5</sup> Using 1<sup>st</sup> order kinetics, the ratio  $r_{\text{after}}$  of two isomers (S and U) after photodegradation in air for time  $t$  would be:  $R_{\text{after}} = R_{\text{emission}} e^{(k_U - k_S)t}$ , where  $k$  is the photodegradation constant of the respective analytes for a certain particle color.

account for other kinds of degradation (biotic or abiotic), if a model describes them adequately. Several authors have evaluated the different types of degradation that affects PAH ratios (e.g., Costa and Sauer 2005; Stout et al. 2003; Uhler and Emsbo-Mattingly 2006; Wang et al. 1998). Hence, different PAH ratios may also be used as a simple means of evaluating degradation.

## 5.2 *Sum of PAHs*

A way to quantify the amount of pollution for a specific area, and also to take the first step in characterizing a PAH source, is to compare the sum of PAHs with the amounts released by a suspected source (Dupree and Ahrens 2007; Saber et al. 2005, 2006; Stout 2007). “Total PAHs” is commonly defined as the sum of identified three- to six-ringed parent PAH compounds, which is denoted as  $\Sigma$ PAH or EPA 16 (i.e., the U.S. EPA sixteen priority PAHs). To account for uncombusted petroleum sources that are rich in alkyl PAHs, TPAH is defined as the sum of all quantified parent and alkyl PAHs (Stout et al. 2003; Yan et al. 2006). Sometimes naphthalene, perylene and retene are excluded from TPAH estimation because the naphthalene is a common laboratory contaminant and perylene and retene could have a non-anthropogenic origin (Boehm et al. 2001, 2002, 2007; Gogou et al. 2000).

## 5.3 *Low Molecular Weight PAH Ratios*

### 5.3.1 *Naphthalene Indices*

Naphthalene and alkyl naphthalene ratios find several applications in source identification, as they constitute potentially useful thermal (Stout et al. 2002) or weathering parameters for crudes, coals, bitumen and other sources. Roush and Mauro (2009) used the N0/N1 ratio (parent naphthalene over methylnaphthalene) to detect coal tar residues enriched in naphthalene oil. The ratio  $MNR = 2-N1/1-N1$  (2-methylnaphthalene to 1-methylnaphthalene) is unaffected by light weathering and can be used to distinguish products that have different methylnaphthalene content, such as lightly weathered distillates (Stout and Wang 2007). MNR and other alkylnaphthalenic ratios were used for the characterization of coals of different ranks (Radke et al. 1982). For minimally weathered sediments, the petrogenic background may be deduced simply from a high N0/F0 (naphthalene to fluorene) ratio (Neff et al. 2006).

In the initial weathering stages of an oil spill, the loss of naphthalene and methylnaphthalenes relative to dimethylnaphthalenes (N0+N1/N2) can be used as a measure for the loss of PAHs due to dissolution (Diez et al. 2007). The N3/P3 (trimethyl naphthalenes over trimethylphenanthrenes) ratio is useful for estimating the weathering state of light crude oils (Peters et al. 2005). Heavier weathering may be evaluated by the sum of alkylated naphthalenes over TPAH or over the recalcitrant

alkylated chrysenes (e.g., N1-N4/C1-C3) (Bence et al. 1996; Boehm et al. 2008; Wang et al. 2006). After the rapid dissolution of the parent naphthalene and methyl-naphthalenes, these ratios decrease more slowly (Bence et al. 1996).

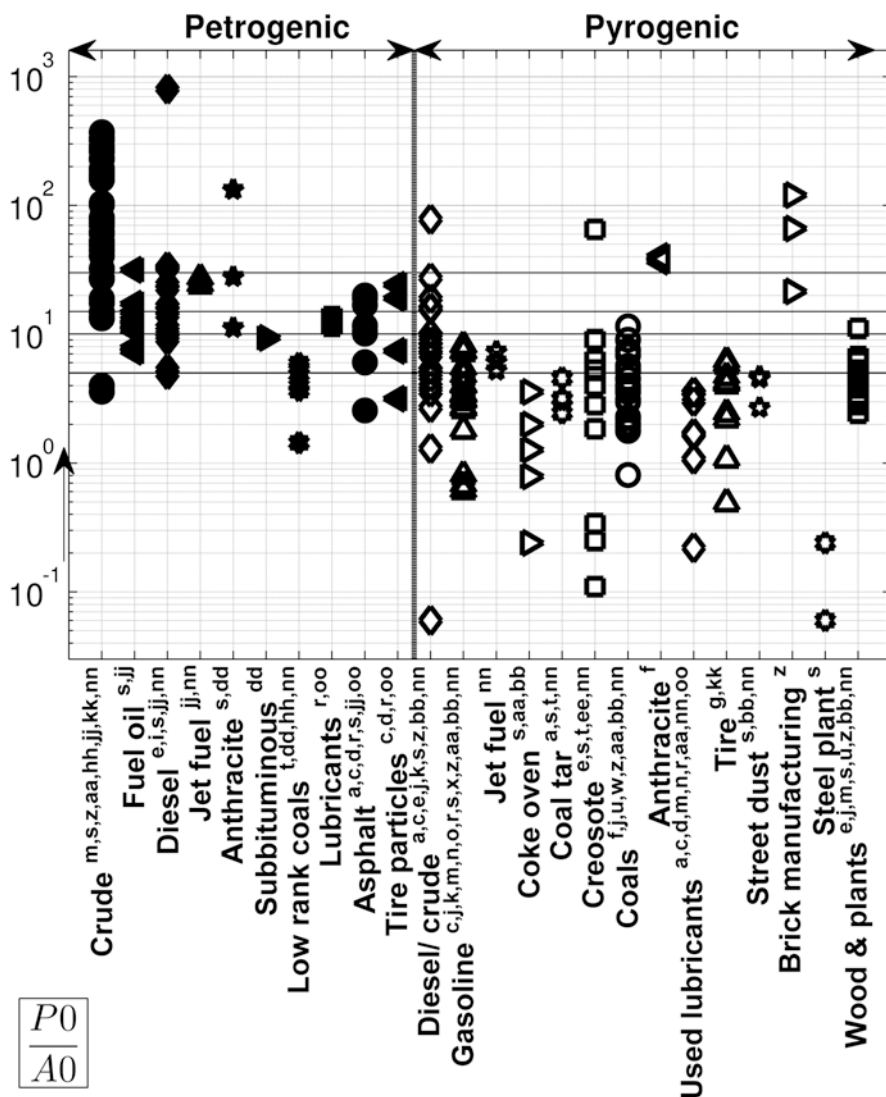
### 5.3.2 The Ratio of Phenanthrene to Anthracene

The ratio of parent phenanthrene to parent anthracene (P0/A0) redundant has been extensively used to differentiate between petrogenic and pyrogenic PAH pollution in sediments (e.g., Grimmer et al. 1981; Gschwend and Hites 1981; Guo et al. 2007; Lake et al. 1979; Sicre et al. 1987). Thermodynamically, this ratio is temperature-dependent (Budzinski et al. 1997 and references therein). Phenanthrene is the thermodynamically most stable triaromatic isomer, and its prevalence over A0 supports petrogenesis (Budzinski et al. 1997; De Luca et al. 2004, 2005; Gogou et al. 2000). High-temperature (800–1,000 K) processes yield low P0/A0 ratio values (4–10), usually less than 5. The slow thermal maturation of organic matter in petroleum leads to much higher P0/A0 values (50 at 373 K) (Budzinski et al. 1997; De Luca et al. 2005; Neff et al. 2005; Wang et al. 2001). However, fresh petroleum products occasionally exhibit small P0/A0 values (down to 4), whereas some combustion sources have a higher value (Budzinski et al. 1997; Colombo et al. 1989; Wang et al. 1999a).

P0/A0 ratios in different literature data sources are summarized in Fig. 9. Also shown in Fig. 9 are the P0/A0 threshold values that researchers used to distinguish petrogenic from pyrogenic sources. For example,  $P0/A0 > 15$  for likely petrogenic inputs (or  $> 30$  for negligible pyrogenic) and  $P0/A0 < 15$  for the dominance of pyrolytic sources ( $< 5$  according to Neff et al. 2005), such as fuel combustion or other high-temperature processes (Budzinski et al. 1997; De Luca et al. 2004; Morillo et al. 2008a). Yunker et al. (2002) concluded that a lowest P0/A0 boundary of 9 or 10 appears applicable for petrogenics, except that P0/A0 ratios overlap for certain sources such as diesel oils, coals, and coal emissions (Fig. 9).

In summary: i)  $P0/A0 > 30$  shows crude oil contamination, but creosote and the combustion of some coals or crude occasionally exhibit high P0/A0 ratios, ii) values  $30 > P0/A0 > 10$  show a mixed source profile, but if diesel and coal combustion and creosote are ruled out, then such values indicate a probable petrogenic source, iii) values  $10 > P0/A0 > 5$  define a mixed source profile, and iv) values smaller than 5 indicate pyrogenic origin except for gasoline fuel, some road fingerprints, and low rank coals that exhibit  $5 < P0/A0 < 9$ .

The different thermodynamic stabilities of P0 and A0 allow biogeochemical processes to alter the P0/A0 value (Bucheli et al. 2004; Lake et al. 1979; Yan et al. 2006). The phenanthrenes photodegrade much more slowly than anthracenes (Behymer and Hites 1988; Hwang et al. 2003). As a result, smaller quantities of A0 are observed during the daytime in urban areas (Yunker et al. 2002). However, Zhang et al. (2005) calculated an air-to-sediment (i.e., receptor-to-source) ratio to be approximately 1 for P0/A0. This indicated that the P0/A0 ratio does not change significantly during deposition from atmospheric emissions to sediment. Nevertheless, the P0/A0 is sensitive to parameters such as molecular mobility and volatility (Zhang et al. 2005).



**Fig. 9** Mean, maximum and minimum values of  $P0/A0$  ratio (Y-axis in logarithmic scale) for different PAH sources (X-axis), as reported in the literature (see Table 5 in appendix). The vertical dashed line divides the graph into petrogenic (left) and pyrogenic (right) sources. Horizontal continuous lines indicate the thresholds used to distinguish pyrogenic and petrogenic products discussed in the text. Degradation arrow (left of graph, by the Y-axis) shows the change in  $P0/A0$  with most types of degradation. However,  $P0$  is more soluble than  $A0$  (see text for more information)

In water, both  $P0$  and  $A0$  follow similar first order photodegradation kinetics when not attached to particles, although humic substances protect  $P0$  but not  $A0$  (Bertilsson and Widenfalk 2002).  $P0$  is more soluble than  $A0$  ( $P0/A0$  decreases as dissolution increases) (Table 2), otherwise  $A0$  is more degradable than  $P0$  (ratio increases as the degradation proceeds). However,  $P0$  in soils biodegrades more

readily than A0 (Tobiszewski and Namiesnik 2012 and references cited by these authors). Iqbal et al. (2008) noted that the P0/A0 ratio also depends on analytical matrix effects.

When degradation significantly changes the P0/A0 ratio, consistency with other ratios such as FL0/PY0 and P1/P0 has to be checked (Hwang et al. 2003). De Luca et al. (2004, 2005) noted that a prerequisite for the applicability of the P0/A0 is that  $\Sigma\text{PAH} > 0.22 \mu\text{g/g}$  dry weight. Furthermore, when P0/A0 values are close to the pyrogenic/petrogenic thresholds, the ratio may be misleading for certain sources such as automobile exhausts (Morillo et al. 2008b). Dvorska et al. (2011) reported that the P0/A0 ratio is not very useful for distinguishing between traffic and domestic heating sources.

The P0/A0 ratio and other ratios such as FL0/PY0, BaA/C0 have been widely applied (Budzinski et al. 1997; Sicre et al. 1987; Wang et al. 2001, 2006; Yunker et al. 2002). However, caution needs to be exercised when applying the P0/A0 ratio for intermediate values (e.g., 4–15), on sediment that contains weathered PAH, or for solely pyrogenic discriminations (Bucheli et al. 2004; Dvorska et al. 2011; Hwang et al. 2003; Karlsson and Viklander 2008; Yan et al. 2005; Zhang et al. 2005). Thus, P0/A0 is more useful for petrogenic–pyrogenic discriminations.

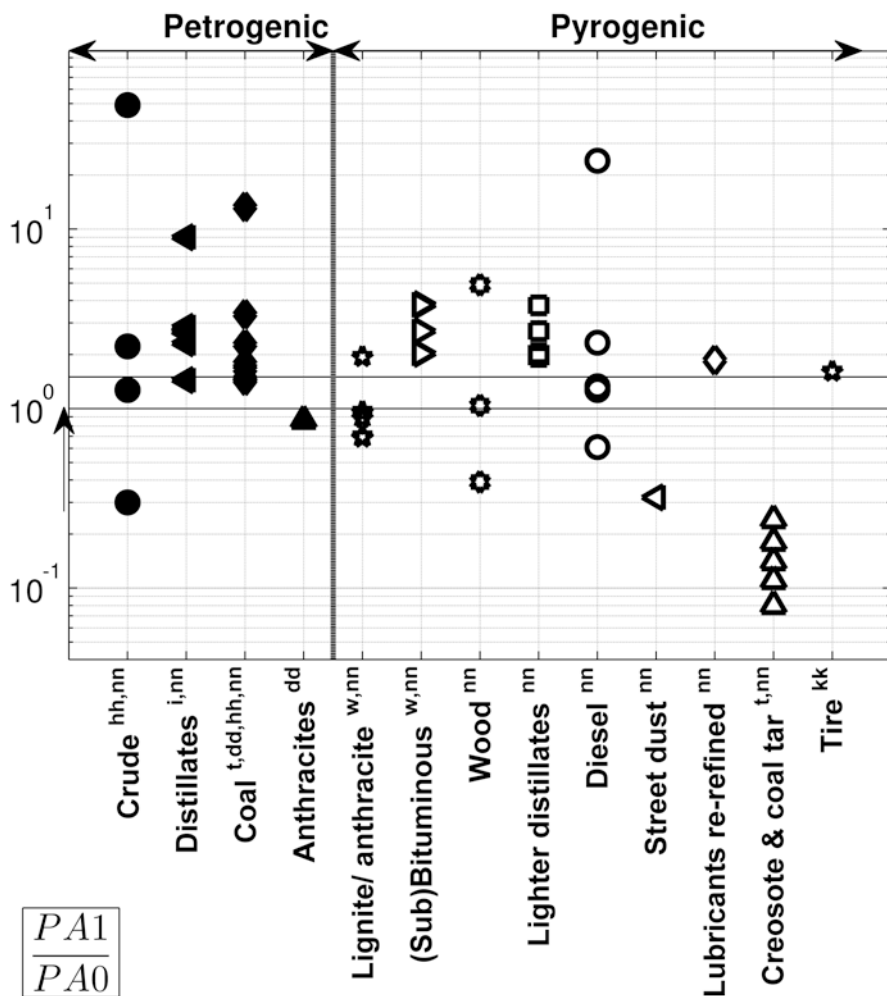
### 5.3.3 The Ratio of Methylphenanthrenes to Methylanthracene

Methylphenanthrenes can be used to distinguish between petrogenic and pyrogenic sources by comparing them with methylanthracenes that are mainly products of catalytic or thermal cracking (Lake et al. 1979; Stout and Wang 2007; Uhler et al. 2007; Walker and Dickhut 2001). Such pyrolytic processes reduce the proportions of 9-, 4-, and 1-methylphenanthrenes in favor of methylanthracenes (Stout and Wang 2007). Therefore, a  $\Sigma\text{P1/2-A1}$  (sum of methylphenanthrenes to 2-methylanthracene) ratio might serve as an indicator of the presence of coal tar, or of cracked gas-oil blending stock in heavy fuel oils (Uhler et al. 2007). Using this ratio it is also possible to distinguish heavy fuel oil from crude oil (Uhler et al. 2007).

Methylphenanthrenes are thermodynamically stable, and thus the  $\Sigma\text{P1/2-A1}$  ratio should be high for most crudes and higher rank coals, which are produced during different geologic periods and under different heating conditions. Methylanthracenes may rapidly decompose to methylphenanthrenes (Walker and Dickhut 2001). Furthermore, the  $\Sigma\text{P1/2-A1}$  ratio is sensitive to different source inputs, which may significantly alter its value (Walker and Dickhut 2001).

### 5.3.4 Methylphenanthrene Plus Methylanthracene Versus Their Parents

A sensitive indicator for tracing petrogenic and pyrogenic PAHs is the ratio of methylphenanthrene plus methylanthracene to the sum of parent phenanthrene plus parent anthracene:  $\frac{P1+A1}{P0+A0}$ , or PA1/PA0 in short (Fig. 10) (Da Silva and Bicego 2010; Mitra et al. 2009; Yan et al. 2005; Yunker et al. 2002). High PA1/PA0 ratios (>1.5) generally indicate petroleum, but occasionally PA1/PA0 is greater than 1.5



**Fig. 10** The ratio of methylalkylated PAHs of PA1 to their parents. See Fig. 9 for the symbols and to the text for explanation

for combustion samples, too (Fig. 10; Yunker et al. 2002). Accordingly,  $PA1/PA0 < 1$  indicates the combustion of coal or wood, or weathered urban aerosols. The  $PA1/PA0$  ratio is lower ( $< 0.2$ ) in creosotes or coal tar than in any other pyrogenic or petrogenic sources (Fig. 10) and seems appropriate for differentiating creosotes or coal tar from other sources (Fig. 10).

According to Yan et al. (2005), further study is required to fully exploit the potential of the  $PA1/PA0$  ratio for pyrogenic PAH source apportionment.  $PA1/PA0$  should preferably be used along with other ratios such as (see also Sect. 5.8): alkyl/ $\Sigma PAH$ ,  $FP1/FP0$ , Ring456/ $TPAH$  (Yan et al. 2005). For petroleum products, Yunker et al. (2002) assumed that the  $PA1/PA0$  ratio is more reliable than the  $P0/A0$  ratio, especially if the latter has a value close to 9.



### 5.3.5 Ratio of Methylphenanthrenes to Phenanthrene

After carbonaceous materials are combusted at 600–1,500 °C, phenanthrene dominates over its alkylated homologues, which are negligible (Lehndorff and Schwark 2009). High ratios of methylphenanthrenes (the sum of 1- plus 2-, and optionally 3- plus 9-methylphenanthrenes) over phenanthrene (P1/P0) indicate combustion at low temperatures that preserve the petrogenic alkylation pattern, e.g., fossil fuels, products of petroleum diagenesis, inefficient combustion, etc. (Elmquist et al. 2007; Lehndorff and Schwark 2009; Luo et al. 2008; Mitra et al. 1999; Takada et al. 1990).

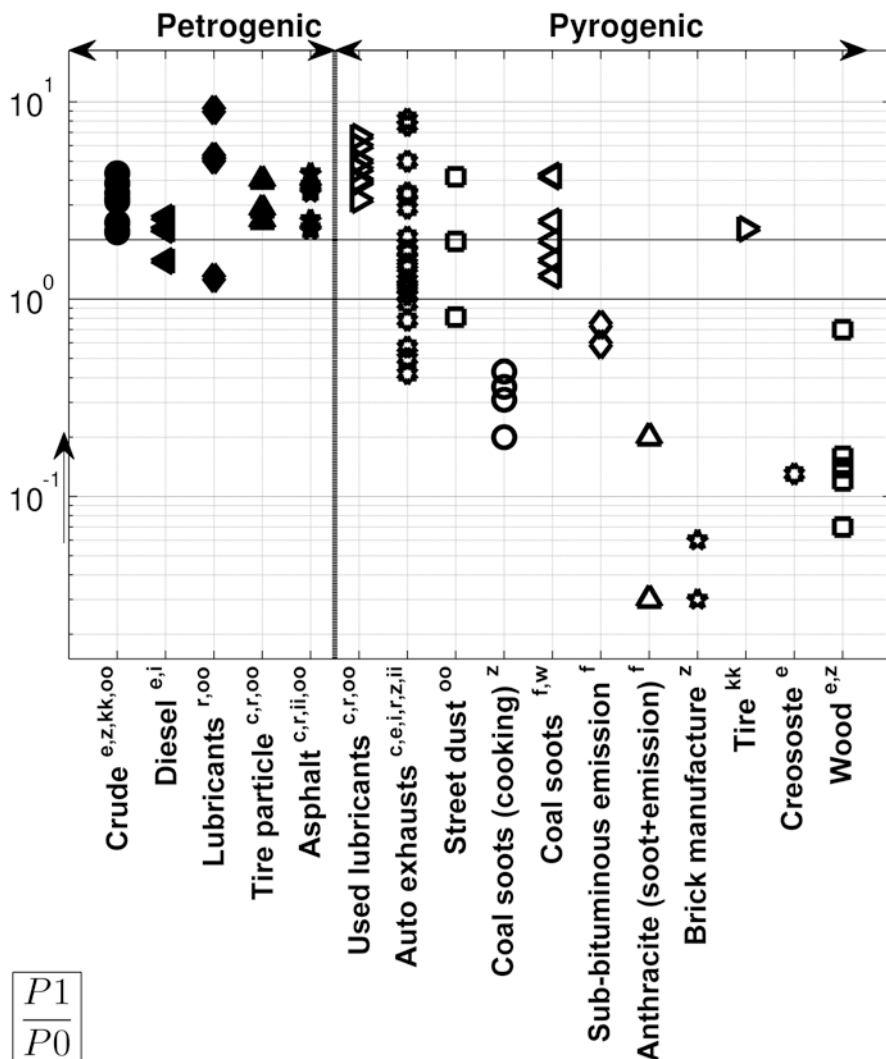
In petrogenic sources such as unburned fossil organic material, petroleum, oil shales, and their refined products, the P1/P0 ratio displays values over 2 (Gschwend and Hites 1981; Hwang et al. 2003; Kim et al. 2008; Luo et al. 2008; Takada et al. 1990; Zakaria et al. 2002). When  $P1/P0 < 1$  (Budzinski et al. 1997; Hwang et al. 2003; Takada et al. 1990), or  $0.4 < P1/P0 < 0.7$ , according to Elmquist et al. (2007) a pyrogenic origin may be inferred. Indeed, in Fig. 11, the area of overlap between pyrogenic and petrogenic sources (coal, used lubricants, automobile exhausts) is mainly the interval  $1 < P1/P0 < 2$ . Because phenanthrene is less stable than its methyl homologues, the degradation of crude or diesel increases the P1/P0 (Burns et al. 1997).

The methylphenanthrenes to phenanthrene ratio has been used to identify pyrogenic or petrogenic hydrocarbon contaminants (e.g., Farrington et al. 1977; Guo et al. 2007; Luo et al. 2008), or, together with the dimethylphenanthrene (DMP) ratio, to trace PAH sources over time (Sect. 5.3.8) (Elmquist et al. 2007). The P1/P0 ratio has also been used to distinguish asphalt from vehicle emissions (along with the D1/P1 ratio—methyl dibenzothiophenes to methylphenanthrenes), and vehicle traffic (0.7 to 8.2) from background domestic pollution (0.7–1.2) in Tokyo (Takada et al. 1990).

Used oil or diesel emissions have both petrogenic (unburned fuel,  $P1/P0 > 2$ ) and pyrogenic (HMW) PAH signatures (Mostafa et al. 2009; Zakaria et al. 2002). Therefore, the P1/P0 ratio is usually higher in diesel vehicle emissions than in gasoline ones (Hwang et al. 2003; Larsen and Baker 2003). Accordingly, Hwang et al. (2003) calculated the diesel and gasoline vehicle contributions to pine needles via a mass balance model. Furthermore, pyrogenic contribution from used crankcase oil could cause the P1/P0 ratio to be correlated with chrysene, benzo[*a*]pyrene, benzo[*ghi*]perylene and the total PAHs (Zakaria et al. 2002).

### 5.3.6 Distribution of Methylphenanthrenes

Alkylphenanthrene homologues are considered as petrogenic markers and enable petrogenic PAHs to be recognized (Gogou et al. 2000). For example, if  $P2 > P1 + P0$  (dimethylphenanthrenes concentration is higher than the sum of the concentrations of methylphenanthrene plus phenanthrene), then the dominant source is petroleum (Gogou et al. 2000; Sicre et al. 1987). However, coal combustion and wood smoke may show maxima in the parent PAH, or the methyl-PAH, or the dimethyl-PAH (Sicre et al. 1987; Yunker et al. 2002). Furthermore, coal PAHs (Fig. S27, Supporting Material) do not follow the “usual” pyrogenic or petrogenic



**Fig. 11** The ratio of  $P1/P0$  for different sources. See Fig. 9 for the symbols and to the text for explanation

distributions, and so other methylphenanthrenic indices (MPIs) such as the  $MPI3 = \frac{2 - P1 + 3 - P1}{9 - P1 + 1 - P1}$  are frequently used to distinguish between coals or oils of different thermal maturity (Achten and Hofmann 2009; Boehm et al. 2001; Dzou et al. 1995; Lehndorff and Schwark 2009; Radke et al. 1982; Stout and Emsbo-Mattingly 2008; Wang and Brown 2009).

Methylphenanthrene (1-, 2-, 3- and 9-P1) ratios of the more stable  $\beta$  isomers to the less stable  $\alpha$  isomers (9-, 4- and 1-P1) have been developed for monitoring the thermal maturity of oil and middle distillate fuels (Faksness et al. 2002; Stout et al. 2002; Uhler et al. 2007). The European Committee for Standardization (CEN) includes the ratio of 2-P1/1-P1 (sometimes called the methylphenanthrene ratio or MPR) in its methods for identifying different oil products, such as IFO 380 heavy fuel oil (Hansen et al. 2007; Uhler et al. 2007). However, preferential biodegradation of 2-methylphenanthrene (Faksness et al. 2002) may reduce the value of 2-P1/1-P1, which can then be used as a biodegradation ratio (Wang and Brown 2009). In such a case, caution is necessary when utilizing this biodegradation index for bunker fuels that may represent a blend of different oils and fuels, which consequently have altered physicochemical properties (Wang and Brown 2009).

Another methylphenanthrenic ratio, the 4-P1 + 5-P1/P1, may be used to discriminate wood fires from coal combustion or asphalt (Simcik et al. 1999). Low values of this ratio have been observed for oil (0.02), which can thus be discriminated from other pyrogenic sources (Gschwend and Hites 1981).

### 5.3.7 Retene

The ratio of retene to chrysene (RET/C0) has been used to apportion softwood (e.g., fir and pine) combustion sources (RET/C0=4.5) and other combustion sources (RET/C0=0.35) (Bogdal et al. 2011; Mathieu and Friese 2012; Yan et al. 2005, 2007). However, hardwood combustion may significantly reduce the RET/C0 ratio (similar to the dimethylphenanthrene ratio: Sect. 5.3.8), which is insensitive to inputs from the combustion of petroleum or of coal. It is thus recommended to use the RET/C0 ratio together with other ratios such as the DMP ratio (Yan et al. 2005). Roush and Mauro (2009) suggested that the RET/C0 ratio be used to distinguish between coal fines (high value) and coal tar or petroleum products (low value).

Other RET ratios have occasionally been used. Dupree and Ahrens (2007) used the retene to methylpyrene (RET/PY1) (three-/four-ringed alkyl PAHs) ratio to distinguish wood soot in urban runoff samples. The retene to pyrene (RET/PY0) ratio was used to trace wood combustion in air (0.25–0.4) and sediments (Bucheli et al. 2004 and references cited by these authors). The RET/P4 ratio has been used to distinguish different spilled oil products according to the CEN methodology (Hansen et al. 2007). Grimalt et al. (2004) suggested that the ratio of retene to benzo[*b*]naphtho[2,1-*d*]thiophene, can be used together with the DMP ratio to distinguish between wood combustion and sulfur pyrogenic sources such as coal combustion.

### 5.3.8 Dimethylphenanthrenes

The  $\frac{1,7}{1,7+2,6}$  dimethylphenanthrene ratio (DMP ratio) is useful for distinguishing between vehicle emissions and wood combustion. The 1,7-dimethylphenanthrene isomer is thermally unstable relative to 2,6-dimethylphenanthrene (by 3.3 kcal/

mol). As petroleum matures, the DMP ratio decreases; softwood combustion however, is associated with high DMP values (Benner et al. 1995; Gogou et al. 2000; Yunker et al. 2002).

Yunker et al. (2002) suggested that  $DMP > 0.7$  indicates strong wood combustion sources, and (Yan et al. 2005, 2007) state that a  $DMP < 0.7$  indicates that vehicle/petroleum/fossil fuel or non-softwood emissions are dominant. Others (Lehndorff and Schwark 2009 and references therein) have suggested that a ratio of  $DMP < 0.43$  indicates vehicle emissions exclusively. Yunker et al. (2002) point out that DMP ratios in the range of 0.45–0.7 may indicate marine or terrestrial oils, terrestrial source rocks or even a mix of vehicle emissions and wood combustion. Thus, DMP ratios in these ranges may imply multiple mixed sources.

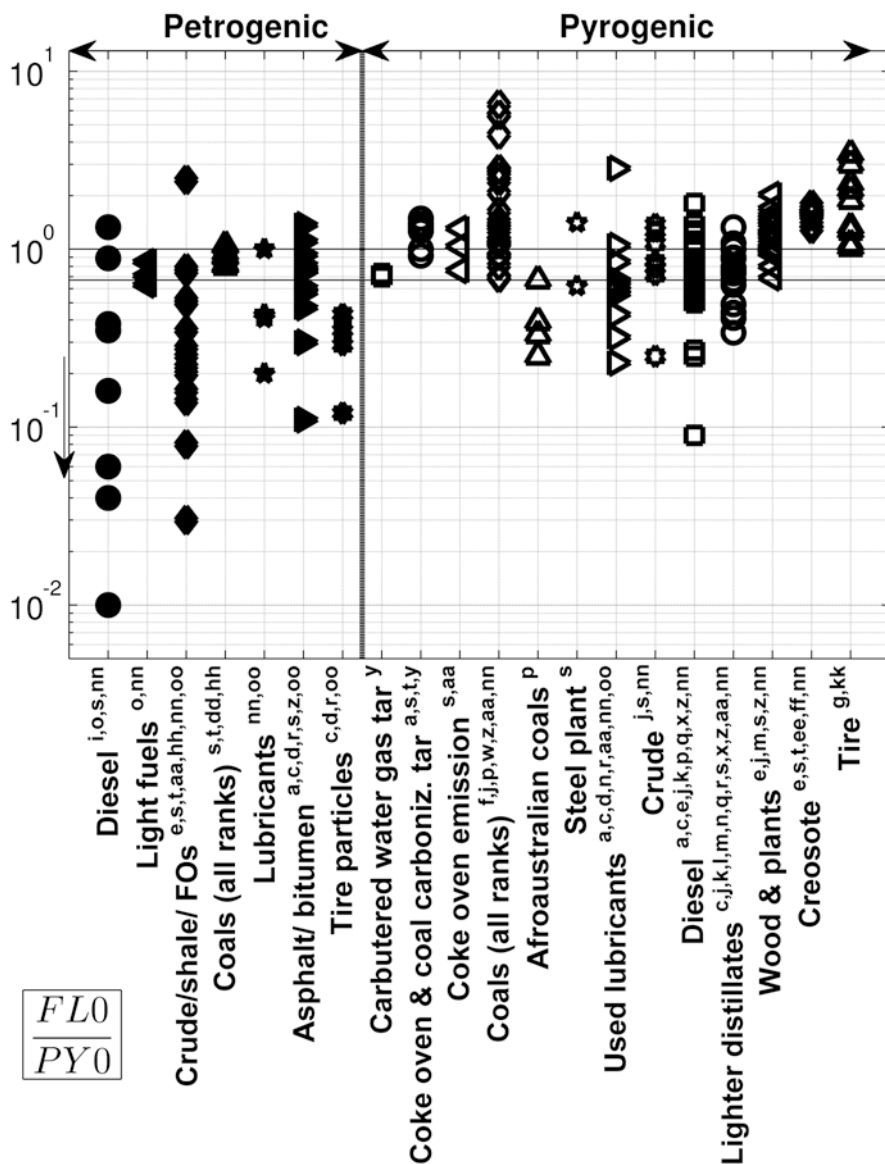
The DMP ratio in aerial particulate matter was used to apportion softwood combustion and motor vehicle emissions (Benner et al. 1995). It has also been used to estimate the present and historic relative contributions of softwood, coal, and petroleum combustion sources to sediments (Yan et al. 2005; Yunker et al. 2002). In these studies, the DMP ratio was used together with the fluoranthene to pyrene ratio. However, for wood and coal combustion the DMP ratio is best used in conjunction with the ratio of retene to chrysene (Yan et al. 2005). The DMP ratio has been used together with the acenaphthylene to acenaphthene (AY/AE) ratio, which is a marker for MGP tars, to distinguish coal soot from coal tar or other sources such as tires, oil, or bitumen (Craig and Mauro 2012; Dupree and Ahrens 2007).

In sources other than softwood combustion, the DMP ratio has a low value and should not be applied to distinguish petroleum or its combustion products, particularly in sediments with background contamination (Bogdal et al. 2011; Yunker et al. 2002). Biodegradation increases the DMP ratio (Jimenez et al. 2006 and references therein). The DMP and RET/C0 ratios may also be compromised by hardwood emissions, which produce lower ratios than softwood emissions (Yan et al. 2005). Therefore, DMP-based source apportionment may be inaccurate in areas affected by multiple combustion sources (Elmqvist et al. 2007; Mandalakis et al. 2004). Yan et al. (2005) have argued that 7,9-dimethylphenanthrene may be used instead of 2,6 DMP to apportion PAHs from fresh bituminous coal and brown-coal smoke. These two substances are present in similar amounts in bituminous sources, although softwood combustion emissions contain much greater amounts of 1,7 DMP than 1,6 DMP.

## 5.4 Four-Ringed PAHs

### 5.4.1 The Ratio of Fluoranthene to Pyrene

Similar to the P0/A0 ratio, the fluoranthene to pyrene (FL0/PY0) ratio correlates with the temperature of formation (e.g., Budzinski et al. 1997). Thermodynamically, fluoranthene is less stable than its isomer pyrene (Yan et al. 2005). FL0 is less favored than PY0 under fossil fuel formation conditions (Iqbal et al. 2008). As a result,  $FL0/PY0 < 1$  for petrogenic products, except for certain coals, crudes and diesels (Fig. 12).



**Fig. 12** The ratio of  $FL0/PY0$  for different sources. Note that  $PY0$  is more prone to biodegradation than  $FL0$ . See Fig. 9 for the symbols and to the text for explanation. *FO*: fuel oil

Coal combustion usually yields values of  $FL0/PY0$  greater than 1 (Gschwend and Hites 1981; Sicre et al. 1987). Creosotes exhibit a narrow range of  $FL0/PY0$  values (Stout et al. 2001a), which also exceed 1 (Fig. 12). Similarly,  $FL0/PY0 > 1$  occur for coke oven tars and other pyrogenic materials produced at relatively high temperatures (Costa et al. 2004; Saber et al. 2006).

Pyrogenic sources that could have  $FL0/PY0 < 1$  include used lubricants, emissions from automobiles and diesel trucks, and the combustion of gasoline, diesel, fuel oil and crude oil (Fig. 12; Yunker et al. 2002). Accordingly, pyrene can dominate over fluoranthene ( $FL0/PY0 = 0.6-0.8$ ) in atmospheric urban aerosols (Budzinski et al. 1997; Sicre et al. 1987). Tars from former manufacturing gas plants operating the relatively low-temperature carbureted water gas process also have low  $FL0/PY0$  ratios, which typically range from about 0.6–0.8 (Saber et al. 2006).

A relatively reliable threshold could be  $FL0/PY0 \leq 0.5$  for petrogenic sources, but diesel combustion and some used lubricants can also have  $FL0/PY0$  values below 0.5 (Fig. 12). Ratios between 0.5 and 1.0 are indicative of a mixed source profile, although automobile emissions are also in that interval. If  $FL0/PY0 > 1$ , then pyrogenic sources such as the combustion of coal or of biomass are probably predominant (Laflamme and Hites 1978; Yan et al. 2005; Yunker et al. 2002). A ratio of 1.2 was used as an upper limit for petroleum sources, depending on the reference oil used (Colombo et al. 1989; Iqbal et al. 2008; Neff et al. 2005).

The  $FL0/PY0$  ratio has been used in conjunction with other PAH ratios (e.g., Budzinski et al. 1997; Morillo et al. 2008a) or PAH isotopic signatures (Stark et al. 2003; Yan et al. 2005). Yunker et al. (2002) reported differences between the  $FL0/PY0$  ratios of the effluents of waste water treatment plants (WWTP) receiving stormwater and the  $FL0/PY0$  ratios of WWTP effluents that did not receive stormwater. These differences (also evident for the indeno[1,2,3-*cd*]pyrene to benzo[*ghi*]perylene ratio) were attributed to the stormwater runoff that contained petrogenic PAH signatures. De Luca et al. (2004) were able to distinguish pyrogenic from petrogenic sources in harbor sediments by using both the  $FL0/PY0$  and the phenanthrene to anthracene ( $P0/A0$ ) ratios (De Luca et al. 2004, 2005; Yunker et al. 2002).

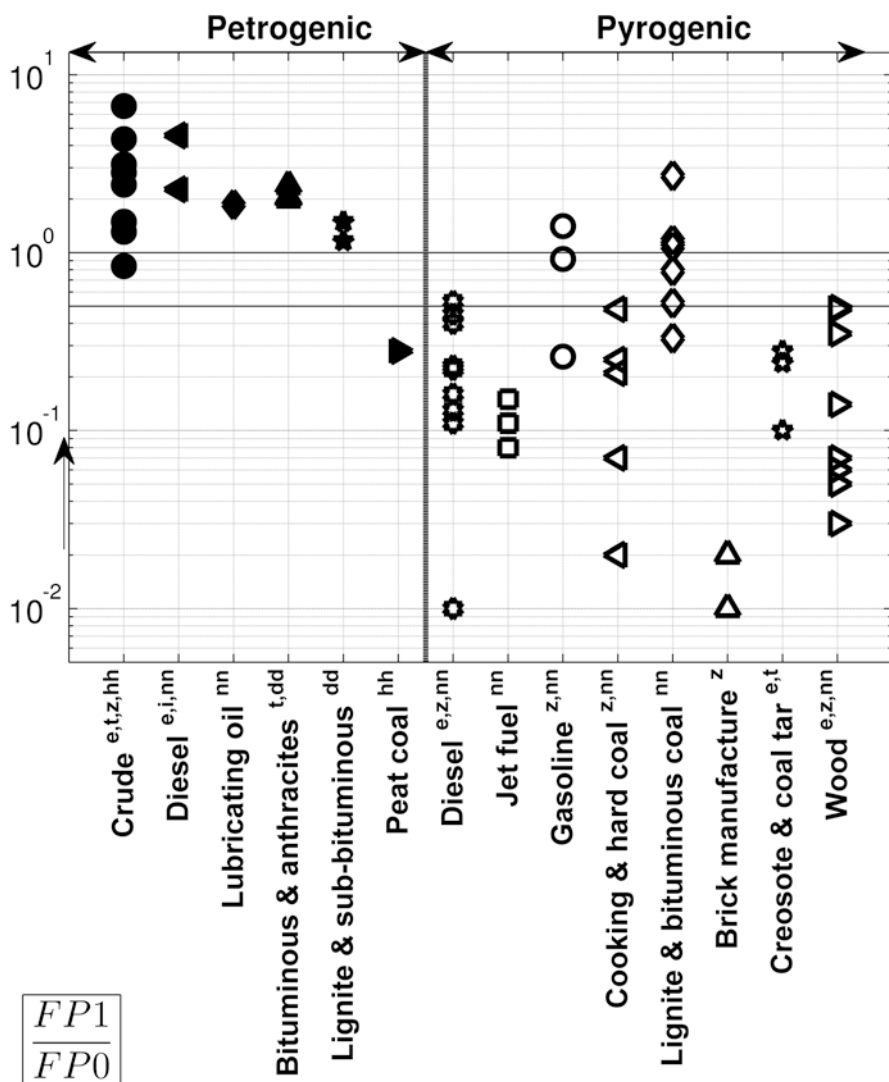
The  $FL0/PY0$  ratio is more sensitive as a source indicator than the  $P0/A0$  ratio (Yunker et al. 2002). The  $FL0/PY0$  is probably more reliable at elevated PAH values, but caution is necessary when applying it in heavily industrialized areas that have pyrogenic sources, which exhibit a low value of this ratio (Yan et al. 2006; Yunker et al. 2002). The  $FL0/PY0$  pair is more stable than the  $P0/A0$  pair over large concentration ranges and in regard to degradation, because both  $FL0$  and  $PY0$  degrade at almost the same rate in the atmosphere and in other matrices (Behymer and Hites 1988; Budzinski et al. 1997; Costa and Sauer 2005; Saber et al. 2006; Uhler and Emsbo-Mattingly 2006; Yunker et al. 2002). Nevertheless,  $FL0$  is more difficult for organisms to metabolize and is not easily photodegraded (Behymer and Hites 1988; Yunker et al. 2011), but is more prone to evaporation and dissolution than  $PY0$  (Table 2). In contrast,  $FL0$  biodegrades preferentially over  $PY0$  in soil (Tobiszewski and Namiesnik 2012 and references therein).

#### 5.4.2 Other Fluoranthenic and Pyrenic Ratios

For petrogenic–pyrogenic discriminations, several less common ratios use fluoranthenic ( $FL_n$ ) and pyrenic ( $PY_n$ ) isomers in conjunction with alkyl PAHs. The ratio of methylfluoranthene plus methylpyrene to pyrene ( $FP1/PY0$ ) can be used to

distinguish pyrogenic ( $\approx 0.3$ ) from petrogenic ( $\approx 4$ ) sources (Bucheli et al. 2004). If multiple sources influence the P1/P0 ratio, then the FP1/FL0 ratio can be used to detect anthropogenic inputs (Gustafsson 1997; Pereira et al. 1999 and references therein); in such cases, an FP1/FL0 > 1 indicates petroleum contamination. However, such ratios (e.g., FP1/FL0) may be influenced by weathering (Neff et al. 2005).

Ratios of FP1/FP0 < 1 (Fig. 13) are said to indicate combustion (Yunker et al. 2002). Saha et al. (2009) used a more conservative upper FP1/FP0 value of 0.5 for



**Fig. 13** The ratio of FP1/FP0 for different sources. *Degradation arrow* drawn assuming that parent PAHs are less stable than their alkylated homologues. See Fig. 9 for the symbols and the text for explanation

pyrogenic inputs, probably because  $FP1/FP0 < 1$  for some petrogenic sources such as coals (Fig. 13; Yunker et al. 2002). The  $FP1/FP0$  and the  $PA1/PA0$  ratios may not correlate with emissions from old vehicles (Yan et al. 2006; Yunker et al. 2002). Yunker et al. (2002) suggested that the  $FP1/FP0$  ratio is better used for detecting combustion and is less variable than the  $PA1/PA0$ .

Sporstol et al. (1983) showed that the alkyl fluoranthene plus pyrene (alkylation level: 1-3) homologue distributions of soot and oil differ significantly. The ratios of  $\frac{FP0}{FP2 + FP3}$  and  $\frac{BC0}{C2 + C3}$  (proportion of alkylated PAHs) were used by Stout et al. (2003) to classify pyrogenic and petrogenic sources. These thermal parameters range from 1.9 to 3.6 for pyrogenic sources, whereas petrogenic values (crudes) range from 0.05 to 0.06 (Stout 2007). In coal tars, the  $\frac{FP0}{FP2 + FP3}$  ratio is more prone to changes from evaporation than from biodegradation (Uhler and Emsbo-Mattingly 2006). Thus, caution is advised when applying  $FP0/FP2 + FP3$  to different matrices.

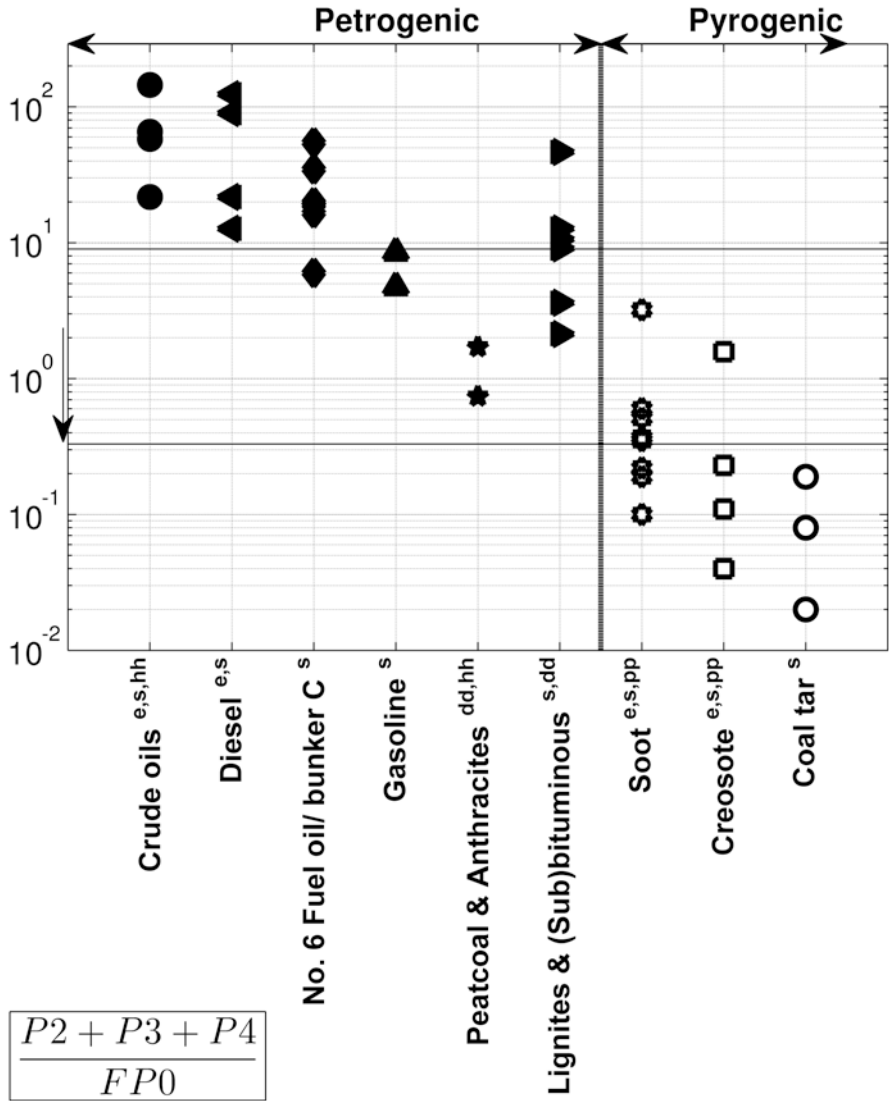
Methylpyrenes and benzofluorenes (MW 216) are relatively stable isomers that are suitable for comparing light fuel oils (e.g., gas oil), which rapidly degrade in the environment (Dahlmann 2003; Hansen et al. 2007; Uhler and Emsbo-Mattingly 2006). In addition, the ratios of benzo[*a*]fluorene/4-PY1, benzo[*b+c*]fluorene/4-PY1, 1-PY1/4-PY1 and 2-PY1/4-PY1 are recommended in the oil spill identification methodology of the European Committee for Standardization (Hansen et al. 2007).

Roush and Mauro (2009) used the benzofluorenes to methylpyrene ratio to exclude petroleum as having contaminated soils and sediments. Contamination from coal tar or creosote is possible if this ratio is  $>1$ . Craig and Mauro (2012) reported that, in sediments contaminated with coal tar, the ratio of benzo[*b+c*]fluorene to monomethylpyrenes is little changed by weathering and can be used to discriminate sources such as coal tar (3.9) and MGP tar (1.5).

The PAH pyrogenic indicator (PPI)—not to be confused with the pyrogenic index (Sect. 5.8)—is the  $\frac{P2 + P3 + P4}{FP0}$  ratio (Fig. 14). It reflects the relative abundance of petrogenic PAHs and decreases as the pyrogenic contamination increases (Bence et al. 2007; Luo et al. 2008; Page et al. 1999). According to Neff et al. (2005), the PPI is almost always higher than 9 for petrogenics (50–100 for Exxon Valdez crude at different stages of weathering) and lower than 0.3 for pyrogenic PAHs. If  $TPAH > 0.1 \mu\text{g/g}$ , and  $PPI < 4$ , then the PAH contamination probably has a pyrogenic component (Bence et al. 2007; Neff et al. 2006; Page et al. 1999). Values of PPI for wood burning and creosote have also been reported (Fig. 14; Neff et al. 2006; Page et al. 1999).

The PPI has been used to show that forest fire fallout contributed to PAHs in nearshore subtidal sediments (Page et al. 1999). The PPI was used to differentiate petrogenic from pyrogenic PAHs in sediments and biological samples at the site of the 1989 Exxon Valdez oil spill, and also in other cases (Neff et al. 2005, 2006; Pies et al. 2008). Bence et al. (2007) showed that PPI is unaffected by weathering.





**Fig. 14** The ratio of  $P2 + P3 + P4/FP0$  or  $PPI$  for different sources. See Fig. 9 for the symbols and the text for explanation

The degradation rates of FL0 and PY0 are similar to that of P4, and when mass losses of spilled oil approach 60%, the PPI is undefined (Bence et al. 2007; Neff et al. 2006). Extensively weathered oils have reduced PPI values which are higher than 5.5 (Neff et al. 2006).

### 5.4.3 The Ratio of Benz[*a*]anthracene to Chrysene<sup>6</sup>

Benz[*a*]anthracene (BaA) is preferentially produced over chrysene (C0) during the combustion of fossil fuel or of biomass (Dvorska et al. 2011; Yunker et al. 2002). Yunker et al. (2002) have suggested that  $BaA/C0 < 0.25$  indicates petroleum sources,  $0.25 < BaA/C0 \leq 0.5$  indicates mixed sources and  $BaA/C0 \geq 0.5$  indicates combustion (e.g., vehicular emissions). In contrast, De Luca et al. (2004) have suggested that the transition point from petrogenesis to pyrogenesis is at  $BaA/C0 = 1$ . Nevertheless, the  $BaA/C0$  ratio is well above 1 for gasoline and above 0.5 for coals (Fig. 15). Examples of pyrogenic sources below the threshold of 0.5 are creosote and the combustion of some coals, diesel and gasoline. Only anthracite combustion and some combusted diesels have  $BaA/C0$  values below 0.25.

The  $BaA/C0$  ratio has sometimes been used in conjunction with the IP/*ghi* ratio, to distinguish between automobile and domestic heating sources (e.g., Dvorska et al. 2011; Sofowote et al. 2008), or to apportion the contributions from coal tar and paving bitumen to urban runoff and sediments (Ahrens and Depree 2010; Dupree and Ahrens 2007). BaP/BbF (five-ringed PAHs) and  $BaA/C0$  have been successfully used to differentiate Al smelter sludge from creosote pilings (Boehm and Saba 2008). The combination of A0/P0 (the inverse of P0/A0) and the  $BaA/C0$  ratio can be used to distinguish between pyrogenic sources and crude oils because both ratios are higher for pyrogenic sources (Wang et al. 1999b, 2001). Sofowote et al. (2009) factorized both the A0/P0 and the  $BaA/C0$  ratios into a new ratio that is more robust than both constituent ratios. Zeng and Vista (1997) found that the  $BaA/C0$  ratio correlated with the P1/P0 and P0/A0 ratios. However, the  $BaA/C0$  ratio correlates only weakly with the FL0/PY0 ratio (De Luca et al. 2004). Yunker et al. (2002) observed negligible amounts of BaA in wood combustion and used the  $BaA/C0$  ratio plus the DMP ratio to trace wood combustion.

The  $BaA/C0$  ratio is stable over different concentration ranges and aerobic degradation and evaporation conditions (Costa and Sauer 2005; Uhler and Emsbo-Mattingly 2006). However, caution is advised when only the  $BaA/C0$  ratio is used to distinguish different types of creosotes in sediments, especially if influences from urban background (lower ratio) or weathering are possible (Mauro 2008; Stout et al. 2003; Yan et al. 2005, 2006). Compared with C0, BaA is more easily photolyzed and has a different environmental behavior (Dvorska et al. 2011; Tobiszewski and Namiesnik 2012; Yunker et al. 2002). Yunker et al. (2002) reported that the photolysis patterns for the  $BaA/C0$  and the P0/A0 ratios were similar. Chrysene is the more stable isomer and BaA can convert to C0 during degradation (De Luca et al. 2004; Soclo et al. 2000). Therefore, the applicability of  $BaA/C0$  in weathered sediments may be questionable (Stout et al. 2003; Yan et al. 2005; Yunker et al. 2002).

---

<sup>6</sup>The  $BaA/228$  (i.e., the denominator is the sum of PAHs that have MW = 228) is sometimes used instead of  $BaA/C0$ , because of the coelution of triphenylene (TPH) and chrysene (e.g., Gogou et al. 2000). In this paper no discrimination is made between the two ratios.

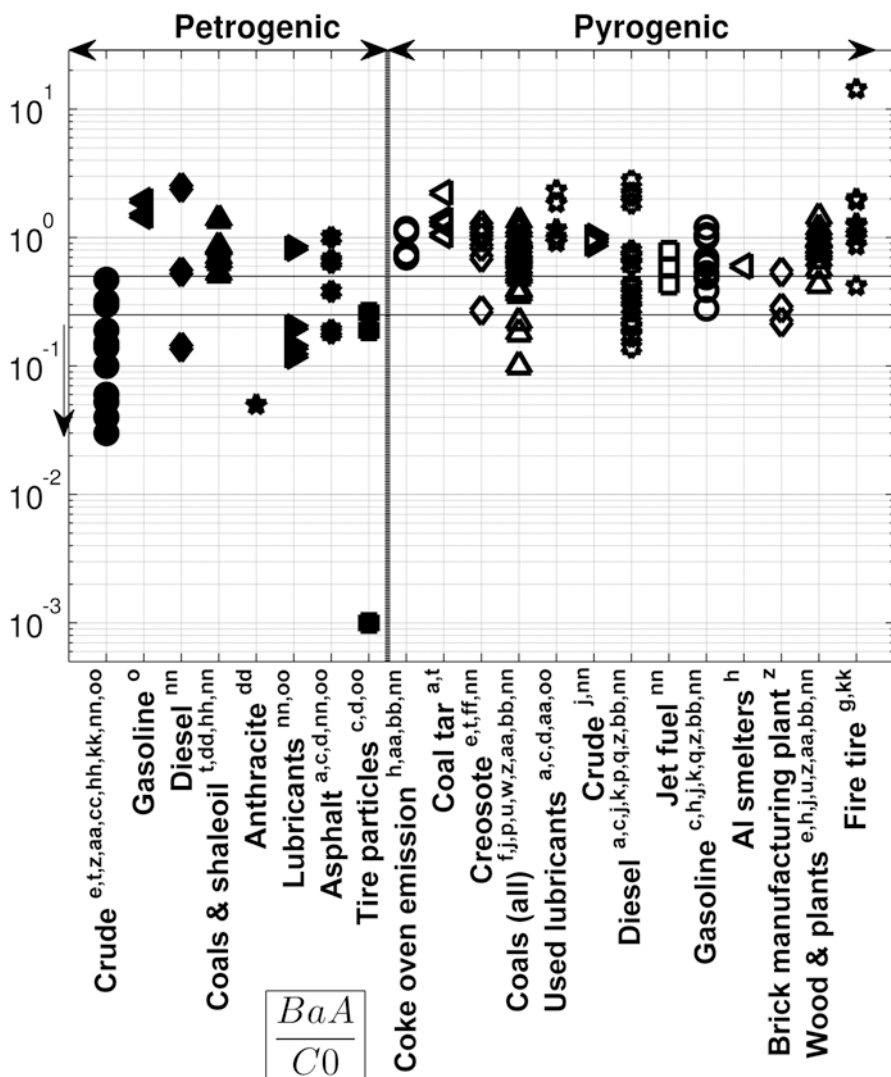


Fig. 15 The ratio of  $BaA/C_0$  for different sources. See Fig. 9 for the symbols and the text for explanation

#### 5.4.4 Alkylated Chrysenes

Combustion usually yields the characteristic pyrogenic distribution ( $C_0 > C_1 > C_2 > C_3$ ) for chrysenes in soots of diesel, wood, coal, refined petroleum products, etc. However, the dominance of parent over alkylated PAHs in diesel soots is unique for chrysenes (Wang et al. 1999b). Other LMW (2–4 ringed) PAHs volatilize and are

incorporated uncombusted into diesel soots, retaining the bell-shaped distribution (Fig. 4 and Fig. S16, Supporting Material), which readily modifies to a PAH0 < PAH1 < PAH2 < PAH3 profile during weathering. Furthermore, the ratio of alkylated chrysenes to the *five target alkylated PAH homologues* is significantly higher in diesel soots (0.1–0.2) or in diesel burn residues than in diesel fuel (0.001) or other weathered fuels (Wang et al. 1999b).

Urban background or pyrogenic impact on sediments can be deduced from high ratios of chrysene to dimethylchrysenes (i.e., predominance of non-alkylated parent PAHs over their dimethyl- or ethyl-alkylated equivalents) (Stout et al. 2004). This C0/C2 ratio is minimally affected by degradation, can indicate pyrogenic origin if higher than 1 (Battelle Memorial Institute et al. 2003), and can be used to distinguish between different pyrogenic sources (Roush and Mauro 2009). Similarly, Wang et al. (2001) used the relative distribution of the highly degradation-resistant alkyl (C0 to C3) chrysene series to apportion sources by using mass balance equations.

The  $\frac{BC0}{C2 + C3}$  ratio is a measure of the alkylation (Stout et al. 2003) and can be used to determine pyrogenic or petrogenic origin. For example, the contribution of a petroleum component (lubricating oil) to urban background enabled Stout et al. (2003) to distinguish creosote from urban background by using the BC0/C2 + C3 ratio. The measured values for the BC0/C2 + C3 ratio given by Stout (2007) for contributions to sediments are 0.11–0.12 for crude, 0.28–0.27 for petrogenic and 4.11–7.86 for pyrogenic. In coal tars, the biodegradability of the BC0/C2 + C3 ratio is moderate and its evaporability is negligible (Douglas et al. 2007a; Uhler and Emsbo-Mattingly 2006). Saha et al. (2009) suggested that the BC0/BC1 ratio can be used to distinguish pyrogenic (>1) from petrogenic sources. Costa et al. (2004) used the Cn/FPn double ratio plot ( $n = 1, 2$ ) to distinguish MGP tars from background pyrogenic contamination.

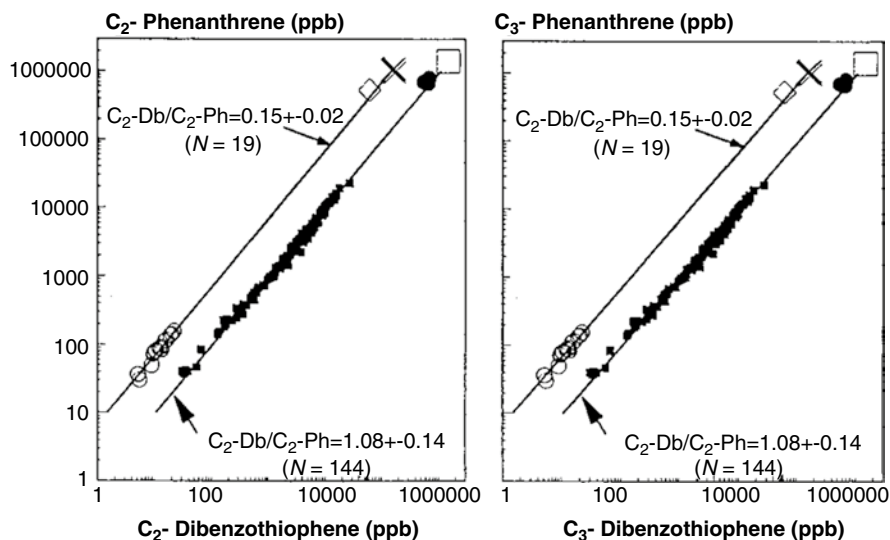
Several weathering ratios that use chrysenes have been reported. Degradation increases the ratios C2/P2 and C3/P3 at a relatively constant rate (Barakat et al. 2001; Bence et al. 1996). Additionally, these ratios can assist in discriminating distillates such as diesel (when alkylated chrysenes are absent the ratios approach zero) from unweathered crude oil (Bence et al. 1996). Similarly, the ratio of the C2-C4 alkylchrysenes to the P2-P4 alkylphenanthrenes increases as the weathering proceeds, because phenanthrenes are more soluble in water and are thus removed from the oil faster (Page et al. 2003). In general, ratios of chrysenes to the more degradable two- and three-ringed PAHs can be used to ascertain the weathering state of sediments (partly because of the low solubility of chrysenes in water) (Kim et al. 2008; Page et al. 1999). Such ratios are called weathering ratios (weathering and biodegradation greatly affect them). Weathering-sensitive ratios are usually combined with ratios that are unaffected by weathering, to resolve multiple sources and the extent of weathering (Barakat et al. 2001).

## 5.5 Sulfur PAH Indices

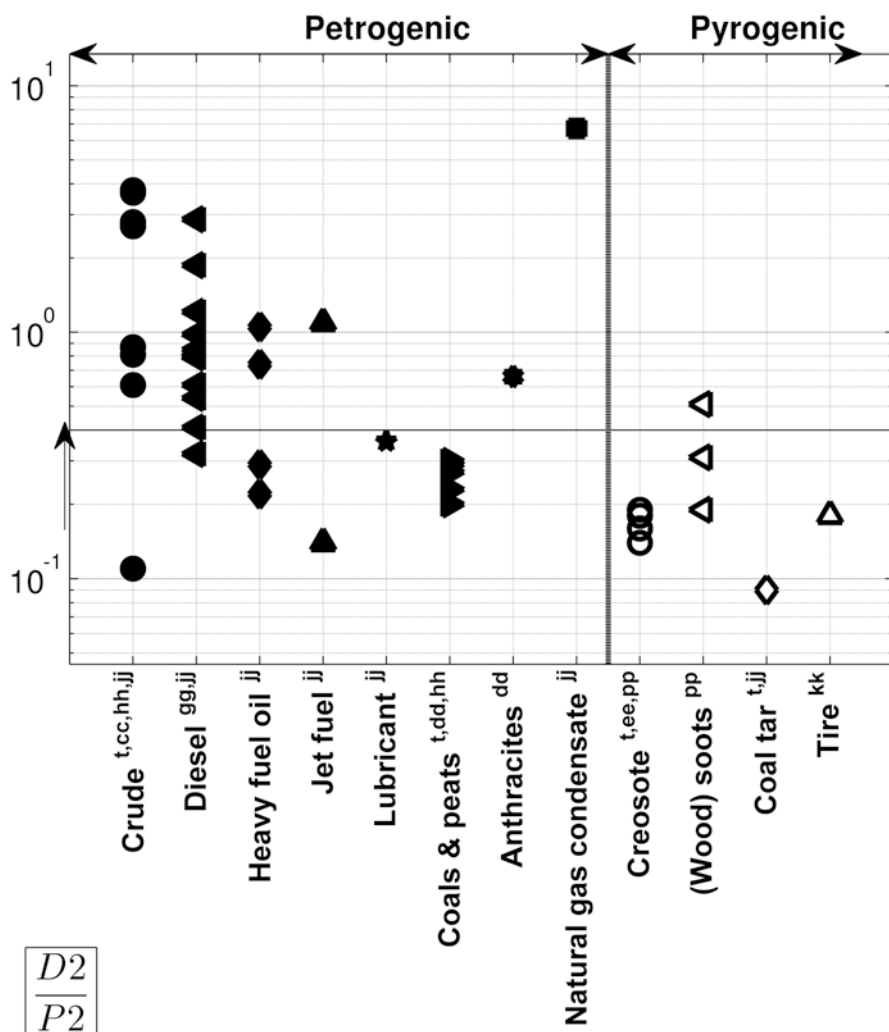
### 5.5.1 Ratios of Alkylated Dibenzothiophenes to Alkylated Phenanthrenes

The methyl dibenzothiophene/methylphenanthrene (D1/P1) ratio is an expression of the relative abundance of alkyl-substituted dibenzothiophenes, and has been used to apportion diesel and pyrogenic sources in sediments (Wang et al. 2001). The D1/P1 was used by Takada et al. (1990) to distinguish asphalt (0.78), diesel emissions (0.40) and fuel oil soot (0.05) in street dusts. Used in conjunction with the weathering ratio N2/P2, the D1/P1 ratio was useful for source identification in groundwater samples having dibenzothiophene concentrations  $>0.07$  ng/cm<sup>3</sup> (Hegazi and Andersson 2007).

Among the most popular ratios in oil spill identification are the D2/P2 and D3/P3 ratios (Dn/Pn-alkyldibenzothiophene/alkylphenanthrene). They are source ratios (almost constant because the compounds degrade at the same rate). They are also called “the petrogenic source ratios” (because they distinguish different petroleum sources) and “sulfur to non-sulfur ratios” (Wang et al. 1999a). Both ratios vary among products having different sulfur contents (e.g., diesel, crude) (Fig. 16; Fig. S3a, b, Supporting Material) and are useful in identifying such oil sources (e.g., distillate fuels from sour or sweet crude) (Hegazi and Andersson 2007; Stout et al. 2006). Small differences in the crude oil supplied by a refinery may greatly change these ratios (Hostettler et al. 2007; Stout 2007).



**Fig. 16** The discriminating power of the Dn/Pn ratios for different crudes (filled square weathered Exxon Valdez Crude, open circle prespill cores, filled circle Exxon Valdez, multiplication sign Katalla, open square ANS diesel, open diamond Cook Inlet). Adapted from Wang et al. (1999a), with permission, © Elsevier Science BV



**Fig. 17** The ratio of  $D2/P2$ . Evaporation leads to opposite *degradation arrow* direction (i.e., decreases ratio). See Fig. 9 for the symbols and the text for explanation

Using the double ratio plot of  $D2/P2$  versus  $D3/P3$ , Wang et al. (1999b) sufficiently resolved burn products and diesel fuel. Pyrogenic sources (coal tar, creosote and fire tire wipe) have values below 0.4 for both ratios (Fig. 17; Neff et al. 1998; Stout et al. 2001a; Wang et al. 1999b, 2006). Together with other PAH markers (e.g.,  $D1$ ,  $FL0$ ,  $PY0$ ), the  $Dn/Pn$  ratios have been used to characterize pyrogenic products mixed with petrogenic ones (Wang et al. 1999a, 2001).

The  $Dn/Pn$  ratios have been used to identify petrogenic sources (crudes, diesels, etc.) of different origin; for example, in the studies of the Gulf War and of the 1989 Exxon Valdez oil spills and their weathering products (Hostettler et al. 2007; Kim

et al. 2008; Page et al. 1999; Stout 2007; Stout et al. 2006; Wang et al. 1999a). Page et al. (1996, 1999) applied a two-component mixing model that used both  $Dn/Pn$  ratios and apportioned petroleum and background sources. However, this model cannot discriminate a source contribution of less than 3–8%. Similarly, Stout et al. (2006) apportioned different historic oil inputs (diesels of different blends) in non-aqueous phase liquids. Douglas et al. (2007b) used the  $Dn/Pn$  ratios in combination with the Nordtest method, to rule out spilled fuel oils in tarballs and mousse samples.

The success of the  $Dn/Pn$  ratios as diagnostic tools for heavy fuel oils that contain LMW or HMW PAHs is based on the fact that these ratios are not a strong function of TPAH (Douglas et al. 2007b). However, if all sources have the same sulfur content, or their upper boiling point (bp) is below those of D2, D3, P2, P3 (e.g., kerosene), then the  $Dn/Pn$  ratios are not applicable (Stout et al. 2006).

Both  $Dn/Pn$  ratios, especially the trimethyl one, are not significantly affected by heavy (bio) degradation—up to 98% depletion of total PAHs—for a range of petrogenic products (Douglas et al. 1996; Uhler and Emsbo-Mattingly 2006). Wang et al. (1999b) noted that both combustion and heavy degradation decrease the  $Dn/Pn$ . Natural weathering, long-term biodegradation and photo-oxidation will increase the  $Dn/Pn$  ratios, but evaporation is thought to slightly decrease them, rendering them inapplicable for source characterization (Hegazi and Andersson 2007; Kim et al. 2008; Page et al. 1999; Stout et al. 2006; Uhler and Emsbo-Mattingly 2006; Wang et al. 1999a, b).

Costa et al. (2004) used a version of the  $Dn/Pn$  ratio slightly modified by the addition of the respective anthracenic homologues to the denominator to distinguish between background and petroleum contamination. The  $D3/PA3$  and  $D2/PA2$  (alkyldibenzothiophenes to the sum of alkylphenanthrenes and alkylanthracenes, all with the same alkylation degree) are slightly affected by weathering and biodegradation of coal tars in the laboratory, although in field samples, degradation can significantly alter such ratios (Douglas et al. 2007a; Uhler and Emsbo-Mattingly 2006).

### 5.5.2 Other Dibenzothiophenic Ratios

The  $D3/P3$  ratio in conjunction with the  $Dn/Cn$  ( $n=2, 3$ ) ratios has been used to describe oil depletion and identify sources in subtidal sediment data (Hegazi and Andersson 2007; Stout et al. 2002; Wang and Fingas 2003; Wang et al. 1999a). Furthermore, the double ratio plot of  $P2/P3$  versus the  $D2/D3$  has been used as a weathering index for oil residues from the Exxon Valdez oil spill (Hegazi and Andersson 2007 and references therein).

### 5.5.3 Alkyldibenzothiophene and Benzonaphthothiophene Distributions

The distribution of methyldibenzothiophenes (1-D1, 2-D1, 3-D1, 4-D1) is characteristic for particular crudes, and the methyldibenzothiophene ratios exhibit excellent consistency with weathering (so they can be used as weathering ratios), even for

burned oils (Hegazi and Andersson 2007; Wang and Fingas 1995). Wang and Fingas (1995, 2003) established a database of the methyl dibenzothiophene ratios for crudes, weathered and biodegraded oils, and other petroleum products. The ratios pair of  $\frac{1-D1}{4-D1}$  versus  $\frac{2-D1+3-D1}{4-D1}$  exhibits a satisfactory discriminating ability for different oils (Hegazi and Andersson 2007). Alternatively, such ratios may be used as biodegradation indicators, because 1-D1 is most affected by biodegradation, whereas 2-D1 and 3-D1 are the least affected by biodegradation (Faksness et al. 2002; Hegazi and Andersson 2007). Therefore, prior knowledge of the weathering state of a sample is necessary before the methyl dibenzothiophene ratios can be used either as source or weathering indicators (Wang and Fingas 1995). Furthermore, the 1-D1/4-D1 ratio correlates with coal vitrinite reflectance (Dzou et al. 1995; Hansen et al. 2007; Stout and Emsbo-Mattingly 2008). As the coals mature, the value of the 1-D1/4-D1 increases, because the less stable 4-D1 decreases (Dzou et al. 1995).

The dimethyl dibenzothiophenes, together with the methyl dibenzothiophene distributions, may further assist in the identification of oils (Hegazi and Andersson 2007), or to distinguish between coal combustion and automobile emissions (Allan 1999; Marvin et al. 2000 and references therein). According to these authors, the D1/D0 ratio is distinct for diesel emissions (1.6–2.9) and coal tars or coke oven condensates (0.11–0.18). Similarly, the D2/D0 ratio ranges from 2.7 to 4.2 for diesel vehicles, vs. a range of 0.03–0.04 for coal tars and coke oven condensates. Allan (1999) points out that coke oven emissions yield  $D2/D0 < 2.4$ . The D2/D0 ratio is increased by biodegradation, solubilization and evaporation, whereas photo-oxidation decreases it (Allan 1999).

Benzonaphthothiophenes are sometimes used for source discrimination tasks. For example, the ratio of IP to benzo[*b*]naphtho[2,1-*d*]thiophene has been used to distinguish vehicle emissions (<0.4) from urban heating sources (>0.9) in Gliwice, Poland (Bylina et al. 2005). However, this ratio is insensitive to coke oven emissions. Allan (1999) reported that the benzo[*b*]naphtho[2,1-*d*]thiophene/benzo[*b*]naphtho[2,3-*d*]thiophene is characteristic for diesel emissions (>3.2), whereas coal tar or coke oven emissions exhibit lower values of this ratio. For such sources, D0 and dibenzonaphthothiophene ratios are far superior to other PAH ratios (BeP/BaP, *ghi*/BeP, BkF/BeP, *ghi*/BaP) (Allan 1999).

## 5.6 HMW Five- and Six-Ringed PAHs

### 5.6.1 Ratio of Benzo[*e*]pyrene to Benzo[*a*]pyrene

The benzo[*e*]pyrene/benzo[*a*]pyrene (BeP/BaP) ratio is indicative of aging particles when >1, and has been used as a photodegradation indicator in atmospheric aerosols (Okuda et al. 2002; Tan et al. 2009; Tobiszewski and Namiesnik 2012). The BeP/BaP ratio is not affected by biodegradation and evaporation in sediments, tarballs, tars and in creosote-contaminated sites (Costa and Sauer 2005; Stout et al. 2003; Uhler and Emsbo-Mattingly 2006; Zakaria and Takada 2007).



Together with the FL0/PY0 ratio, the BeP/BaP has successfully been used to differentiate MGP tar residues from background contamination (Costa et al. 2004), and other combustion sources (Dickhut et al. 2000). Ahrens and Depree (2010) discriminated bitumen from coal tar in sediments by using the BeP/BaP ratio in conjunction with IP/ghi and BaA/CO.

The literature ratios of BeP/BaP are >1 for most petrogenic sources, except for some coals (Fig. 18). BeP/BaP is usually <2 for pyrogenic sources, and this

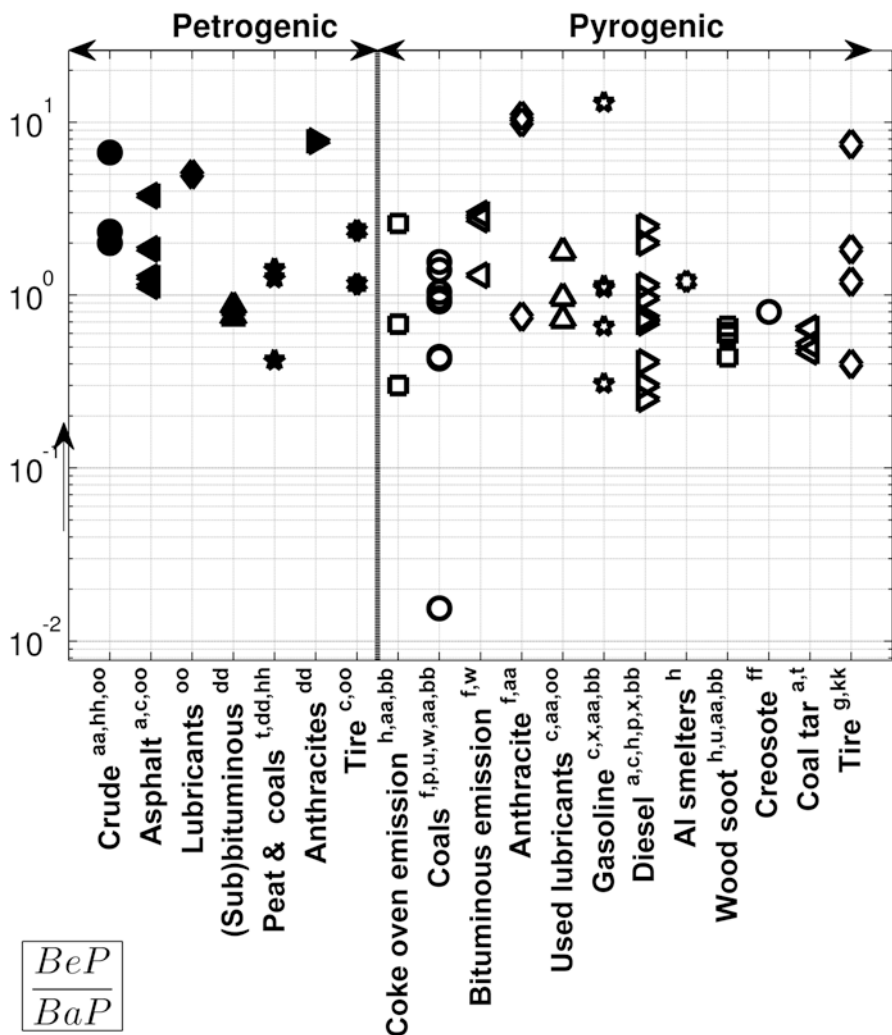


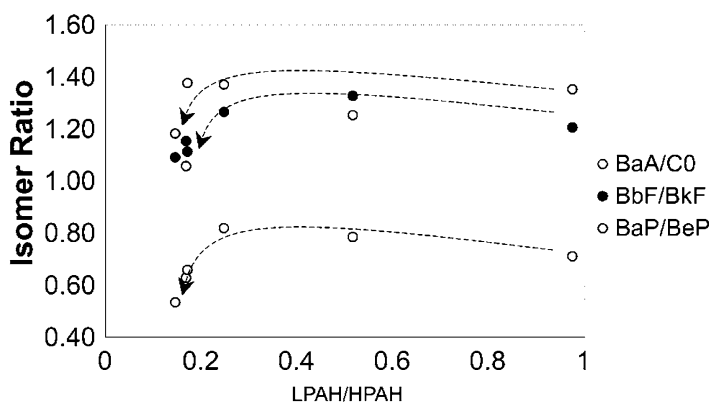
Fig. 18 The ratio of BeP/BaP for different sources. See Fig. 9 for the symbols and the text for explanation

range overlaps with the range of BeP/BaP in petrogenic sources. The combustion of bituminous and anthracite coals yields BeP/BaP ratios higher than 1.5 and 2.5, respectively. The combustion of diesel and gasoline occasionally yields higher ratios. Therefore, a limited number of sources may be discriminated by using the BeP/BaP ratio (e.g., wood soots seem to have a narrow range for BeP/BaP; Fig. 18). Further study is necessary to verify the applicability of the BeP/BaP ratio under environmental conditions, especially in regard to the reactivity of BaP in air (Abrajano et al. 2003). Thus, the BeP/BaP ratio is suitable for non-atmospheric pyrogenic characterization (BeP/BaP <1) because of the low concentrations of these isomers in petrogenic products (e.g., fuel oils, crudes) and because sediments protect BeP and BaP from degradation to the same degree.

### 5.6.2 Ratio of Benzo[*b*]fluoranthene to Benzo[*k*]fluoranthene

The ratio of benzo[*b*]fluoranthene to benzo[*k*]fluoranthene (BbF/BkF) has been used to differentiate between two or more pyrogenic sources in urban soils or in sediments (e.g., Morillo et al. 2008b; Walker and Dickhut 2001). The BbF/BkF has distinct values for pyrogenic emissions for an aluminum smelter (2.5–2.9), coke oven (3.7), motor vehicles (1.3), creosote (1.2) and wood soot (0.9) (Dickhut et al. 2000; Fig. 19; Stout et al. 2003; Tobiszewski and Namiesnik 2012). BbF/BkF correlates with coal rank or with other petrogenic PAHs (Jiang et al. 2009; Stout and Emsbo-Mattingly 2008).

Weathering or urban background may limit the applicability of BbF/BkF for different creosote types (Stout et al. 2003). However, under aerobic degradation and evaporation conditions, the BbF/BkF ratio is minimally influenced (Uhler and Emsbo-Mattingly 2006).



**Fig. 19** LPAH/HPAH as a proxy of weathering and how certain ratios may be compromised after weathering. See Table 1 for PAH abbreviations. Adapted from Stout et al. (2003)

### 5.6.3 Perylene

Perylene (PER) ratios are useful for discriminating between natural and coal-derived PAHs. Low abundance of PER (<10% of TPAH, or of total five-ringed PAHs) may indicate non-natural production (Calvacante et al. 2009; Gogou et al. 2000; Wang et al. 2014). Conversely, high amounts of perylene (>10% of TPAH) indicate that the PAHs have a natural origin, and when PER is >10% of the total five-ringed PAHs, the main PER source is regarded to be diagenesis under reducing conditions (Boll et al. 2008; Calvacante et al. 2009; Fan et al. 2011; Stout et al. 2001a). The relative abundance of PER over five-ringed PAHs ( $B[b+k]F + BaP + BeP + DA$ ) has been used to identify whether the PAH contamination in intertidal sediments in Brazil was of natural or petrogenic origin (De Fatima et al. 2007), and to estimate the contribution of fluvial PAHs to coastal sediments (Luo et al. 2008).

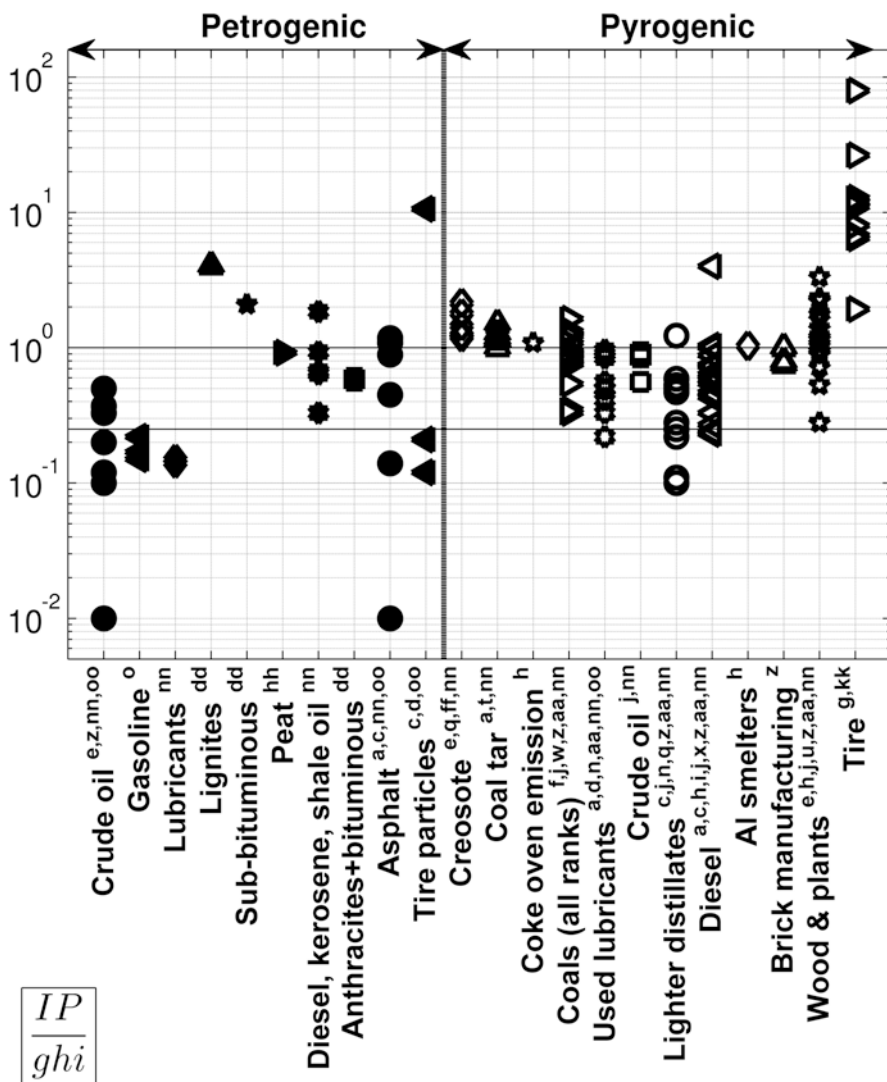
The PER/BeP (Gogou et al. 2000) and PER/BaP (Stout et al. 2001a) ratios can be used to identify that PAHs have a natural origin. The PER/PY0 ratio has been used by Abrajano et al. (2003) to indicate diagenetic origin for retene. If such ratios are high, the PER is from natural or petrogenic sources (e.g., coals). The PER/BaP ratio is recalcitrant under aerobic and evaporative conditions in sediments (Uhler and Emsbo-Mattingly 2006).

### 5.6.4 Ratio of Indeno[1,2,3-*cd*]pyrene to Benzo[ghi]perylene

The indeno[1,2,3-*cd*]pyrene/benzo[ghi]perylene (IP/*ghi*) ratio has been used by several researchers to distinguish/apportion distinct pyrolytic sources (and, specifically, automobile sources) of contamination in sediments (Agarwal 2009; Larsen and Baker 2003; Magi et al. 2002; Morillo et al. 2008b; Park et al. 2002; Sicre et al. 1987; Van Drooge et al. 2012; Zhang et al. 2005). Examples include automobile exhausts, gasoline emissions, coal-fired domestic heaters, biomass combustion and other forms of combustion. Sometimes the IP/*ghi* ratio is studied in conjunction with the dimethylphenanthrene ratio (DMP), the BaA/C0 or the FL0/PY0 ratios (Dvorska et al. 2011; Walker and Dickhut 2001; Yunker et al. 2002).

In Fig. 20, the IP/*ghi* is greater than 0.25 for most pyrogenic sources except for used lubricants and the combustion of gasoline, of jet fuel, and occasionally of diesel. If such specific sources are absent, an IP/*ghi* < 0.25 implies strong petroleum inputs (Yunker et al. 2002). If  $0.25 < \text{IP}/\text{ghi} < 1$ , mixed sources are possible. Ratios > 1 imply combustion sources if certain petrogenics (e.g., asphalt, tire particles, coals) are excluded. Wood and coal combustion may be discriminated by the IP/*ghi* ratio, but they sometimes yield IP/*ghi* < 1 (Fig. 20; Guillon et al. 2013). Furthermore, patterns for pyrogenic sources (e.g., automobile) are hardly distinguishable from each other in Fig. 20 because IP/*ghi* ratios for vehicle, diesel emissions and other pyrogenic sources overlap. For this reason, PAH patterns from local sources should be scrutinized before the IP/*ghi* is used as a pyrogenic indicator for atmospheric emissions.

It has been argued that there is uncertainty about the IP/*ghi* ratio, its threshold values, and its correlation with other ratios (Yunker et al. 2002). Yan et al. (2006) reported that the IP/*ghi* had little to no correlation with the  $\delta^{13}\text{C}_{\text{py}}$  or with the FL0/



**Fig. 20** The ratio of  $IP/ghi$  for different sources. Degradation depends heavily on particle color for pyrogenics and is highly variable. See Fig. 9 for the symbols and the text for explanation

PY0 in New York sediments. By means of fugacity model calculations, Zhang et al. (2005) classified the  $IP/ghi$  ratio as being superior to  $FL0/PY0$ ,  $A0/P0$ ,  $BaP/ghi$ ,  $BbF/BkF$  and  $BaA/C0$  for source apportionment in different media, when the contamination resulted from atmospheric emissions. Uhler and Emsbo-Mattingly (2006) reported that the  $IP/ghi$  ratio is stable in tar-contaminated sediment under aerobic and evaporation conditions. However, weathering and urban background may render the  $IP/ghi$  not applicable to creosote characterization (Stout et al. 2003).

A probable explanation for the uncertainty of the  $IP/ghi$  is the differential degradation of the two PAHs in the atmosphere. Both isomers degrade at about the same rate when they are attached to black particles, but IP attached to gray particle degrades faster than  $ghi$ , whereas IP attached to white particles degrades more slowly than  $ghi$ , and IP attached to red particles degrades more variably than  $ghi$  (Behymer and Hites 1988). Other studies have also suggested that particle association is very important for understanding photodegradation effects on the  $IP/ghi$  ratio (Tobiszewski and Namiesnik 2012 and references therein).

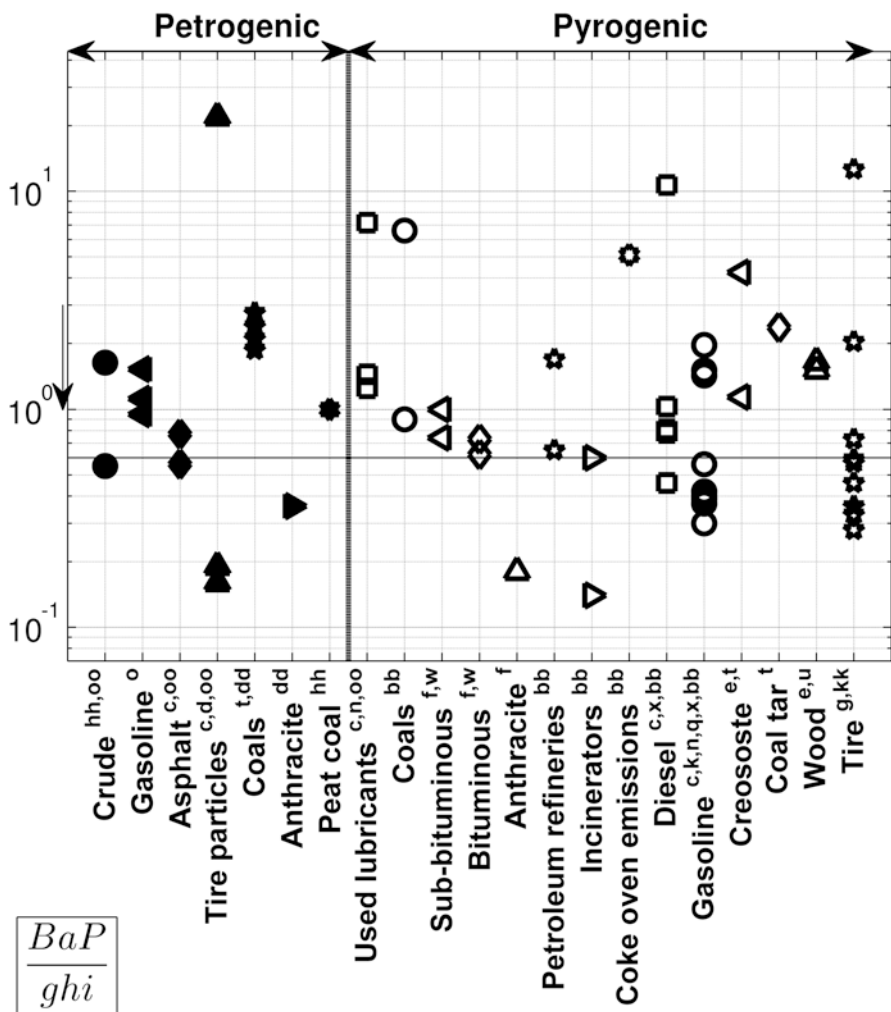
## 5.7 Non Isomer Ratios

According to Costa and Sauer (2005), when the more recalcitrant PAH isomer pairs (e.g., 4ring/4ring or 5ring/5ring) cannot provide enough resolution in double ratio plots, then non isomer ratios (e.g., five- over six-ringed PAHs) may be used. It is also possible to input non isomer ratios into a PCA/PMF model. For such a case, Christensen and Tomasi (2007) proposed an external normalization of the ratio (i.e., using a reference material).

### 5.7.1 Ratios of Five- to Six-Ringed PAHs

Some authors (Boitsov et al. 2009; Bucheli et al. 2004) have found that the  $BaP/ghi$  ratio is correlated with pyrogenic PAHs, whereas other researchers (Alam et al. 2013; Bucheli et al. 2004; Jiang et al. 2009; Ravindra et al. 2008) have investigated whether traffic sources in soils can be discriminated (e.g., by a  $BaP/ghi$  ratio  $< 0.6$ ) from the combustion of coal, wood or oil. Jiang et al. 2009 used both the  $BaP/ghi$  and the  $IP/ghi$  ratios to identify PAHs from automobile exhausts. Lehndorff and Schwark (2004) used the  $BaP/ghi$  ratio together with the  $FL0/PY0$  ratio to investigate biomass burning (indicated by a high ratio). The  $BaP/ghi$  ratio is prone to photodegradation, as BaP decomposes faster in the atmosphere (e.g., Alves et al. 2009). The literature data in Fig. 21 show the low discriminating power of the  $BaP/ghi$  ratio. For example, the  $BaP/ghi$  ratio for traffic sources has intermediate values that overlap the values of other pyrogenic and petrogenic products. Nevertheless, the  $BaP/ghi$  ratio may be used in certain situations, for example, when PAH sources are limited and have  $BaP/ghi$  values in a relatively narrow range (e.g., wood combustion, some coals, etc.; see Fig. 21).

Another traffic indicator, the ratio of  $BeP/ghi$ , is sometimes studied together with the  $IP/ghi$  (Alves et al. 2009; Tan et al. 2009). In a study conducted in Malaysia (Okuda et al. 2002),  $BeP/ghi$  values for diesel vehicles (1.1), gasoline vehicles (0.4), wood burnings (0.9), smoke hazes (0.3) and coal burnings (2.2) were reported. Therefore,  $BeP/ghi$  has been used to discriminate traffic sources, specifically gasoline, from non-traffic sources such as wood burning (Jensen et al. 1993; Larsen and Baker 2003; Okuda et al. 2002).



**Fig. 21** The ratio of  $BaP/ghi$  for different sources. See Fig. 9 for the symbols and the text for explanation

Together with the  $BeP/ghi$  ratio, the  $Cor/BeP$  ratio (six over five rings) has been used to distinguish or apportion traffic sources (1.8) and non-traffic sources (0.3) (Daisey et al. 1986; Jensen et al. 1993; Larsen and Baker 2003 and references cited by these authors). When doing so, there are two equations to be solved simultaneously (Larsen and Baker 2003). Applying this method at different locations revealed significant differences for the  $Cor/BeP$  ratio (>20%). Thus, location-specific source inventories are required prior to application. If only the  $Cor/BeP$  is available, then it can be assumed that the excess  $BeP$  is unrelated to traffic (Larsen and Baker 2003). Alternatively, the  $Cor/IP$  ratio may be used to distinguish gasoline from wood burnings (Okuda et al. 2002).

### 5.7.2 Ratios of Four- to Five-Ringed PAHs

The benz[*a*]anthracene/benzo[*a*]pyrene (BaA/BaP) ratio is little influenced by photodegradation and has been used (sometimes together with the FL0/PY0 ratio) to identify enhanced industrial emissions or to distinguish diesel or wood emissions from gasoline emissions (Lehndorff and Schwark 2004; Zhu et al. 2011). The BaA/BaP ratio may be adequate to distinguish coal tar and creosote residues from urban background PAHs (Costa and Sauer 2005; Costa et al. 2004). Wood combustion has a BaA/BaP ratio of about 1 (Lai et al. 2011 and references therein).

Low pyrene/benzo[*a*]pyrene (PY0/BaP) ratios indicated a negligible contribution of terrigenous flows into the aquatic system, whereas PY0/BaP > 10 indicated petrogenic sources (De Luca et al. 2004). The PY0/BaP ratio may be used to discriminate coal from wood combustion, but may not be applied to discriminate between combustion products of different wood species (Guillon et al. 2013). PY0/BaP values have been reported for diesel ( $\approx 10$ ), gasoline emissions ( $\approx 1$ ) and wood combustion ( $\approx 0.7$ ) (Lai et al. 2011; Ravindra et al. 2008 and articles cited by these authors).

## 5.8 Assignment of PAHs to Sources

One way to estimate the different source contributions to a sample is to empirically classify PAHs into pyrolytic, petrogenic or natural, even if some PAHs could have more than one origin (Page et al. 2006; Stout et al. 2004; Table 3). For instance, a typical urban background sediment containing approximately 74% of pyrogenic and 26% of petrogenic PAHs is distinctly different from some pyrogenic fingerprints (Battelle Memorial Institute et al. 2003). Assignment of PAHs to sources depends on the specific region examined (local sources) and on the analytical methods applied (number of PAH analytes), which is why the lists of PAHs assigned to sources differ between different studies (Jeanneau et al. 2008).

### 5.8.1 PCA/PMF Classification

PAH classification schemes occasionally emerge from a successful discriminant analysis application for a certain contamination case. The resulting compilation of PAH indices may have a local or wider applicability, and offers adequate resolution,

**Table 3** PAH apportionment to sources according to Stout et al. (2004)

Pyrogenic	Petrogenic	Mixed	Biogenic
A0, FL0, PY0, FP1, BaA, C0, C1, BbF, BkF, BeP, BaP, IP, DA, ghi	N0, N1, N2, N3, N4, B, F0, F1, F2, F3, AE, AY, DF, PA2, PA3, PA4, D0, D1, D2, D3, D4, FP2, FP3, C2, C3, C4	C0, PA1	PER

See Table 1 for PAH abbreviations

particularly in non-trivial cases, e.g., when urban background has to be discriminated from a petrogenic or, more often, a pyrogenic source. Using PMF in conjunction with PCA for the EPA16 PAHs and advanced chemical fingerprinting, Stout and Graan (2010) differentiated between creosote and urban background runoff. One confounding factor contributing to PAH contamination was two four-ringed parent PAHs (FP0). The other factor was eight HMW PAHs (BaA, C0, BbF, BjF, BaP, IP, DA, *ghi*). An increase in the abundance of the eight PAHs was attributed not to weathering, but to increased urban contribution.

Walker and Dickhut (2001) intrigued by abundances of FP0 (MW=202) or of the isomer sum BbF+BkF+BeP+BaP+PER (MW=252), plotted ratios of these sums to the parent compounds that have MW=202-276 (i.e., FL0+PY0+BbF+BkF+BeP+BaP+PER+IP+DA). Using double PAH ratio plots and PCA, they showed that both isomer-sum ratios ( $\Sigma\text{PAH}_{202}/\Sigma\text{PAH}_{202-276}$  and  $\Sigma\text{PAH}_{252}/\Sigma\text{PAH}_{202-276}$ ) explained a significant proportion of the variability (1st principal component). These results show that parent PAH compilations (e.g., fluoranthene-pyrene pair and HMW PAHs) are suitable for discriminating pyrogenic sources. However, it remains important to consider the influence of weathering or urban background when interpreting the results, in order to attribute the explained variability to the correct source factor (Stout et al. 2003; Walker and Dickhut 2001).

### 5.8.2 Low Versus High Molecular Weight Parent PAHs

A numeric index related to the pyrogenic-petrogenic differentiation into LMW and HMW PAHs is the ratio of these PAH fractions (De Luca et al. 2004; Fig. 22; Magi et al. 2002; Soclo et al. 2000):

$$L / H = \frac{\text{PA0} + \text{FP0}}{\text{BaA} + \text{C0} + \text{BkF} + \text{BaP} + \text{IP} + \text{DA} + \text{ghi}}$$

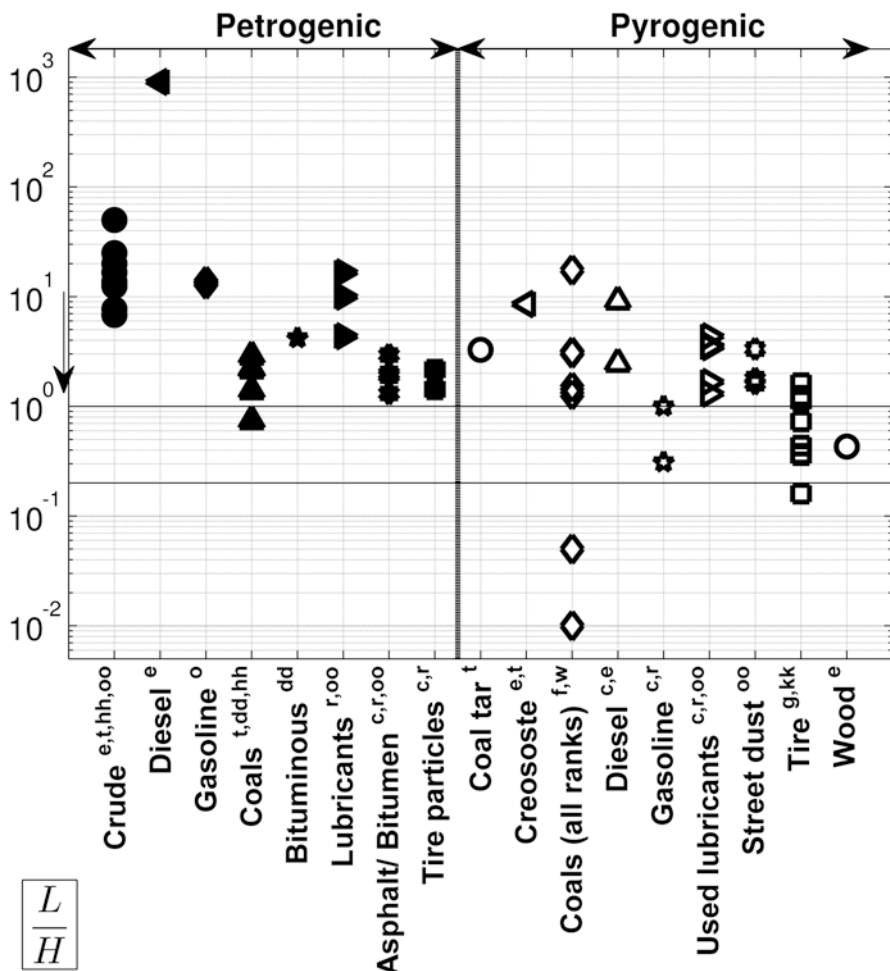
Others (Boonyatumanond et al. 2007; Zakaria et al. 2002) add P1 to “L”, and B[*b+j*]F, BeP, and optionally, Cor and PER to “H”, without the DA.

In some studies (De Luca et al. 2004; Karlsson and Viklander 2008; Mathieu and Friese 2012), the EPA 16 are divided into low molecular weight (LPAH, i.e., naphthalene to anthracene, 2-3 rings) and high molecular weight PAHs (HPAH, i.e., fluoranthene to indeno[1,2,3-*cd*]pyrene, 4-6 rings):

$$\text{LPAH} / \text{HPAH} = \frac{\text{N0} + \text{AE} + \text{AY} + \text{F0} + \text{PA0}}{\text{FP0} + \text{BC0} + \text{BbF} + \text{BkF} + \text{BaP} + \text{IP} + \text{DA} + \text{ghi}}$$

Chen and Chen (2011) add 2-P1 to the numerator. Stout et al. (2003) used all quantified compounds, including alkylated ones. The LPAH/HPAH ratio has been reported for several substances, including gasoline, diesel fuel, used lubricating oil and bitumen (Fig. 23; Karlsson and Viklander 2008). The ratio can differ for different brands of gasoline, diesel, and oil, depending on the differences in the crude oil properties and refinery processes.

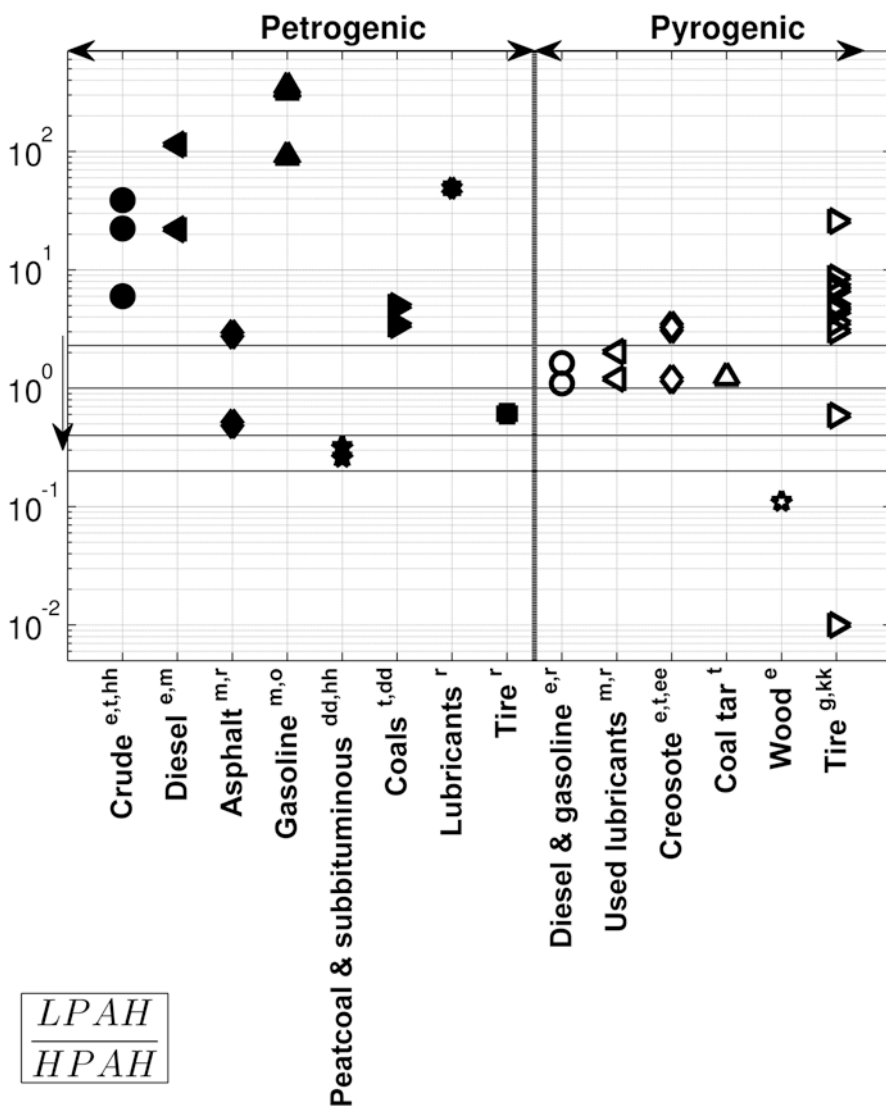




**Fig. 22** The  $L/H$  ratio for different sources. See Fig. 9 for the symbols and the text for explanation

For both ratios ( $L/H$  and  $LPAH/HPAH$ , Figs. 22 and 23), values  $<1$  indicate pyrogenic pollution and values  $>1$  indicate petrogenic contamination (De Luca et al. 2004; Karlsson and Viklander 2008; Magi et al. 2002). Nevertheless, several pyrogenics (coals, coal tars, diesel combustion etc.) show  $L/H >1$  (Fig. 22). Similarly,  $LPAH/HPAH$  lies in the range of 0.6-2.3 for pyrogenics, whereas petrogenics usually have  $LPAH/HPAH >2$  (Fig. 23).

The sum of concentrations of ten major non-alkylated PAHs (FL0, PY0, BaA, C0, B(b+k)F, BaP, BeP, IP, and *ghi*) is usually referred to as  $\Sigma$ COMB, and serves as a PAH indicator of combustion (Bucheli et al. 2004; Gogou et al. 2000; Hwang et al. 2003; Mostafa et al. 2009; Takada et al. 1990). Sometimes, BeP is not included in the  $\Sigma$ COMB expression (Bucheli et al. 2004; Ou et al. 2004). If BeP is added to the



**Fig. 23** The *LPAH/HPAH* ratio for different sources. See Fig. 9 for the symbols and the text for explanation

HPAH, then:  $\frac{\Sigma\text{COMB}}{\Sigma\text{PAH}} = \left( \frac{LPAH}{HPAH} + 1 \right)^{-1}$ . Accordingly, pyrolytic PAHs =  $\Sigma\text{COMB} /$

$\Sigma\text{PAH}$ , and  $\Sigma\text{COMB} / \Sigma\text{PAH} < 0.3$  (or  $LPAH / HPAH \geq 2.3$ ) indicates petroleum. When  $\Sigma\text{COMB} / \Sigma\text{PAH} > 0.7$  (or  $LPAH / HPAH \leq 0.4$ ) a pyrolytic origin is likely (Hwang et al. 2003; Tobiszewski and Namiesnik 2012). Phenanthrene and anthracene (MW = 178) are not included in  $\Sigma\text{COMB}$  because they may be of petrogenic origin, whereas perylene usually originates from natural sources (Gogou et al. 2000).

Since LMW PAHs are more susceptible to degradation (microbial, volatilization, and dissolution), sediments exhibit lower LMW/HMW ratios than the contamination source (Zakaria et al. 2002). As a workaround, De Luca et al. (2005) suggested using P0 as a possible marker of LPAH pollution in Olbia harbor (Italy). Furthermore, some combustion sources may produce LMW PAHs (Guo et al. 2007). Hence, source apportionment assignments using two- to three-ringed parent PAHs may become compromised after moderate weathering (Yan et al. 2006), rendering the LMW/HMW ratios (i.e., L/H, LPAH/HPAH) inadequate for discriminating crude oil from other major sources of sedimentary PAHs.

For the above reasons, the LPAH/HPAH ratio was used as a proxy of PAH weathering by Stout et al. (2003), who noted that if the LPAH/HPAH ratio becomes low ( $\approx 0.2$ ), then the ratios of BaA/C0, BbF/BkF, BeP/BaP decrease sharply and may fail to indicate the contaminant sources (Fig. 19). However, Costa and Sauer (2005) did not observe such trends for these ratios, and used the LPAH/HPAH ratio as a weathering index. Consequently, the L/H ratio is consistent with degradation and as such it was used to interpret the degradation in oil tarballs in Malaysia (Zakaria and Takada 2007). Summarizing, if LPAH/HPAH  $> 2.3$ , then recent input of petrogenic products is implied. Degradation or pyrogenic sources are likely when  $0.2 < \text{LPAH/HPAH} < 0.4$ , whereas at values of LPAH/HPAH  $< 0.2$ , degradation is likely to have occurred.

### 5.8.3 Ratios of Alkyl to Parent PAHs

The sum of the parent PAHs with masses 128, 178, 202, and 228, divided by the total PAH1-PAH4 homologues of these PAHs (N0, P0, A0, FL0, PY0, BaA, C0) is called the parent to alkyl (Par/Alkyl) ratio:

$$\left( \frac{N1 + N2 + N3 + N4 + PA1 + PA2 + PA3 + FP1 + FP2 + BC1}{N0 + PA0 + FP0 + BC0} \right)$$

The Par/Alkyl ratio was used by Yan et al. (2005, 2006, 2007) to distinguish petrogenic ( $> 2.3-4$ ) and pyrogenic ( $< 1$ ) sources (e.g., in oil spills even after extensive weathering in sediments). Apportionment values for petroleum combustion (1.1) and coal combustion (0.35) have also been reported (Yan et al. 2007). The correlation of Par/Alkyl with  $\delta^{13}\text{C}_{\text{py}}$ , FL0/PY0 and Ring456/TPAH (discussed below), implies that Par/Alkyl is a reliable PAH source indicator over large geographic areas or even long timespans (Yan et al. 2005, 2006).

Yunker et al. 2002 used an alkyl/ $\Sigma$ PAH ratio to infer pyrogenic or petrogenic sources in sediments. In this case,  $\Sigma$ PAH is the  $\Sigma(178-278)$  parent PAHs:

$$\frac{N1 + N2 + N3 + N4 + D1 + D2 + PA1 + PA2 + PA3}{PA0 + FP0 + BC0 + BeP + BaP + BbF + BjF + BkF + ghi + IP + DA + DcA}$$

and when alkyl/ $\Sigma$ PAH  $\leq 0.35$ , coal is ruled out, since natural background sources (e.g., shales, coal, and bitumen) have a ratio of 2.3–3.2 (Yunker et al. 2002).

The ratio of the sum total of four- to six-ringed PAHs (including parent and alkylated homologues) to total PAHs (Ring456/TPAH) is minimally influenced by the degradation of LMW PAHs (Yan et al. 2005, 2006). Ring456/TPAH is sensitive to inputs from fresh oil spills, and thus can be used to distinguish petrogenic (<0.4) and pyrogenic (>0.5) inputs (Yan et al. 2005, 2006). In the study of Yan et al. (2006), Ring456/TPAH correlated with FLO/PY0, but weathering rendered the Ring456/TPAH insensitive to petrogenic contributions. Furthermore, the applicability of the Ring456/TPAH is currently limited because of the small amount of data available to validate this ratio, particularly for environments where petrogenic sources are dominant (Yan et al. 2006).

#### 5.8.4 Pyrogenic Index

The pyrogenic index (PI) is the ratio of the sum of the concentrations of EPA priority unsubstituted three- to six-ring PAHs (sometimes coronene is also added: Wang et al. 2006) to the sum of the concentrations of the *five target alkylated PAH homologues* ( $\Sigma 5$ alkylated: naphthalenes, fluorenes, dibenzothiophenes, phenanthrenes and chrysenes) (Wang et al. 1999b, 2001, 2014):

$$PI = \frac{AY + AE + A0 + FP0 + BaA + BbF + BkF + BeP + BaP + Per + ghi + IP + DA}{N(1-4) + P(1-4) + D(1-4) + F(0-4) + C(0-4)}$$

PI ranges from 0.8 to 2.0 for pyrogenic sources and is much lower for petrogenics: <0.01 for crudes and <0.05 for heavy oils and heavy fuels (Fig. 24; Wang et al. 1999a, b, 2001, 2009). Thus, PI can be useful for distinguishing heavy fuels from crude oils or light refined products, and soot from crude oils or petroleum products (De Fatima et al. 2007; Wang et al. 1999a, b, 2001).

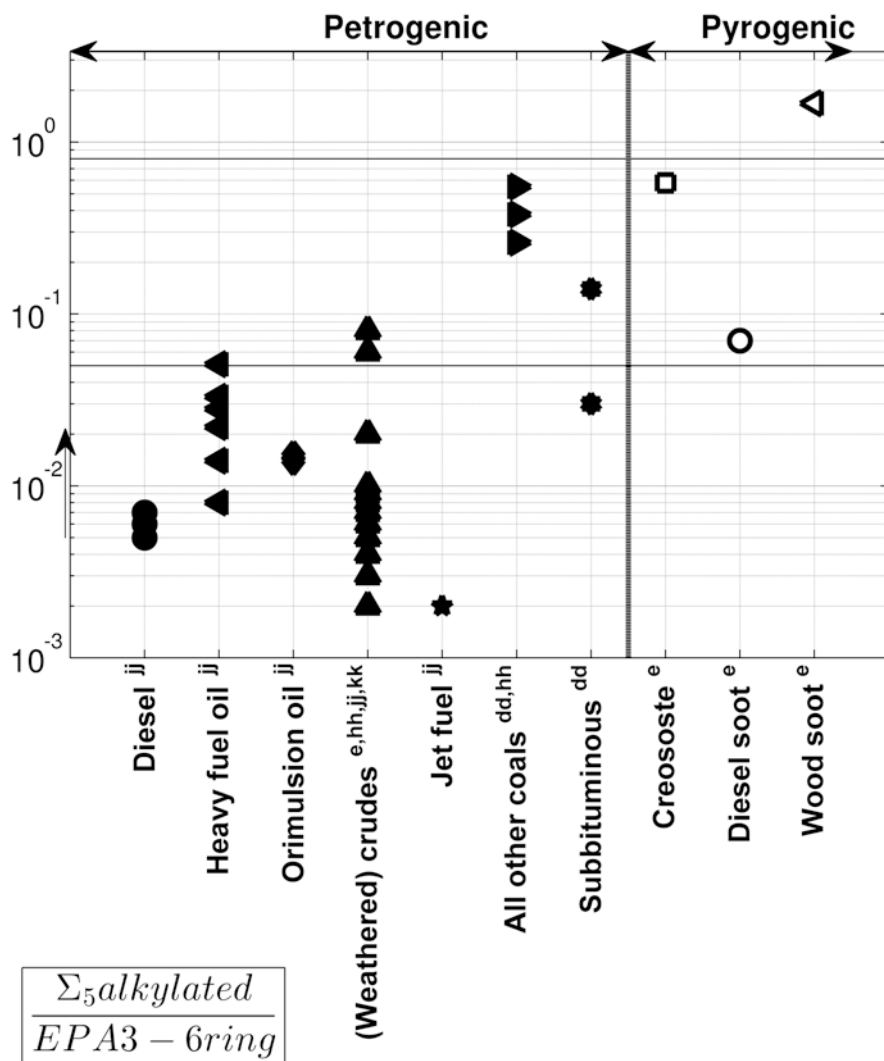
Compared with other indices, PI better resolves pyrogenic and petrogenic products (combustion significantly alters the value of PI) and is more accurate and consistent (Wang et al. 1999a, b). In contrast to combustion, weathering has little effect on PI, which makes it one of the most reliable PAH indices.

#### 5.8.5 Fossil Fuel Pollution Index

A precursor to PI for differentiating pyrogenic and petrogenic products is the fossil fuel pollution index (FFPI) (Iqbal et al. 2008; Stout et al. 2001b), defined as:

$$FFPI = \frac{N0 + N1 + N2 + N3 + N4 + D0 + D1 + D2 + D3 + \frac{1}{2}(P0 + P1) + P2 + P3 + P4}{TPAH}$$

FFPI is close to zero for most pyrogenic PAHs, whereas for sediments containing significant amounts of fossil-fuel PAH constituents, the FFPI is close to 1 (Iqbal et al. 2008). FFPI can thus be used as a method for apportioning the contribution of different PAH sources.



**Fig. 24** The *PI* for different sources. PER was omitted for data estimations from Burns et al. (1997). Degradation arrow is assumed as inferred from EVC crude weathering data from Burns et al. (1997). See Fig. 9 for the symbols and the text for explanation

## 6 Discussion and Conclusions

The various PAH distributions, which differ from refinery feedstocks, refinery fractionation/processes, differential degradation/weathering, formation or combustion temperatures, provide a basis for differentiating and identifying the sources of PAHs in sediments. Below, we reproduce and answer the questions posed in the introduction section.

### **6.1 What Are the Most Important PAH Sources in the Aquatic Environment and Which PAH Indicators Can Be Used to Unequivocally Identify Them?**

Thermal, source and degradation PAH indicators produce fingerprint physicochemical gradients that are developed during pyrogenic and petrogenic PAH formation, transport, and deposition. One of the most widely applicable and robust approaches to PAH source characterization is to apply different discriminant analysis techniques (e.g., ratios, PMF) to the PAH pattern of parent versus alkylated (e.g., reflected in PI, PPI), stable versus unstable isomer, and HMW versus LMW forms.

Mathematically, it is not possible to discriminate more sources (times their temporal, climatic and geographical variations) than the known variables (PAH analytes). Therefore, to limit the number of possible suspected sources, knowledge of current and historic records of contamination is helpful. PAHs are classified according to their origin or temperature of formation into three classes: pyrogenic, petrogenic, and biogenic/natural. The multitude of PAH sources in the aquatic environment, their variability and the differential fate of PAHs have resulted in a plethora of PAH indicators for the purposes of PAH source assessment.

Each class of indicator is based upon a physicochemical aspect of the contaminant (source, degradation, and thermodynamic) and has been designated to solve a particular problem, but also indicates an existing gradient in the PAH chemistry. For example, the sulfur gradient (dibenzothiophenes) was initially applied for petroleum sources, but it can also be used to discriminate pyrogenic ones. There are extensive databases for PAHs and their sources. Table 4 gives an overview of the PAH indices used to characterize or apportion the pyrogenic or petrogenic nature of a sample.

Of special importance is the spatial extent of the PAH analysis, which is ascertained by distinguishing between point and non-point sources and measuring background concentrations. Background PAH concentrations always make it necessary to proceed with caution when using PAH ratios, because some degraded PAH source fingerprints (e.g., coal tar, creosote, etc.) are similar to urban background fingerprints. PAH indices such as  $N0/F0$ ,  $C2/C0$ ,  $FP0/(C0 + BaA + BaP + BjF + ghi + IP + D A)$  have been used to discriminate different sources that contribute to urban background. If urban background concentrations are high, it is possible to break down the composite urban background into individual sources by examining the inventory of sources contributing to it (e.g., asphalt, automobile soot, etc.).

PAH ratios are a fast and simple means to overview and understand the origin of pollution, particularly when coupled with a discriminant analysis approach. In general, two- to three-ringed PAHs (including alkylated) are good for distinguishing petrogenic contamination, whereas four- to six-ringed PAHs are appropriate for discriminating between pyrogenic sources. One of the most successful approaches for deducing the pyrogenic or petrogenic character of sedimentary contamination is the apportionment of PAHs to sources (e.g., the PI). The PPI and the FLO/PY0 ratio are robust and simple to use.

When petrogenic contamination is suspected, chrysenes, PAHs that are lighter than C0, and definitely alkylated PAHs are useful. For example, the  $Dn/Pn$  ratios are

**Table 4** Safe PAH ratios and threshold values for initial screening/identification of pyrogenic and petrogenic PAHs

Ratios	Fig	List	Pyrogenic	Petrogenic	Degr <sup>d</sup>	Comments
P0/A0	9	U, V	$\leq 4-10^b$	$>15^b-30$	↑	-
P1/P0	11	-	$\leq 1-2$	$>2-5$	↑	-
PA1/PA0	10	-	$\leq 1^b$	$>1.5^b$	↑	-
DMP	-	-	-	-	↓	$>0.7 = >$ Softwood combustion, $<0.45 = >$ non softwood, $0.9 =$ softwood combustion, $\sim 0.4 =$ vehicle
RET/C0	-	-	-	-	↓	$4.5 =$ Softwood, $0.35 =$ other combustion sources
FLO/PY0	12	U	$>1.5$	$<0.5^b$	↓	-
FPI/PY0	-	-	$\approx 0.3$	$\approx 4$	↓	-
FPI/FP0	13	-	$\leq 0.5-1$	$>1^b$	↑	-
P2+P3+P4/FP0	14	-	$<0.3$	$\geq 5.5-9$	↓	Intermediate values indicate weathering/mixing
BaA/C0	15	U	$>0.5b-1$	$<0.25^b-0.5^b$	↓	-
D1/P1	-	-	-	-	↑	Source ratio for crudes, $0.78 =$ asphalt, $0.4 =$ diesel emissions, $0.04 =$ fuel oil soot
D2/P2	17	-	$\leq 0.4$	-	↑	Source ratio for crudes, up to 98% degradation
PY0/BaP	-	B, U, V	$\leq 10$	$\geq 10$	↓ <sup>c</sup>	-
BaP/ghi	21	B, U, V	-	-	↓	$<0.6^b = >$ Non traffic
BeP/BaP	18	-	$\leq 1$	-	↑	Atmospheric weathering ratio
IP/ghi	20	U	$>1$	$<0.25$	~	Degradation depends on particle color for pyrogenics
ΣPAH/Alkyl	-	-	$>0.5$	$\leq 0.2-0.3$	Minor ↑	-
L/H	22	U	$<1$	$\geq 1$	↓	Weathering ratio, extensive degradation at low values
LPAAH/HPAAH	23	U	$<0.4-2^b$	$\geq 1-2.3$	↓	Weathering ratio, $<0.2 = >$ extensive degradation
Pyrogenic index	24	-	$>0.05^b$	$<0.05$	Minor ↑	-

Most safe thresholds in **bold**. Underlined: the side (values) of the ratio that will not be compromised by degradation (opposite direction). Intermediate ratio values indicate either mixed or unclear origin. Fig figure in manuscript which shows the respective ratio for different sources. List: priority list which can be used to estimate the ratio (U U.S, EPA 16, V FROM 10, B Borneff 6)

<sup>a</sup>Degradation effects on this ratio (↓ decrease, ↑ increase, ~ variable) based on thermodynamic assumption under "common" environmental conditions (i.e., stability of PAH isomers in the environment) but differences in environmental conditions and degradation types may differentially affect the value of the indicators

<sup>b</sup>Serious caveat when this value of this ratio is applied (see text for more)

<sup>c</sup>According to evaporation and dissolution potential as seen in Table 2

=Apportionment value (all apportionment values for one ratio refer to a single case in literature)

good for distinguishing weathered crudes, whereas C2/P2 can be used to distinguish crude from diesel, and 2-P1/1-P1 can be used to discriminate between fuel oils. For coal PAHs, the phenanthrenic ratios (MPIs), the 1-D1/4-D1, and BbF/BkF correlate with vitrinite reflectance (coal ranks). Unfortunately, little is known about the PAH composition of coals, which is geographically very variable (Achten and Hofmann 2009; Stout and Emsbo-Mattingly 2008).

Three-ringed PAHs such as  $D_n$  ( $n=1,2,\dots$ ), P1/A1, AY/AE, F0, and the two-ringed N0 are useful for distinguishing coal-derived liquids such as unweathered creosotes and coal tars, which do not follow the usual pyrogenic/petrogenic distributions. Weathered creosotes are rich in benzofluoranthenes, BaA, benzopyrenes, C0, FL0, PY0 (Fig. S28, Supporting Material). Ratios of four- or five-ringed (methyl) PAHs such as C0/BaA, BbF/BkF, FP0/FP2+FP3, may prove useful for distinguishing (un)weathered creosote from background contamination and other high-temperature processes.

Useful indicators of biomass combustion are alkylphenanthrenic indices such as DMPs and retene (RET/C0, RET/PY1, RET/benzo[*b*]naphtho[2,1-*d*]thiophene etc.), and PAH markers such as coronene. Of these, coronene is also a vehicle combustion marker, as are five- to six-ringed PAHs such as BeP, *ghi*, PY0, and other LMW PAHs (e.g., P1, F0, D0, benzonaphthothiophenes, etc.), which can assist in discriminating automobile-related emissions from other combustion forms (wood, coal, etc.).

Perylene, even though not of anthropogenic origin, can help yield information as to the source, depositional environment and the transport dynamics of the PAHs before or during their deposition.

In summary, a full scan analysis (all suspected sources included) should include the EPA16 parent PAHs (mostly pyrogenic discrimination), the *five target alkylated* (PI and petroleum products), the fluoranthenes/pyrenes homologues (pyrogenic/petrogenic discrimination), BeP (vehicle), PER (Biogenic), RET, and DMPs (biomass/softwood). This “initial screening” yields a set of candidate substances to be analyzed. A faster, cost-effective solution can narrow down the number of PAH analytes, but it depends on the case in question.

## ***6.2 What Are the Inherent Uncertainties in These Indicators and How Does the Value of the Indicator Change After Undergoing Biogeochemical Processes (i.e., Photochemical Oxidation, Degradation, Volatilization, etc.) in the Aquatic Environment?***

PAH degradation, background contamination, mixing of multiple sources and similarities between the PAH sources are functions of anthropogenic, environmental, and geographic conditions that differentially affect all but a few PAH molecular indices. It is possible to take these uncertainties into account by using suitable degradation/weathering PAH ratios.



Generally, HMW and alkylated PAHs are more recalcitrant than LMW and less alkylated PAHs. Furthermore, PAHs attached to particles are protected from several types of degradation (such as photodegradation and biodegradation). As a result, pyrogenic PAH distributions retain their signature better than petrogenic ones. PAH ratios such as P1/P0, 2-P1/1-P1, C0/C2, Ring456/TPAH, and the PPI are all inevitably affected by degradation. Ratios such as BbF/BkF, BaA/C0, P0/A0, FP0/FP2 + FP3, and BeP/BaP should be applicable in moderate weathering conditions, although they depend on sample matrix effects (differential weathering in air, aerobic or anaerobic conditions). More stable are the FL0/PY0 and IP/*ghi*—but only in certain compartments and substrates, not everywhere. For such ratios, the degradation effects for different matrices should be considered (e.g., empirically or by a degradation rate kinetic model) prior to application.

Differential degradation has been established for numerous ratios. The ratios of D2/D0 and P0/A0 are decreased by photo-oxidation and solubilization. Most other forms of degradation increase these ratios. Degradation does not significantly affect the alkyl/ $\Sigma$ PAH and PI. By definition, source parameters such as D0/P0 ratios are constant even after severe degradation, although if these substances do not associate with particles, long-term weathering also affects them. Other ratios such as benzo-fluorenes to methylpyrenes or the 2-N1/1-N1 ratio are resistant in certain cases or at certain degradation stages. In sediments and water matrices, biodegradation (oxic or anoxic) often has opposite effects than other forms of degradation for the same PAH ratio. For example, biodegradation usually increases the values of DMP and FL0/PY0 ratios, although other forms of degradation reduce them.

Empirical and theoretical models have been used to account for the differential degradation patterns. Weathering ratios of the more stable PAHs to the less recalcitrant PAHs (e.g., LMW/HMW or alkylated/less alkylated) are often used. The methyl-dibenzothiophene isomer ratios are useful biodegradation indicators. The ratio N0 + N1/N2 can account for dissolution in oil spills. The ratios of N2 or N3 alkyl-naphthalenes to the respective phenanthrenes are used as weathering indicators at early weathering stages (dissolution and evaporation). The ratios of two- or three-ringed PAHs (naphthalenes, dibenzothiophenes, phenanthrenes) to HMW PAHs (chrysenes or TPAH) are frequently used as general-purpose degradation indicators. Ratios such as P2/P3 (or the respective alkylated dibenzothiophenes) make use of the fact that the more alkylated the isomer is, the more recalcitrant it is. Notice that certain weathering ratios such as C2/P2 and C3/P3 are also source ratios when unweathered. Both BaP and the BeP/BaP ratio are applicable as photodegradation indicators in the atmosphere. Otherwise, the L/H and the LPAH/HPAH can be used to indicate the degradation level at which other PAH ratios may fail.

The charts (Figs. 9, 10, 11, 12, 13, 14, 15, 17, 18, 20, 21, 22, 23, and 24, summary in Table 4) summarize literature values for the PAH ratios in sources and show the possibilities for source characterization. Comparing the sediment contamination with these charts can assist in deducing the nature of contamination and its uncertainty. The degradation arrow shows how degradation will change a specific ratio

and assists in finding whether the ratio is compromised by degradation. Ranges and reliable (degradation-independent) threshold values of PAH ratios can be estimated, either for individual sources or for a group of sources of interest. Because of the higher degradability of petrogenic PAHs, petrogenic assessments should take into account at least dissolution and evaporation.

### ***6.3 Can the Borneff-6, 16 EPA, and 10 VROM PAHs Be Used to Calculate the Proposed Indicator—and, if so, Which Uncertainties are Introduced by This Approach?***

All the proposed indicators contain parent PAHs only, which make it difficult to trace petrogenic sources. We believe that after a local case study has taken into account a wider range of alkylated and parent PAHs, it is possible to establish the EPA16 as an indicator of pyrogenic and petrogenic sources.

All three indicators are suitable mainly for pyrogenic sources. Specifically, Borneff-6 has only one LMW parent PAH (easily degradable), making it inadequate to detect petrogenic contamination. Even though some LMW PAHs are included in the VROM10 PAH compilation, important ones such as pyrene (useful for discriminating petrogenic/pyrogenic or different combustion sources) are omitted.

Alkylated homologues are petroleum-specific, but they cannot be measured by using the standard EPA methods. Of the three proposed PAH compilations, the most adequate for identifying pyrogenic or petrogenic sources seems to be the  $\Sigma$ PAH16, although it does not take into account certain important parent PAHs (e.g., N0, BeP, PER, D0) nor, most importantly, does it take account of alkylated PAHs. Under degradation conditions, the parent compounds are those that are lost first—sometimes preferentially over the alkylated ones.

Certain ratios within the  $\Sigma$ PAH16 (e.g., LPAH/HPAH) are able either to describe patterns, in which degradation has occurred, or in which the targets are recalcitrant. Even for very complex systems, it should be possible to establish a diagnostic set of PAH indicators (e.g., the EPA16 indicators) after implementing a full scan analysis and a tiered approach (historic records, source inventories, background concentrations, weathering check, and parent and alkylated PAHs and data analysis). If the compounds that we expect to be present or absent in the sources are empirically known, the number of analytes to be investigated can be reduced. Establishing the levels and correlations of a small subset of indicators can reduce the effort of extensive analysis of PAHs while providing adequate data analysis and resolution, which are necessary for monitoring programs. We suggest that the next step in using a small subset of all the PAHs for the source characterization in sediments would be to implement an inference protocol (e.g., a multi-valued logic, or a PMF), in which conclusions drawn from multiple PAH ratio combinations are applied to weight the  $\Sigma$ PAH16 ratios in a standardized manner on the basis of source composition and degradation.

## 7 Summary

In recent decades, an exponential increase in the concentration of anthropogenic Polycyclic Aromatic Hydrocarbons (PAHs; see Table 1 for a list of PAH abbreviations) has been observed worldwide. Regulators need to know the sources if concentrations are to be reduced and appropriate remediation measures taken. “Source characterization of PAHs” involves linking these contaminants to their sources. Scientists place PAH sources into three classes: pyrogenic, petrogenic, and natural.

In this review, we investigate the possibility of using PAH molecular ratios individually or in combination for the purpose of deducing the petrogenic or pyrogenic origin of the contamination in sediments. We do this by reviewing the characteristic PAH patterns of the sources and by taking into account the fate of PAHs in the aquatic environment. Many PAH indicators have been developed for the purpose of discriminating different PAH sources. In Table 4 we summarize the applicability of different PAH ratios and threshold values.

The analysis of two- to four-ringed alkylated PAHs offers the possibility to distinguish two or more single sources or categories of pollution in greater detail. For example, the FL0/PY0, the PPI, and P0/A0 ratios can be used to discriminate between pyrogenic and petrogenic sources of contamination. When petrogenic contamination is suspected, chrysenes, PAHs lighter than C0, and in particular, alkylated PAHs can usually be of use. For unburned coal PAHs, the methylphenanthrenic ratios (MPIs), the 1-D1/4-D1, and BbF/BkF are promising, since they are sometimes correlated with vitrinite reflectance (coal ranks). Alkylphenanthrenes can be used to detect biomass combustion. Higher molecular weight parent and alkylated PAHs are appropriate for pyrogenic discriminations. When PAH indices are coupled with discriminant analysis techniques such as PMF (positive matrix factorization), the origin of multiple sources in even the most complex environments can be traced and measured.

Even so, the most stable isomer pairs degrade differentially, depending on their thermodynamic stability, the environmental conditions, and the type of degradation. If PAH ratios are to be used, it is usually necessary to have prior knowledge of the degradation state of the matrices examined (air, sediment, etc.) and of how the PAH ratio behaves under such conditions. PAH indices (e.g., N0/C0 or LPAH/HPAH) can be applied for distinguishing differential degradation gradients (photodegradation, biodegradation, etc.). Degradation does not significantly affect the ratio of parent to alkylated PAHs and the PI. The degradation arrow in Table 4 and Figs. 9, 10, 11, 12, 13, 14, 15, 17, 18, 19, 20, 21, 22, 23, and 24 shows how the ratio usually changes with degradation.

Merely detecting the six PAHs of Borneff-6 is not enough to establish petrogenic contamination, because Borneff6 includes mainly HMW PAHs. The  $\Sigma$ PAH16 appears to be the most suitable for identifying pyrogenic and petrogenic sources. For more specific information on sources and their discrimination it is recommended to further take into account important parent PAHs such as N0, BeP, PER, D0, and—most importantly—alkylated PAHs.

**Acknowledgments** We wish to thank Dr. J. Haftka, Prof. Dr. P. de Voogt and an anonymous reviewer for their helpful and critical comments and suggestions. Dr. J. Burrough was our language editor.

## Appendix

**Table 5** Key to literature data cited in figures

a	Ahrens and Depree (2010)	b	Benner et al. (1995)	c	Boonyatumanond et al. (2007)
d	Breault et al. (2005)	e	Burns et al. (1997)	f	Chen et al. (2005)
g	Chen et al. (2006)	h	Dickhut et al. (2000)	i	Dobbins et al. (2006)
j	Galarneau (2008)	k	Geller et al. (2006)	l	Jiao et al. (2009)
m	Karlsson and Viklander (2008)	n	Lim et al. (2007)	o	Marr et al. (1999)
p	Masclet et al. (1987)	q	Miguel et al. (1998)	r	Mostafa et al. (2009)
s	Neff et al. (2005)	t	Neff et al. (1998)	u	Oanh et al. (1999)
v	Okuda et al. (2002)	w	Oros and Simoneit (2000)	x	Riddle et al. (2007)
y	Saber et al. (2006)	z	Saha et al. 2009	aa	Sicre et al. (1987)
bb	Simcik et al. (1999)	cc	Stout (2007)	dd	Stout and Emsbo-Mattingly (2008)
ee	Stout et al. (2001a)	ff	Stout et al. (2003)	gg	Stout et al. (2006)
hh	Stout et al. (2007)	ii	Takada et al. (1990)	jj	Wang et al. (1999b)
kk	Wang et al. (2006)	ll	Yan et al. (2005)	mm	Yan et al. (2007)
nn	Yunker et al. (2002)	oo	Zakaria et al. (2002)	pp	Page et al. (1999)

## References

- Abrajano TA, Yan B, O'Malley V (2003) High molecular weight petrogenic and pyrogenic hydrocarbons in aquatic environments. In: Sherwood B (ed) Treatise on geochemistry, vol 9. Elsevier Ltd, Oxford, pp 475–509
- Achten C, Hofmann T (2009) Native polycyclic aromatic hydrocarbons (PAH) in coals – a hardly recognized source of environmental contamination. *Sci Total Environ* 407:2461–2473
- Agarwal T (2009) Concentration level, pattern and toxic potential of PAHs in traffic soil of Delhi, India. *J Hazard Mater* 171:894–900
- Ahrens MJ, Depree CV (2010) A source mixing model to apportion PAHs from coal tar and asphalt binders in street pavements and urban aquatic sediments. *Chemosphere* 81:1526–1535
- Alam MS, Delgado-Saborit JM, Stark C, Harrison RM (2013) Using atmospheric measurements of PAH and quinone compounds at roadside and urban background sites to assess sources and reactivity. *Atmos Environ* 77:24–35
- Allan LM (1999) Thia-arenes as pollution source tracers in urban air particulate. PhD Thesis, McMaster University, Hamilton, ON, pp 43–74, 178–221
- Alves CA, Vicente A, Evtuyugina M, Pio CA, Hoffer A, Kiss G, Decesari S, Hillamo R, Swietlicki E (2009) Characterisation of hydrocarbons in atmospheric aerosols from different European sites. *World Acad Sci Eng Tech* 33:236–242

- Andersson M, Klug M, Eggen OA, Ottesen RT (2014) Polycyclic aromatic hydrocarbons (PAHs) in sediments from lake Lille Lungegårdsvannet in Bergen, western Norway; appraising pollution sources from the urban history. *Sci Tot Environ* 470–471:1160–1172
- Bakhtiari AR, Zakaria MP, Yaziz MI, Hj Lajis MN, Bi X, Abd Rahim MC (2009) Vertical distribution and source identification of polycyclic aromatic hydrocarbons in anoxic sediment cores of Chini Lake, Malaysia: perylene as indicator of land plant-derived hydrocarbons. *Appl Geochem* 24:1777–1787
- Barakat AO, Qian Y, Kim M, Kennicutt M II (2001) Source and weathering dependent changes in PAH molecular ratios during naturally weathering of oil residues over a period of 15 years in the Egyptian Western Desert. *ACS Div Environ Chem Prepr* 41:38–43
- Barra R, Castillo C, Torres JPM (2007) Polycyclic aromatic hydrocarbons in the South American environment. *Rev Environ Contam Toxicol* 191:1–22
- Battelle Memorial Institute, Earth Tech Inc, Newfields Inc (2003) Guidance for environmental background analysis Volume II: Sediment. NFESC User's Guide UG-2054-ENV DC 20374-5065. Naval Facilities Engineering Command, Washington, DC, pp 153–180
- Behymer TD, Hites RA (1988) Photolysis of polycyclic aromatic hydrocarbons adsorbed on fly ash. *Environ Sci Technol* 22:1311–1319
- Bence AE, Kvenvolden KA, Kennicutt MC II (1996) Organic geochemistry applied to environmental assessments of Prince William Sound, Alaska, after the Exxon Valdez oil spill – a review. *Org Geochem* 24:7–42
- Bence AE, Page DS, Boehm PD (2007) Advances in forensic techniques for petroleum hydrocarbons: the Exxon Valdez experience. In: Wang Z, Stout SA (eds) *Oil spill environmental forensics. Fingerprinting and source identification*. Elsevier, Boston, MA, pp 449–488
- Benner BA, Wise SA, Currie LA, Klouda GA, Klinedinst DB (1995) Distinguishing the contributions of residential wood combustion and mobile source emissions using relative concentrations of dimethylphenanthrene isomers. *Environ Sci Technol* 29:2382–2389
- Bertilsson S, Widenfalk A (2002) Photochemical degradation of PAHs in freshwaters and their impact on bacterial growth – influence of water chemistry. *Hydrobiologia* 469:23–32
- Boehm P, Saba T (2008) Identification and allocation of polycyclic aromatic hydrocarbons (PAHs). *Exponent Environ Forens Notes* 4:1–5
- Boehm PD, Douglas GS, Brown JS (1995) Advanced chemical fingerprinting for oil spill identification and natural resource damage assessment. In: *Proceedings of the 1995 International Oil Spill Conference*. American Petroleum Institute, Washington, DC, pp 967–969
- Boehm PD, Page DS, Burns WA, Bence AE, Mankiewicz PJ, Brown JS (2001) Resolving the origin of the petrogenic hydrocarbon background in Prince William Sound, Alaska. *Environ Toxicol Chem* 35:471–479
- Boehm PD, Burns WA, Page DS, Bence AE, Mankiewicz PJ, Brown JS, Douglas GS (2002) Total organic carbon, an important tool in an holistic approach to hydrocarbon source fingerprinting. *Environ Forens* 3:243–250
- Boehm PD, Neff JM, Page DS (2007) Assessment of polycyclic aromatic hydrocarbon exposure in the waters of Prince William Sound after Exxon Valdez oil spill: 1989–2005. *Mar Pollut Bull* 54:339–367
- Boehm PD, Page DS, Brown JS, Neff JM, Bragg JR, Atlas RM (2008) Distribution and weathering of crude oil residues on shorelines 18 years after the Exxon Valdez spill. *Environ Sci Technol* 42:9210–9216
- Bogdal C, Bucheli TD, Agarwal T, Anselmetti FS, Blum F, HungerBuhler K, Kohler M, Schmid P, Scheringer M, Sobek A (2011) Contrasting temporal trends and relationships of total organic carbon, black carbon, and polycyclic aromatic hydrocarbons in rural low-altitude and remote high-altitude lakes. *J Environ Monit* 13:1316–1325
- Boitsov S, Jensen HK, Klungsoyr J (2009) Natural background and anthropogenic inputs of polycyclic aromatic hydrocarbons (PAH) in sediments of South-Western Barents Sea. *Mar Environ Res* 68:236–245
- Boll ES, Christensen JH, Holm PE (2008) Quantification and source identification of polycyclic aromatic hydrocarbons in sediment, soil, and water spinach from Hanoi, Vietnam. *J Environ Monit* 10:261–269

- Boonyatumanond R, Murakami M, Wattayakorn G, Togo A, Takada H (2007) Sources of polycyclic aromatic hydrocarbons (PAHs) in street dust in a tropical Asian mega-city, Bangkok, Thailand. *Sci Total Environ* 384:420–432
- Breault RF, Smith KP, Sorenson JR (2005) Residential street-dirt accumulation rates and chemical composition, and removal efficiencies by mechanical- and vacuum-type sweepers, New Bedford, Massachusetts, 2003–04. Scientific Investigations Report 2005-5184. Department of the Interior, U.S. Geological Survey, Reston, VA, pp 1–27
- Brenner RC, Magar VS, Ickes JA, Abbott JE, Stout SA, Crecelius EA, Bingler LS (2002) Characterization and fate of PAH-contaminated sediments at the Wyckoff/Eagle Harbor Superfund site. *Environ Sci Technol* 36:2605–2613
- Bucheli TD, Blum F, Desaulles A, Gustafsson O (2004) Polycyclic aromatic hydrocarbons, black carbon, and molecular markers in soils of Switzerland. *Chemosphere* 56:1061–1076
- Budzinski H, Jones I, Bellocq J, Pierard C, Garrigues P (1997) Evaluation of sediment contamination by polycyclic aromatic hydrocarbons in the Gironde estuary. *Mar Chem* 58:85–97
- Burns WA, Mankiewicz PJ, Bence AE, Page DS, Parker KR (1997) A principal-component and least-squares method for allocating polycyclic aromatic hydrocarbons in sediment to multiple sources. *Environ Toxicol Chem* 16:1119–1131
- Bylina BG, Rakwicz B, Pastuszka JS (2005) Assessment of exposure to traffic-related aerosol and to particle-associated PAHs in Gliwice, Poland. *Pol J Environ Stud* 14:117–123
- Cailleaud K, Forget-Leray J, Souissi S, Hilde D, LeMenach K, Budzinski H (2007) Seasonal variations of hydrophobic organic contaminant concentrations in the water-column of the Seine Estuary and their transfer to a planktonic species *Eurytemora Affinis* (Calanoida, copepoda). Part 1: PCBs and PAHs. *Chemosphere* 70:270–280
- Calvacante RM, Sousa FW, Nascimento RF, Silveira ER, Freire GSS (2009) The impact of urbanization on tropical mangroves (Fortaleza, Brazil): evidence from PAH distribution in sediments. *J Environ Manage* 91:28–335
- Chen CW, Chen CF (2011) Distribution, origin, and potential toxicological significance of polycyclic aromatic hydrocarbons (PAHs) in sediments of Kaohsiung Harbor, Taiwan. *Mar Pollut Bull* 63:417–423
- Chen SJ, Su HB, Chang JE, Lee WJ, Huang KL, Hsieh LT, Huang YC, Lin WY, Lin CC (2006) Emissions of polycyclic aromatic hydrocarbons (PAHs) from the pyrolysis of scrap tires. *Atmos Environ* 41:1209–1220
- Chen Y, Sheng G, Bi X, Feng Y, Mai B, Fu J (2005) Emission factors for carbonaceous particles and polycyclic aromatic hydrocarbons from residential coal combustion in China. *Environ Sci Technol* 39:1861–1867
- Chien SM, Huang YJ (2010) Sizes and polycyclic aromatic hydrocarbon composition distributions of nano, ultrafine, fine, and coarse particulates emitted from a four-stroke motorcycle. *J Environ Sci Health A* 45:1768–1774
- Christensen JH, Tomasi G (2007) Practical aspects of chemometrics for oil spill fingerprinting. *J Chromatogr A* 1169:1–22
- Christensen JH, Hansen AB, Tomasi G, Mortensen J, Andersen O (2004) Integrated methodology for forensic oil spill identification. *Environ Sci Technol* 38:2912–2918
- Colombo JC, Pelletier E, Brochu C, Khall M (1989) Determination of hydrocarbon sources using n-alkane and polyaromatic hydrocarbon distribution indexes. Case study: Rio de La Plata Estuary, Argentina. *Environ Sci Technol* 7:888–894
- Comero S, Capitani L, Gawlik BM (2009) Positive Matrix Factorisation (PMF). An introduction to the chemometric evaluation of environmental monitoring data using PMF. JRC Scientific and Technical reports EUR 23946 EN–2009. European Commission Joint Research Centre, Institute for Environment and Sustainability, Ispra, Italy, pp 1–59
- Compaan H, Laane RWP (1992) Polycyclic aromatic hydrocarbons in the North Sea, an inventory. TNO-report IMW-R 92/392, 130p
- Costa HJ, White KA, Ruspantini JJ (2004) Distinguishing PAH background and MGP residues in sediments of a freshwater creek. *Environ Forens* 5:171–182
- Costa HJ, Sauer JTC (2005) Forensic approaches and considerations in identifying PAH background. *Environ Forens* 6:9–16

- Craig DR, Mauro DM (2012) Benzofluorene/methylpyrene ratios as a source identification tool. In: Liptai LL, Micheals A (eds) *Forensic engineering sciences, Proceedings 2002-2011*. American Academy of Forensic Sciences, Colorado Springs, CO, pp 215–245
- Dahlmann G (2003) Characteristic features of different oil types in oil spill identification. BSH 31/2003, *Berichte des Bundesamtes für Seeschifffahrt und Hydrographie*, Germany, pp 1–48
- Daisey JM, Cheney JL, Liou PJ (1986) Profiles of organic particulate emissions from air pollution sources—status and needs for receptors source apportionment modeling. *J Air Pollut Control Assoc* 36:17–33
- Da Silva DAM, Bicego MC (2010) Polycyclic aromatic hydrocarbons and petroleum biomarkers in Sao Sebastiao Channel, Brazil: assessment of petroleum contamination. *Mar Environ Res* 69:277–286
- Davis JC (2002) *Analysis of multivariate data*. John Wiley and Sons, New York, NY, pp 461–600
- Dean JA (ed) (1999) *Lange's handbook of chemistry*, 15th edn. McGraw-Hill, New York, NY
- De Fatima M, Meniconi G, Barbanti SM (2007) Case study: evaluation of hydrocarbon sources in Guanabara Bay, Brazil. In: Wang Z, Stout SA (eds) *Oil spill environmental forensics. Fingerprinting and source identification*. Elsevier, Boston, MA, pp 505–536
- De Luca G, Furesi A, Leardi R, Micera G, Panzanelli A, Piu PC (2004) Polycyclic aromatic hydrocarbons assessment in the sediments of the Porto Torres Harbor (Northern Sardinia, Italy). *Mar Chem* 86:15–32
- De Luca G, Furesi A, Micera G, Panzanelli A, Piu PC, Pilo MI, Spano N, Sanna G (2005) Nature, distribution and origin of polycyclic aromatic hydrocarbons (PAHs) in the sediments of Olbia harbor (Northern Sardinia, Italy). *Mar Pollut Bull* 50:1223–1232
- Denton E (2006) Characterization of used oil in stormwater runoff in California. Office of Environmental Health Hazard Assessment, California Environmental Protection Agency, p 3. Available from: <http://oehha.ca.gov/water/reports/OilInRunoff0906.pdf>. Accessed on 30 October 2012
- Dickhut RM, Canuel EA, Gustafson KE, Liu K, Arzayus KM, Walker SE, Edgecombe G, Gaylor MO, Macdonald EH (2000) Automotive sources of carcinogenic polycyclic aromatic hydrocarbons associated with particulate matter in the Chesapeake Bay region. *Environ Sci Technol* 34:4635–4640
- Diez S, Jover E, Bayona JM, Albaiges J (2007) Prestige oil spill. III. Fate of a heavy oil in the marine environment. *Environ Sci Technol* 41:3075–3082
- Dobbins RA, Fletcher RA, Benner JBA, Hoelt S (2006) Polycyclic aromatic hydrocarbons in flames, in diesel fuels, and in diesel emissions. *Comb Flame* 144:773–781
- Douglas GS, Bence AE, Prince RC, McMillen SJ, Butler EL (1996) Environmental stability of selected petroleum hydrocarbon source and weathering ratios. *Environ Sci Technol* 30:2332–2339
- Douglas GS, Emsbo-Mattingly SD, Stout SA, Uhler AD, McCarthy KJ (2007a) Chemical fingerprinting methods. In: Murphy BL, Morisson RD (eds) *Introduction to environmental forensics*, 2nd edn. Academic, New York, NY, pp 311–454
- Douglas GS, Stout SA, Uhler AD, McCarthy KJ, Emsbo-Mattingly SD (2007b) Advantages of quantitative chemical fingerprinting in oil spill source identification. In: Wang Z, Stout SA (eds) *Oil spill environmental forensics. Fingerprinting and source identification*. Elsevier, Boston, MA, pp 257–292
- Dupree C, Ahrens A (2007) Polycyclic aromatic hydrocarbons in Auckland's aquatic environment: sources, concentrations and potential environmental risks. Technical Publication No. TP378, Auckland Regional Council, New Zealand, pp 1–71
- Dvorska A, Lammel G, Klanova J (2011) Use of diagnostic ratios for studying source apportionment and reactivity of ambient polycyclic aromatic hydrocarbons over Central Europe. *Atmos Environ* 45:420–427
- Dzepina K, Arey J, Marr LC, Worsnop DR, Salcebo D, Zhang Q, Onasch TB, Molina LT, Molina MJ, Jimenez JL (2007) Detection of particle-phase polycyclic aromatic hydrocarbons in Mexico City using an aerosol mass spectrometer. *Int J Mass Spectrom* 263:152–170
- Dzou LIP, Noble RA, Senftle JT (1995) Maturation effects on absolute biomarker concentration in a suite of coals and associated vitrinite concentrates. *Org Geochem* 23:681–697

- Elmqvist M, Zencak Z, Gustafsson O (2007) A 700 year sediment record of black carbon and Polycyclic Aromatic Hydrocarbons near the EMEP Air Monitoring Station in Aspövreten, Sweden. *Environ Sci Technol* 41:6926–6932
- European Commission (2001) Decision No 2455/2001/EC of the European parliament and of the council of 20 November 2001 establishing the list of priority substances in the field of water policy and amending Directive 2000/60/EC. *Official Journal of the European Communities*, L331/1. European Commission.
- Fabbri D, Vassura I, Sun CG, Snape CE, Merae C, Fallick AE (2003) Source apportionment of polycyclic aromatic hydrocarbons in a coastal lagoon by molecular and isotopic characterisation. *Mar Chem* 84:123–135
- Faksness LG, Daling PS, Hansen AB (2002) CEN/BT/TF 120 oil spill identification. Summary report: Round Robin test series B. SINTEF report STF66 A02038, SINTEF, Trondheim, Norway, pp 1–50
- Fan CW, Shiue J, Wu CY, Wu CY (2011) Perylene dominance in sediments from a subtropical high mountain lake. *Org Geochem* 42:116–119
- Farrington JW, Frew NM, Gschwend PM, Tripp BW (1977) Hydrocarbons in cores of Northwestern Atlantic coastal and continental margin sediments. *Estuar Coast Mar Sci* 5:793–808
- Galarneau E (2008) Source specificity and atmospheric processing of airborne PAHs: implications for source apportionment. *Atmos Environ* 42:8139–8149
- Geller MD, Ntziachristos L, Mamakos A, Samaras Z, Schmitz DA, Froines JR, Sioutas C (2006) Physicochemical and redox characteristics of particulate matter (PM) emitted from gasoline and diesel passenger cars. *Atmos Environ* 40:6988–7004
- Giger W, Blumer M (1974) Polycyclic aromatic hydrocarbons in the environment: isolation and characterization by chromatography, visible, ultraviolet, and mass spectrometry. *Anal Chem* 46:1663–1671
- Gogou A, Bouloubassi I, Stephanou EG (2000) Marine organic geochemistry of the Eastern Mediterranean: 1. Aliphatic and polyaromatic hydrocarbons in Cretan Sea surficial sediments. *Mar Chem* 68:265–282
- Grimalt JO, van Drooge BL, Ribes A, Fernandez P, Appleby P (2004) Polycyclic aromatic hydrocarbon composition in soils and sediments of high altitude lakes. *Environ Pollut* 131:13–24
- Grimmer G, Jacob J, Naujack KW (1981) Profile of the polycyclic aromatic hydrocarbons from lubricating oils inventory by GCGC/MS - PAH in environmental materials, Part 1. *Fresenius Z Anal Chem* 306:347–355
- Grimmer G, Jacob B, Naujack KW (1983) Profile of the polycyclic aromatic compounds from crude oils Part 3. inventory by GCGC/MS. - PAH in environmental materials. *Fresenius Z Anal Chem* 314:29–36
- Gschwend PM, Hites RA (1981) Fluxes of polycyclic aromatic hydrocarbons to marine and lacustrine sediments in the northeastern United States. *Geochim Cosmochim Acta* 45:2359–2367
- Guillon A, Le Menach K, Flaud PM, Marchand N, Budzinski H, Villenave E (2013) Chemical characterization and stable carbon isotopic composition of particulate Polycyclic Aromatic Hydrocarbons issued from combustion of 10 Mediterranean woods. *Atm Chem Phys* 13:2703–2719
- Guo Z, Lin T, Zhang G, Zheng M, Zhang Z, Hao Y, Fang M (2007) The sedimentary fluxes of polycyclic aromatic hydrocarbons in the Yangtze River Estuary coastal sea for the past century. *Sci Total Environ* 386:33–41
- Gustafsson O (1997) Physico-chemical speciation and ocean fluxes of polycyclic aromatic hydrocarbons. PhD Thesis, Massachusetts Institute of Technology, Woods Hole Oceanographic Institution, Cambridge, MA, p 189
- Haftka J (2009) Bioavailability of polycyclic aromatic hydrocarbons in sediments: experiments and modelling. PhD Thesis, Universiteit van Amsterdam, Amsterdam, Netherlands
- Hailwood M, King D, Leoz E, Maynard R, Menichini E, Moorcroft S, Pacyna J, Ballesta P, Schneider PJ, Westerholm R, Wichmann-Fiebig M, Woodfield M, van Bree L, Conolly C (2001) Ambient air pollution by polycyclic aromatic hydrocarbons (PAH). In: European Commission (ed) Position paper annexes, annex 2:3–43



- Hansen AB, Daling PS, Faksness LG, Sorheim KR, Kienhuis P, Duus R (2007) Emerging CEN methodology for oil spill identification. In: Wang Z, Stout SA (eds) Oil spill environmental forensics. Fingerprinting and source identification. Elsevier, Boston, MA, pp 229–256
- Harris KA, Yunker MB, Dangerfield N, Ross PS (2011) Sediment-associated aliphatic and aromatic hydrocarbons in coastal British Columbia, Canada: concentrations, composition, and associated risks to protected sea otters. *Environ Pollut* 159:2665–2674
- He J, Balasubramanian R (2010) Semi-volatile organic compounds (SVOCs) in ambient air and rainwater in a tropical environment: concentrations and temporal and seasonal trends. *Chemosphere* 78:742–751
- Hegazi AH, Andersson JT (2007) Characterization of polycyclic aromatic sulfur heterocycles for source identification. In: Wang Z, Stout SA (eds) Oil spill environmental forensics. Fingerprinting and source identification. Elsevier, Boston, MA, pp 147–168
- Hostettler FD, Wang Y, Huang Y, Cao W, Bekins BA, Rostad CE, Kulpa CF, Laursen A (2007) Forensic fingerprinting of oil-spill hydrocarbons in a methanogenic environment—Mandan, ND and Bemidji, MN. *Environ Forens* 8:139–153
- Hwang HM, Wade TL, Sericano JL (2003) Concentrations and source characterization of polycyclic aromatic hydrocarbons in pine needles from Korea, Mexico, and United States. *Atmos Environ* 37:2259–2267
- Iqbal J, Overton EB, Gisclair D (2008) Polycyclic aromatic hydrocarbons in Louisiana Rivers and coastal environments: source fingerprinting and forensic analysis. *Environ Forens* 9:63–74
- Irwin RJ, van Mouwerik M, Stevens L, Seese MD, Basham W (1997) Environmental contaminants encyclopedia. National Park Service, Water Resources Division, Fort Collins, CO
- Jeanneau L, Faure P, Montarges-Pelletier E (2008) Quantitative multimolecular marker approach to investigate the spatial variability of the transfer of pollution from the Fensch River to the Moselle River (France). *Sci Total Environ* 389:503–513
- Jensen A, Nielsen GG, Gundersen V, Nielsen OJ, Ostergard H, Aarkrog A (1993) Environmental science and technology department annual report 1992, Riso-R-680(EN). Riso National Laboratory, Roskilde, Denmark, pp 16–17
- Jiang JJ, Lee CL, Fang MD, Liu JT (2009) Polycyclic aromatic hydrocarbons in coastal sediments of southwest Taiwan: an appraisal of diagnostic ratios in source recognition. *Mar Pollut Bull* 58:752–760
- Jiao L, Zheng GJ, Minh TB, Richardson B, Chen L, Zhang Y, Yeung LW, Lam JCW, Yang X, Lam PKS, Wong MH (2009) Persistent toxic substances in remote lake and coastal sediments from Svalbard, Norwegian Arctic: levels, sources and fluxes. *Environ Pollut* 157:1342–1351
- Jimenez N, Vinas M, Sabate J, Diez S, Bayona JM, Solanas AM, Albaiges J (2006) The prestige oil spill. 2. Enhanced biodegradation of a heavy fuel oil under field conditions by the use of an oleophilic fertilizer. *Environ Sci Technol* 40:2578–2585
- Johnson GW, Ehrlich R, Full W, Ramos S (2007) Principal components analysis and receptor models in environmental forensics. In: Murphy BL, Morrison RD (eds) Introduction to environmental forensics, 2nd edn. Academic, New York, NY, pp 207–272
- Johnson-Restrepo BJ, Verbel JO, Lu S, Fernandez JG, Avila RB, Hoyos IO, Aldous KM, Addink R, Kannan K (2008) Polycyclic aromatic hydrocarbons and their hydroxylated metabolites in fish bile and sediments from coastal waters of Colombia. *Environ Pollut* 151:452–459
- Karlsson K, Viklander M (2008) Polycyclic aromatic hydrocarbons (PAH) in water and sediment from gully pots. *Water Air Soil Pollut* 188:271–282
- Kim D, Kumfer BM, Anastasio C, Kennedy IM, Young TM (2009) Environmental aging of polycyclic aromatic hydrocarbons on soot and its effect on source identification. *Chemosphere* 76:1075–1081
- Kim M, Kennicutt MC II, Yaorong Q (2008) Source characterization using compound composition and stable carbon isotope ratio of PAHs in sediments from lakes, harbor and shipping waterway. *Sci Total Environ* 389:367–377
- Klamer JC, Hegeman WJM, Smedes F (1990) Comparison of grain size correction procedures for organic micropollutants and heavy metals in marine sediments. *Hydrobiologia* 208:213–220

- Laane RWPM, Sonneveldt HLA, Van der Weyden AJ, Loch JPG, Groenvelde G (1999) Trends in the spatial and temporal distribution of metals (Cd, Cu, Zn and Pb) and organic compounds (PCBs and PAHs) in Dutch coastal zone sediments from 1981 to 1996: a model case study for Cd and PCBs. *J Sea Res* 41:1–17
- Laane RWPM, De Voogt P, Bik MH (2006) Assessment of organic compounds in the Rhine estuary. *Hdb Env Chem* 5:307–368
- Laane RWPM, Vethaak AD, Gandrass J, Vorkamp K, Kohler A, Larsen MM, Strand J (2013) Chemical contaminants in the Wadden Sea: Sources, transport, fate and effects. *J Sea Res* 82:10–53
- Lafamme RE, Hites RA (1978) The global distribution of polycyclic aromatic hydrocarbons in recent sediments. *Geochim Cosmochim Acta* 42:289–303
- Lai IC, Lee CL, Zeng KY, Huang HC (2011) Seasonal variation of atmospheric polycyclic aromatic hydrocarbons along the Kaohsiung coast. *J Environ Manage* 92:2029–2037
- Lake JL, Norwood C, Dimock C, Bowen R (1979) Origins of polycyclic aromatic hydrocarbons in estuarine sediments. *Geochim Cosmochim Acta* 43:1847–1854
- Lang YH, Yang X, Wang H, Yang W, Li GL (2013) Diagnostic ratios and positive matrix factorization to identify potential sources of PAHs in sediments of the Rizhao Offshore, China. *Polycycl Aromat Compd* 33:161–172
- Larsen RK, Baker JE (2003) Source apportionment of polycyclic aromatic hydrocarbons in the urban atmosphere: a comparison of three methods. *Environ Sci Technol* 37:1873–1881
- Lehndorff E, Schwark L (2004) Biomonitoring of air quality in the Cologne Conurbation using pine needles as a passive sampler—Part II: polycyclic aromatic hydrocarbons (PAH). *Atmos Environ* 38:3793–3808
- Lehndorff E, Schwark L (2009) Biomonitoring airborne parent and alkylated three-ring PAHs in the Greater Cologne Conurbation I: temporal accumulation patterns. *Environ Pollut* 157:1323–1331
- Lide DR (ed) (2004) *Handbook of chemistry and physics*, 84th edn. CRC Press LLC., Boca Raton, FL
- Lim MCH, Ayoko GA, Morawska L, Ristovski DZ, Jayaratne ER (2007) Influence of fuel composition on polycyclic aromatic hydrocarbon emissions from a fleet of in-service passenger cars. *Atmos Environ* 41:150–160
- Lorenzi D, Entwistle JA, Cave M, Dean JR (2011) Determination of polycyclic aromatic hydrocarbons in urban street dust: implications for human health. *Chemosphere* 83:970–977
- Luo XJ, Chen SJ, Mai BX, Sheng GY, Fu JM, Zeng EY (2008) Distribution, source apportionment, and transport of PAHs in sediments from the Pearl River delta and the northern South China Sea. *Arch Environ Contam Toxicol* 55:11–20
- Mackay D, Shiu WY, Ma K-C, Lee SC (eds) (2006) *Handbook of physical-chemical properties and environmental fate for organic chemicals*, 2nd edn. CRC Press, Boca Raton, FL
- Magi E, Bianco R, Di Carro M (2002) Distribution of polycyclic aromatic hydrocarbons in the sediments of the Adriatic Sea. *Environ Pollut* 119:91–98
- Mandalakis M, Gustafsson O, Reddy C, Xu L (2004) Radiocarbon apportionment of fossil versus biofuel combustion sources of polycyclic aromatic hydrocarbons in the Stockholm metropolitan area. *Environ Sci Technol* 38:5344–5349
- Mansuy-Huault L, Regier A, Faure P (2009) Analyzing hydrocarbons in sewer to help in PAH source apportionment in sewage sludges. *Chemosphere* 75:995–1002
- Marr L, Kirchstetter TW, Harley RA, Miguel AH, Sussane VH, Hammond KS (1999) Characterization of polycyclic aromatic hydrocarbons in motor vehicle fuels and exhaust emissions. *Environ Sci Technol* 33:3091–3099
- Marvin CH, McCarty BE, Villella J, Allan LM, Bryant W (2000) Chemical and biological profiles of sediments as indicators of sources of genotoxic contamination in Hamilton Harbour. Part I: Analysis of polycyclic aromatic hydrocarbons and thia-arene compounds. *Chemosphere* 41:979–988
- Masclat P, Bresson MA, Mouvier G (1987) Polycyclic aromatic hydrocarbons emitted by power stations, and influence of combustion conditions. *Fuel* 66:556–562

- Masclat P, Mouvier G, Nikolaou K (1986) Relative decay index and sources of polycyclic aromatic hydrocarbons. *Atmos Environ* 20:439–446
- Mathieu C, Friese M (2012) PBT chemical trends in Washington state determined from age-dated lake sediment cores 2011 sampling results. Environmental Assessment Program, Publication No. 12-03-045. Washington State Department of Ecology, Olympia, Washington, DC, pp 1–53
- Mauro D (2008) PAHs in urban background: distribution, regulatory relief, and forensic value. In: MGP 2008 Proceedings. The Third International Symposium and Exhibition on the Redevelopment of manufactured gas plant sites. Mystic, CT, USA
- Micic V, Kruge MA, Koster J, Hofmann T (2011) Natural, anthropogenic and fossil organic matter in river sediments and suspended particulate matter: A multi-molecular marker approach. *Sci Total Environ* 409:905–919
- Miguel AH, Kirchstetter TW, Harley RA (1998) On-road emissions of particulate polycyclic aromatic hydrocarbons and black carbon from gasoline and diesel vehicles. *Environ Sci Technol* 32:450–455
- Mitra S, Dellapenna TM, Dickhut RM (1999) Polycyclic aromatic hydrocarbon distribution within Lower Hudson River estuarine sediments: physical mixing vs sediment geochemistry. *Estuar Coast Shelf Sci* 49:311–326
- Mitra S, Lalicata JJ, Allison MA, Dellapenna TM (2009) The effects of hurricanes Katrina and Rita on seabed polycyclic aromatic hydrocarbon dynamics in the Gulf of Mexico. *Mar Pollut Bull* 58:851–857
- Morillo E, Romero AS, Madrid L, Villaverde J, Maqueda C (2008a) Characterization and sources of PAHs and potentially toxic metals in urban environments of Sevilla (Southern Spain). *Water Air Soil Pollut* 187:41–51
- Morillo E, Romero AS, Maqueda C, Madrid L, Ajmone-Marsan F, Grcman H, Davidson CM, Hursthouse AS, Villaverde J (2008b) Soil pollution by PAHs in urban soils: a comparison of three European cities. *J Environ Monit* 9:1001–1008
- Mostafa AR, Hegazi AH, El-Gayar MS, Andersson JT (2009) Source characterization and the environmental impact of urban street dusts from Egypt based on hydrocarbon distributions. *Fuel* 88:95–104
- Nasher E, Heng LY, Zakaria Z, Surif S (2013) Concentrations and sources of polycyclic aromatic hydrocarbons in the seawater around Langkawi island, Malaysia. *J Chem* 2013, Article ID 975781
- Neff JM, Ostazeski SA, Macomber SC, Roberts LG, Gardiner W, Word KQ (1998) Weathering, chemical composition and toxicity of four Western Australian crude oils. Report to Apache Energy Ltd. Apache Energy Ltd., Perth, WA
- Neff JM, Stout SA, Gunster DG (2005) Ecological risk assessment of polycyclic aromatic hydrocarbons in sediments: identifying sources and ecological hazard. *Integr Environ Assess Manag* 1:22–33
- Neff JM, Bence AE, Parker KR, Page DS, Brown JS, Boehm PD (2006) Bioavailability of polycyclic aromatic hydrocarbons from buried shoreline oil residues thirteen years after the Exxon Valdez oil spill: a multispecies assessment. *Environ Toxicol Chem* 25:947–961
- Nordtest (1991) Nordtest method. NT Chem 001, 2nd edn. Nordtest, Espoo, Finland, p 7
- O'Malley VP, Abrajano TA, Hellou J (1994) Determination of the  $^{13}C/^{12}C$  ratios of individual PAH from environmental samples: can PAH sources be apportioned? *Org Geochem* 21:809–822
- O'Malley VP, Burke RA, Schlotzhauer WS (1997) Using GC-MS/Combustion/IRMS to determine hydrocarbons produced from the combustion of biomass materials – application to biomass burning. *Org Geochem* 27:567–581
- O'Reilly K, Pietari J, Boehm P (2012) Forensic assessment of refined tar-based sealers as a source of polycyclic aromatic hydrocarbon (PAHs) in urban sediments. *Environ Forens* 13:185–196
- O'Reilly KT, Pietari J, Boehm PD (2014) Parsing pyrogenic polycyclic aromatic hydrocarbons: forensic chemistry, receptor models, and source control policy. *Integr Environ Assess Manag* 10:279–285. doi:10.1002/ieam.1506

- Oanh NTK, Reutergardh LB, Dung NT (1999) Emission of polycyclic aromatic hydrocarbons and particulate matter from domestic combustion of selected fuels. *Environ Sci Technol* 33: 2703–2709
- Oanh NTK, Kongpran J, Hang NT, Parkpian P, Hung NTQ, Lee SB, Bae GN (2013) Characterization of gaseous pollutants and PM<sub>2.5</sub> at fixed roadsides and along vehicle traveling routes in Bangkok Metropolitan Region. *Atmos Environ* 77:674–685
- Okuda T, Kumata H, Zakaria MP, Naraoka H, Ishiwatari R, Takada H (2002) Source identification of Malaysian atmospheric polycyclic aromatic hydrocarbons nearby forest fires using molecular and isotopic compositions. *Atmos Environ* 36:611–618
- Ollivon D, Blanchard M, Garban B (1999) PAH fluctuations in rivers in the Paris region (France): impact of floods and rainy events. *Wat Air Soil Poll* 115:429–444
- Orecchio S (2010) Contamination from polycyclic aromatic hydrocarbons (PAHs) in the soil of a botanic garden localized next to a former manufacturing gas plant in Palermo (Italy). *J Hazard Mater* 180:590–601
- Oros DR, Simoneit BRT (2000) Identification and emission rates of molecular tracers in coal smoke particulate matter. *Fuel* 79:515–536
- Ou S, Zheng J, Zheng J, Richardson BJ, Lam PKS (2004) Petroleum hydrocarbons and polycyclic aromatic hydrocarbons in the surficial sediments of Xiamen Harbour and Yuan Dan Lake China. *Chemosphere* 56:107–112
- Page DS, Boehm PD, Douglas GS, Bence AE, Burns WA, Mankiewicz PJ (1996) The natural petroleum hydrocarbon background in subtidal sediments of Prince William Sound, Alaska, USA. *Environ Toxicol Chem* 15:1266–1281
- Page DS, Boehm PD, Douglas GS, Bence AE, Burns WA, Mankiewicz PJ (1999) Pyrogenic polycyclic aromatic hydrocarbons in sediments record past human activity: a case study in Prince William Sound, Alaska. *Mar Pollut Bull* 38:247–260
- Page DS, Bence AE, Burns WA, Boehm PD, Brown JS, Douglas GS (2003) The role of petroleum geochemistry in defining oil spill recovery: examples from the Exxon Valdez spill in Prince William Sound, Alaska. In: *Proceedings of the 2003 International Oil Spill Conference*: Publication No. I 4730 B. American Petroleum Institute, Washington, DC, pp 1–8
- Page DS, Brown JS, Boehm PD, Bence AE, Neff JM (2006) A hierarchical approach measures the aerial extent and concentration levels of PAH-contaminated shoreline sediments at historic industrial sites in Prince William Sound, Alaska. *Mar Pollut Bull* 52:367–379
- Pavlova A, Ivanova R (2003) Determination of petroleum hydrocarbons and polycyclic aromatic hydrocarbons in sludge from wastewater treatment basins. *J Environ Monit* 5:319–323
- Park SS, Kim YJ, Kang CH (2002) Atmospheric polycyclic aromatic hydrocarbons in Seoul, Korea. *Atmos Environ* 36:2917–2924
- Pereira WE, Hostettler FD, Luoma SN, Van Geen A, Fuller CC, Anima RJ (1999) Sedimentary record of anthropogenic and biogenic polycyclic aromatic hydrocarbons in San Francisco Bay, California. *Mar Chem* 64:99–113
- Peters KE, Walters CC, Moldowan M (2005) *The biomarker guide. Biomarkers and isotopes in the environment and human history, vol 1, 2nd edn.* Cambridge University Press, Cambridge, pp 296–312
- Philp RP (2007) The emergence of stable isotopes in environmental and forensic geochemistry studies: a review. *Environ Chem Lett* 5:57–66
- Pies C, Hoffman B, Petrowsky J, Yang Y, Ternes TA, Hofmann T (2008) Characterization and source identification of polycyclic aromatic hydrocarbons (PAHs) in river bank soils. *Chemosphere* 72:1594–1601
- Radke M, Willsch H, Leythaeuser D, Teichmuller M (1982) Aromatic components of coal: relation of distribution pattern to rank. *Geochim Cosmochim Acta* 46:1831–1848
- Ravindra K, Sokhi R, Van Grieken R (2008) Atmospheric polycyclic aromatic hydrocarbons: source attribution, emission factors and regulation. *Atmos Environ* 42:2895–2921
- Riddle SG, Jakober CA, Robert MA, Cahill TM, Charles MJ, Kleeman MJ (2007) Large PAHs detected in fine particulate matter emitted from light-duty gasoline vehicles. *Atmos Environ* 41:8658–8668

- Roush JA, Mauro DM (2009) Site assessment for proposed coke point dredged material containment facility at Sparrows Point. Baltimore County, Maryland Attachment IV. Analytical report – environmental forensics for soil and sediment samples, T06006Forensic 090717, META Environmental Inc, Watertown, MA
- Saber DL, Mauro D, Sirivedhin T (2005) Applications of forensic chemistry to environmental work. *J Ind Microbiol Biotechnol* 32:665–668
- Saber D, Mauro D, Sirivedhin T (2006) Environmental forensic investigation in sediments near a former manufactured gas plant site. *Environ Forens* 7:65–75
- Saha M, Togo A, Mizukawa K, Murakami M, Takada H, Zakaria MP, Chiem NH, Tuyen BC, Prudente M, Boonyatumanond R, Sarkar SK, Bhattacharya B, Mishra P, Tana TS (2009) Sources of sedimentary PAHs in tropical Asian waters: differentiation between pyrogenic and petrogenic sources by alkyl homolog abundance. *Mar Pollut Bull* 58:189–200
- Sander LC, Wise SA (1997) Polycyclic aromatic hydrocarbon structure index. NIST Special Publication 922, NSPUE2. United States Department of Commerce Technology Administration, National Institute of Standards and Technology, Gaithersburg, MD, pp 1–105
- Schwarzenbach RP, Gschwend PM, Imboden DM (2003) Environmental organic chemistry, 2nd edn. Wiley-Interscience, Totowa, NJ, pp 1197–1208
- Short JW, Irvine GV, Mann DH, Maselko JM, Pella JJ, Lindeberg MR, Payne JR, Driskell WB, Rice SD (2007) Slightly weathered Exxon Valdez oil persists in gulf of Alaska beach sediments after 16 years. *Environ Sci Technol* 41:1245–1250
- Shreadah MA, Said TO, Abd El Monem MI, Fathallah EMI, Mahmoud ME (2011) PAHs in sediments along the semi-closed areas of Alexandria. *Egypt J Environ Prot* 2:700–709
- Sicre MA, Marty JC, Saliot A, Aparicio X, Grimalt J, Albaiges J (1987) Aliphatic and aromatic hydrocarbons in different sized aerosols over the Mediterranean Sea: occurrence and origin. *Atmos Environ* 21:2247–2259
- Simcik MF, Eisenreich SJ, Liroy PJ (1999) Source apportionment and source/sink relationships of PAHs in the coastal atmosphere of Chicago and Lake Michigan. *Atmos Environ* 33:5071–5079
- Simoneit BRT (1985) Application of molecular marker analysis to vehicular exhaust for source reconciliations. *Int J Environ Anal Chem* 22:203–233
- Soclo HH, Garrigues PH, Ewald M (2000) Origin of polycyclic aromatic hydrocarbons (PAHs) in coastal marine sediments: case studies in Cotonou (Benin) and Aquitaine (France) areas. *Mar Pollut Bull* 40:387–396
- Sofowote UM, McCarry BE, Marvin CH (2008) Source apportionment of PAH in Hamilton Harbour suspended sediments: Comparison of two factor analysis methods. *Environ Sci Technol* 42:6007–6014
- Sofowote UM, Allan LM, McCarry BE (2009) Evaluation of PAH diagnostic ratios as source apportionment tools for air particulates collected in an urban-industrial environment. *J Environ Monit* 12:417–424
- Sofowote UM, Hung H, Rastogi AK, Westgate JN, Deluca PF, Su Y, McCarry BE (2011) Assessing the long-range transport of PAH to a sub-Arctic site using positive matrix factorization and potential source contribution function. *Atmos Environ* 45:967–976
- Sporstol S, Gjøs N, Lichtenthaler RG, Gustavsen KO, Urdal K, Orelid F, Skel J (1983) Source identification of aromatic hydrocarbons in sediments using GC/MS. *Environ Sci Technol* 17:282–286
- Stark A, Abrajano T, Hellou J, Metcalf-Smith JL (2003) Molecular and isotopic characterization of polycyclic aromatic hydrocarbon distribution and sources at the international segment of the St. Lawrence River. *Org Geochem* 34:225–237
- Stout SA (2007) Characterization and source of unknown “tar-like material” and “slag” in a former oil field in Compton, California. *Environ Forens* 8:265–282
- Stout SA, Wang Z (2007) Chemical fingerprinting of spilled or discharged petroleum – methods and factors affecting petroleum fingerprints in the environment. In: Wang Z, Stout SA (eds) Oil spill environmental forensics. Fingerprinting and source identification. Elsevier, Boston, MA, pp 1–54

- Stout SA, Emsbo-Mattingly SD (2008) Concentration and character of PAHs and other hydrocarbons in coals of varying rank – implications for environmental studies of soils and sediments containing particulate coal. *Org Geochem* 39:801–819
- Stout SA, Graan TP (2010) Quantitative source apportionment of PAHs in sediments of Little Menomonee River, Wisconsin: weathered creosote versus urban background. *Environ Sci Technol* 44:2932–2939
- Stout SA, Magar VX, Uhler RM, Ickes J, Abbott J, Brenner R (2001a) Characterization of naturally occurring and anthropogenic PAHs in urban sediments Wyckoff/Eagle Harbor Superfund site. *Environ Forens* 2:287–300
- Stout SA, Uhler AD, Boehm PD (2001b) Recognition of and allocation among multiple sources of PAH in urban sediments. *Environ Claims J* 13:141–158
- Stout SA, Magar VX, Uhler RM, McCarthy KJ, Emsbo-Mattingly S (2002) Chemical fingerprinting of hydrocarbons. In: Murphy BL, Morrison RD (eds) *Introduction to environmental forensics*, 1st edn. Academic, New York, NY, pp 137–260
- Stout SA, Leather JM, Corl WE III (2003) A user's guide for determining the sources of contaminants in sediments. Technical report 1907. Spawar Systems Center, San Diego, CA, pp 1–85
- Stout SA, Uhler AD, Emsbo-Mattingly SD (2004) Comparative evaluation of background anthropogenic hydrocarbons in surficial sediments from nine urban waterways. *Environ Sci Technol* 38:2987–2994
- Stout SA, Douglas GS, Uhler AD, McCarthy KJ, Emsbo-Mattingly SD (2005) Identifying the source of mystery waterborne oil spills – a case for quantitative chemical fingerprinting. *Environ Claims J* 17:71–88
- Stout SA, Uhler AD, McCarthy KJ (2006) Chemical characterization and sources of distillate fuels in the subsurface of Mandan, North Dakota. *Environ Forens* 7:267–282
- Stout SA, Liu B, Millner GC, Hamlin D, Healey E (2007) Use of chemical fingerprinting to establish the presence of spilled crude oil in a residential area following hurricane Katrina, St. Bernard Parish, Louisiana. *Environ Sci Technol* 41:7242–7251
- Swietlik R, Kowalczyk D, Dojlido J (2002) Influence of selected physicochemical factors on the degradation of PAHs in water. *Pol J Environ Stud* 11:165–169
- Takada H, Onda T, Ogura N (1990) Determination of polycyclic aromatic hydrocarbons in urban street dusts and their source materials by capillary gas chromatography. *Environ Sci Technol* 24:1179–1186
- Tan JH, Duan JC, Chen DH, Wang XH, Guo SJ, Bi XH, Sheng GY, He KB, Fu JM (2009) Chemical characteristics of haze during summer and winter in Guangzhou. *Atm Res* 94:238–245
- Tobiszewski M, Namiesnik J (2012) PAH diagnostic ratios for the identification of pollution emission sources. *Environ Pollut* 162:110–119
- Uhler AD, Emsbo-Mattingly SD (2006) Environmental stability of PAH source indices in pyrogenic tars. *Bull Environ Contam Toxicol* 76:689–696
- Uhler AD, Stout SA, Douglas GS (2007) Chemical heterogeneity in modern marine residual fuel oils. In: Wang Z, Stout SA (eds) *Oil spill environmental forensics. Fingerprinting and source identification*. Elsevier, Boston, MA, pp 327–348
- Valle S, Panero MA, Shor L (2007) *Pollution prevention and management strategies for polycyclic aromatic hydrocarbons in the New York/New Jersey Harbor*. Academy of Sciences, New York, NY
- Van Drooge BL, Crusack M, Reche C, Mohr C, Alastuey A, Querol X, Prevot A, Day DA, Jimenez JL, Grimalt JO (2012) Molecular marker characterization of the organic composition of submicron aerosols from Mediterranean urban and rural environments under contrasting meteorological conditions. *Atmos Environ* 61:482–489
- Van Metre PC, Mahler BJ (2010) Contribution of PAHs from coal-tar pavement sealcoat and other sources to 40 U.S. lakes. *Sci Total Environ* 409:334–344
- Venkatesan MI (1988) Occurrence and possible sources of perylene in marine sediments—a review. *Mar Chem* 25:1–27
- Walker SE, Dickhut RM (2001) Sources of PAHs to sediments of the Elizabeth River, VA. *Soil Sedim Contam* 10:611–632

- Wang Z, Fingas M (1995) Use of methyl dibenzothiophenes as markers for differentiation and source identification of crude and weathered oils. *Environ Sci Technol* 29:2842–2849
- Wang Z, Fingas MF (2003) Development of oil hydrocarbon fingerprinting and identification techniques. *Mar Pollut Bull* 47:423–452
- Wang Z, Brown C (2009) Chemical fingerprinting of petroleum hydrocarbons. In: Mudge SM (ed) *Methods in environmental forensics*. CRC Press, Boca Raton, FL, pp 43–112
- Wang Z, Fingas M, Blenkinsopp S, Sergy G, Landriault M, Sigouin L (1998) Comparison of oil composition changes due to biodegradation and physical weathering in different oils. *J Chromatogr A* 809:89–107
- Wang Z, Fingas M, Page DS (1999a) Oil spill identification. *J Chromatogr A* 843:369–411
- Wang Z, Fingas M, Shu YY, Sigouin L, Landriault M, Lambert P, Turpin R, Campagna P, Mullin J (1999b) Quantitative characterization of PAHs in burn residue and soot samples and differentiation of pyrogenic PAHs from petrogenic PAHs – the 1994 mobile burn study. *Environ Sci Technol* 33:3100–3109
- Wang Z, Fingas M, Sigouin L (2001) Characterization and identification of a “mystery” oil spill from Quebec (1999). *J Chromatogr A* 909:155–169
- Wang Z, Fingas M, Lambert P, Zeng G, Yang C, Hollebone B (2004) Characterization and identification of the Detroit River mystery oil spill (2002). *J Chromatogr A* 1038:201–214
- Wang Z, Li K, Lambert P, Yang C (2006) Identification, characterization and quantitation of pyrogenic polycyclic aromatic hydrocarbons and other organic compounds in tire fire products. *J Chromatogr A* 1139:14–26
- Wang Z, Yang C, Brown C, Hollebone B, Landriault M (2009) A case study: distinguishing pyrogenic hydrocarbons from petrogenic hydrocarbons. In: *Proceedings of 2008 International Oil Spill Conference*. American Petroleum Institute, National Research Council (NRC) 1999, National Academy Press, Washington, DC, pp 311–320
- Wang Z, Yang C, Parrot JL, Frank RA, Yang Z, Brown CE, Hollebone BP, Landriault M, Fieldhouse B, Liu Y, Zhang G, Hewitt LM (2014) Forensic source differentiation of petrogenic, pyrogenic, and biogenic hydrocarbons in Canadian oil sands environmental samples. *J Hazard Mater* 271:166–177
- Wickramasinghe AP, Karunaratne DG, Sivakanesan R (2011) PM10-bound polycyclic aromatic hydrocarbons: Concentrations, source characterization and estimating their risk in urban, suburban and rural areas in Kandy, Sri Lanka. *Atmos Environ* 45:2642–2650
- Wilcke W, Krauss M, Amelung W (2002) Carbon isotope signature of polycyclic aromatic hydrocarbons (PAHs): evidence for different sources in tropical and temperate environments? *Environ Sci Technol* 36:3530–3535
- Williams PT, Bartle KD, Andrews GE (1986) The relation between polycyclic aromatic compounds in diesel fuels and exhaust particulates. *Fuel* 65:1150–1158
- Windsor JG, Hites RA (1979) Polycyclic aromatic hydrocarbons in Gulf of Maine sediments and Nova Scotia soils. *Geochim Cosmochim Acta* 43:27–33
- Yan B, Abrajano TA, Bopp RF, Chaky DA, Benedict L, Chillrud SN (2005) Molecular tracers of saturated and polycyclic aromatic hydrocarbon inputs into Central Park Lake, New York City. *Environ Sci Technol* 39:7012–7019
- Yan B, Abrajano TA, Bopp RF, Benedict LA, Chaky DA, Perry E, Song J, Keane DP (2006) Combined application of  $\delta^{13}\text{C}$  and molecular ratios in sediment cores for PAH source apportionment in the New York/New Jersey harbor complex. *Org Geochem* 37:674–687
- Yan B, Bopp RF, Chaky DA, Chillrud SN, Abrajano TA (2007) Organic contaminant sources to the lower Hudson basin. *Environmental monitoring and protection in New York: linking science and policy*, Poster Abstracts, NYSERDA, 15–16 November, New York, NY
- Yang HH, Lai SO, Hsieh LS, Hsueh LJ, Chi TW (2002) Profiles of PAH emission from steel and iron industries. *Chemosphere* 48:1061–1074
- Youngblood WW, Blumer M (1975) Polycyclic aromatic hydrocarbons in the environment: homologous series in soils and recent marine sediments. *Geochim Cosmochim Acta* 39:1303–1314

- Yunker MB, Macdonald RW, Vingarzan R, Mitchel RH, Goyette D, Sylvestre S (2002) PAHs in the Fraser River basin: a critical appraisal of PAH ratios as indicators of PAH source and composition. *Org Geochem* 33:489–515
- Yunker MB, Lachmuth CL, Cretney WJ, Fowler BR, Dangerfield N, White L, Ross PS (2011) Biota-sediment partitioning of aluminium smelter related PAHs and pulp mill related diterpenes by intertidal clams at Kitimat, British Columbia. *Mar Environ Res* 72:105–126
- Zakaria MP, Takada H, Tsutsumi S, Ohno K, Yamada J, Kound E, Kumata H (2002) Distribution of polycyclic aromatic hydrocarbons (PAHs) in rivers and estuaries in Malaysia: a widespread input of petrogenic PAHs. *Environ Sci Technol* 36:1907–1918
- Zakaria MP, Takada H (2007) 16 Case study: oil spills in the strait of Malacca, Malaysia. In: Wang Z, Stout SA (eds) *Oil spill environmental forensics. Fingerprinting and source identification*. Elsevier, Boston, MA, pp 489–504
- Zeng EY, Vista CL (1997) Organic pollutants in the coastal environment off San Diego, California. 1. Source identification and assessment by compositional indices of polycyclic aromatic hydrocarbons. *Environ Toxicol Chem* 16:179–188
- Zhang XL, Tao S, Liu WX, Yang Y, Zuo Q, Liu Z (2005) Source diagnostics of polycyclic aromatic hydrocarbons based on species ratios: A multimedia approach. *Environ Sci Technol* 39:9109–9114
- Zhu X, Fan ZT, Wu X, Jung KH, Ohman-Strickland P, Bonanno LJ, Liou PJ (2011) Ambient concentrations and personal exposure to polycyclic aromatic hydrocarbons (PAH) in an urban community with mixed sources of air pollution. *J Expos Sci Environ Epidemiol* 21:437–449



# Respiratory and Cardiovascular Effects of Metals in Ambient Particulate Matter: A Critical Review

Deborah L. Gray, Lance A. Wallace, Marielle C. Brinkman, Stephanie S. Buehler, and Chris La Londe

## Contents

1	Introduction .....	136
2	Approach .....	137
2.1	Exposure.....	138
2.2	Epidemiology .....	138
2.3	Toxicology.....	139
3	Results .....	140
3.1	Exposure.....	140
3.2	Epidemiology .....	146
3.3	Toxicology.....	154
4	Summary .....	196
	References.....	197

---

D.L. Gray (✉)  
Stantec Consulting Services, Inc., 1500 Lake Shore Drive, Suite 100,  
Columbus, OH 43204, USA  
e-mail: [deb.gray@stantec.com](mailto:deb.gray@stantec.com)

L.A. Wallace  
Santa Rosa, CA, USA

M.C. Brinkman • S.S. Buehler  
Battelle Centers for Public Health Research and Evaluation, Columbus, OH, USA

C. La Londe  
Stantec Consulting Services, Inc., 1500 Lake Shore Drive, Suite 100, Columbus,  
OH 43204, USA

## 1 Introduction

There is a large body of community-level epidemiologic evidence showing positive associations between increases in morbidity and mortality from respiratory and cardiovascular causes, and increases in the mass of ambient particulate matter (PM) in air in the preceding 1–3 days (Dockery and Pope 1994; Schwartz and Morris 1995; Laden et al. 2000). The evidence has been sufficiently convincing to support the development of ambient air quality standards and regulations to reduce air particulate emissions in the U.S., Canada and Europe. Ambient PM is a dynamic and complex mixture that varies in composition over both time and location; and, it is not clear which components of ambient PM are most active in producing respiratory and cardiovascular health effects. Identifying which components of ambient PM present the greatest risk is potentially important for refining strategies to protect public health (Grahame and Schlesinger 2007).

Rohr and Wyzga (2012) recently summarized the epidemiological, controlled human exposure, and toxicological literature related to the role of PM components in health effects. They concluded that the epidemiological studies that they reviewed most strongly implicated carbon-containing PM components, but they did not fully exonerate any major component class. They also noted that the toxicology literature suggests that several elements including aluminum, silicon, vanadium, and nickel have been associated with health effects, in addition to carbon-containing components. In this critical review, we review studies in which metal components have had a role in producing health effects attributed to ambient PM.

In late 2013 the Health Effects Institute (HEI) National Particle Component Toxicity (NPACT) Initiative published two comprehensive reports of coordinated toxicological and nationwide epidemiologic studies of the health effects of PM and its components. Report No. 177 presents the findings of Lippmann and colleagues (2013) from studies with mice and human cell lines which identified the coal combustion, residual oil combustion, traffic, and metals source categories as most frequently associated with cardiovascular effects. In Report No. 178 Vedal and colleagues (2013) investigated the cardiovascular effects of traffic related PM by evaluating data from two national epidemiologic studies—the Multi-Ethnic Study of Atherosclerosis (MESA) and the Women’s Health Initiative Observational Study (WHI-OS). Their analysis of the epidemiologic data was supported by toxicological studies, in which mice were exposed to mixtures of diesel and gasoline emissions. Both the particulate and gas phases of motor vehicle exhaust were found to play a role in cardiovascular effects. These reports add significant new information regarding the cardiovascular effects of PM. However, as observed by the HEI review panel implicating (or exonerating) any specific PM component is difficult given the complexity of the exposures.

Several epidemiologic studies conducted during the late 1980s and 1990s (Pope 1989, 1991, 1992) introduced the hypothesis that metal constituents of ambient PM may contribute to the increases in respiratory and cardiovascular morbidity and mortality that are associated with small increases in ambient PM. Pope (1989) reported that the incidence of respiratory ailments in the community near an open hearth steel mill in the Utah Valley decreased during a year (1987) when the mill was closed for repairs, compared to the two adjacent years (1986, 1988). Since the

levels of some metals in ambient PM in the region were also lower during the year that the mill was closed, it was suggested that PM-bound metals may be associated with changes in the incidence of respiratory ailments. The results of these studies in the Utah Valley are so central to the hypothesis that metals may be causally related to the respiratory and cardiovascular illnesses associated with particulate air pollution, that archived particulate matter from those 3 years has been used as the source of exposure in several of the toxicology studies that we review in this paper.

Over the past 20 years, numerous studies have been conducted to characterize metal constituents in ambient PM and to apportion the relative contributions of source categories (e.g., industrial, motor vehicle, crustal elements) to the composition of ambient PM in various geographic regions. A relatively smaller number of epidemiologic studies have been conducted that explored associations between specific transition metals and health effects in members of the general population. There is a growing body of *in vivo* and *in vitro* toxicology studies, in which the potential has been tested for PM metals to induce inflammation and alter gene expression along pathways potentially involved in respiratory and cardiovascular illnesses. To our knowledge, the adequacy of the current body of evidence to determine the risk posed by specific metals in ambient PM has not been critically evaluated, although previous reviews of the literature have been published (Schlesinger 2007). In particular, the review by Chen and Lippmann (2009) served as a spring-board for our current work.

Chen and Lippmann (2009) detailed available epidemiological studies through 2006, summarizing the health effects of PM-associated metals on exposed populations. They found that there were limited data on metallic elements as tracers for source apportionment of health effects, and many of the studies that they cited did not report metal-specific data that were associated with PM. They concluded that extrapolations would have to be made, based on the source and the known general components of that source, to estimate what metals might be causing the health effects. However, such extrapolation is only an indirect means of identifying particular metals or their amounts that constitute a significant factor from a given source.

## 2 Approach

Our objective was to better understand how the metal content of ambient air PM contributes to the health effects associated with particulate air pollution. We searched the peer-reviewed literature that was published from 1993 to October, 2012, to review the health effects of specific transition metals that were associated with airborne particulate matter in normal and/or at-risk sub-populations. We narrowed the selection of articles to those containing exposure assessment and dose-response data, such that results from this review can be integrated into a future risk analysis. Although the strongest associations for health effects that are linked to ambient particulates reported in the epidemiological literature are for fine particles having aerodynamic diameters of  $\leq 2.5 \mu\text{m}$  ( $\text{PM}_{2.5}$ ), we reviewed all relevant studies regardless of the size category. These size categories included the following particulate classes: coarse particles (with an aerodynamic diameter larger than  $\text{PM}_{2.5}$  but smaller than  $10 \mu\text{m}$ ), ultrafine particles (particles with an aerodynamic diameter  $\leq 0.1 \mu\text{m}$ ), and

Total Suspended Particulate in air (TSP). During a preliminary review of the literature, we identified ten metals and metalloids (arsenic and selenium) that posed the greatest potential risk to human health, based on their prevalence in ambient air, and their toxicity: arsenic (As), chromium (Cr), copper (Cu), iron (Fe), manganese (Mn), nickel (Ni), selenium (Se), titanium (Ti), vanadium (V), and zinc (Zn). We excluded lead and mercury, because the health effects literature for both elements is sufficiently voluminous and convincing to support the regulatory and public health actions already taken that have greatly reduced exposures to the general population.

Only studies that incorporated univariate analyses for specific metals of interest and health effects were included in this review. Thus, numerous studies that only inferred, rather than directly evaluated, the role of metals in ambient PM were excluded. Unless otherwise stated, appropriate statistical methods were used in the studies presented in this review; statistical significance equates to a p value less than 0.05.

## **2.1 Exposure**

In the exposure section, we focus on ambient measurements of the target metals as provided by the two national monitoring networks operated by the United States Environmental Protection Agency (US EPA) the Speciation Trends Network (STN) and the Interagency Monitoring of Protected Visual Environments (IMPROVE) network. Information from the IMPROVE network reference in this review was obtained online from <http://epa.gov/ttnamtiI/visdata.html> (US EPA 2010a); and information from the STN network was obtained on-line from <http://ttn/amtic/specieg.html> (US EPA 2010b). Moreover, we briefly address method detection limits in each network. Since the STN includes primarily urban areas and IMPROVE mostly rural ones, we present mean results from the most recent full year available from each study to indicate the range of concentrations to be expected. Major multicity studies of ambient concentrations from Canada and Europe are also presented. A brief section on indoor and personal exposures follows.

## **2.2 Epidemiology**

Using Chen and Lippmann (2009) as a starting point, we performed a similar search and included many of the studies they reviewed, because they continue to have relevance. In addition, we focused on two sensitive subpopulations that have been linked with PM-associated metals and adverse health effects. These subpopulations were a) individuals with compromised cardiopulmonary function, and b) those aged 65 years old or older, and children (0–17 years old). Occupational studies were excluded from our review since worker exposure conditions may not emulate those of the general population. The majority of epidemiology studies included in this review focused on respiratory and cardiovascular outcomes. Although we used general search terms for health effects that would not have excluded cancer as an outcome, there were few if any studies that attempted to correlate specific transition metals in ambient PM with cancer morbidity and mortality.

## 2.3 Toxicology

We searched the toxicology literature for *in vivo* and *in vitro* studies, including human studies that were designed to elucidate the role of PM-associated metals in the respiratory and cardiovascular health effects most frequently reported in epidemiologic studies. We selected studies that provided data on metal exposures from a source of ambient PM, such as archived particulates from regional air monitors, concentrated ambient particles (CAPs), or residual oil fly ash (ROFA). In several studies, laboratory animals or cell cultures were treated with solutions of the major metal constituents that had been identified in ambient PM sources. The *in vitro* studies summarized in this review were often designed to reveal the mechanisms by which PM-associated metals may contribute to adverse health effects.

The *in vivo* studies summarized herein utilized different dosing routes (e.g., inhalation, intratracheal instillation), animal models (e.g., mouse, rat, dog, human), dosage levels, and often expressed doses in different units. To allow comparison across studies, when sufficient information was available, we recalculated all dosages on a mass per body weight basis. For reference to typical human daily dosages, we used the annual mean concentrations of our target metals in the STN 2008 data (Table 1). We assumed a daily breathing rate of 10 m<sup>3</sup> and a human body weight of

**Table 1** Mean annual concentrations of PM<sub>2.5</sub> and transition metals in ambient air in the U.S. as reported by the Speciation Trends Network (STN 2008) and Interagency Monitoring of Protected Visual Environments (IMPROVE 2006)

Analyte	STN 2008				IMPROVE 2006				Ratio means, STN/IMPROVE
	N	Mean	Standard error	Fraction of PM <sub>2.5</sub>	N	Mean	Standard error	Fraction of PM <sub>2.5</sub>	
Particulate Matter <sub>2.5</sub> —μg/m <sup>3</sup>									
PM <sub>2.5</sub>	13,990	12.5	0.67	—	19,272	5.4	0.037	—	2.3
Target Metals—ng/m <sup>3</sup>									
As	13,607	0.8	0.01	0.006%	19,002	0.2	0.003	0.004%	4.0
Cr	13,607	2.3	0.23	0.018%	18,861	0.1	0.003	0.002%	23
Cu	13,702	5.4	0.11	0.043%	19,019	0.8	0.014	0.015%	6.7
Fe	13,702	94	2.21	0.752%	19,094	46	0.547	0.852%	2.1
Mn	13,607	3.0	0.18	0.024%	19,088	1.3	0.018	0.024%	2.3
Ni	13,607	1.3	0.09	0.010%	18,956	0.3	0.008	0.006%	4.3
Se	13,607	0.5	0.01	0.004%	18,838	0.4	0.005	0.007%	1.3
Ti	13,702	2.5	0.05	0.020%	19,079	3.9	0.05	0.072%	0.6
V	13,702	1.1	0.02	0.009%	18,918	0.5	0.007	0.009%	2.3
Zn	13,702	14	0.28	0.112%	19,093	4.3	0.081	0.080%	3.2

\*STN Detection Limits (US EPA 2010b): As (2.5), Cr (1.6), Cu (1.4), Fe (2.0), Mn (2.3), Ni (1.3), Se (2.1), Ti (2.1), V (1.5), Zn (1.5)

<sup>b</sup>IMPROVE Detection Limits (US EPA 2010a): As (0.094), Cr (0.028), Cu (0.043), Fe (0.039), Mn (0.026), Ni (0.059), Se (0.026), Ti (0.051), V (0.034), Zn (0.039)

70 kg to convert these concentrations into a daily dose for our “standard human”. Representative body weights for dogs, rats and mice were 10 kg, 0.3 kg and 0.02 kg, respectively. The ratio of the study dosage to this mean daily human dose provides a common metric for all studies. (Please see the footnote to Table 6 for additional assumptions, e.g., breathing rates and body weights of the test animals, etc.).

## 3 Results

### 3.1 Exposure

Understanding the range of ambient concentrations of PM-associated metals is essential to putting epidemiological and toxicological studies into perspective. We limited our analysis to data collected in support of large human exposure studies and national networks and those studies containing ambient, indoor and personal air data for the ten target metals.

#### 3.1.1 Concentrations of Transition Metals in Ambient Air

Epidemiology studies rely upon measurements of ambient PM and its components to represent exposure to populations of interest. Airborne elements are generally measured using actively pumped samplers and analyzing the resulting filter loadings by one of several methods. The most common are X-ray fluorescence (XRF), proton-induced X-ray emission (PIXE), atomic absorption spectrometry (AAS), and inductively coupled plasma mass spectrometry (ICP-MS), which is becoming more popular, because smaller concentrations of some metals are detectable by using this technique.

The two main large-scale networks operating in the United States (U.S.), the IMPROVE and the STN provide useful information on ambient concentrations of transition metals in urban and rural areas. The IMPROVE network of 110 sites (US EPA 2010a) was set up in 1987 to measure visibility and particle and elemental concentrations in areas where visibility is protected by stringent regulations, such as National Parks. Approximately 24 elements are being analyzed by XRF in about 60 sites. The STN (US EPA 2010b) was designed in the 1990s to more completely analyze the various components of PM<sub>2.5</sub>, and by 2000 it was operating in 174 urban and suburban sites. STN performs analyses for 48 elements.

Thus, the two networks are expected to represent the range of ambient concentrations experienced by the vast majority of the U.S. population. Both networks report a detection frequency of 85–100% for Fe, Zn, and Cu. The remaining seven metals are detected at least 40% of the time in the STN. Ni and As are found more often in the STN; and, some crustal metals such as Ti and Se are found more often in IMPROVE. The urban/rural ratios of mean concentrations range between 2 and 4 for 7 of the 10 target metals. Mean ambient concentrations in the PM<sub>2.5</sub> fraction

from the STN network range from about 1–5 ng/m<sup>3</sup> for 8 of the 10 target metals; Zn (14 ng/m<sup>3</sup>) and Fe (94 ng/m<sup>3</sup>) are the exceptions (Table 1).

The STN network has confirmed that the highest metal concentrations are found in heavily industrialized cities such as Birmingham, AL, Pittsburgh, PA, and East Saint Louis, IL. Since these high-concentration areas are the most likely to show health effects, if such exist, it is important to have confirmation that measured concentrations are a reliable representation of potential exposures. Hyslop and White (2008; 2009) compared the STN and IMPROVE network detection limits for six elements, five of which are included in our ten targeted metals: As, Cu, Fe, Ti, Mn, and Se; they found that the detection limits for all metals were approximately 10 times lower for the IMPROVE network than for the STN network. Detection limits in ng/m<sup>3</sup> for the STN 2008 data and the IMPROVE 2006 data, for the major metals of interest in this review were, respectively: Cu (1.4 and 0.043); Fe (2.0 and 0.039); Mn (2.3 and 0.026); Ni (1.3 and 0.059); V (1.5 and 0.034); and Zn (1.5 and 0.039). Reff et al. (2009) provides a complete discussion of major sources of the target elements. The laboratories contributing to the two networks have recently agreed to “harmonize” their measures of uncertainty and detection limits by adopting similar or identical methods (Gutknecht et al. 2010). It is anticipated that recent progress in determining empirical method detection limits (MDLs) for duplicate monitors in the STN and IMPROVE systems will provide more reliable detections and measurements for PM metals across geographic locations, and ultimately benefit the conduct of epidemiological studies.

The Canadian National Air Pollution Surveillance Network (NAPS) monitors the largest cities in Canada and other sites that are chosen mainly for their intensity of industrial activity. The European Environment Agency also monitors several air quality parameters, including PM<sub>10</sub>, PM<sub>2.5</sub>, As, Cd, Ni and Pb. Maps of monitored sites can be found on-line at <http://www.eea.europa.eu/themes/air/airbase/>. Useful data on a large number of samples in eight Canadian cities (Burnett et al. 2000) were collected in two additional studies, and in one U.S. city (Steubenville, OH), long studied closely for its relatively high levels of ambient PM (Connell et al. 2006). Table 2 summarizes the average ambient concentrations of PM<sub>2.5</sub> and metals of interest and the percent of PM<sub>2.5</sub> mass from several studies.

Recent progress has been made in estimating emissions of metals on a nationwide geographic grid. A special analysis in this report suggested that, at least for the highest observed ambient concentrations, the emissions estimates are often consistent with those measurements. A far more complete study is needed on the entire STN data (not just the top 2% as in our analysis) for the years surrounding the latest emission inventory.

Although much more information is now available on metal concentrations in ambient air due to the STN network, additional work needs to be done in first collecting data from duplicate monitors over a period of years on empirical precision, and then using that information to detect areas of sampling and analysis that can be improved. When completed, such work will improve detection limits and will produce more accurate results for the less-common elements.

**Table 2** Mean ambient concentrations of  $PM_{2.5}$  and target elements and target metal concentration as a percent of  $PM_{2.5}$  reported by nationwide networks and in selected studies

Network name or study/reference	Location	$PM_{2.5}$		As	Cr	Cu	Fe	Mn	Ni	Se	Ti	V	Zn
		$\mu\text{g}/\text{m}^3$	$\text{ng}/\text{m}^3$										
Network name or study/reference IMPROVE 2006	National Parks	5.4		<b>0.2 a</b>	<b>0.1</b>	<b>0.8</b>	<b>46</b>	<b>1.3</b>	<b>0.3</b>	<b>0.4</b>	3.9	<b>0.5</b>	<b>4.3</b>
				<b>0.003</b>	<b>0.002</b>	<b>0.015</b>	<b>0.855</b>	<b>0.024</b>	<b>0.005</b>	<b>0.007</b>	<b>0.072</b>	<b>0.010</b>	<b>0.079</b>
NAPS 2008	25 Canadian Sites	7.5		-- <sup>b</sup>	0.3	--	53	2.7	1.9	0.5	2.6	1.0	12
STN 2008	U.S. Urban Areas	12		0.8	2.3	5.4	94	3.0	1.3	0.5	<b>2.5</b>	1.1	14
				0.006	0.019	0.043	0.759	0.024	0.010	0.004	<b>0.020</b>	0.009	0.111
Götschi (2005)	21 European Cities	17		<b>5.8<sup>c</sup></b>	--	6.5	76	3.3	--	--	4.0	3.6	39
				<b>0.035</b>		0.039	0.461	0.020			0.024	0.022	0.233
Burnett (2000)	8 Canadian Cities	13		0.9	2.2	7.7	81	13	1.6	1.0	6.2	3.7	26
				0.007	0.017	0.058	0.611	0.101	0.012	0.008	0.047	0.028	0.194
Connell (2006) TEACH (Kinney 2008) <sup>d</sup>	Steubenville, OH Los Angeles, CA	NR		1.6	NR	3.2	272	<b>15</b>	1.1	<b>3.3</b>	<b>17</b>	1.5	<b>84</b>
		13		0.4	1.8	4.9	144	5.1	6.9	2.0	12	4.9	43
				0.003	0.014	0.038	1.114	0.039	0.053	0.015	0.095	0.038	0.333



TEACH (Kinney 2005) <sup>d</sup>	New York City, NY	13	0.4	1.4	7.4	121	2.3	<b>23</b>	0.9	3.3	6.2	36
			0.003	0.011	0.058	0.949	0.018	<b>0.178</b>	0.007	0.026	0.048	0.281
RIOPA (Turpin 2007) <sup>d</sup>	Southern CA	19	0.5	0.6	5.5	163	2.9	2.0	1.4	10	5.3	16
			0.003	0.003	0.029	0.847	0.015	0.011	0.007	0.054	0.027	0.085
	Elizabeth, NJ	20	1.2	<b>7.0</b>	11	282	5.7	5.3	1.6	14	<b>6.7</b>	48
			0.006	<b>0.034</b>	0.054	1.380	0.028	0.026	0.008	0.068	<b>0.033</b>	0.233
	Houston, TX	15	1.0	1.1	1.9	117	4.3	2.2	0.7	8.8	5.5	14
			0.007	0.008	0.013	0.797	0.029	0.015	0.004	0.060	0.038	0.094
EPA-RTP <sup>e</sup>	Research Triangle Park, NC	19	1.5	0.5	3.3	133	3.2	1.1	1.7	9.4	2.2	14
			0.008	0.002	0.017	0.684	0.017	0.006	0.009	0.048	0.011	0.070
EPA-PTEAM (Thomas 1993, Clayton 1993; Ozkaynak et al. 1996)	Riverside, CA	<b>50</b>	--	--	<b>9.6</b>	<b>330</b>	11	--	--	--	--	40
					<b>0.019</b>	<b>0.660</b>	0.022					0.079

<sup>a</sup>“**Bold and Italic**” indicates the lowest reported value for each metal

<sup>b</sup>“--” Metal not evaluated by Network or Study

<sup>c</sup>**Bold** and “Shading” indicates the highest reported value for each metal

<sup>d</sup>Studies sponsored by Health Effects Institute (HEI) and the Mickey Leland National Urban Air Toxics Research Center (NUATRC)

<sup>e</sup>Unpublished data from 37-person study described in Wallace and Williams (2005)

### 3.1.2 Summary of Indoor and Personal Concentrations of Target Metals

Outdoor concentrations are not necessarily good guides to actual exposures. Most people spend most of their time indoors. Homes and buildings can act as a partial barrier to outdoor particles. However, indoor sources of particles also exist. Certain elements, such as sulfur, tend to have lower concentrations indoors, because few indoor sources exist, whereas levels of other elements tend to be higher indoors from sources such as cigarette smoke, cooking, and resuspension from clothes and floors because of particle mobility or cleaning processes (Wallace et al. 2008). Two valuable sources of particulate exposures levels are available and are the Toxicity and Exposure Assessment for Children's Health (TEACH) (Kinney et al. 2005, 2008) studies, and the Relationships of Indoor, Outdoor, and Personal Air (RIOPA): part II. analyses of concentrations of particulate matter species (Turpin et al. 2007), in which indoor and outdoor  $PM_{2.5}$  and elemental concentrations at 60–100 homes were measured in each of five cities or larger regions. The indoor and outdoor results for the target elements found in  $PM_{2.5}$  are summarized in Table 3. The indoor/outdoor (I/O) ratios, based on these results, are also shown. Metals such as V and Mn have I/O ratios <1 in all five areas, indicating few indoor sources. Metals with I/O ratios that often exceed one include Zn and Cu, indicating the presence of indoor sources (Adgate et al. 2007). Therefore, we expect human exposure for these two metals to be several times higher than their reported ambient levels. The RIOPA and TEACH studies did not include smokers. In a separate study, the target metals associated with tobacco smoke (viz., Cr, Ni, Zn, and As) were increased by factors of 8–22, compared to reference indoor atmospheres (Slezakova et al. 2009).

Personal daytime exposures to 14 elements in the  $PM_{10}$  fraction were shown to be elevated by more than 50% compared to concurrent indoor concentrations in the Particle TEAM study performed in Riverside, CA (Ozkaynak et al. 1996). The source of this “personal cloud” has not been unambiguously identified, but may arise from resuspension of particles from clothes or floors, or it may be due to a proximity effect, in that personal activities such as cooking or vacuuming involve closer distances to the source than the fixed location of the indoor monitor. The  $PM_{10}$  personal cloud was shown to be about  $35 \mu\text{g}/\text{m}^3$  in the Personal Total Exposure Assessment Methodology (PTEAM) (Clayton et al. 1993; Ozkaynak et al. 1996; Thomas et al. 1993) and other studies (Pellizzari et al. 1999). However, multiple studies of the  $PM_{2.5}$  fraction have shown a much smaller personal cloud, on the order of 2–3  $\mu\text{g}/\text{m}^3$ , suggesting that the  $PM_{10}$  personal cloud consists mostly of coarse particles (Wallace 2000). Coarse particles are more easily resuspended than fine particles due to Van der Waals forces attracting the fine particles to surfaces.

Although a small personal cloud has been reported in most  $PM_{2.5}$  studies, a very large personal cloud ranging from 13 to 25  $\mu\text{g}/\text{m}^3$  was reported in the RIOPA study, in which the concurrent indoor concentrations were about a factor of 2 higher. In contrast to the other studies, no personal cloud was reported in the TEACH study. Even larger personal/indoor factors, ranging up to 6.9, were found in the RIOPA study for metals such as Cr, Cu, Fe, Mn, Ni, Ti, and Zn. Increased personal exposures for these metals were reported in the TEACH study, but at more modest ratios <1.5, except for Ni in Los Angeles (2.6) and Cr, Fe, and Mn in New York City (5.4, 3.0, and 2.6, respectively).

**Table 3** Indoor, outdoor, personal PM<sub>2.5</sub> and target-metal concentrations as reported in the Toxicity and Exposure Assessment for Children's Health (TEACH) and Relationships of Indoor, Outdoor, and Personal Air (RIOPA studies)<sup>a</sup>

Location	Analyte										
	PM <sub>2.5</sub>	Fe	Zn	Ti	Ni	Cu	V	Mn	Cr	Se	As
	µg/m <sup>3</sup>	ng/m <sup>3</sup>									
Indoor											
L.A.	21.0	106.0	40.0	8.8	6.6	5.7	4.1	3.4	1.5	1.4	0.4
NYC	20.1	102.0	52.0	3.5	22.2	7.2	5.0	2.0	1.1	0.7	0.4
CA	16.2	109.0	16.0	10.8	1.6	5.4	4.1	2.0	0.9	0.8	0.5
NJ	20.1	72.0	106.0	4.1	3.0	11.4	4.1	2.2	3.8	0.9	0.9
TX	17.1	49.0	52.0	5.4	1.2	4.4	2.7	2.0	1.2	0.3	0.9
Outdoor											
L.A.	12.9	144.0	43.0	12.4	6.9	4.9	4.9	5.1	1.8	2.0	0.4
NYC	12.8	121.0	36.0	3.3	22.8	7.4	6.2	2.3	1.4	0.9	0.4
CA	19.2	163.0	16.0	10.4	2.0	5.5	5.3	2.9	0.6	1.4	0.5
NJ	20.4	282.0	48.0	13.9	5.3	11.0	6.7	5.7	7.0	1.6	1.2
TX	14.7	117.0	14.0	8.8	2.2	1.9	5.5	4.3	1.1	0.7	1.0
Personal <sup>b</sup>											
L.A.	16.7	156.0	56.0	12.7	17.2	7.5	3.9	4.6	1.9	1.4	0.4
NYC	17.9	546.0	48.0	4.1	23.5	8.0	5.1	6.2	3.0	0.7	0.5
CA	29.2	187.0	75.0	20.0	3.9	17.1	3.7	3.1	2.7	0.9	0.5
NJ	44.8	206.0	208.0	22.9	7.3	17.4	3.6	4.0	5.4	0.8	0.9
TX	37.2	168.0	69.0	28.5	4.1	12.3	2.6	4.2	2.3	0.4	1.2
Indoor/outdoor ratio											
L.A.	1.6	0.7	0.9	0.7	1.0	1.2	0.8	0.7	0.8	0.7	1.0
NYC	1.6	0.8	1.4	1.1	1.0	1.0	0.8	0.9	0.8	0.8	1.0
CA	0.8	0.7	1.0	1.0	0.8	1.0	0.8	0.7	1.5	0.6	1.0
NJ	1.0	0.3	2.2	0.3	0.6	1.0	0.6	0.4	0.5	0.6	0.8
TX	1.2	0.4	3.7	0.6	0.5	2.3	0.5	0.5	1.1	0.4	0.9
Personal/outdoor ratio											
L.A.	1.3	1.1	1.3	1.0	2.5	1.5	0.8	0.9	1.1	0.7	1.0
NYC	1.4	4.5	1.3	1.2	1.0	1.1	0.8	2.7	2.1	0.8	1.3
CA	1.5	1.1	4.7	1.9	2.0	3.1	0.7	1.1	4.5	0.6	1.0
NJ	2.2	0.7	4.3	1.6	1.4	1.6	0.5	0.7	0.8	0.5	0.8
TX	2.5	1.4	4.9	3.2	1.9	6.5	0.5	1.0	2.1	0.6	1.2

<sup>a</sup>Source: Turpin et al. (2007), Kinney et al. (2008)

<sup>b</sup>Samples collected using Personal Sampling Pumps at breathing zone height

Indoor and outdoor concentrations (from the TEACH and RIOPA studies) are generally within a factor of 2, with outdoor concentrations larger in about 60% of the comparisons and indoor concentrations larger in about 20% (Table 3). Mean personal concentrations (again from TEACH and RIOPA) were greater than mean indoor concentrations in 76% of the comparisons; mean indoor concentrations were greater in only 12% of the comparisons. Although indoor and personal exposures would be more closely associated with outcomes of interest to us, the epidemiological studies we reviewed were not designed to account for them. More studies are

required in different geographical areas to determine important parameters that potentially affect metal (and other constituents) exposures; such parameters include infiltration factors for house construction and insulation, air conditioning and occupant behaviors.

## 3.2 *Epidemiology*

It has been reported in a large number of studies that incremental increases in ambient PM concentrations are followed 1–3 days later by increases in respiratory and cardiovascular morbidity and mortality. Fewer studies have investigated the role of specific components of the total mass of ambient PM, including the transition metals of interest to this review. Table 4 summarizes the concentrations of metals (when reported), population of interest, and health effects evaluated in each of the studies discussed in this section.

### 3.2.1 *Aging Population*

Four studies that focused specifically on associations between metals in ambient PM<sub>2.5</sub> and hospital admissions or mortality in the aging population were identified for this review (Bell et al. 2009; Lipfert et al. 2006; Ostro et al. 2007; and Suh et al. 2011). All of the studies reported statistically significant effects (either  $p < 0.10$  or  $p < 0.05$ ) for one or more transition metals and increases in respiratory and/or cardiovascular outcomes. The studies are briefly discussed below.

Bell et al. (2009) examined respiratory and cardiovascular hospitalizations for persons 65 years or older from exposure to county-specific levels of PM<sub>2.5</sub> As, Cu, Fe, Ni, Ti, Zn, and V, in 106 U.S. counties. Bayesian hierarchical regression modeling showed a statistically significant relationship between short-term changes in V (average conc. 3 ng/m<sup>3</sup>) and Ni (average conc. 2 ng/m<sup>3</sup>) concentrations and a higher risk of cardiovascular and respiratory hospitalization. Concentrations of the other metals were not significantly associated with hospitalizations.

Ostro et al. (2007) examined associations between 12 metals in PM<sub>2.5</sub> and daily mortality in a time-trend study of residents 65 years and older in six California counties. Increases in mortality were significantly associated with Zn for 1 and 3-day lags. There were significant associations for Cu, Fe, Mn, Ti, V, and Zn (but not for Ni), and daily mortality deaths during the cooler months. The average concentration for Fe was 124 ng/m<sup>3</sup>, with averages for the other metals ranging from 2 to 12 ng/m<sup>3</sup>, (similar to the nationwide means from the STN shown on Table 1).

Lipfert et al. (2006) investigated the effects of 15 PM<sub>2.5</sub>-associated metals on long-term mortality for U.S. military veterans, aged 60 years or older. In a proportional hazards model, Ni and V, but not As, Cu, Fe, Mn, Se or Zn, had significant effects on mortality. The average concentrations of Ni and V were 1.73 ng/m<sup>3</sup> and 1.90 ng/m<sup>3</sup>, respectively.

**Table 4** PM<sub>2.5</sub> metal concentrations (ng/m<sup>3</sup>) and associated health effects reported in epidemiological studies

Sources or location	Size fraction	As	Cr	Cu	Fe	Mn	Ni	Se	Ti	V	Zn	Significant findings
<i>Effects of PM metals on sensitive populations</i>												
Bell et al. (2009)—Persons 65 years or older												
106 US Counties	PM <sub>2.5</sub>	2	-- <sup>a</sup>	5	101	--	2	--	--	3	17	V and Ni significantly associated with higher risk of cardiovascular and respiratory hospitalization
Hirshon et al. (2008)—Children aged 17 or younger in Greater Baltimore												
Baltimore, MD	--	--	--	--	--	--	--	--	--	--	22.4	"Low" levels (<8.63) and "high" levels (>20.76) of Zn were significantly associated with risk of pediatric asthma the following day. No dose response relationship
Lipfert et al. (2006)—US military veterans over the age of 60 years												
US	PM <sub>2.5</sub>	1.5	--	4.3	82	3	1.7	1.4	--	1.9	12	V and Ni significantly associated with mortality
Ostro et al. (2007)—Persons 65 years or older												
6 California Counties	PM <sub>2.5</sub>	--		7	124	3	5	--	9	2	12	Zn significantly associated with mortality (1–3 days lag). Cu, Fe, Mn, Ti and Zn significantly associated with mortality in cooler months.
Ostro et al. (2009)—Children less than age of 19												
6 California Counties	PM <sub>2.5</sub>			7.7	130						12	Cu, Fe, K and Zn were significantly associated with hospital admissions for respiratory symptoms at 1 and 3 days lags
Patel et al. (2009)—Children 2 years and younger												
New York, NY	PM <sub>2.5</sub> <sup>b</sup>			--	--		14			3	18	V and Ni significantly associated with "Wheeze" symptoms.
Suh et al. (2011)—Persons 64 years and older in Atlanta												
Atlanta GA	PM <sub>2.5</sub> <sup>b</sup>	--	--	*** <sup>c</sup>	***	***	--	***	***	--	***	Cu, Fe, Mn, Ti and Zn significantly associated with increased odds of hospital admission for cardiovascular disease

(continued)

**Table 4** (continued)

Sources or location	Size fraction	As	Cr	Cu	Fe	Mn	Ni	Se	Ti	V	Zn	Significant findings
<i>Effects of PM metals on general populations</i>												
Burnett et al. (2000)—8 Canadian cities												
8 Canadian Cities	PM <sub>2.5</sub>	1	2.2	7.7	81	13	1.6	1	6.2	3.7	26	PM <sub>2.5</sub> , Fe, Ni and Zn significantly associated with mortality (1 day lag)
Dominici et al. (2007)—60 US cities												
60 US Cities	PM <sub>2.5</sub>	***	***	***	***	***	1.9	1.2	--	1.9	***	Reanalysis of data (Lippmann et al. 2006). When NYC is removed from analyses significant effects of V and Ni were no longer significant
Franklin et al. (2008)												
25 US Cities	PM <sub>2.5</sub>	1.5 <sup>d</sup>	***	--	***	***	1.5 <sup>d</sup>	--	--	***	***	Al, As, sulfate, Si and Ni as individual components and combinations of Al, sulfate and Ni significantly associated with mortality.
Laden et al. (2000)												
6 US cities	PM <sub>2.5</sub>	--	--	6.4–30	62–542	3.2–30	0.5–8.8	--	--	0.1–23	14–138	In models with all individual elements, sulfur, Pb and Ni significantly associated with mortality. V and Fe significantly related to mortality individually.
Lippmann et al. (2006)												
60 US cities	PM <sub>2.5</sub>	***	***	***	***	***	1.9	1.2	--	1.9	***	V and Ni significantly associated with CV mortality rates.
Ostro et al. (2008)—Ethnic Subpopulation												
California	PM <sub>2.5</sub>	--	--	7	124	--	--	--	9	--	12	Cu and Fe significantly associated with cardiovascular mortality

<sup>a</sup>“--” Metal not evaluated

<sup>b</sup>Only IQR values were provided

<sup>c</sup>“\*\*\*” Metal evaluated, but no concentration provided

<sup>d</sup>Values were estimated from a graph

In a more recent study, Suh et al. (2011) evaluated associations between levels of 65 air pollutants measured in the Aerosol Research and Inhalation Epidemiology Study and specific causes for hospital admissions in Atlanta, GA for Medicare recipients 64 years of age or older from 1998 to 2006. These authors reported that the 24-h concentrations of certain transition metals (viz., Cu, Fe oxides, Mn, Ti and Zn) were associated with increased odds of hospital admissions for cardiovascular disease; including ischemic heart disease, congestive heart disease and atrial fibrillation. No information was provided on the concentrations of the individual transition metals.

### 3.2.2 Children

Other authors focused on the sensitive subpopulation of children, who are thought to be especially susceptible to the effects of PM<sub>2.5</sub> (Binkova et al. 2004; Kleinman 2000; Miller et al. 2002; Schwartz 2004). Exposure to PM<sub>2.5</sub> has been linked to the development of chronic respiratory disease, lung function changes, and exacerbation of asthma in children. Three studies (Hirshon et al. 2008; Ostro et al. 2009; Patel et al. 2009) that specifically investigated associations between transition metals in ambient PM and respiratory symptoms in children are discussed below.

Patel et al. (2009) investigated associations between PM<sub>2.5</sub> Ni, V, and Zn concentrations and respiratory symptoms reported for children aged 2 years and younger of African American and Dominican Republic heritage, living in Northern Manhattan and the South Bronx. The study used generalized additive mixed effect models to evaluate the effects of each metal alone and metals with co-pollutants for each symptom-reporting period. The authors found significant positive associations between wheeze and Ni and V exposure, with the largest effect observed for Ni. An increase of one interquartile range (IQR) unit concentration of Ni was related significantly to a 28% increased probability of wheeze. The inclusion of co-pollutants and removal of the highest 5% of Ni concentrations did not alter this relationship. V and wheeze were only significantly associated in the multi-pollutant model. Ni and V remained significantly associated with wheeze during the cold and flu season. Zn was significantly negatively associated with cough during the cold and flu season. Average concentrations of Ni and V during cold and flu season were 12 ng/m<sup>3</sup> and 3.3 ng/m<sup>3</sup>, respectively. These Ni concentrations were about 10 times the nationwide (STN) mean for urban areas, and the V concentrations about 3 times (see Table 2).

Ostro et al. (2009) investigated the effects of Cu, Fe, K, and Zn on hospital admissions for respiratory symptoms in general and subcategories of pneumonia, acute bronchitis, and asthma in children <5 years of age, and children aged 5–18 years for six counties in California. Poisson regression was used to evaluate the effects of individual metals for each county using single-day lags of 0–3; and results then were combined into a meta-analysis using a random-effects model. Changes in concentrations of Cu, Fe, K and Zn were significantly associated with increases at 1 and 3-day lags in hospital admissions for all respiratory symptoms, and for asthma, pneumonia, and acute bronchitis for children <19 years of age. Average concentrations for these metals ranged from 7 ng/m<sup>3</sup> for Cu to 124 ng/m<sup>3</sup> for Fe. An excess risk of 4.7% for respiratory hospital admissions was found for Fe

for children <19 years old. Children <5 years old were particularly sensitive to the Fe component of PM<sub>2.5</sub> for respiratory admissions, with significant associations at both 1- and 3-day lags.

Hirshon et al. (2008) correlated Zn levels reported from the STN network sampler located at the Baltimore “Supersite” in Greater Baltimore, and urgent health care visits for children 0–17 years old. The authors reported that “medium” levels of Zn (8.63–20.76 ng/m<sup>3</sup>) on the previous day were associated with greater than 1.2 times the risk of pediatric asthma problems that day than if “low” levels of Zn (<8.63 ng/m<sup>3</sup>) occurred on the previous day; but, “high” levels of Zn (>20.76 ng/m<sup>3</sup>) on the previous day were associated with only a 1.16 times higher risk of asthma emergency department (ED) visits and hospitalization. There were no significant associations between levels of Zn and same day emergency department admissions, and no consistent “dose-response” relationships in this study.

### 3.2.3 General Population

Ostro et al. (2008) evaluated differences in cardiovascular mortality for whites and Hispanics associated with PM<sub>2.5</sub> metals. Changes in concentrations of Cu, Fe, K and Ti (but not Mn, Ni, V and Zn) were associated with increased risk for the categories of non-high school graduates and being Hispanic. A 2–3% increase in risk of cardiovascular mortality was associated with an IQR increase for Cu for Hispanics, and a 1–2% increase in risk of cardiovascular mortality associated with an IQR increase of Zn for whites. Increased risks of 3% and 5% for cardiovascular mortality were associated with IQR increases in Fe and Zn in people who did not graduate from high school. IQR values for these metal components ranged from 7 ng/m<sup>3</sup> for Cu to 99 ng/m<sup>3</sup> for Fe (see Table 4).

In a study conducted by Burnett et al. (2000) regression models and principal components analysis were used to evaluate daily mortality rates and particulate- and gas-phase air pollutants in eight Canadian cities. A positive and statistically significant relationship was found for PM<sub>2.5</sub> Zn, Ni, and Fe and mortality from lag 1 day data. Both single and multi-pollutant models showed similar percent increases for Zn, Fe, and Ni in daily non-accidental deaths. Statistically significant relationships were not found for As, Cr, Cu, Mn, Se, Ti, and V.

Laden et al. (2000) correlated daily all-causes mortality in six U.S. cities with PM<sub>2.5</sub> metal concentrations from crustal (soil), mobile sources, and coal combustion sources using Poisson regressions in a generalized additive model. The authors reported that a 10 µg/m<sup>3</sup> increase in PM<sub>2.5</sub> from mobile sources and the same incremental increase in PM<sub>2.5</sub> from coal combustion accounted for a 3.4% and 1.1% increase in daily mortality, respectively. In models with all individual elements included simultaneously, sulfur, Pb and Ni were found to be significantly associated with total mortality across all cities. The authors state that V and Fe were statistically associated with increases in daily mortality when evaluated separately, but were no longer significant if modeled simultaneously with sulfur, Ni and Pb.

Lippmann et al. (2006) investigated associations between PM metals and cardiovascular outcomes across 60 cities in the National Mortality and Morbidity Air Pollution



Study (NMMAPS). These authors reported that daily cardiovascular mortality rates were significantly associated with Ni and V and that mortality risk coefficients were high in areas where Ni and V concentrations were in the 95th percentile, versus those areas where the Ni and V component concentrations were in the 5th percentile. No significant associations were reported for As, Cr, Cu, Fe, Mn, Se, or Zn.

Using Bayesian hierarchical regression models, Dominici et al. (2007) re-analyzed the relationships between Ni and V and daily mortality from the NMMAPS data previously evaluated by Lippmann et al. (2006). Dominici found that when specific areas from New York City were excluded from the analysis, the effect of Ni and V on mortality was no longer statistically significant, indicating that the results found by Lippmann et al. (2006) were affected by inclusion of these New York Communities where the  $PM_{2.5}$  Ni and V were 8.9 and 3.4 times higher than the average values found in the other study areas. Both Lippmann et al. (2006) and Dominici et al. (2007) used NMMAPS mortality data (1987–1994 for Lippmann and 1987–2000 for Dominici) that significantly pre-dated the  $PM_{2.5}$  speciation data for metals (2000–2003 for Lippmann and 2000–2005 for Dominici). It is not clear how Ni and V concentrations measured in the air 1–13 years *after* the time period of the mortality data can be effectively used to represent exposures during the previous time period, and no evidence was presented to indicate that Ni and V concentrations remained consistent across time. Lippmann et al. (2006) acknowledged that changes in Clean Air Act Regulations between 1990 and 1995 might have led to a reduced Ni concentrations. No accommodations were made in either the Lippmann et al. (2006) or Dominici et al. (2007) studies to account for the possible reduced Ni and V concentrations or the impact this might have on the results.

Franklin et al. (2008) evaluated associations between STN data for  $PM_{2.5}$  metals (see Table 4) and mortality in 25 U.S. cities, adjusting for time spent indoors, socioeconomic factors, and the locations of the  $PM_{2.5}$  monitors used in their analysis of the data. The authors reported that higher proportions of Al, As, sulfate, Si and Ni existed as individual components in the  $PM_{2.5}$ ; moreover, combinations of Al, sulfate and Ni averaged over 2 days were associated with an increase in non-accidental deaths. No significant associations were found for Cr, Fe, Mn, V, or Zn.

Using the same California PM metal data as in related studies, Ostro et al. (2007) reported associations in general population mortality that were consistent across seasons between Cu, Fe, Ti, V, and Zn, but not Mn or Ni (see Table 4 for concentrations). All-cause mortality was associated most strongly with Cu at a 1-day lag. Cardiovascular mortality was associated most strongly with Fe (2-day lag), Ti (1- and 2-day lag), and Zn (3-day lag). An excess risk of 2.2% per IQR of Zn was found for cardiovascular mortality at the 3-day lag. Respiratory mortality was most strongly associated with Cu and Ti (3-day lag) and to a lesser extent with V and Zn (1-day lag).

### 3.2.4 Critical Comments on the Epidemiology Studies

A relatively small number of epidemiological studies were identified, in which the study design allowed for the correlation of morbidity and mortality with levels of individual transition metals in ambient PM. The studies included in this review are

consistent with the general literature in showing positive associations between increased concentrations of constituents of  $PM_{2.5}$  and increased risk of respiratory and cardiovascular morbidity; mortality lagged 1–3 days following the change in ambient PM. The majority of the studies have the advantage of having included large populations. None of the epidemiology studies covered in our review conclusively implicated specific transition metals as being the cause of the increased cardio-pulmonary morbidity and mortality observed following incremental increases in levels of PM. However, the major findings presented in the eleven epidemiology studies included in our review (Bell et al. 2009; Burnett et al. 2000; Hirshon et al. 2008; Laden et al. 2000; Lipfert et al. 2006; Lippmann et al. 2006; Ostro et al. 2007, 2008, 2009; Patel et al. 2009; Suh et al. 2011) tended to be internally consistent in identifying some metals (Fe, Ni, V, Zn) more often than others (As, Cu, Mn, Se) as potentially affecting health.

The fact that Fe and Zn are the two most abundant transition metals in ambient PM may have contributed to these findings. As discussed previously, the studies conducted by Bell et al. (2009) and Lippmann et al. (2006) included New York City, wherein levels of V and Ni were relatively high during the time period of data collection, and the Dominici study (2007) showed that the associations disappeared when New York City was removed from the other NMMAPS cities. The multiple studies by Ostro did not report significant effects associated with Ni, and significant associations between V and health outcomes were reported in only one study. In those studies, in which transition metals in addition to Ni and V were evaluated, the majority showed no effects of these other metals on health outcomes. Furthermore, the metals identified by the investigators as being more toxic were chosen *a priori* as targets of these investigations (e.g., in the many ROFA studies) far more often than the others, biasing the ability to uncover potential associations.

The studies used to define the role of metals in causing the respiratory and cardiovascular health effects had limitations that included: the characterization of exposure from PM monitoring data, the presence of co-pollutants in ambient PM, and individual risk factors for the same outcomes in members of the subject populations.

All of the studies used data from “centrally” located monitors to quantify the concentrations of  $PM_{2.5}$ ,  $PM_{10}$ , and individual transition metals to which the study populations were exposed. In the California studies (Ostro et al. 2007, 2008, 2009) characterization of exposure was based on relatively few measurements, the monitors were not co-located in most counties and data were reported every third or sixth day. The study conducted by Hirshon et al. (2008) in Greater Baltimore inferred exposure from a single sampling location as being representative of the entire 2.6 million population. Relying upon measurements from a single monitoring location can be particularly problematic for constituents such as Zn, Ni and V that have high spatial variability (Patel et al. 2009; Bell et al. 2009), even when the model accounted for random effects. For example, when New York County and Queens County were excluded from the analysis by Bell et al. (2009), the association between Ni and respiratory hospitalizations was no longer significant. It is also important to recognize that the concentrations of Ni and V in the ambient PM in certain areas of

New York City (Bell et al. 2009; Patel et al. 2009; Lippmann et al. 2006; and Dominici et al. 2007) were influenced by the historical use of residual oil (which is high in these metals) to heat residential and commercial buildings in those neighborhoods during the time periods covered by the studies. Thus, conclusions regarding associations between Ni and respiratory and cardiovascular health effects in those studies should be viewed within the unique context of air quality in residential neighborhoods of Manhattan and the Bronx.

Ambient PM is a complex mixture, and thus, exposure is to multiple agents that may interact in undefined ways. For any study discussed in this review article, the associations found for any given PM<sub>2.5</sub>-associated metal component and the resulting health effect may not wholly reflect the effects of the single metal in question, but may represent the effect of another co-pollutant, particularly those that are unmeasured, that may be part of that particular source (Ostro et al. 2009).

The majority of the studies are population-based. Therefore, despite the (generally) large number of subjects, the influence of individual risk factors and exposures that are related to the same health outcomes, and are sources of many of the same transition metals, such as tobacco smoke, could not be completely accounted for in the study designs.

Observations from even a relatively large number of subjects in a specific geographic location may or may not be relevant to other geographic locations or to other demographic groups. Different mixtures of PM components, weather conditions, and even general population health in different areas may contribute to the results in unknown ways. For example, the group of studies published by Ostro et al. focused on a select set of California counties, and the Ostro et al. (2008) study looked specifically at differences between whites and Hispanics. The study by Patel focused on children of Dominican Republic and African American heritage living in Northern Manhattan and the South Bronx. The studies were designed to address specific populations in specific geographic locations, and thus caution must be used in extrapolating the findings from them to the general US population.

Even when appropriate statistical methods were used to control bias introduced by chance, the very large number of associations tested in some of the studies may have produced findings that were significant by chance alone. For example, Patel et al. (2009) tested over 400 potential associations.

The limitations of the epidemiological studies to define the role of transition metals in health effects are primarily related to characterization of exposure on an individual and population level and the presence of co-pollutants that may contribute to the same effects. For the majority of the epidemiological studies that we reviewed, the levels of exposure to PM and its components were estimated from centrally-located monitors that may or may not have been representative for the populations of interest. The indoor and personal environments of the study subjects may have been additional sources of exposure to particulate and some transition metals. Furthermore, most study designs were limited in the ability to account for other personal risk factors that could be associated with morbidity and mortality from respiratory and cardiovascular causes.

### 3.3 Toxicology

#### 3.3.1 Human Exposure Studies

Epidemiology study results have suggested that the metals content of ambient PM may be associated with increases in the incidence of adverse cardio-respiratory outcomes in the general population. Source factor analyses have correlated concentrations and groupings of specific metals (particularly transition metals) in ambient air masses with particulate sources such as coal or oil combustion, motor vehicle traffic, industrial complexes and agricultural soil. In particular, studies conducted in the Utah Valley during the late 1980s (Pope 1989, 1991, 1992) suggested a decrease in respiratory illness during a 1 year period in 1987, when a local open-hearth steel mill was temporarily shut down. During the shutdown period, the levels of PM in the Utah Valley declined dramatically compared to the years preceding and following the shutdown. Samples of ambient PM collected on filters during those years were archived and have subsequently been used for human, animal and *in vitro* studies. The results reported from this natural experiment suggest that metals may be a contributory factor in the toxicity of PM.

A logical progression from the epidemiology studies is to test the hypothesis that the metal constituents in ambient PM play a role in the health effects. Dose-response has been evaluated by correlating changes in response parameters with variations in the levels and content of metals in ambient PM over time in the same or different geographic locations, or by administering known levels of metals to human subjects.

The human studies reviewed in this section fall into three major categories that are based on the source of exposure to PM metals and the effects measured: 1) indicators of pulmonary function correlated with changes in the levels of metals in ambient PM or in CAPs; 2) indicators of cardiovascular function correlated with metals in inhaled CAPs; and 3) changes in inflammatory markers from inhalation of CAPs or from PM extracts instilled directly into the lungs of volunteers. Where sufficient data were available, we compared the concentrations reported in the studies to the mean ambient concentrations in US urban areas reported by STN 2008 concentrations (Table 1). The relevant findings from studies in each of these categories are summarized below. The average concentrations of metals in ambient PM are presented in Table 5 for those studies, in which this information was readily available.

#### Effects of PM Metals on Indicators of Pulmonary Function

The studies by Hong et al. (2007 and 2010) and Roemer et al. (2000) correlated the daily changes in peak expiratory flow (PEF) rates in grade school age children with changes in levels of ambient PM<sub>10</sub> and/or PM<sub>2.5</sub> and associated metals. The two studies by Hong and co-workers were conducted in Seoul, Korea; the latter study (Hong et al. 2010) was conducted during the Asian Dust Storm of May-June 2007. The study by Roemer et al. (2000) was part of a larger European initiative to evaluate Pollution Effects on Asthmatic Children in Europe (PEACE), and correlated PEF (Peak Expiratory Flow) and respiratory symptoms reported by children living in

industrialized and non-industrialized cities with levels of ambient PM and metals by source (e.g., industrial, agricultural, etc.). Lagorio et al. (2006) attempted to correlate levels of metals associated with particulate air pollution on changes in pulmonary function parameters in adults with compromised lung and/or cardiovascular function.

Although all four of these studies employed changes in PEF or PEV (Peak Expiratory Volume) as indicators of effect correlated to daily changes in levels of ambient PM, the study designs and individual metals that were quantified were sufficiently different as to make direct comparisons amongst studies challenging.

The two studies with Korean school children were of similar design, but yielded seemingly conflicting conclusions. The first study (Hong et al. 2007) with 43 children (not specified as asthmatic) reported a significant reduction in the morning and mean PEFs lagged 1 day after increases in  $PM_{2.5}$ , with an estimated mean decrement in PEF of  $-0.54$  L/min per  $1 \mu\text{g}/\text{m}^3$   $PM_{2.5}$  increase on the preceding day. Concentrations of Mn and Pb in the  $PM_{10}$  were significantly associated with changes in morning and mean PEF. Hong et al. (2010) conducted the second study with 110 children during the 2007 Asian Dust Storm, when concentrations of particulate were very high ( $>130,000 \mu\text{g}/\text{m}^3$  in Seoul); results were that  $PM_{2.5}$  and  $PM_{10}$  concentrations were not associated with significant decreases in PEF rates except in asthmatic children, where the effect was strongest with  $PM_{10}$ . The concentrations of many of the  $PM_{10}$  bound metals, including Cd, Mn, Pb and Zn (Table 5), were reportedly associated with significant decreases in PEF rates in the children (Hong et al. 2010).

In both studies, the daily measurements of PEF were self-reported and the number of subjects was fairly small, which may limit statistical power. The second study (Hong et al. 2010) seemed incongruous, because, whereas the authors indicated significant associations between decreases in PEF and several individual metals of anthropogenic origin, they found no difference in the effect for metals from anthropogenic (As, Cd, Mo, Pb, Zn) vs. natural sources (Al, Ca, Fe, Mn, Si). Because the 2010 study was conducted during the Asian Dust Storm of 2007, which originated in desert regions to the west of Korea, it would have been more logical to find associations between metals in natural as opposed to anthropogenic sources, if the metals were actually contributing to the reported changes in PEF.

The Korean studies identified significant associations between changes in concentrations of Mn and Pb and changes in PEF. Roemer et al. (2000) studied 1,208 asthmatic children divided among 17 panels based on city of residence in the countries of Sweden, Finland, the Netherlands, Germany, Poland, Hungary and Greece. Changes in PEF and symptom prevalence were significantly correlated with changes in Si and Fe concentrations. As for the two studies by Hong et al. (2007, 2010), the study by Roemer (2000) had several limitations. Although the total number of subjects was larger, it did not appear that individual-level characteristics potentially related both to metal exposure and to respiratory conditions were collected or used in the analysis. Symptoms were self-reported and thus potentially biased. Moreover, other possible exposures to respiratory irritants and causes of the effects being measured were not well characterized. In particular, none of the four transition metals identified in the original hypothesis (Ni, Zn, V, and Fe) was found to be significantly associated with respiratory symptoms, and the range of Si and Fe concentrations in urban and suburban locations had significant overlap.

Lagorio et al. (2006) conducted a hospital-based study to evaluate whether exposures to air pollutants in Rome, including  $PM_{2.5}$  and associated selected metals (Cd, Cr, Fe, Ni, Pb, Pt, and V), had a measurable impact on the lung function of adult subjects aged 40–64 years who possessed pre-existing pulmonary or cardiovascular conditions. Three panels consisting of 12 patients with chronic obstructive pulmonary disease (COPD), 11 patients with asthma, and 9 patients with ischemic heart disease (IHD), who had not smoked for at least a 1 year, participated in the study. The study took place over a total of 67 days in 1999 (May to June and November to December) during periods of high variability in air pollutant concentrations. Pulmonary function tests were performed on each subject every 3 days during the study periods. Sixty-two 24-h samples of  $PM_{2.5}$  and  $PM_{10}$  were collected at two fixed monitoring locations, representing a low and a high traffic area in Rome, and were quantified for Cd, Cr, Fe, Ni, Pb, Pt, V, and Zn.

Amongst COPD patients, a  $10 \mu\text{g}/\text{m}^3$  increase in  $PM_{2.5}$  was significantly correlated with a 1.1% decrease in forced vital capacity (FVC) and a 1.06% decrease in forced expiratory volume (FEV) based on the mean concentration of  $PM_{2.5}$  for the previous 3 days. Zn showed the most consistent associations with decrements in FVC and FEV, and was also the metal most highly correlated with  $PM_{2.5}$  concentrations. The authors stated that Fe and Ni had less consistent associations with pulmonary function, and the concentrations of these metals were moderately correlated with  $PM_{2.5}$ . The overall mean concentrations of  $PM_{2.5}$  Ni ( $4.8 \text{ ng}/\text{m}^3$ ), Fe ( $283 \text{ ng}/\text{m}^3$ ) and Zn ( $45.8 \text{ ng}/\text{m}^3$ ), along with a mean  $PM_{2.5}$  concentration of  $27.2 \mu\text{g}/\text{m}^3$ , appeared to be threshold exposure levels that were correlated with decreased pulmonary function parameters amongst patients with COPD. Changes in  $PM_{2.5}$  (or metal constituents) appeared to have no effects on pulmonary function parameters in the asthmatic and IHD patients.

To put the ambient exposures in perspective, average levels of  $PM_{2.5}$  recorded in the U.S. (Table 1) ranged from  $5.4$  to  $12.5 \mu\text{g}/\text{m}^3$ , as compared to the level of  $27.2 \mu\text{g}/\text{m}^3$  in Rome. Similarly, average concentrations of the metals of interest—Ni, Fe, and Zn—are many times lower in U.S. ambient air as compared to Rome. A few aspects of this study that must be interpreted with caution include the small number of subjects, the relatively minor changes (less than 1%) in FVC and FEV, and the influence of unaccounted for individual health factors on the responses being measured.

### Effects of PM Metals on Indicators of Cardiovascular Function

Urch and co-workers (2004) investigated the acute vascular effects of exposure to CAPs (approximately  $10\times$  ambient levels) from Toronto plus ozone as compared to filtered air, by measuring changes in brachial artery diameter in 24 healthy adult volunteers. This study used a cross-over design, in which each subject served as his/her own control, being exposed to either filtered air or CAPs plus ozone for a 2-h period on different occasions. The median and range of transition metals concentrations (in  $\text{ng}/\text{m}^3$ ) in the CAPs to which the volunteers were exposed are presented in Table 5. Linear regression revealed no statistically significant associations with total

**Table 5** Exposure concentrations of target metals reported in ambient air studies with human volunteers

Sources or location	Size fraction	As	Cu	Fe	Mn	Ni	V	Zn	Significant findings
<i>Effects of PM metals on pulmonary function</i>									
Bell et al. (2009)—Reported concentrations in Air, ng/m <sup>3</sup> (Ratio to U.S. Average (STN)) <sup>a</sup>									
Korea	PM <sub>2.5</sub>	-- <sup>b</sup>	--	208 (2.2)	8 (2.7)	--	--	21 (1.5)	PEFR significantly reduced with increases in PM. Mn and Pb significantly associated with reduction in PEFR.
Hong et al. (2010)—Inhalation Ambient Air in Children—Reported Concentrations in Air, ng/m <sup>3</sup> (Ratio to U.S. Average (STN))									
Asian Dust Storm/	PM <sub>2.5</sub>	8 (10)	--	264 (2.8)	22 (7.3)	--	--	101 (7.2)	PM <sub>10</sub> and PM <sub>2.5</sub> not significantly associated with decreased PEFR, except in asthmatic children (PM <sub>10</sub> ). Metals bound to particulates significantly associated with decrease in PEFR.
Korea	PM <sub>10</sub>	17 (21.3)	--	563 (6.0)	43 (14.3)	--	--	153 (10.9)	
Lagorio et al. (2006)—Inhalation ambient PM; Subjects with Asthma or COPD—Reported Concentrations in Air, ng/m <sup>3</sup> (Ratio to U.S. Average (STN))									
Rome, Italy	PM <sub>2.5</sub> (overall mean)	--	--	283 (3.0)	--	4.8 (3.7)	1.8 (1.6)	45.8 (3.3)	In COPD patients, PM <sub>2.5</sub> significantly associated with decrease in FVC and FEV. Zn consistently associated with decreased FVC and FEV
Roemer et al. (2000)—Inhalation Ambient PM in Asthmatic Children—Reported Concentrations in Air, ng/m <sup>3</sup> (Ratio to U.S. Average (STN))									
Umea, Sweden	Urban	--	--	124 (1.3)	--	0.8 (0.6)	1.5 (1.4)	15.4 (1.1)	SI and Fe significantly associated with changes in PEF and prevalence of symptoms.
	Suburban	--	--	65 (0.7)	--	1 (0.8)	2 (1.8)	14.6 (1.0)	
Kuopio, Finland	Urban	--	--	124 (1.3)	--	1 (0.8)	3.8 (3.5)	18.9 (1.4)	
	Suburban	--	--	32 (0.3)	--	1.3 (1.0)	2.2 (2.0)	13.3 (1.0)	
Oslo, Norway	Urban	--	--	105 (1.1)	--	0.2 (0.2)	2 (1.8)	6.9 (0.5)	
	Suburban	--	--	49 (0.5)	--	0 (0)	1.3 (1.2)	3.1 (0.2)	
Amsterdam	Urban	--	--	187 (2.0)	--	2.8 (2.2)	6.6 (6.0)	54.1 (3.9)	
	Suburban	--	--	70 (0.7)	--	0 (0)	3.3 (3.0)	15.9 (1.1)	
Berlin	Urban	--	--	536 (5.7)	--	2.9 (2.2)	5.7 (5.2)	91.5 (6.5)	
	Suburban	--	--	283 (3.0)	--	2.4 (1.8)	4.9 (4.5)	86.6 (6.2)	
Hettstedt, Germany	Urban	--	--	146 (1.6)	--	1 (0.8)	2.2 (2.0)	309.1 (22.1)	
	Suburban	--	--	133 (1.4)	--	1.1 (0.8)	1.9 (1.7)	60.9 (4.4)	

(continued)

**Table 5** (continued)

Sources or location	Size fraction	As	Cu	Fe	Mn	Ni	V	Zn	Significant findings
Katowice, Poland	Urban	--	--	881 (9.4)	--	4 (3.1)	4.2 (3.8)	121.3 (8.7)	
	Suburban	--	--	517 (5.5)	--	2.2 (1.7)	2.8 (2.5)	69 (4.9)	
Budapest	Urban	--	--	363 (3.9)	--	4.2 (3.2)	7.4 (6.7)	71.9 (5.1)	
	Urban	--	--	1,110 (11.8)	--	5.3 (4.1)	8.6 (7.8)	92.8 (6.6)	
Athens	Urban	--	--	147 (1.6)	--	2.4 (1.8)	5.3 (4.8)	22.7 (1.6)	
	Suburban	--	--						
<i>Effects of PM metals on cardiovascular function</i>									
Urch et al. (2004)—Inhalation ambient CAPS in Healthy Adults—Reported Concentrations in Air, ng/m <sup>3</sup> (Ratio to U.S. Average (STN))									
Ontario	PM <sub>2.5</sub> Ambient	--	3.7 (0.7)	84 (0.9)	6.5 (2.2)	0.9 (0.7)	0.8 (0.7)	19 (1.4)	No significant associations for total PM <sub>2.5</sub> or transition metals with brachial artery diameter.
<i>Effects of PM metals on indicators of inflammation</i>									
Ghio and Devlin (2001), Ghio (2004)—Instillation PM Extract in Healthy Non-Smoking Adults, µg metal/g PM (Ratio to U.S. Average (STN))									
Utah Valley; Steel Mill operating vs not operating	PM Extract 1986	--	402.8 (3.7)	82.2 (0.04)	--	17.6 (0.7)	6.0 (0.3)	1,276.5 (4.6)	Exposure to aqueous extracts of PM collected while mill was operational produced significantly greater inflammatory response compared to extract of PM when mill was not operational.
	PM Extract 1987	--	29.1 (0.3)	14.8 (0.01)	--	3.8 (0.1)	7.4 (0.3)	20.2 (0.1)	
	PM Extract 1988	--	471.8 (4.4)	257.5 (0.14)	--	11.0 (0.4)	37.7 (1.7)	690.2 (2.5)	
Huang et al. (2003)—Inhalation of CAPS in Adults—Reported Concentrations in Air, ng/m <sup>3</sup> (Ratio to U.S. Average (STN))									
Chapel Hill, NC	<PM <sub>2.5</sub>	2.2 (2.8)	13.1 (2.4)	42.6 (0.5)	--	1.2 (0.9)	2.1 (1.9)	66.4 (4.7)	Factor consisting of sulfate/Fe/Se was associated with an increase in neutrophils in BALF. Factor consisting of Cu/Zn/V was associated with increase of fibrinogen in blood.



Lay et al. (1999)—Instilled 2.6 µm-Diameter Ferric Oxide Particles into Lungs of Non-Smoking Adults									
NA	Fe <sub>2</sub> O <sub>3</sub> particles <sup>c</sup>	--	3E +08	--	--	--	Iron particles produced transient inflammation during the first day after instillation.		
Schaumann et al. (2004)—Instilled into lung: non-smoking adults (100 µg extract) Metal Concentrations, µg metal/L of PM extract									
Hettstedt, Germany	PM Extract	--	123.6 (0.23)	93.9 (0.01)	--	17.2 (0.13)	9.0 (0.08)	691.7 (0.49)	PM extracts from both locations increased total cell counts, only extract from smelter town (Hettstedt) increased ROS, IL-6, TNF-alpha and monocytes
Zerbst, Germany	PM Extract	--	35.6 (0.07)	83.1 (0.01)	--	7.2 (0.06)	7.4 (0.07)	148.3 (0.11)	
Schins et al. (2004a)—Inhalation Ambient PM in Children—µg/g PM (Ratio to U.S. Average (STN))									
Borken, Germany	PM <sub>2.5</sub>	--	125.5 (170)	1,440 (1110)	--	59.0 (340)	7.04 (48)	--	Platinum significantly associated with increased number of neutrophils and epithelial cells.
	PM <sub>10</sub>	--	93.1 (130)	192.1 (15)	--	198.6 (1,100)	4.65 (32)	--	Vanadium weakly associated with increased concentration of epithelial cells
Duisburg, Germany	PM <sub>2.5</sub>	--	126.6 (180)	2,390 (190)	--	87.2 (500)	10.56 (72)	--	
	PM <sub>10</sub>	--	91.8 (130)	83.5 (6.6)	--	46.3 (270)	6.48 (44)	--	
Sorensen et al. (2005)—Inhalation of Ambient PM <sub>2.5</sub> in Non-Smoking Adults—Median Concentrations, µg Metal/L of PM Extract									
Copenhagen, Denmark	PM <sub>2.5</sub> Autumn	--	19.6	35.5	--	13.1	3.0	--	Transition metals not significantly associated with 8-oxodG levels in urine or lymphocytes.
	PM <sub>2.5</sub> Summer	--	31.7	44.6	--	42.9	3.2	--	

<sup>a</sup>Based on STN data, Table 1

<sup>b,-:</sup> Indicates metals were not measured in the study

<sup>c</sup>Authors do not provide mass of PM per extract, making it impossible to express units in µg metal/g PM or calculate ratio to U.S. average  
NOTE: No concentrations were reported for Cr, Se and Ti in any of the studies

PM<sub>2.5</sub> concentration or the concentration of any transition metal and changes in brachial artery diameter, whereas there were significant negative associations for both the organic and elemental carbon concentrations of the PM<sub>2.5</sub>.

### Effects of PM Metals on Indicators of Inflammation

Two of the six studies reviewed in this section attempted to correlate concentrations of metals in ambient PM with inflammatory markers in nasal lavage fluid (Schins et al. 2004b) or to indicators of oxidative DNA damage in blood and urine (Sorensen et al. 2005). In the other four studies (Ghio and Devlin 2001; Ghio 2004; Lay et al. 1999; and Schaumann et al. 2004), particulate extracts and/or metal particles were instilled into the lungs of volunteers and inflammatory markers were measured in bronchiolar lavage fluid.

In a cross-sectional survey of 67 children living in four areas of Germany that have different traffic densities, Schins et al. (2004a) tested the utility of measuring platinum (Pt) in nasal lavage fluid as a potential biomarker for traffic related PM exposure. The authors stated that the four locations had significantly different concentrations of PM, NO, NO<sub>2</sub>, CO and Cr, but not Pt or V, although the actual concentrations could not be gleaned from the study. Levels of IL-8 and differential cell counts of neutrophils, eosinophils, monocytes, lymphocytes and epithelial cells were measured in nasal lavage fluid from the subjects. Pt was significantly correlated with an increased number of neutrophils and epithelial cells. There was only a weak association between V and epithelial cell concentration. No other statistically significant correlations were reported, and no other potential explanations were offered for differences in cell counts.

Sorensen et al. (2005) attempted to correlate ambient PM<sub>2.5</sub> and transition metals with concentrations of 7-hydro-8-oxy-2'-deoxyguanosine (8-oxodG) as an indicator of oxidative damage in the blood and urine of 49 young, healthy, non-smoking adults, aged 20–33 years living in central Copenhagen. Summer and winter concentrations of transition metals in ambient PM<sub>2.5</sub> are presented in Table 5. Mixed-model repeated measures analysis did not reveal statistically significant associations between the concentrations of 8-oxodG in urine, and water soluble transition metal concentrations or 8-oxodG levels in lymphocytes. Since it appears that blood and 24-h urine samples were only collected on two occasions for each subject, it is not possible to determine individual variability in 8-oxodG over time. Other exposures were not well-accounted for, and there were a relatively small number of subjects enrolled in the study.

### Controlled Exposures to Human Volunteers

The four human dosing studies that will be discussed in this section share features with the rodent intratracheal instillation studies found in the next part of this review. In the following group of studies, volunteers were exposed to known amounts of the

target metals of interest extracted from ambient PM by instillation, or were exposed to known concentrations of metals in CAPs by inhalation for a specified length of time. These studies are the human equivalent of the *in vivo* animal studies that will be reviewed in subsequent sections. Exposure levels of the target metals used in the human exposure studies below are summarized in Table 5.

Ghio and Devlin (2001) conducted a study to correlate clinical evidence of airway inflammation with epidemiologic findings of a reduction in respiratory ailments during a 1-year period in 1987 when an open hearth steel mill in the Utah Valley was temporarily closed, as compared to the adjacent years, 1986 and 1988, when the mill was operating. Aqueous extracts of PM collected from the Utah Valley in 1986, 1987, and 1988 containing a 500  $\mu\text{g}$  equivalent mass of Fe, Zn, Cu, Pb, Ni, and V were instilled into the left bronchi of three groups of 8 non-smokers. An equal volume of saline was instilled into the right bronchi to serve as a control. Twenty-four hours after instillation of the PM extract, the same bronchial segments were lavaged for analysis of the following indicators of inflammation: total cell counts, protein, albumin, fibronectin, neutrophils, alpha-1-antitrypsin, fibrinogen, IL-8, and TNF-alpha. Exposure to aqueous extracts of PM collected during the years that the steel mill was operating produced greater inflammatory response than extracts of PM collected during the year that the mill was shut down. Aqueous extracts from 1986 and 1988, when the mill was in operation, had higher concentrations of Fe, Cu, Zn, Pb, and Ni, and produced significantly greater reactive oxygen species (ROS)—as measured by the thiobarbituric acid reaction products of deoxyribose—than extracts from the 1987 PM. Because the chelating agent deferoxamine inhibited oxidant generation by all three extracts, the authors inferred that transition metals in the extracts were the cause of the ROS. In a follow-up paper, Ghio (2004) expanded the discussion of findings from the bronchoalveolar lavage fluid (BALF) study and added a summary of results from an *in vitro* study, in which human respiratory epithelial BEAS-2 cells were incubated with PM extracts from the 3 years of interest, and in which the oxidative activity was determined. The results of the *in vitro* studies corroborate the findings from the human exposure studies, suggesting that soluble transition metals in ambient PM play a role in inflammatory damage.

In a study similar to those of Ghio (2001), Schaumann and co-workers (2004) conducted a study on 12 human volunteers to determine whether metal constituents of ambient  $\text{PM}_{2.5}$  may be related to increased prevalence of allergic asthma amongst children residing in a German copper mining and ore-processing town (Hettstedt) vs. children from a rural area of Germany (Zerbst). Concentrations of Cu and Zn were much higher in PM from the smelter town of Hettstedt than from the rural town of Zerbst. Each volunteer was instilled with 10 mL saline (right upper lobe of the lung), 100  $\mu\text{g}$  suspension of PM from Hettstedt in 10 mL saline (middle lobe) and 100  $\mu\text{g}$  suspension of PM from Zerbst in 10 mL saline (lingula of the left lung). After 24 h, bronchiolar lavage fluid was obtained and levels of the following inflammatory indicators were compared for the control and the two PM extracts: total cell count, macrophages, monocytes, lymphocytes, neutrophils, ROS generation, IL-1, IL-6, IL-8, TNF-alpha, albumin, and lactate dehydrogenase (LDH). PM extracts

from both Hettstedt and Zerbst increased total cell counts, but only extracts from the smelter town of Hettstedt increased ROS, IL-6, TNF-alpha, and monocytes. The authors concluded that soluble metals in ambient PM play a role in the mechanism of injury, but the contribution(s) of other constituents in PM is not known.

Lay et al. (1999) examined the role of Fe in the inflammatory response caused by PM by instilling 2.6  $\mu\text{m}$ -diameter ferric oxide particles into the lungs of human subjects and sampling cells by bronchoalveolar lavage and biochemical components in lung air from 1 to 91 days after instillation. The iron particles produced transient inflammation during the first day after instillation, evidenced by increased numbers of neutrophils, alveolar macrophages, and increased amounts of protein, LDH and IL-8. In addition to the human subjects, similar studies were also performed, in which iron oxide particles were instilled into the trachea of Fisher rats. The authors suggested that acute inflammation immediately after instillation may be related to oxidant generation by residual amounts of ferric iron, ferric hydroxides, or oxyhydroxides.

Huang et al. (2003) expanded on earlier work by Ghio et al. (1999b) to quantify concentrations of metals in the water soluble fraction of CAPs in Chapel Hill, North Carolina, and to correlate the concentrations with cellular and biochemical changes by expanding and re-analyzing data from 38 healthy young human volunteers who had previously been exposed for 2 h to either filtered air or CAPs. The maximum aerosol concentrations varied depending upon the ambient  $\text{PM}_{2.5}$  (ranging from 5 to 30  $\mu\text{g}/\text{m}^3$ ). Eighteen hours following inhalation of CAPs or filtered air, bronchoalveolar lavage was performed on the subjects to collect cells and indicators of acute inflammation. Huang et al. (2003) quantified the nine most abundant components of the water soluble fraction (As, Cu, Fe, Ni, Pb, Se,  $\text{SO}_4$ , V and Zn) and correlated the concentrations of these constituents with cellular and biochemical endpoints in the BALF and pre- and post-treatment blood samples. BALF responses measured were: total cell count, IL-6, IL-8, leukotriene B4, macrophage inflammatory protein, PGE-2, fibrinogen, fibronectin, and nitric oxide. Response variables in peripheral blood were: complete blood count (CBC), differential blood count (DBC), ferritin, and fibrinogen.

These investigators (Huang et al. 2003) used principal components analysis to determine how the nine constituents varied together. Median concentrations and range of the nine soluble components in  $\text{PM}_{2.5}$  are shown in Table 5. A factor consisting of sulfate/Fe/Se was associated with an increase in neutrophils in BALF, whereas a factor consisting of Cu/Zn/V was associated with increased levels of fibrinogen in blood. No other factors were evaluated in this study.

## Comments on Human Exposure Studies

The human studies presented in this review attempted to correlate individual measurements of pulmonary (PEF) or cardiac function (brachial artery diameter), easily obtainable indicators of inflammation and ROS (viz., blood, nasal lavage or BALF), or quantifiable measurement of PM-related metals in biological samples with either 1) temporal/regional variations in ambient PM metal levels (Hong et al. 2007, 2010; Lagorio et al. 2006; Roemer et al. 2000; Schins et al. 2004b; Sorensen et al. 2005),

or 2) controlled administration of PM metals by bronchial instillation (Ghio and Devlin 2001; Ghio 2004; Lay et al. 1999; Schaumann et al. 2004) or inhalation of CAPs (Huang et al. 2003; Urch et al. 2004).

Unlike the epidemiological studies that we reviewed, the exposures to human volunteers are well defined. Major limitations of some, but not all of the studies correlating individual responses with ambient PM were: relatively small numbers of subjects; self-measurement and self-reporting of PEF and respiratory symptoms (especially in the studies with young children); personal-level exposures to metals or other factors (e.g., community respiratory infections) associated with the response. Innate individual variability in the response being measured over time complicates interpretation of the results, but reflects the variability in individual responses in the general population. In studies in which volunteers were instilled with PM metals, the investigators controlled both the exposure and the measurement of response, but the number of subjects was necessarily small and the administration method far removed from breathing ambient air. Inhalation exposure of human volunteers to CAPs is a relevant route of administration, and only increases concentrations by factors of 10–40, so can be considered environmentally relevant to exposures at the upper levels of ambient PM constituents. However, the gaseous components of air pollution, such as ozone, NO<sub>x</sub>, and SO<sub>x</sub>, etc., and any transformation products, are not represented in exposure to CAPs, so their contribution to any effects cannot be determined.

The studies that attempted to correlate exposure to metals in ambient PM with changes in readily-measured indicators of respiratory and vascular function provide only weak evidence for the involvement of metals. This hardly seems surprising given the inherent variability in the exposure(s) of interest and variability in response among subjects, and for the same subject at different times. These study results may also indicate that metals play little or no role in producing these health effects. Potential bias from self-reported measurements of PEF and respiratory symptoms in the Korean and European children studies further compounds the variability. To some extent, the possibility of finding statistically significant associations between changes in the concentrations of PM-bound metals and changes in the responses being measured may also have been a matter of luck, with regard to the time period and locations selected for the studies.

Experiments, in which volunteers were instilled with PM extracts or breathed CAPs essentially follow the same protocols used in the majority of the *in vivo* animal studies (except that the human subjects survived the procedures). Moreover, the findings of increased inflammatory indicators in the lungs in response to metal-containing PM extracts are consistent with those observed in the animal studies. The results are also subject to the same caveats as the *in vivo* studies, with regard to amount of material deposited in a limited anatomical location, i.e., by-passing landscape of the nose, sinuses and upper respiratory tract, and potential effects related to the surgical procedure.

It should also be recognized that invasive studies (e.g., bronchoscopy) with humans are costly to conduct, and the number of subjects is necessarily small. However, the investigators optimized the information obtained by having each subject serve as his/her own control. The numbers of human subjects in each treatment

“group” in the previous studies were similar to the typical number of rats or mice used per treatment group in the *in vivo* studies that follow. In both the human and animal instillation studies, the method of exposure and the physical form of the PM metals are not “natural,” raising the possibility that invasive physical manipulation of the subjects may influence the responses being measured. The response to a bolus of aqueous metal extract deposited in a relatively small anatomical region of the respiratory tract cannot be discounted as a potential explanation for some of the effects on BALF parameters observed in both the human and animal studies.

The CAPs inhalation studies conducted by Huang et al. (2003) and Urch et al. (2004) represent a more “natural” exposure scenario than the bronchial instillation studies. Although these exposures cannot be considered “real world”, because the levels of transition metals are many times higher than ambient levels, the components in the PM mixture are in the same proportions. It should be noted that the activity of other components of ambient PM, other than ozone (Urch et al. 2004) that would also be concentrated by the technology, was not accounted for in these studies. Although the levels of metals in CAPs are many times the ambient levels, this exposure method seems potentially relevant for conducting future human and animal studies that maximize the chances of detecting responses potentially associated with PM metals.

### 3.3.2 In Vivo Studies

As discussed in the previous section, human exposure studies provide some limited support for the role of metals in the increased morbidity and mortality associated with increases in ambient PM reported in epidemiologic studies. Human exposure studies introduce sources of variability in both exposure and response variables that are difficult to control. *In vivo* studies with laboratory animals (primarily rats and mice) allow for greater control of the exposure, greater numbers of (almost) genetically identical subjects, and optimal evaluation of multiple response parameters in an intact biological system. In contrast, *in vivo* animal studies do not capture the inherent (but problematic) variability in either exposures to PM metals or to individual human responses. Also, the doses administered to laboratory animals on a body weight basis are typically several orders of magnitude higher than encountered by people breathing ambient air containing metals in the low ng/m<sup>3</sup> concentration range. Extrapolating from animals to humans and from high dose to low dose is not a straightforward exercise.

The majority of the laboratory animal studies discussed in this section were conducted by multi-institutional teams of researchers in collaboration with the US EPA National Health and Environmental Effects Research Laboratory (NHEERL), and followed similar experimental designs. Another distinct group of studies were conducted by investigators in Europe and primarily focused on the activity of PM from regional airsheds with differing source contributions. In most of the *in vivo* studies that we reviewed, the response parameters that were measured are cellular and chemical indicators of respiratory tract inflammation and cell damage/death.

Indicators of cardiovascular effects such as changes in heart rate, body temperature, and frequency/intensity of arrhythmias were also measured in a smaller number of the studies.

The *in vivo* studies are grouped by the predominate source of the PM metals used for exposure: ambient PM samples, CAPs, ROFA and individual metals. Within a given study, multiple sources of PM metals may have been used for comparisons, thus these groupings are not mutually exclusive. Tables 6 and 7 present the concentrations of individual metals in the sources of PM or ROFA, respectively, in  $\mu\text{g/g}$  of particulate mass. Where sufficient information was available, we made a rough comparison of the dose levels used in the animal studies to the dose of the same metals that a member of the general U.S. population would receive from inhaling the aver-

**Table 6** Target metal concentrations reported in ambient PM sources for *in vivo* studies

Sources	Concentration of metal in source PM ( $\mu\text{g/g}$ )						
	As	Cu	Fe	Mn	Ni	V	Zn
Adamson et al. (2000), Prieditis and Adamson (2002)							
Ottawa, Canada EHC-93 <sup>a</sup>	–	144	149	–	5	–	4,784
Costa and Dreher (1997)							
St Louis, Missouri (NIST No. 1648)	–	111	35.6	–	38.5	33	2,599
Dusseldorf, Germany		420	48.3		117.6	55.8	2,516
Ottawa, Canada		147.6	145.6		81	1.9	6,059
Washington DC		46.2	308.8		20	152	1,356
ROFA (power plant in Florida) <sup>b</sup>		230	23,310		37,510	41,710	1,010
DOFA <sup>c</sup>		2,070	154,510	–	120	–	9,000
CFA <sup>d</sup>		30	14,570		700	370	80
Dye et al. (2001) Exp. #1							
Utah Valley 1986	9.4	55.2	26.4	4.3	4.3	0.72	74.0
Utah Valley 1987	7.6	22.0	3.03	3.8	1.2	0.76	6.8
Utah Valley 1988	11.7	140.0	54.0	8.9	4.7	0.47	13.1
Molinelli et al. (2002)							
Provo Utah 1982	–	294.5	88.2	9.73	16.7	10.9	597
Gavett et al. (2003)	–						
Hettstedt, Germany <sup>a</sup>	57	1,181	355	127	62	172	6,546
Zerbst, Germany <sup>a</sup>	21	179	561	133	128	345	3,907
Schins et al. (2004b)							
Borken, Germany PM <sub>2.5</sub>	–	125.5	1,440	–	59.0	7.04	–
Borken PM <sub>10</sub>		93.1	192.1		198.6	4.65	
Duisburg, Germany PM <sub>2.5</sub>		126.6	2,390		87.2	10.56	
Duisburg PM <sub>10</sub>		91.8	83.5		46.3	6.48	

<sup>a</sup>Aqueous extract

<sup>b</sup>Residual Oil Fly Ash

<sup>c</sup>Domestic Oil Fly Ash

<sup>d</sup>Coal Fly Ash

**Table 7** Summary of *in vivo* study effects from intratracheal administration of metal extracts of ambient PM<sup>a,b</sup>

Source of PM	Animal	Dose (mass of extract)	Significant responses						
Costa and Dreher (1997)									
Ambient Air: 1. St. Louis 2. Washington, DC 3. Ottawa 4. Dusseldorf	Rats— Sprague Dawley	2.5 mg Extract (46 µg total metal)	Bronchoalveolar Lavage Fluid (BALF) responses similar for all PM normalized to total metals						
Dye et al. (2001)									
Utah Valley 1986 (Mill Open)	Rats— Sprague Dawley	2.5 mg	<b>1986 and 1988 Extracts:</b> Significant increase BALF parameters, acute pathology compared to controls <b>1987 Extract:</b> No difference from controls						
1987 (Mill Closed)		0.25 mg or 1.0 mg	<b>1986 Extract:</b> Significant increase in BALF parameters compared to controls						
1988 (Mill Open)		5.0 mg	<b>1987 Extract:</b> Significant increase in BALF parameters compared to controls						
Gavett et al. (2003)									
Zerbst (non-industrial) Hettstedt (industrial)	Balb/c Mice Allergic Non-Allergic	100 µg Extract	PM <sub>2.5</sub> Extract from Hettstedt Significantly increased BALF parameters in non-allergic and allergic mice as compared to saline controls						
Gerlofs-Nijland et al. (2009)									
Duisburg (industrial) Amsterdam Barcelona	Rats— Hypertensive	7 mg	Significant increase in BALF parameters associated with exposure to Amsterdam Extract (highest metals); Also significant association with PAHs						
Happo et al. (2008)									
Course PM <sub>2.5-10</sub> Fine PM <sub>0.2-1</sub> Duisburg (industrial) Amsterdam Barcelona Athens Helsinki Prague	C57BL/ 6J mice	10 mg/ kg/bw	No significant association with metals						
Utah Valley 1982 1. Extract 2. Chelated Extract 3. Chelated Extract + Metals				Rats— Sprague Dawley	1,000 µg	Significant increase in proteins and LDH in rats dosed with both <b>chelated</b> and <b>un-chelated extract</b>			
Schins et al. (2004b)									
Course PM <sub>2.5-10</sub> Fine PM <sub>1-2.5</sub> Borken (rural) Duisburg (industrial)							Rats— Wistar	0.32 mg Extract	Coarse PM from both locations significant increase in BALF parameters; endotoxin also associated with response

<sup>a</sup>PM extract administered by intratracheal instillation in all studies

<sup>b</sup>Response Parameters in BALF (bronchoalveolar lavage fluid): inflammatory markers-total protein, cells, soluble factors (cytokines)



age concentrations of the same metals in ambient PM using the STN concentrations in Table 1. This common dose metric is based on assumptions regarding body weight, breathing rate, and particle size; the derivation of this metric is more fully described in the introduction section of this paper. These estimated “animal to human” ratios were based on the concentration of the specific metals in the PM source in  $\mu\text{g metal/g PM mass}$  and using conservative assumptions for the weight and volume of air breathed per day for an average human, dog, rat, and mouse. In the majority of the studies reviewed, the results were analyzed using ANOVA with appropriate after tests (e.g., Bonferroni or Tukey’s) for multiple comparisons.

### In Vivo Exposures to Metals in Ambient PM

The seven studies discussed in this section addressed the effects of ambient PM extracts on cellular and soluble markers of inflammatory response in BALF. The studies share common design features in that doses of PM extracts in saline were directly instilled into the lungs of rats or mice, the animals sacrificed at one or more time intervals post-instillation (e.g., 24 and 96 h), and inflammatory markers in BALF examined. The sources of ambient PM, experimental animals, and significant responses from this group of studies are summarized below. The concentrations of specific metals in the source material (Table 6) was readily available for five (Dye et al. 2001; Molinelli et al. 2002; Costa and Dreher 1997; Gavett et al. 2003; Schins et al. 2004b) of the studies. In the remaining two studies (Gerlofs-Nijland et al. 2009; and Happo et al. 2008), the investigators used extracts of ambient PM from airsheds in Europe that differed with regard to industrial vs. non-industrial sources. Concentrations of metals in the source material used in many of the studies are presented in Table 6 and the findings are summarized in Table 7.

#### *Ambient PM from the Utah Valley*

Dye et al. (2001) conducted a series of three experiments to evaluate the toxicity of aqueous extracts of TSP from the Utah Valley in 1986, 1987, and 1988 corresponding to the time period of the epidemiology studies published by Pope (1989, 1991) to test the hypothesis that the decrease in respiratory illnesses reported in 1987 while an open-hearth steel mill was closed for repairs, as compared to the two adjacent years, could have been associated with decreased exposure to the water/acid soluble fraction of airborne metals. The concentrations ( $\mu\text{g metal/g TSP}$ ) of transition metals of interest in the Utah Valley PM samples are presented in Table 6, along with concentrations of metals in National Institute of Standards and Technology (NIST) No. 1648 (St. Louis). On a mass basis, the concentrations of Cu, Zn, Fe, Ni, and V were much greater in the NIST reference sample than concentrations for these metals in any of the three Utah Valley TSP samples. Three experiments, using varying doses of PM extracts in saline, were performed with healthy Sprague Dawley rats to assess non-specific airway responsiveness, BALF indicators of cellular response, and general lung pathology at 24 and 96 h post-instillation. Data

were analyzed by ANOVA with Sheffe's post-test correction or t-test for single comparisons at a significance level of  $p < 0.05$ . Rats treated with 2.5 mg extract (8.33 mg extract/ml saline) of TSP from 1986 and 1988 (steel mill operating) developed acute lung injury characterized by increases in BALF indicators of response. Response to treatment with the same dose of the 1987 extract was not different from controls. Instillation of 0.25 or 1.0 mg extract from the 1986 PM extract produced increases in some BALF parameters (LDH, total cells and neutrophils) that were significantly greater than controls. Instillation with 5.0 mg/rat of the 1987 (steel mill closed) extract produced a significant increase in LDH, total protein, total BAL cells and neutrophils compared to saline controls.

In a related study, Molinelli et al. (2002) used a chelating agent to further examine the role of acid-extractable metals (Table 7) in the toxicity of PM collected from the Utah Valley in the winter of 1982 on Sprague Dawley rats exposed *in vivo*, and on human airway epithelial cell (BEAS-2B) cultures. Rats instilled with 1,000  $\mu\text{g}$  of extract, Chelex-treated extract, and Chelex-treated extract with metals added back all showed significant increases in BALF proteins and LDH. BEAS-2B cells were incubated with 100  $\mu\text{L}$  of PM extract at concentrations of 0, 62.5, 125, 250, 500 or 1,000  $\mu\text{g}/\text{mL}$ , Chelex-treated PM extract, or Chelex-treated PM extract with metals added back to concentrations in untreated extract, or solutions of metals. Chelex decreased the mass of, but did not entirely remove Fe, Ni, V, Cu, Zn, Mn, and Pb. Extract concentrations greater than 125  $\mu\text{g}/\text{mL}$  increased IL-8 levels in the cell cultures. IL-8 production was not significantly increased in cultures incubated with Chelex-treated, Chelex-treated-with-metals, and metals-only groups compared to the controls.

#### *Ambient PM from Regional Airsheds*

In one earlier animal study, Costa and Dreher (1997) used PM samples from three emission sources, including Domestic Oil Fly Ash (DOFA); ROFA; and Coal Fly Ash (CFA); and four ambient airsheds: St. Louis, MO; Washington, DC; Dusseldorf, Germany; and Ottawa, Canada, to investigate the role of bioavailable (extractable in 1 M HCl) transition metals (Cu, Fe, Ni, V, and Zn) in a rat model of adverse cardiopulmonary outcomes. Healthy Sprague Dawley rats were instilled with 2.5 mg (equal dose by mass to yield a total metal content of 46  $\mu\text{g}/\text{dose}$ ) of the PM extracts and sacrificed 24 or 96 h later. When the mass from each of the seven PM sources was normalized to a dose of 46  $\mu\text{g}$  total metals/rat, the BALF cellular responses were similar for all PM samples, suggesting that toxicity was related to the bioavailability of the constituent transition metals. Rats with monocrotaline-induced pulmonary hypertension instilled with the metal-rich ROFA had significant higher mortality than healthy rats instilled with ROFA. It should be noted that the PM samples used in these experiments had been in storage from 3 to 15 years, and there was considerable variability in the acid-extractable concentrations of metals (Table 6) in the seven different sources.

In four studies (Gavett et al. (2003), Gerlofs-Nijland et al. (2009), Happo et al. (2008), and Schins et al. (2004b)), the toxicity of metals in ambient PM from various

airsheds in Europe were evaluated, using *in vivo* rodent models. In the studies conducted by Gerlofs-Nijland et al. (2009) and Happo et al. (2008), the actual metal concentrations were not given for the various locations, but rather were inferred from previous studies or were based on the presence of industrial sources.

Gavett et al. (2003) conducted experiments by using an allergic mouse model to determine if the metals composition of ambient  $PM_{2.5}$  could help to explain reports that children in the industrialized Hettstedt area of eastern Germany have a higher prevalence of sensitization to common allergens than children in the less industrialized City of Zerbst (Table 7). Normal non-allergic Balb/c mice instilled with saline, or 100  $\mu\text{g}$  of either Hettstedt or Zerbst PM. Hettstedt  $PM_{2.5}$  had significantly increased BALF protein levels and indicators of epithelial cell injury as compared to mice instilled with saline). In allergic mice (sensitized with ovalbumin), exposure to both the Hettstedt and Zerbst PM extracts increased airway response to methacholine, with only the Hettstedt PM response being significantly greater than controls. From the transition metal composition of the two PM samples, it is apparent that the concentrations of As and Mn were similar, the sample from Zerbst had somewhat higher levels of Fe, Ni and V, and the sample from Hettstedt had much higher concentrations of Cu and Zn, suggesting that the effects on inflammatory markers and allergic airway response may have been related to these two metals. However, this was not confirmed by exposing the animals to concentrations of these metals equivalent to those in the PM samples.

Schins et al. (2004b) evaluated the inflammatory response to coarse ( $PM_{2.5-10}$ ) and fine ( $PM_{1.0-2.5}$ ) particulates from a rural area (Borken) and an industrialized area (Duisburg) in Germany (total of four PM samples, concentrations in Table 6). The hydroxyl-radical generating capability of the PM fractions was determined and inflammatory potential evaluated in Wistar rats. Both Duisburg fine and Duisburg coarse PM generated significantly more hydroxyl-radicals than either fraction from Borken, with the Duisburg coarse PM fraction producing significantly more radicals than the Duisburg fine fraction. This finding seems counter-intuitive because the concentrations of soluble metals in the fine PM samples from both locations were greater than in the coarse fractions. Furthermore, the concentrations of Fe and Ni in the coarse fraction from the rural area of Borken were more than three times higher than the concentrations of these metals in the coarse fraction from the industrialized area of Duisburg. Wistar rats were then instilled with 0.32 mg of aqueous extract from each of the four PM samples, or saline control, and indicators of inflammatory response were evaluated in BALF 18 h after exposure. Coarse PM from both airsheds produced changes in some, but not all, inflammatory markers in BALF that were significantly different from controls. It should also be noted that the coarse PM from both locations contained higher levels of endotoxin than did the fine fraction. In the majority of the studies that we reviewed, in which the size fractions were examined, the fine PM fraction typically produced a greater inflammatory response than the coarse fraction.

As the authors (Schins et al. 2004b) acknowledged, the fact that the metal doses applied to the experimental animals were at least 15–1,100 times higher than a human would receive from ambient exposure (Table 6), and the heterogeneity of the

metal composition of the samples made it difficult to define the role of the individual metals in the inflammatory response. On the other hand, the endotoxin content of the PM samples was associated with the differences in response. Unlike the metal doses, the endotoxin levels measured in this study were the same order of magnitude as the median for ambient air, 1.085 endotoxin/EU m<sup>3</sup> (95% CI 0.915–1.251), reported by Carty et al. (2003) for Munich, Germany. This study (Schins et al. 2004b) is unusual in that it accounted for the presence of endotoxin as a potential contributor to the inflammatory response.

Gerlofs-Nijland et al. (2009) investigated the potential contributions of transition metals and polycyclic aromatic hydrocarbons (PAHs) to inflammation and pulmonary toxicity in spontaneously hypertensive rats instilled with extracts of PM from the cities of Prague, Duisburg and Barcelona at a dose of 7 mg extract/kg body weight of the animals. In some experiments, a chelating agent was added to the extract prior to administration. Extracts of both fine and coarse PM from Duisburg (highest metal content) significantly increased in inflammatory markers in BALF. Chelated extracts still produced a significantly greater inflammatory response than controls. When interpreting the results from these studies, it should be considered that these researchers also found positive correlations between PAHs and some indicators of inflammatory damage.

Happo et al. (2008) evaluated the toxicity of water-soluble and water-insoluble coarse (PM<sub>2.5-10</sub>) and fine (PM<sub>0.2-2.5</sub>) particulate from six European cities having different airshed characteristics. C57BL/6J mice were instilled with 10 mg PM extract/kg body wt, sacrificed at 4 or 12 h post-treatment and inflammatory markers in BALF were measured. Results were analyzed using Spearman's rank correlation. The authors reported that dicarboxylic acids and transition metals (Ni and V) in PM<sub>2.5</sub> had a positive correlation with inflammatory indicators; secondary inorganic ions (nitrate and ammonium) were negatively correlated with inflammatory markers. None of the correlations were statistically significant and the actual concentrations of the individual metals in the PM mass were not given.

### Comments on In Vivo Studies with Ambient PM

As a group, the seven studies reviewed in this section provide some limited evidence for the role of metals in the inflammatory response to ambient PM. Although the general epidemiology literature suggests that fine particulate (PM<sub>2.5</sub>) is more strongly associated with increases in morbidity and mortality from respiratory and cardiovascular causes than coarse particulate, the ambient PM source samples available to the authors of these studies did not always allow evaluation of toxicity by size fraction. In fact, the findings of Schins et al. (2004b) are not consistent with the hypothesis that fine PM is more active with regard to metals. It must also be emphasized that the doses of total PM and associated transition metals administered to the animals in some of the studies reviewed above in this section were as much as four orders of magnitude greater than humans are exposed to by breathing ambient air in most areas of the U.S.

## In Vivo Exposures to Metals in CAPs

The particulate fraction of ambient air can be concentrated while maintaining the same proportions of constituents. Inhalation studies performed with the resulting concentrated ambient particulates (CAPs) are representative of exposures to the source air, only at higher concentrations of particulates. Since there are relatively few particle concentrators in existence, the majority of studies with CAPs have been conducted by researchers affiliated with institutions that have this technology, such as the Harvard School of Public Health, University of North Carolina, or New York University School of Medicine. We discuss six studies in this section that are of similar design and were conducted to examine the cardio-pulmonary responses of dogs (Clarke et al. 2000 and Wellenius et al. 2003), rats (Batalha et al. 2002; Kodavanti et al. 2005; and Saldiva et al. 2002), or mice (Lippmann et al. 2006).

Clarke et al. (2000) exposed healthy dogs to CAPs or filtered air for 6 h/day for 3 days using a paired experimental design. CAPs concentration factors ranged from 17 to 28, with considerable variability in the relative concentrations of metals over the days of exposure. Samples of blood and BALF were analyzed for fibrinogen, cell counts and protein levels. Responses were highly variable and there were no significant differences in BALF or blood parameters in controls or CAPs exposed dogs compared to pre-exposure baseline levels. The authors suggested that pulmonary inflammatory responses, after ambient PM inhalation may not be a major contributor to the morbidity and mortality reported in epidemiologic studies.

In a subsequent study, Wellenius et al. (2003) investigated the effect of CAPs (concentration factor approximately 30 times ambient levels) on myocardial ischemia in a canine model of coronary artery occlusion. Six pairs of dogs were randomly assigned to breathe CAPs or filtered air, followed by coronary artery occlusion and electrocardiographic examination, for a total of 21 exposure cycles. Exposure to CAPs as compared to filtered air was significantly (mixed effects and multivariate analysis) associated with indicators of myocardial ischemia during occlusion. Although not a target metal for this review, the Pb concentration in CAPs was significantly associated with ischemic changes, but this finding may be an artifact of multiple comparisons.

In companion studies, Batalha et al. (2002) and Saldiva et al. (2002) evaluated an 18-day exposure to CAPs at particulate concentrations ranging from 73.5 to 733.0  $\mu\text{g}/\text{m}^3$  (approximately 30 times ambient). The authors measured vasoconstriction of small pulmonary arteries in normal rats and in rats with chronic bronchitis (Batalha et al. 2002) exposed to CAPs. Pulmonary inflammation (Saldiva et al. 2002) was measured in healthy Sprague Dawley rats and in rats with chronic bronchitis exposed to CAPs. Chronic bronchitis was induced by exposing the rats to  $\text{SO}_2$  for 5 weeks prior to conducting studies with CAPs. In the study by Batalha et al. (2002), normal and bronchitic rats were exposed to CAPs or filtered air for 5 h/day for three consecutive days, and were then sacrificed 24 h after the final exposure, after which the lungs and blood vessels were examined for histological changes. Silicon was significantly associated with vasoconstriction in both normal and bronchitic rats, but no significant associations were found for Ni (10–160  $\text{ng}/\text{m}^3$ ) and V (ND to 260  $\text{ng}/\text{m}^3$ ).

In the companion study by Saldiva (2002), inhalation exposure to CAPs for both the normal and bronchitic rats caused variable increases in pulmonary neutrophils and total BALF cell counts as compared to controls. Many of the rats exposed to CAPs developed acute pulmonary inflammation. Significant overall associations were found for CAPs, V, and bromine due to changes in normal rats; the changes in bronchitic rats were not significantly associated with V. The authors suggested that because the bronchitic rats had more inflammatory changes than the normal animals as a result of their disease status, further change was difficult to detect, and therefore was likely underestimated.

Kodavanti et al. (2005) described multiple exposure studies, in which the responses of spontaneously hypertensive (SH) and normo-tensive Wistar Kyoto (WKY) exposed to CAPs (concentration factor from 40 to 60 times ambient) were compared. Concentrations of CAPs and individual water-soluble metals were highly variable. Ventilatory parameters were measured during six repeat studies of 4 h/day for 1-day exposures in late autumn 2000, and seven repeat studies of 4 h/day for 2-day exposures in late summer/early autumn 2001. At necropsy, all hematologic parameters evaluated were higher in SH than WKY rats, although none of the biochemical and inflammatory parameters showed a consistent change. There were no consistent relationships between metals in CAPs and strain-specific changes in the responses being measured.

Lippmann et al. (2006) investigated the effects of metals in New York City CAPs (concentration factor 10 times ambient levels) on cardiovascular responses in atherosclerotic ApoE<sup>-/-</sup> mice fed a high fat diet and exposed for 6 h/day, 5 days/week, for 6 months (summer through fall). In this study, Ni, but not V was significantly associated with changes in cardiac function. The peak Ni concentration in CAPs was 175 ng/m<sup>3</sup>, with the average concentration being 26 ng/m<sup>3</sup>. To put this in perspective, the long-term average concentration of Ni across the U.S. is 1.9 ng/m<sup>3</sup> and in New York City it is 19 ng/m<sup>3</sup>.

### Critical Comments on In Vivo Studies with CAPs

In summary, the studies we reviewed, in which animals were exposed to CAPs by inhalation were reasonably analogous to the human condition, only at somewhat exaggerated concentrations of constituents. It should be considered that the transition metals of interest comprise a relatively minor fraction of ambient PM, and would be expected to comprise a similarly minor fraction of CAPs. The contributions of the other constituents (e.g., endotoxin) in ambient PM and subsequently CAPs are not well accounted for in these studies.

### In Vivo Exposures to Metals in Residual Oil Fly Ash (ROFA)

The burning of heavy oils in boilers and electrical power generating plants produces particulates that are enriched with metals. The resulting ash particulates contribute to ambient PM in some regions of the U.S. and internationally. Relative to other emission

sources, ROFA has high concentrations of the transition metals Fe, Ni and V. Consequently, the majority of studies reviewed in this section focus on the role of these three metals in the inflammatory and immune system effects produced by ROFA.

The studies discussed in this section were conducted by investigators affiliated with NHEERL (Dreher et al. 1997; Ghio et al. 1998; Kadiiska et al. 1997; Kodavanti et al. 1998, 2001; Lambert et al. 2000; Nadadur and Kodavanti 2002), and used samples of ROFA collected downstream of the cyclone of a Florida power plant, and which burned low sulfur #6 residual oil as the source of particles. Another four studies (Antonini et al. 2004; Hamada et al. 2002; Lewis et al. 2003; and Roberts et al. 2004) were conducted by teams affiliated with the Harvard School of Public Health and/or National Institute for Occupational Safety and Health (NIOSH). The concentrations of the target metals in the ROFA sources used in the following studies are summarized in Table 8, and are presented along with estimated ratios of experimental animal exposures to ambient human exposures that are based on average STN metal concentrations (Table 1).

The fact that these studies were conducted by groups of affiliated researchers using the same source(s) of ROFA leads to a similarity of experimental designs, especially within laboratory groups. In most studies, suspensions of ROFA and solutions of Fe, Ni and V were administered to rats by intratracheal instillation and the responses of interest measured at two or more time periods after dosing (most commonly 24 and 96 h). As with the majority of *in vivo* studies included in this review, chemical and cellular indicators of inflammation were evaluated in BALF. In a number of studies, a chelating agent was used to bind the transition metals to confirm that the responses observed were largely (or at least partially) mediated by divalent cations.

#### *ROFA from a Florida Power Plant*

In two early studies, researchers at NHEERL investigated the relative activity of various soluble and insoluble formulations of ROFA on markers of acute lung injury (Dreher et al. 1997) and production of free radical damage (Kadiiska et al. 1997) in BALF from Sprague Dawley rats at 24 or 96 h post-treatment. Sulfate solutions of Fe, Ni and V at doses equivalent to ROFA were administered to mimic the activity of the ROFA. Dreher et al. (1997) also added a chelating agent to a soluble suspension of ROFA particles to confirm the activity of the transition metals.

Dreher et al. (1997) found that ROFA preparations containing soluble metals produced significantly more injury as measured by increases in BALF parameters than the non-soluble forms of ROFA. Although administration of equivalent doses of the individual Fe, Ni or V sulfates (dose equivalent to 2.5 mg ROFA/rat; or 8.3 mg ROFA/kg body wt) produced significant injury compared to controls, the extent of the injury was not as great as that produced by ROFA suspension. Neutralization to a more physiologic range (pH 6.0) of the normally acidic ROFA suspension, ROFA leachate, and V and Ni sulfates produced a fine precipitate. Rats dosed with the neutralized ROFA and metal sulfates either died or exhibited severe respiratory distress. The addition of chelating agent to soluble ROFA enhanced rather than diminished the overall toxic response. In mixtures of individual metal sulfates, chelation

**Table 8** Summary of *in vivo* studies performed with Residual Oil Fly Ash (ROFA)

Concentrations in µg metal/mg ROFA extract (ratio of animal dose to human on body wt basis) <sup>a</sup>							Outcomes and indicators of effect evaluated
Sources	Fe	Mn	Ni	V	Zn		
Antonini et al. (2004)							
Precipitator	(t)157.0 (120,000)	(t)1.41 (33,000)	(t)35.7 (1,900,000)	(t)48.6 (3,100,000)	-		Inflammatory cellular response; Bacterial clearance
Boston_Mystic Power Plant	(s)15.0 (12,000)	(s)0.74 (17,000)	(s)21.4 (1,200,000)	(s)0.63 (40,000)			
Air Heater	(i)91.4 (68,000)	(i)0.36 (8,400)	(i)7.71 (420,000)	(i)42.9 (2,700,000)			
Boston_Mystic Power Plant	(t)45.7	(t)0.29	(t)12.3	(t)20.0	-		Inflammatory cellular response; Bacterial clearance
	(s)2.71	(s)0.23	(s)3.43	(s)0.05			
	(i)62.9	(i)0.12	(i)7.0	(i)18.6			
Dreher et al. (1997)							
ROFA (FL power plant)	51.3 (32,000)	0.4 (7,800)	36.6 (1,600,000)	58.2 (3,100,000)	-		Inflammatory cellular response
Ghio et al. (1998)							
ROFA (FL power plant)	35.5 (4,300)	-	37.5 (340,000)	188.0 (2,000,000)	-		Metal transport and storage
Hamada et al. (2002) <sup>b</sup>							
Precipitator	(s)0.0	(s)0.316	(s)6.824	(s)6.468	-		Inflammatory cellular response; allergic sensitization
Boston_Mystic Power Plant							
Kaditska et al. (1997)							
ROFA (FL power plant)	51.2 (6,400)	0.4 (1,600)	36.6 (330,000)	58.2 (620,000)	-		Inflammatory cellular response; reactive oxygen species





**Table 8** (continued)

Concentrations in µg metal/mg ROFA extract (ratio of animal dose to human on body wt basis) <sup>a</sup>						
Sources	Fe	Mn	Ni	V	Zn	Outcomes and indicators of effect evaluated
Lambert et al. (2000)						
ROFA (power plant in Florida)	51.3 (13,000)	0.4 (3,100)	36.6 (660,000)	58.2 (1,200,000)	–	Inflammatory cellular response; Allergic Sensitization
Lewis et al. (2003)						
Boston_Mystic Power Plant	(t)122.0 (1,200,000)		(t)38.4 (380,000)	(t)46.0 (460,000)	(t)5.34 (53,000)	Inflammatory cellular response; reactive oxygen species
	(s)18.6 (190,000)		(s)27.9 (280,000)	(s)0.58 (5,800)	(s)4.34 (43,000)	
	(i)93.2 (930,000)		(i)5.5 (55,000)	(i)41.6 (420,000)	(i)0.56 (5,600)	
Nadadur et al. (2002)						
ROFA (power plant in Florida)	51.300 (13,000)	0.4 (3,100)	36.6 (650,000)	58.2 (1,200,000)	–	Cardiovascular effects
Roberts et al. (2004)						
Precipitator	(t)122.0 (91,000)	–	(t)38.4 (2,100,000)	(t)46.0 (2,900,000)	(t)5.34 (27,000)	Cellular inflammatory response; Bacterial Clearance
Boston_Mystic Power Plant	(s)18.6 (14,000)		(s)27.9 (1,500,000)	(s)0.58 (37,000)	(s)4.34 (22,000)	
	(i)93.2 (69,000)		(i)5.5 (300,000)	(i)41.6 (2,600,000)	(i)0.56 (2,800)	
Wallenborn et al. (2007)						
HP-12 Boston Power Plant	(t)47.0 (390,000)	(t)0.56 (4,600)	(t)43.1 (360,000)	(t)62.95 (520,000)	(t)29.86 (250,000)	Metal translocation
	(s)1.09 (9,000)	(s)0.31 (2,600)	(s)6.61 (55,000)	(s)7.18 (60,000)	(s)11.55 (96,000)	
	(hcl)13.74 (110,000)	(hcl)0.13 (1,100)	(hcl)9.12 (76,000)	(hcl)26.5 (220,000)	(hcl)6.62 (55,000)	
	(i)32.21 (270,000)	(i)0.12 (1,000)	(i)27.37 (230,000)	(i)29.27 (240,000)	(i)11.69 (97,000)	

<sup>a</sup>Dose expressed as ratio of animal to man on body weight basis, based on STN annual means (Table 3), body mass = 70 kg, 10 kg, 0.3 kg and 0.02 kg for man, dog, rat and mouse, respectively, and volume of air breathed/day = 10 m<sup>3</sup>, 1 m<sup>3</sup>, 0.262 m<sup>3</sup>, and 0.01 m<sup>3</sup> for man, dog, rat and mouse, respectively

<sup>b</sup>Authors do not provide mass of PM aerosolization rate, making it impossible to calculate ratio of dose to ambient

<sup>c</sup>Animal/man dosage ratios shown in parentheses are based on the lowest dose of 0.83 mg/kg; multiply ratios by 10 to correspond to the highest dose of 8.3 mg/kg

<sup>d</sup>Animal/man dosage ratios shown in parentheses are based on the lowest dose of 0.83 mg/kg; multiply ratios by 4 to correspond to the highest dose of 3.33 mg/kg

(t)—total; (i)—insoluble fraction; (s)—soluble fraction; (hcl)—acid soluble

of Fe and V increased the lung injury produced by Ni, illustrating the complexity of the interactions amongst these metals *in vivo*.

In the companion study to Dreher et al. (1997), Kadiiska et al. (1997) instilled Sprague Dawley rats with a lower dose (500 µg) of soluble or insoluble preparations of the ROFA sample, or with a mixture of V(II), Ni(II) and Fe(III) sulfates in concentrations approximately equivalent to those in 500 µg of ROFA. Twenty four (24) hours after instillation, acute inflammatory lung damage was ascertained through examination of cellular and chemical markers in BALF; the production of free radicals was evaluated using electron spin resonance (ESR) in conjunction with  $\alpha$ -(4-pyridyl-1-oxide)-N-tert-butyl nitron (4-POBN) spin-trap. Although no p values were given, Kadiiska et al. (1997) reported that the soluble components of ROFA produced a significant influx of neutrophils and proteins indicative of acute inflammation, and significant increases in the formation of free radicals. The authors suggested that V may play the most significant role in the inflammatory response produced by ROFA.

Kodavanti et al. (1998) instilled Sprague Dawley rats with doses of 0, 0.833, 3.33, or 8.33 mg/kg of water soluble and acid-extractable fractions of ROFA samples collected from ten locations within the same oil burning power plant (Table 8); the metals present were primarily Fe, V and/or Ni. Twenty four hours after instillation, dose-dependent increases in inflammatory markers in BALF were observed, with ROFA samples containing the highest concentrations of water-extractable Fe, V and Ni, or V and Ni showing statistically significant increases in some markers. In particular, a significant positive correlation was found between increased BALF protein levels and the water-extractable Ni content of the ROFA sample. However, the chemiluminescence assay indicated that ROFA containing water-extractable V was more potent in producing oxidative damage than ROFA containing Ni in addition to V and Fe.

Ghio et al. (1998) tested the hypothesis that concentrations of the iron transport and storage proteins lactoferrin and ferritin in rat lung would increase in response to exposure to ROFA-containing concentrations of Fe, Ni and V. Sprague Dawley rats were instilled with 500 µg ROFA, were sacrificed at 4, 25, 48 or 96 h post-exposure, and ferritin, transferrin and lactoferrin concentrations and activity in the lungs determined. Measurable concentrations of Fe were present in the lungs of both exposed and un-exposed rats; but Ni and V were only measurable in exposed animals. Ferritin and lactoferrin concentrations in the lower respiratory tract of ROFA-treated animals were transiently increased with signs of visible tissue injury, but the respiratory tract displayed no influx of inflammatory cells. Concentrations of transferrin in BALF were significantly increased at 4, 24 and 48 h after ROFA exposure as compared to control animals. The authors suggested that increases in iron-binding and transporting proteins may be related to control of oxidative stress produced by the metals.

Using the same ROFA sample as used by Kadiiska (1997) and Dreher (1997), Kodavanti et al. (2001) investigated the acute lung toxicity of the ROFA and constituent metals in healthy normotensive Wistar Kyoto (WKY) and spontaneously hypertensive (SH) rats instilled with either saline, 0.83 or 3.33 mg ROFA/kg, or 1.5 µmol/kg of either V or Ni sulfates in saline equivalent to a 2–3 mg dose of ROFA. BALF markers of acute injury and histological changes in the lung were

evaluated at 24 and 96 h for animals exposed to ROFA, and at 6 and 24 h for animals instilled with metal sulfates. Basal levels of BALF protein, macrophages, and neutrophils were significantly higher in SH rats than normotensive animals. Exposure to ROFA produced dose-related increases in BALF markers in both SH and WKY rats, with the effect being more severe in the SH rats. Sulfate solutions of Ni and V produced inconsistent effects on inflammatory markers. Ni caused more severe progressive increases in LDH activity in both strains of rat than V; however, total BALF cells were significantly increased only at 24 h in Ni exposed rats. V produced an increase in protein and LDH at 6 h in WKY but not SH rats. Ni and V acted differently in SH as compared to WKY rats. The authors concluded that rats with compromised cardiovascular systems are more susceptible to pulmonary injury from ROFA metals than normal rats.

Lambert et al. (2000) evaluated the effects of the same ROFA source used in the previous studies on sensitization of Brown Norway rats to house dust mite (HDM) allergens. Rats were instilled with 1,000  $\mu\text{g}$  of ROFA, or 105.12  $\mu\text{g}$  Ni, or 98.2  $\mu\text{g}$  V, or 58.49  $\mu\text{g}$  Fe as sulfates, with mixtures of the metals, or saline controls, followed 3 days later with a sensitization dose of HDM. Some of the animals were sacrificed at day 7 after sensitization. At 14 days, the remaining animals were exposed to a challenge dose of HDM and monitored for immediate bronchoconstriction in response to the allergen, were then sacrificed and evaluated for IgE and inflammatory markers. Significant increases in HDM-specific IgE were apparent in all treatment groups, with the greatest increases occurring in animals exposed to ROFA, Ni, V, or a mixture of metals. Although Fe had only a modest adjuvant effect on IgE, it produced a greater increase in inflammatory markers than ROFA or the other two metals.

The final study using the ROFA obtained from the Florida power plant discussed here was conducted by Nadadur and Kodavanti (2002) to investigate effects on the expression of 84-cardiopulmonary genes coding for proteins involved in inflammatory response, tissue repair, structural and matrix alterations, and vascular contractility. Following a similar protocol to that used in the previous studies, Sprague Dawley rats were instilled with saline, 3.3 mg/kg ROFA, 1.3 mmol/kg  $\text{NiSO}_4$ , or 2.2 mmol/kg  $\text{VSO}_4$  (Table 8). Rats were sacrificed at 3 or 24 h post-instillation and blood and lung tissue were evaluated for mRNA activity representing the 84 gene protein products of interest by gene array data analysis. The authors reported that the gene expression profiles observed in this study indicate that pulmonary injury caused by ROFA is different than injury produced by Ni or V acting alone, suggesting potential interactions amongst the constituents in ROFA.

#### *ROFA from a Boston Area Power Plant*

Wallenborn et al. (2007) used ROFA designated as PM (HP-12) obtained from the precipitator of a Boston area power plant to determine if water-soluble metals from inhaled particulate could translocate to other parts of the body. The water-soluble concentrations of Fe, Ni and V were lower in the HP-12 sample than in the Florida power-plant ROFA used in the previously described studies. Wistar Kyoto rats were instilled

with saline or 8.33 mg/mL HP-12 suspension, sacrificed 4 or 24 h post-instillation, and samples of blood, lung, heart and liver collected and analyzed for transition metals. Significantly higher levels of V and Ni were found in the lung, plasma, heart and liver of animals instilled with HP-12 as compared to saline controls ( $p \leq 0.05$ ), suggesting that the soluble metals are cleared and presumably enter the systemic circulation, while insoluble metals remained in the lungs. However, higher baseline levels of Zn and Mn were found in the tissues of control animals, making it more challenging to detect changes related to instillation of these same metals in HP-12. Of particular relevance to the purpose of this study is the observation that there were no significant differences in the amount of Zn (4 and 24 h) or Mn (24 h) in the heart of HP-12-treated animals, compared to controls.

Hamada et al. (2002) investigated the effects of ROFA from the precipitator of a Boston area power plant on airway hyper-responsiveness in 7–8-week-old, and 2- and 3-week-old BALB/c mice exposed by inhalation for 30 min to nebulized aerosols of ROFA at 0 (controls), 10, 50 and 100 mg/mL; the final pH of the ROFA suspension was acidic (viz., 5.5). To determine the effect of pH, mice were also exposed to aerosols adjusted to a pH of 7.2. Airway responsiveness was measured by exposing control and ROFA-exposed mice to increasing concentrations of methacholine aerosol at periods up to 120 h post-ROFA. The potential role of ROS in the response of ROFA-exposed mice to methacholine challenge was explored by pre-treating groups of mice with the antioxidant dimethylthiourea (DMTU) at doses of 5, 10, 50 or 100 mg/kg 30 min prior to exposure to 50 mg/mL ROFA aerosol. Inflammatory markers were evaluated in BALF from 8-week-old mice exposed to 50 mg/mL ROFA at 6, 12, 24 and 48 h post-exposure. As a side study to determine if age and maturation determine airway responsiveness, mice aged 2, 3, and 7–8 weeks old were exposed to 50 mg/mL ROFA and examined 6 and 12 h later for inflammatory response in BALF. Exposure to 50 or 100 mg/mL ROFA, but not to 10 mg/mL, significantly amplified the airway hyper-responsiveness to all challenge concentrations of methacholine at 12, 24 and 48 h after exposure. A mixture containing the individual metals, but not the individual metals alone, produced approximately the same level of significant response as the complete ROFA suspension. ROFA suspensions adjusted to pH 7.2 or 5.5 both produced significantly higher airway responsiveness than saline; moreover, filtered ROFA produced significantly greater responsiveness than saline. The authors did not indicate if adjusting the acidic ROFA suspension to physiologic pH resulted in the formation of a fine precipitate as observed by Dreher (1997).

Treatment with DMTU prior to inhaling ROFA decreased the magnitude of response to subsequent methacholine challenge. Maturation of the respiratory and immune system was relevant to the response to methacholine in the following order: very young 2-week <3- <7–8-week-old mice. Although this series of experiments was conducted with high, non-ambient doses of ROFA and constituent metals, the findings suggest that some type of interactions of the constituent metals in the ROFA are involved in provoking the inflammatory response and that oxidative mechanisms may be at least partially responsible for the injury. This is also one of the few *in vivo* studies, in which animals were exposed to PM by inhalation.

Lewis et al. (2003) further examined the role of ROS induced by transition metals on lipid peroxidation as a mechanism of lung injury by exposing rats to ROFA that had been separated into soluble and insoluble fractions that were taken from the a Boston power plant (Table 8). Sprague Dawley rats were instilled with 1 mg/100 g body wt with total ROFA suspension, ROFA-soluble fraction, ROFA-insoluble fraction, total ROFA suspension plus the chelating agent deferoxamine and antioxidant enzyme catalase, or saline controls. At 4, 24 and 72 h post-instillation, animals were sacrificed and BALF analyzed for total and differential cell counts. Non-lavaged lungs were evaluated for evidence of lipid peroxidation as an indicator of inflammatory injury. The presence of ROS was determined by ESR in a cell-free system, and cellular oxidant potential was measured by chemiluminescence. ROFA-total and ROFA-soluble preparations had significantly more oxidant potential by ESR than the ROFA-insoluble fraction (no p value given). The oxidant potential was reduced by the addition of deferoxamine. There were no differences in alveolar macrophages amongst any of the treatment groups at any time points. All forms of ROFA increased neutrophils, but had somewhat different time courses. ROFA-total and ROFA-insoluble significantly increased lipid peroxidation at 24 and 72 h, compared to saline controls. ROFA-soluble had no effect on lipid peroxidation at any time interval. This finding contradicts other studies that report significant effects from soluble, but not insoluble fractions.

The effects of ROFA metals on susceptibility to bacterial lung infection in Sprague Dawley rats was investigated by Roberts et al. (2004) by using the same ROFA source as used in the previous study (Lewis et al. 2003). The rats were instilled with 1 mg/100 g body wt with one of the three ROFA solutions or saline and then inoculated with *Listeria monocytogenes* 3 days later. At days 6, 8 and 10, rats were sacrificed and the lungs removed for histology and determination of clearance of *L. monocytogenes*. The ROFA-insoluble treatments had no significant effect on rat survival of *L. monocytogenes* infection. On the other hand, mortality after inoculation was 40% in ROFA-total and 80% in ROFA-soluble treatment groups, with the majority of animals dying 7–8 days post-ROFA instillation. Bacterial lung burdens were also correspondingly much higher in those animals administered the ROFA-total or ROFA-soluble treatments, compared to the saline or ROFA-insoluble ones. Rats exposed to ROFA-soluble treatments in the presence of a chelating agent were able to clear the majority of bacteria from their lungs by day 10 and were similar to controls. The fact that adding a chelating agent appeared to nullify the increased susceptibility to infection caused by the ROFA-soluble fraction supports the hypothesis that soluble metals are involved.

In an extension of the previous study (Roberts et al. 2004), Antonini et al. (2004) tested ROFA collected from the precipitator and air-heater of the same Boston power plant on the response of Sprague-Dawley rats to infection with *L. monocytogenes*. The metal content of the precipitator ROFA was considerably higher, and was more water-soluble than that from the air-heater (Table 8). The dosing protocol with the different ROFA preparations and with silica (positive control) or saline (negative control), infection with *L. monocytogenes*, and determination of pulmonary bacterial clearance was the same as described for the Roberts et al. (2004)

study. Instillation of ROFA fractions from the precipitator produced significant increases in inflammatory markers, ROS (no p value given), and significantly decreased bacterial clearance compared to air heater ROFA and saline controls.

### Critical Comments on In Vivo Studies with ROFA

It should be noted that the metal concentrations used in the ROFA studies discussed here (see Table 8) were extremely high and do not reflect actual ambient exposures. For PM<sub>2.5</sub> metals, ambient concentrations of metals in the ROFA extracts gleaned from STN and IMPROVE (Table 1), and ambient concentrations reported for the epidemiological studies (see Table 4), were up to three million times higher than those found in ambient air. Fe levels reported in the ROFA extracts were up to 120,000 times higher than ambient levels, while ROFA levels of Zn were up to 27,000 times higher. Concentrations of Ni and V in the ROFA extracts were even higher, i.e., respectively up to 1.9 million and 3.1 million times higher than recorded ambient levels. These extreme differences between ROFA and ambient levels of metals should be considered when interpreting the significance of the ROFA study results. It should also be noted that on a mass basis, ROFA contains a higher proportion of Ni and V than ambient PM.

### In Vivo Exposures to Individual Metals

The metals most frequently detected in ambient PM in the U.S. are Cu, Fe and Zn, with Ni, V; other metals are detected less frequently. The studies described below investigated the toxicity of individual metals found in specific-source particulates. The doses of individual metals tested in these studies are summarized in Table 9. No Observed Adverse Effect Levels (NOAEL) and Lowest Observed Adverse Effect Levels (LOAEL) are also presented in this table where sufficient dose-response information was available.

Using the Canadian atmospheric dust sample, EHC-93 (Environmental Health Center-93), Adamson et al. (2000) conducted a series of studies to determine which of the metal constituents in this PM was associated with toxicity. The concentrations of the target metals in the EHC-93 PM are presented in Table 6. Swiss mice were intratracheally instilled with the soluble EHC-93 concentration of Al ammonium nitrate, Cu sulfate, Fe sulfate, Pb nitrate, Mg chloride, Ni chloride, Zn chloride or saline controls. Since the concentration of Zn appeared to have the greatest effect on inflammatory markers in BALFs, additional studies were conducted with Zn chloride and Zn sulfate at one and ten times the concentration of soluble Zn in the EHC-93 sample. The mice developed a strong inflammatory response and lung injury over the 2-week post-instillation period, and after 4 weeks the animals treated with Zn sulfate at ten times the EHC-93 concentration had also developed fibrosis. The authors point out that the doses used were roughly four times ambient levels and that the method of administration was not analogous to ambient human PM

**Table 9** No observable (NOAEL) and lowest observable adverse effect levels (LOAEL) for target metals in *in vivo* studies

Study	Exposure method	Form of metal	Doses (ratio animal/human) <sup>a</sup>	Significant responses			
				Heart rate	Core Temp.	Arrhythmia	
Campan et al. (2001)	Inhalation; rat	VSO <sub>4</sub>	Saline				
			0.3 mg/m <sup>3</sup> (1,700,000)	NOAEL = 0.9 mg/m <sup>3</sup>	NOAEL = 0.9 mg/m <sup>3</sup>	NOAEL = 1.7 mg/m <sup>3</sup>	
			0.6 mg/m <sup>3</sup> (2,800,000)	LOAEL = 1.7 mg/m <sup>3</sup>	LOAEL = 1.7 mg/m <sup>3</sup>	LOAEL = NA	
			0.9 mg/m <sup>3</sup> (5,000,000)				
			1.7 mg/m <sup>3</sup> (9,400,000)				
		NiSO <sub>4</sub>	Saline		NOAEL = 0.49 mg/m <sup>3</sup>	NOAEL = 0.49 mg/m <sup>3</sup>	NOAEL = 0.49 mg/m <sup>3</sup>
			0.37 mg/m <sup>3</sup> (1,700,000)				
			0.49 mg/m <sup>3</sup> (2,300,000)		LOAEL = 1.3 mg/m <sup>3</sup>	LOAEL = 1.3 mg/m <sup>3</sup>	LOAEL = 1.3 mg/m <sup>3</sup>
			1.3 mg/m <sup>3</sup> (6,100,000)				
			2.1 mg/m <sup>3</sup> (9,900,000)				
NiSO <sub>4</sub> + VSO <sub>4</sub>	Saline		NOAEL = NA	NOAEL = NA	NOAEL = NA		
	0.5 mg/m <sup>3</sup> (1,300,000)		LOAEL = 0.5 mg/m <sup>3</sup>	LOAEL = 0.5 mg/m <sup>3</sup>	LOAEL = 0.5 mg/m <sup>3</sup>		
		1.3 mg/m <sup>3</sup> (3,300,000)					



Author	Exposure	Route	Species	Sex	Age	Duration	Parameters	Findings			
Campen et al. (2002)	Instillation; rat	rat	Fe <sub>2</sub> (SO <sub>4</sub> ) <sub>3</sub>				Saline control	BALF total protein	BALF lactate dehydrogenase	BALF microalbumin	BALF glutathione
							105 µg (26,000)	Healthy rats: no diff. from control	Healthy rats: Sig. diff. from controls	Healthy rats: Sig. diff. from controls	Healthy rats: Sig. diff. from controls
							Saline control	Healthy rats: Sig. diff. from control day 2 only	Healthy rats: Sig. diff. from controls	Healthy rats: Sig. diff. from controls	Healthy rats: Sig. diff. from controls
							263 µg (47,000)	MCT rats: No diff. from control day 2 only	MCT rats: No diff. from controls	MCT rats: No diff. from controls	MCT rats: No diff. from controls
							Saline control	Healthy rats: No diff. from control day 1 only	Healthy rats: No diff. from controls	Healthy rats: No diff. from controls	Healthy rats: No diff. from controls
							245 µg (5,200,000)	MCT rats: days 1 and 3	MCT rats: No diff. from controls	MCT rats: No diff. from controls	MCT rats: No diff. from controls
							Saline control	MCT rats: No diff. from controls	MCT rats: No diff. from controls	MCT rats: No diff. from controls	MCT rats: No diff. from controls
							105 µg Fe + 245 µg V (86,000)	MCT rats: No diff. from controls	MCT rats: No diff. from controls	MCT rats: No diff. from controls	MCT rats: No diff. from controls
							Saline control	MCT rats: No diff. from controls	MCT rats: No diff. from controls	MCT rats: No diff. from controls	MCT rats: No diff. from controls
							105 µg Fe + 263 µg Ni (90,000)	MCT rats: No diff. from controls	MCT rats: No diff. from controls	MCT rats: No diff. from controls	MCT rats: No diff. from controls
							Saline control	MCT rats: No diff. from controls	MCT rats: No diff. from controls	MCT rats: No diff. from controls	MCT rats: No diff. from controls
							263 µg Ni + 245 µg V (4,900,000)	MCT rats: No diff. from controls	MCT rats: No diff. from controls	MCT rats: No diff. from controls	MCT rats: No diff. from controls
							Saline control	MCT rats: No diff. from controls	MCT rats: No diff. from controls	MCT rats: No diff. from controls	MCT rats: No diff. from controls
							105 µg Fe + 263 µg Ni + 245 µg V (150,000)	MCT rats: No diff. from controls	MCT rats: No diff. from controls	MCT rats: No diff. from controls	MCT rats: No diff. from controls

(continued)

**Table 9** (continued)

Study	Exposure method	Form of metal	Doses (ratio animal/human) <sup>a</sup>	Significant responses				
				Total inflamm. cells in BALF	Total protein in BALF	Cardiac prothrombomodulin mRNA	Blood coagulation Factors	Red blood cells
Gilmour et al. (2006)	Instillation: rat	ZnSO <sub>4</sub>	Saline control	Sig. increase over controls at 4, 24 and 48 h post exposure			Sig. increase in fibrinogen at 24 and 48 h	Sig. increase in hematocrit at 1, 24 and 48 h
			0.32 mg/kg (160,000)					
Gilmour et al. (2006)	Instillation: rat	ZnSO <sub>4</sub>	Saline control	Sig. increase at 1, 4, 24 and 48 h (greatest at 4 h)	<b>Metallothionein MT-1 mRNA</b>	Lung: Sig. increase only at 1 and 4 h		
			0.32 mg/kg (160,000)					
Prieditis and Adamson (2002)	Instillation: mouse	ZnCl <sub>2</sub>	Saline	Sig. increase at 3 and 7 days post exposure	<b>Alveolar macrophages</b>	Damage at days 1 and 3, return to normal days 7 and 14	No apparent changes	
			4.8 µg (120,000)					
Prieditis and Adamson (2002)	Instillation: mouse	Pb(NO <sub>3</sub> ) <sub>2</sub>	Saline	No sig. difference	<b>Lung epithelial damage</b>	Damage at days 1 and 3, return to normal days 7 and 14	No apparent changes	
			4.8 µg					
Prieditis and Adamson (2002)	Instillation: mouse	CuSO <sub>4</sub>	Saline	Sig. increase at 3 and 7 days post exposure	<b>Lung epithelial damage</b>	Damage at days 1 and 3, return to normal days 7 and 14	No apparent changes	
			4.8 µg (310,000)					
Prieditis and Adamson (2002)	Instillation: mouse	NiCl <sub>2</sub>	Saline	No sig. difference	<b>Lung epithelial damage</b>	Damage at days 1 and 3, return to normal days 7 and 14	No apparent changes	
			4.8 µg (1,300,000)					
Prieditis and Adamson (2002)	Instillation: mouse	V <sub>2</sub> O <sub>5</sub>	Saline	No sig. difference	<b>Lung epithelial damage</b>	Damage at days 1 and 3, return to normal days 7 and 14	No apparent changes	
			4.8 µg (1,500,000)					

Wallenborn et al. (2008)	Inhalation; rat	ZnSO <sub>4</sub>	FA	<b>BAL Cell counts and protein levels</b> NOAEL=100 µg/m <sup>3</sup> LOAEL=NA	<b>Cardiac and pulmonary changes</b> NOAEL=100 µg/m <sup>3</sup> LOAEL=NA	<b>Cardiac mitochondria and cytosol enzymes</b> NOAEL=30 µg/m <sup>3</sup> LOAEL=100 µg/m <sup>3</sup>			
		NiSO <sub>4</sub>	0.05 mg/m <sup>3</sup> (27,000)	<b>Heart rate</b>	<b>Heart rate variability</b>	<b>Abnormal wave forms</b>			
		VOSO <sub>4</sub>	0.05 mg/m <sup>3</sup> (32,000)	NOAEL=0.05 mg/m <sup>3</sup>	NOAEL=0.05 mg/m <sup>3</sup>	NOAEL=0.05 mg/m <sup>3</sup>			
	Muggenburg et al. (2003)	Inhalation; dog	MnO <sub>2</sub>	0.05 mg/m <sup>3</sup> (12,000)					
			V <sub>2</sub> O <sub>5</sub>	0.05 mg/m <sup>3</sup> (32,000)					
			Fe <sub>2</sub> O <sub>3</sub>	0.05 mg/m <sup>3</sup> (37,000)					
			CuO <sub>2</sub>	0.05 mg/m <sup>3</sup> (6,500)					
			NiO <sub>2</sub>	0.05 mg/m <sup>3</sup> (27,000)					
			Fe	FA	<b>Pulmonary cytotoxicity</b> NOAEL=57 µg/m <sup>3</sup> LOAEL=90 µg/m <sup>3</sup>	<b>Ferritin</b> NOAEL=57 µg/m <sup>3</sup> LOAEL=90 µg/m <sup>3</sup>	<b>Oxidative stress</b> NOAEL=57 µg/m <sup>3</sup> LOAEL=90 µg/m <sup>3</sup>	<b>Proinflammatory cytokines</b> NOAEL=57 µg/m <sup>3</sup> LOAEL=90 µg/m <sup>3</sup>	<b>NF-kappa beta</b> NOAEL=90 µg/m <sup>3</sup>
			Zhou et al. (2003)	Inhalation; rat					

<sup>a</sup>Dose expressed as ratio of animal to man on body weight basis, based on STN annual means (Table 3), body mass=70 kg, 10 kg, 0.3 kg and 0.02 kg for man, dog, rat, and mouse, respectively, and volume of air breathed/day=10 m<sup>3</sup>, 1 m<sup>3</sup>, 0.262 m<sup>3</sup>, and 0.01 m<sup>3</sup> for man, dog, rat, and mouse, respectively

exposure. This study provides evidence that at concentrations 8,000 times that of ambient levels, zinc salts can produce inflammatory lung injury.

Following up on the findings of Adamson et al. (2000), Frieditis and Adamson (2002) instilled mice with solutions of Zn, Cu, V, Ni, Fe, and Pb at concentrations (4.8 mg/g in 0.1 mL saline) equal to the concentration of Zn (4.8 mg Zn/g dust) in the EHC-93 dust and observed effects on markers of pulmonary inflammation in BALF and lung morphology. The doses (Table 9) used in this study were approximately 100,000–1,000,000 times higher than people are exposed to in ambient air. Markers of inflammation and injury in BALF and lung morphology were then examined to determine any associations with exposure. Only Zn and Cu were associated with significant lung injury as measured by the increased numbers of alveolar macrophages, leukocytes and BALF protein in the exposed mice versus controls. Morphological changes in the lungs of Cu- and Zn-exposed mice were similar to the mice exposed to EHC-93 dust. The Zn levels found in the EHC-93 samples were approximately four times higher than those found in STN samples (Table 1), and the exposure was more than 100,000 fold ambient levels.

Wallenborn et al. (2008) administered aerosolized zinc sulfate (10–100  $\mu\text{g}/\text{m}^3$ ) to healthy rats via nasal inhalation for 5 h per day, 3 days per week for 16 weeks. The animals were euthanized 48 h after the last exposure. No morphological changes consistent with cardiac or pulmonary pathology were observed. Significantly increased levels of ferritin and decreased levels of glutathione peroxidase and succinate dehydrogenase were observed in cardiac cells, suggesting a mitochondrial-specific effect of inhaled Zn sulfate. Cardiac gene expression was significantly altered at the highest dose of Zn sulfate (100  $\mu\text{g}/\text{m}^3$ ), as evidenced by a microarray analysis. As shown in Table 8, the highest exposure level (100  $\mu\text{g}/\text{m}^3$  of Zn) was equal to the NOAEL for BALF parameters and indicators of cardiac changes, and the LOAEL for effects on cardiac enzymes.

According to the authors, this study demonstrates that inhalation exposures to environmentally plausible concentrations of Zn are associated with cardiovascular effects in healthy rats. However, the exposure concentrations of Zn used in this study were hundreds to thousands of times higher than what has been reported in ambient air (STN Zn=0.014  $\mu\text{g}/\text{m}^3$ ; IMPROVE Zn=0.043  $\mu\text{g}/\text{m}^3$ ); hence, these concentrations would not be considered as environmentally relevant levels. In two related studies that were an extension of the work conducted by Costa and Dreher (1997), Campen et al. (2001 and 2002) examined the effects of Fe, Ni and V on cardiovascular parameters and body core temperature in Sprague Dawley rats. In the first study (Campen et al. 2001), rats were surgically fitted with radiotelemetry transmitters that were used to measure core temperature and ECG. Groups of 4 rats were exposed by inhalation to concentrations (Table 9) of V sulfate, Ni sulfate, Ni and V sulfates concurrently, ranging from 0.3 to 2.4  $\text{mg}/\text{m}^3$ , or filtered air 6 h/day for 4 days. Animals were observed for either 24 or 96 h following the final exposure and then were sacrificed. Blood and BALF were collected. Ni caused delayed bradycardia, hypothermia and arrhythmia at concentrations greater than 1.2  $\text{mg}/\text{m}^3$ . Ni and V together produced cardiovascular effects at lower concentrations than produced by the highest concentration of Ni alone (2.1  $\text{mg}/\text{m}^3$ ), suggesting possible

synergy between Ni and V. Cardiovascular effects became apparent on the third day of exposure and persisted for more than 72 h. Exactly 50% of the rats exposed to the highest concentration of Ni + V ( $1.3 \text{ mg/m}^3$ ) died. The exposure levels to Ni and V used in this study were approximately one million times the mean ambient levels of  $1.3 \text{ ng/m}^3$  and  $1.1 \text{ ng/m}^3$ , respectively, in the 2008 STN data as shown in Table 1.

In the companion study by this research group (Campen et al. 2002), healthy (normotensive) and pulmonary hypertensive induced with monocrotaline (MCT) Sprague Dawley rats were fitted with telemetry devices and instilled with either 0.3 ml saline, or various masses (Table 9) of sulfates of Fe (III), Ni (II), V (II), or combinations of the three metal sulfates in the same volume of saline. Telemetry data were collected for 48 h before instillation and for 96 h following instillation, after which the animals were sacrificed, and BALF and tissue samples collected. In both healthy and MCT-treated rats, instillation of V produced an acute decrease in both heart rate and core temperature and an increase in arrhythmias, which persisted for 3 days post instillation. Somewhat surprisingly, these effects were of lesser magnitude in MCT-treated rats. Ni did not cause an immediate effect but rather produced delayed and prolonged bradycardia, hypothermia and arrhythmogenesis, with similar responses in both healthy and MCT-treated rats; 50% of the MCT-treated rats instilled with Ni subsequently died. The combination of Ni + V produced a greater acute hypothermic and arrhythmic response than V alone. The hypothermic and rhythm effects of Ni + V were somewhat attenuated by the addition of Fe. Treatment with MCT (in the absence of metals) produced significant increases in indicators of cardiac damage and proteins that were associated with cell injury [LDH; microalbumin (MIA); N-acetyl glucosaminidase (NAG); glutathione (GSH)] in BALF as compared to saline controls. In MCT-treated rats, the following metals caused significant increases in BALF proteins compared to controls: Ni (LDH); Fe + Ni (LDH); Ni + V (LDH, GSH); Fe + Ni + V (LDH). In healthy rats, the effects of Fe alone were no different than controls. V produced significant increases in LDH and MIA. Ni produced significant increases in total protein, LDH, MIA, NAG and GSH. In these two studies (Campen et al. 2001 and 2002), instillation of  $263 \mu\text{g}$  of Ni produced significantly greater effects on cardiac function, regulation of core body temperature and BALF indicators of pulmonary injury than did  $245 \mu\text{g}$  of V.

In two companion papers, Gilmour et al. (2006) investigated the following parameters: systemic effects of intratracheal zinc sulfate exposure on metal homeostasis of essential metals (Zn, Cu and Se), changes in cardiac gene expression and changes in sequestering proteins, Zn transporter-2 (ZT-2) and metallothionein-1 (MT-1), in the heart, lung and liver in rats exposed to  $2 \mu\text{mol/kg}$  of zinc sulfate or saline. This Zn concentration is approximately 100,000 times environmentally-relevant concentrations (Table 9), but may be relevant to occupational exposures at levels that could induce Zn fume fever, an acute occupational heavy metal intoxication that is classically associated with welders. Rats were euthanized at various time points and responses were measured in plasma, heart, lung and liver tissue. Plasma Zn levels increased 20% at 1 h post exposure and levels in the liver increased 35% in 24–48 h post exposure. Significant increases in liver levels of Cu and Se were also observed at 24–48 h post exposure, which suggested that disruption of systemic

metal homeostasis was induced by the instilled Zn sulfate. Further evidence suggested disruption of essential metal homeostasis, with the induction of MT-1 and ZT-2 in the heart, lung and liver. Zn exposure was significantly associated with changes in genes affecting calcium homeostasis, mitochondrial activity, cell-signaling pathways, ion channels and transferases. These results suggest a possible direct mechanism and effect of pulmonary Zn exposure on cardiac tissue *in vivo*.

Gilmour et al. (2006) evaluated the relationship between pulmonary exposure to Zn and potential direct and indirect cardiovascular responses by instilling 2  $\mu\text{mol/kg}$  of Zn sulfate or saline (time matched control) in male Wistar Kyoto rats (same dose described in Gilmour et al. 2006). Rats were examined 1, 4, 24 and 48 h post exposure for responses in blood chemistry, BALF, histopathology and gene expression. Circulating levels of Zn increased by 20% above baseline at 1–24 h post-exposure. Significant lung injury/inflammation occurred at 1–24 h intervals post-exposure as evidenced by analyses of BALF and histopathology. Moreover, the level of injury/inflammation produced was severe and could indirectly induce cardiac impairment. Gene expression in both lung and cardiac tissue following Zn exposure was significantly increased for tissue factor (TF) and plasminogen activator-inhibitor-1 (PAI-1), in exposed vs. time-matched control rats, which may lead to increased coagulation and thrombosis. There was extensive pulmonary injury/inflammation, whereas only mild focal cardiovascular lesions were observed with no histological evidence of increased fibrin. However, at 24 and 48 h, blood levels of fibrinogen were significantly increased. The authors suggested that impairments in blood coagulation (pro-coagulative effects), in combination with pulmonary injury induced by Zn exposure may be a potential mechanism for adverse cardiovascular responses to Zn in ambient PM.

Muggenburg et al. (2003) measured electrocardiographic responses to inhalation exposure to single metal oxides (*viz.*, the relatively insoluble oxides of Cu, Fe, Mn, Ni, or V) or single metal sulfates (*viz.*, soluble oxides of Ni or V). Older dogs ( $n=8$ ) that had naturally occurring cardiovascular deficiencies were exposed to 0.05 mg/ $\text{m}^3$  (a concentration of Ni roughly 10,000 times higher than found in ambient PM) of single metal aerosols or filtered air for 3 h on 3 successive days. All particles were respirable and had a mass median aerodynamic diameter range of 0.72–2.93  $\mu\text{m}$ . ECGs were continuously recorded throughout each exposure period and were analyzed for changes in heart rate, heart rate variability and abnormal wave forms. No significant effects of exposure were observed for any aerosol containing a single metal oxide or sulfate (Table 9). In a parallel qualitative study, in which ECG trends were visually analyzed without statistical analyses, no effects were observed in dogs ( $n=4$ ) exposed to high concentrations of ROFA (Muggenburg et al. 2003). The lack of associations in this study (Muggenburg et al. 2003) could result from: 1) not evaluating the effect of metal mixtures or the presence of co-pollutants in ambient PM, 2) the study size being too small ( $n=4$  per group) and, thus, lacking power to detect significant effect differences (no power analysis was reported by the authors), and 3) the length and frequency of exposure were too short. More frequent or longer duration exposures may be required to elicit effects.

Zelikoff et al. (2002) conducted a series of studies to investigate reports from epidemiologic studies that exposure to ambient PM is associated with increased respiratory infections, especially in elderly individuals. Fischer 344 rats that had been previously infected with *Streptococcus pneumoniae* were exposed for 5 h in an inhalation chamber to ambient New York City PM<sub>2.5</sub> (65–90 µg/m<sup>3</sup>) or filtered air. In another set of studies, previously infected rats and uninfected controls were exposed by inhalation to chloride salts of Fe, Mn, or Ni at a concentration of 65–90 µg/m<sup>3</sup> for 5 h. Rats were sacrificed at various intervals after exposure and examined for signs of *S. pneumoniae* infection and markers of inflammation in BALF and blood. By 18 h post-exposure, bacterial burdens in the lungs of rats exposed to the NYC PM<sub>2.5</sub> were significantly greater (300 times,  $p < 0.01$ ) than filtered air controls, and the number of pulmonary lymphocytes (cells responsible for bacterial pathogen removal) in PM-exposed animals was lower than in controls ( $p < 0.05$ ). Exposure to the individual transition metals altered some pulmonary and systemic immune system parameters in uninfected rats. Exposure to Fe or Ni (at  $\geq 1,000$ -fold higher than ambient air), but not Mn significantly altered bacterial clearance. The authors suggested that Fe and Ni in ambient PM may play a role in exacerbating bacterial lung infections.

Zhou et al. (2003) conducted an acute pulmonary inhalation exposure study to determine the association between exposure to Fe in ultrafine PM and adverse pulmonary response. Healthy rats were exposed to ultrafine Fe particulate (57 or 90 µg/m<sup>3</sup>, median particle diameter 72 nm) or filtered air for 6 h/day for 3 consecutive days. Rats were euthanized within 2 h of final exposure and markers of inflammation and injury in BALF and lung homogenate were quantified. Exposure at a concentration of 57 µg/m<sup>3</sup> of Fe did not elicit significant responses that were different from controls. Exposure at the highest dose, 90 µg/m<sup>3</sup>, was significantly associated with increased ferritin expression ( $p < 0.05$ , indicates bioavailable iron), total protein ( $p < 0.05$ , indicator of cytotoxicity), IL-1B ( $p < 0.01$ , marker of inflammation) and an increase in markers of oxidative stress in the lungs ( $p < 0.01$ ). The authors concluded that inhaled Fe in ultrafine particles is bioavailable and is associated with adverse pulmonary effects in rats and that this association appears to be dose-dependent. However, the dose administered in this study that elicited an adverse response was over 900 times higher than ambient concentrations in PM<sub>2.5</sub> (Table 1), and ultrafine particles comprise an extremely small fraction (by mass) of PM<sub>2.5</sub>.

Ghio et al. (2005) explored the role of the transferrin-independent surface protein, divalent metal transporter-1 (DMT-1), and its role in detoxification of Fe in the lung. Homozygous Belgrade rats demonstrate poor Fe absorption and resulting anemia. DMT-1-deficient rats were exposed to either 0.5 mL saline or 500 µg of ROFA in 0.5 mL saline via intratracheal instillation. In another phase of the study, normal Sprague Dawley rats were instilled with 0.5 mL of saline, 0.5 mL of 100 µM ferric ammonium citrate, or 0.5 mL of 10 µM vanadyl sulfate. After 24 h, the same rats were again anesthetized and instilled with either saline or 500 µg ROFA in saline. Sacrifices were then made at 15, 30, or 60 min and/or 24 h after the second instillation, and lungs were then analyzed for Fe and V. At 24 h post exposure, homozygous

DMT-1-deficient rats had significantly higher levels of both Fe and V in their lungs than did controls, and exhibited significantly more lung damage. The results suggest a protective transport role for DMT-1 in rat lung tissue. In normal Sprague-Dawley rats instilled with Fe or V, immunohistochemistry results demonstrate that Fe induced DMT-1 in lungs, whereas V had the opposite effect. The normal Sprague-Dawley rats that were pre-exposed to Fe and later challenged with 500 µg of ROFA exhibited better metal clearance than those pre-treated with saline. However, rats pre-exposed to V had significantly less metal clearance 15 min after exposure to ROFA than did controls (no p value given), although the effect of V pre-exposure was not significantly different than saline from 30 to 60 min post exposure to ROFA. Lung injury/inflammation was greater in the lungs of animals pre-exposed to V (no p value given), suggesting down-regulating effects on metal clearance by V. To evaluate expression of DMT-1, BEAS-2B cells were incubated with either culture medium, 100 µM Fe or 10 µM V, and were then evaluated using RT-PCR and Western blot analysis. *In vitro* and *in vivo* results were similar. This study suggested that lung metal clearance is negatively affected by exposure to V, which is commonly found in ROFA particles, potentially because of down-regulation of Fe sequestration by DMT-1. The authors suggested that decreased lung clearance of Fe may lead to production of ROS and may enhance the growth of pathogens in lung tissue.

#### Critical Comments on In Vivo Studies with Individual Metals

The studies we reviewed in this section focus on Fe, Ni and V and are a logical extension of the studies conducted with ROFA. In general, the studies were appropriately designed and executed. Although the studies confirm that these three metals induce inflammatory and cardiac effects at high doses, we have the same concerns regarding relevance to actual human exposures as with the ROFA studies. Specifically, the exposure levels were much higher than ambient exposure levels, and humans are exposed to mixtures rather than to individual components of the mixtures.

#### Summary Comments on In Vivo Studies

With few exceptions (noted in the individual reviews), the laboratory animal studies summarized in this paper were generally well-designed, followed similar protocols and used appropriate statistical methods (including post-hoc corrections for multiple comparisons), and measured responses relevant to respiratory tract inflammation. The majority of the *in vivo* studies used a limited number of well-characterized particulate sources, archived PM from the Utah Valley during the years referenced in the studies by Pope, and a number of study authors used ROFA from specific power plants. In summary, the results of the *in vivo* studies that we reviewed were supportive of the hypothesis that PM metals play a causal role in the respiratory and cardiovascular morbidity and mortality reported in the epidemiologic literature.



The majority of the animal studies that we reviewed used instillation of PM extracts or metal solutions directly into the trachea as the method of dosing. The delivery of a bolus of particulate to a small area of respiratory tract cells can provoke a response that is not analogous to an inhaled dose that is naturally distributed across the surface area of the human respiratory tract. Although intratracheal instillation of PM extracts or metal solutions increases the confidence that the response(s) of the respiratory tract cells being measured are caused by the substance administered, this route of administration is not analogous to breathing PM in ambient air. Such intratracheal instillation bypasses interactions with the anatomical landscape from the nose to the lungs. Furthermore, particulates in ambient air do not enter airways as an aqueous solution deposited directly on airway epithelial cells. Thus, it is not surprising that instillation of very high doses of particulate or metal solutions cause acute inflammatory response and death in some of the studies. The majority of researchers were diligent in using controls. However, when boluses of concentrated “particle masses” were surgically emplaced, they may have contributed to inflammatory responses.

In studies we reviewed, animals were exposed to various doses of Cu, Fe, Mn, Ni, V and Zn. To estimate a daily dose to humans, we assumed that a 70 kg person would inhale 10 cubic meters of air per day containing the average concentration of each metal represented by the STN data (Table 1). Our estimated human doses were: Cu  $\sim 0.00077$   $\mu\text{g}/\text{kg}\text{-day}$ ; Mn  $\sim 0.00043$   $\mu\text{g}/\text{kg}\text{-day}$ ; Fe  $\sim 0.0134$   $\mu\text{g}/\text{kg}\text{-day}$ ; Ni  $\sim 0.00019$   $\mu\text{g}/\text{kg}\text{-day}$ ; V  $\sim 0.00016$   $\mu\text{g}/\text{kg}\text{-day}$ ; and Zn  $\sim 0.002$   $\mu\text{g}/\text{kg}\text{-day}$ .

The doses used in the majority of in vivo studies are much higher than what people are exposed to in ambient air. By putting all dosages on a common footing (e.g., metal mass per body weight), it is possible to see the extent of the dosage variation across studies and across the target metals. For example, in human exposure studies using ambient or concentrated (CAPs) exposures (Table 5), the median range of dosages is reasonable, from 1 to 10 times the expected human 24-h dose at the STN annual mean values. The ambient concentrations of PM metals reported in industrial regions of Europe were 20–300 times higher than the expected doses in the U.S. based on STN annual mean values.

The ratios of administered doses to expected ambient doses were much higher in the toxicology studies that were performed. The median dosage for the studies in Table 6, for example, exceeded 1,000 times the expected human 24-h dosage for the three metals Cu, Ni, and Zn, and 35 times the expected human dose for Fe. Maximum exposure ratios exceeded one million for Ni and V, but were less than 1,000 for As and Mn. Minimum exposure ratios were not lower than 100 for any metal. Therefore some studies exceeded others in dosage levels by as much as 30,000–90,000 times (Fe, Ni, and V). Moreover, most metals identified as being more toxic were often chosen *a priori* as targets of these investigations (e.g., in the many ROFA studies). In some studies, the concentrations of Ni and V were often two orders of magnitude higher, on an equal body weight basis, than the other metals tested.

The ROFA studies (Table 8) included five target metals, and a wide range of doses. For example, the median dose levels of Ni and V used in the studies were 170,000 and 770,000 times expected human 24-h doses. The doses of Fe and Mn

used in the studies were approximately 100 times lower than the doses of Ni and V. The maximum dosage ratios for Ni and V exceeded one million, one to two orders of magnitude greater than the maximum ratios for Fe, Mn, and Zn. Minimum dosage ratios ranged from 12 (Fe) to 1,600 (V). Therefore some studies used dosages up to 10,000 times as great as others.

The majority of the toxicology studies we reviewed used relatively higher doses of Ni and V than other metals such as As, Cu, Fe, and Mn. It is possible that the larger number of positive associations for Ni and V may partially result from the relatively higher dosages applied. It is also the case that there is considerable variation across studies in the magnitude of the applied dose. This factor alone may account for some of the differences in identifying significant associations.

The target metals of interest to this review account for a minor portion (<1%) of the mass of the ambient PM in the air that most members of the U.S. population breathe. Although transition metals comprise a much larger portion of the mass of ROFA, people in the general population do not breathe ROFA except to the extent that oil combustion sources contribute to local and regional air quality. Relative to the range of metal doses that people experience in ambient air, the dose levels of metals used in laboratory animal experiments range from hundreds to more than a million times higher than ambient levels. It should not be assumed that biological systems, whether animal or human, handle extremely large doses of metals (or other chemicals) in the same way as small doses are handled. Responses observed at extremely high levels of exposure may not be observed at lower, more relevant levels of exposure when normal body defense mechanisms are functional. If application of such high exposure levels are required to produce significant increases in inflammatory indicator parameters (as compared to unexposed controls), then the ability of metals to produce such results at ambient levels is in doubt.

Although there are exceptions, the majority of laboratory studies suggest that the factors present in water-soluble extracts of PM are more biologically active than those in the insoluble fraction; moreover, in general, greater toxicity is associated with fine PM<sub>2.5</sub> rather than coarse PM<sub>10</sub> particles, when applied at high doses to the same anatomical location in experimental animals. Exceptions to this trend are noted in the individual study discussions. Generally, for studies in which exposures were to ambient PM, CAPs or PM extracts, multivariate analysis methods were used to identify individual metals that were statistically associated with the responses being measured. However, statistical significance identified in multivariate analysis does not always portend biological significance. Furthermore, the individual metals most frequently associated with inflammatory responses in human and animal studies are also those that are present in the highest concentrations in the PM sources used in the studies (Fe, Ni, V and Zn).

Study results with individual metals (particularly Fe, Ni, V and Zn) provide convincing evidence that metals, either singly or in simple combinations, induce inflammatory responses when administered at high doses. The activity of major metal constituents usually differs from the activity of the complete mixture. In biological systems, transition metals interact in ways that are not necessarily simple or additive. Among target metals of interest that were frequently identified as being significantly

associated with health in the studies we reviewed, only Ni and V do not have a known role in normal physiological processes. Thus, it is not surprising that high level exposures to these two metals can elicit significant toxic responses.

### 3.3.3 In Vitro Studies

Evidence from the *in vivo* studies previously described indicates that transition metal constituents may have a role, either alone or in mixtures, in producing the responses observed in animals exposed to PM from various sources. Several investigators have studied the mechanisms by which metals may produce inflammation, ROS, and/or altered gene expression, by conducting *in vitro* studies with human or animal cell cultures and/or with cell-free systems. The studies that we summarize in this section have generally shared a common experimental design. That design usually involved exposing cells in culture to ambient particulate extracts and/or to solutions of the target individual transition metals and then measuring the production of inflammatory cytokines or upstream markers of genes active in the inflammatory process and/or cell death at time intervals after exposure. As with many *in vivo* studies, chelating agents were often added to *in-vitro* systems to confirm that observed effects were fully or partially attributable to transition metal exposures, especially iron.

The *in vitro* studies that we reviewed fell into two major groupings according to the responses that were examined. In one group, indicators of cell death (release of LDH), metabolic activity (e.g., glutathione, mitochondrial succinate dehydrogenase) and indicators of inflammation were examined: Alley (2009), Aust et al. (2002), Carter et al. (1997), Duvall et al. (2008), Dye et al. (1999), Ghio et al. (1999a, b), Jalava et al. (2009), Smith et al. (2000), Okeson et al. (2004), Riley et al. (2003), and Zhou and Kobzik (2007). In the second group, the expression of specific genes and upstream signaling pathways involved in inflammation were examined: Graff et al. (2004), Gutierrez-Castillo et al. (2006), Jaspers et al. (2000), Kennedy et al. (1998), Klein-Patel et al. (2006), Nadadur et al. (2009), Prophete et al. (2006), Salnikow et al. (2004), Wu et al. (2003), Wang et al. (2003), and Kim et al. (2006). The major findings of these studies are summarized in Table 10.

We have concluded from the analysis of *in vitro* studies we reviewed that metals associated with particulate matter, especially Ni, V and Zn (in ROFA) can significantly affect the viability and metabolic activity of airway cells in culture, possibly by producing ROS and altering expression of genes involved in inflammation and macrophage anti-microbial activity. Vanadium appears to be the most toxic of the transition metals associated with ROFA and may influence the expression of genes in the signaling pathway that ultimately produces the inflammatory cytokines. There is evidence both for and against the role of Fe as either a participant in inducing the release of inflammatory markers or as a moderating factor in the hypoxic stress produced by other metals (e.g., Ni). These putative cell and molecular-level mechanisms of action are consistent with the findings of the *in vivo* studies demonstrating that exposures to high levels of metals increase markers of inflammatory response in respiratory tract tissues.

**Table 10** Summary of *in vitro* studies with metals from sources of ambient particulate matter

Cell type	Genes/pathways	Metals
<i>Altered gene expression</i>		
Graff et al. (2004)		
Neonatal rat ventricular myocytes	Inflammation, electrical impulse conduction	<ul style="list-style-type: none"> <li>• Vanadium sulfate</li> <li>• Zinc sulfate</li> </ul>
Nadadur et al. (2009)		
HUVEC human umbilical vein endothelial cells	Endothelial cell permeability, membrane integrity, pathway signaling	<ul style="list-style-type: none"> <li>• ROFA</li> <li>• Vanadium sulfate</li> </ul>
Gutierrez-Castillo et al. (2006)		
A549 human lung epithelial cells	Non-specific DNA damage and repair (comet assay)	• Cu, Ni and V from PM <sub>2.5</sub> and PM <sub>10</sub> Mexico City (2002–2003)
Kim et al. (2006)		
BEAS-2B cells	IL-8, and upstream signaling pathway genes MAPK, ERK, JNK, AP-1	• Zn sulfate
Klein-Patel et al. (2006)		
A549 human lung epithelial cells; BTE bovine tracheal epithelial cells	B-defensin-2 gene	<ul style="list-style-type: none"> <li>• ROFA Florida Power Plant</li> <li>• Fe and Ni sulfate</li> <li>• Si and Ti dioxide</li> <li>• V pentoxide and sulfate</li> <li>• Psuedomonas aeruginos LPS</li> </ul>
Salnikow et al. (2004)		
IHEAo <sup>-</sup> human lung cells	NDRG-1/Cap43 cellular hypoxia protein; IL-8	<ul style="list-style-type: none"> <li>• Ferric sulfate</li> <li>• Ferrous sulfate</li> <li>• Ni sulfate</li> </ul>
Prophete et al. (2006)		
NR8383 rat alveolar macrophages	NO; iron response protein IRP; extracellular signal-regulated kinases ERK1 and 2; iNOS	<ul style="list-style-type: none"> <li>• Aluminum chloride hexahydrate</li> <li>• Ferric chloride hexahydrate</li> <li>• Manganese chloride tetrahydrate</li> <li>• Sodium vanadate</li> </ul>
Kennedy et al. (1998)		
BEAS-2B cells	IL-8, NK-κB	<ul style="list-style-type: none"> <li>• TSP Provo, Utah (Winter 1982)</li> <li>• Copper sulfate</li> <li>• Iron sulfate</li> <li>• Lead sulfate</li> <li>• Zinc sulfate</li> </ul>
Jaspers et al. (2000)		
BEAS-2B cells; NHBE cells	NK-κB, TNF-α, p38 MAPK	• Vanadyl sulfate
Wang et al. (2003)		
Rat lung myofibroblasts	STAT-1 (signal transducers and activators of transcription) for IFN-γ and TNF-α	• Vanadium pentoxide

(continued)

**Table 10** (continued)

Cell type	Genes/pathways	Metals
Wu et al. (2003)		
BEAS-2B cells; NHBE cells	PTEN tumor suppressor protein; P13K/Akt pathway	• Zn sulfate
<i>Inflammatory markers</i>		
Alley et al. (2009)		
WTHBF-6 human bronchial fibroblasts	Cytotoxicity	• As, Cu, Mn, Ni and V <sup>a</sup> • PM <sub>10</sub> State of Maine
Duvall et al. (2008)		
Primary human airway epithelial cells	IL-8, COX-2, HO-1	• Cu, Pb and V Fine (<0.1 μm); fine PM <sub>2.5</sub> and coarse PM <sub>10</sub> from six US cities
Jalava et al. (2009)		
Mouse macrophage RAW 246.7	Cytotoxicity, IL-6, NO, TNF-α, MIP-2	• Cr, Cu, Fe, Ni and V PM samples from six European cities
Smith et al. (2000)		
A549 human lung epithelial cells	IL-8, ferritin	• Fe CFA generated by combusting coal from Utah, Illinois and North Dakota
Aust et al. (2002)		
A549 human lung epithelial cells	IL-8, PGE2, intracellular ferritin	• Cu, Fe and Zn CFA generated by combusting coal from Utah, Illinois and North Dakota
Carter et al. (1997)		
NHBE normal human bronchial epithelial cells	IL-6, IL-8, TNF-α	• Fe, Ni and V ROFA Florida power plant
Dye et al. (1999)		
RTE rat tracheal epithelial cells	Cytotoxicity, glutathione, IL-6, MIP-2	• Fe, Ni and V ROFA Florida power plant
Ghio et al. (1999a, b)		
BEAS-2B respiratory epithelial cells	Lactoferrin receptors	• Fe, Ni and V ROFA Florida power plant
Riley et al. (2003); Okeson et al. (2004)		
RL-6TN rat Type II alveolar cells	Cytotoxicity, mitochondrial activity (succinate dehydrogenase activity)	• Cu, Fe, Ni, V and Zn Soluble metal chlorides, individually and in combinations
Zhou and Kobzik (2007)		
Primary mouse alveolar macrophage; and murine macrophage cell line J744	Macrophage interaction with <i>S. pneumoniae</i>	• FE CAPS (Boston/Harvard)

<sup>a</sup>NIST—National Institute of Standards

A number of the *in vitro* studies addressed in this review were conducted as logical extensions of the *in vivo* studies. Consequently, many of the *in vitro* studies employed similar protocols, the same cell culture lines, and the same sources of PM and individual metal solutions. The *in vitro* studies offer the advantages of greater

numbers of replicates, lower cost and shorter timelines, and minimize the need to sacrifice animals. In general, the *in vitro* studies support the findings of the *in vivo* investigations in that they provide evidence that high exposures to PM metal extracts and the dominant transition metals can produce ROS and may also alter gene expression involved in cell-signaling pathways and metal-homeostasis. However, as noted previously, the exposure levels used in the majority of the *in vivo* studies are extremely high and of dubious relevance to actual human exposures. It is also very difficult to extrapolate exposures in cell cultures to either laboratory animal studies or human exposures to ambient PM. Therefore, although the reviewed studies inform the possibility of a hazard, they are of limited usefulness in evaluating the risk that metals in PM pose.

## 4 Summary

In this review, we critically evaluated the epidemiological and toxicological evidence for the role of specific transition metals (As, Cr, Cu, Fe, Mn, Ni, Se, Ti, V and Zn) in causing or contributing to the respiratory and cardiovascular health effects associated with ambient PM. Although the epidemiologic studies are suggestive, and both the *in vivo* and *in vitro* laboratory studies document the toxicity of specific metals (Fe, Ni, V and Zn), the overall weight of evidence does not convincingly implicate metals as major contributors to health effects. None of the epidemiology studies that we reviewed conclusively implicated specific transition metals as having caused the respiratory and cardiovascular effects associated with ambient levels of PM. However, the studies reviewed tended to be internally consistent in identifying some metals (Fe, Ni, V and Zn) more frequently than others (As, Cu, Mn and Se) as having positive associations with health effects. The major problem with which the epidemiological studies were faced was classifying and quantifying exposure. Community and population exposures to metals or other components of ambient PM were inferred from centrally-located samplers that may not accurately represent individual level exposures. Only a few authors reported findings that did not support the stated premise of the study; indeed, statistically significant associations are not necessarily biologically significant. It is likely that “negative studies” are under-represented in the published literature, making it a challenge to achieve a balanced evaluation of the role of metals in causing health effects associated with ambient PM.

Both the *in vivo* and *in vitro* study results demonstrated that individual metals (Cu, Fe, Ni, V and Zn) and extracts of metals from ambient PM sources can produce acute inflammatory responses. However, the doses administered to laboratory animals were many orders of magnitude greater than what humans experience from breathing ambient air. The studies that used intratracheal instillation have the advantage of delivering a known dose to a specific anatomical location, but are not analogous to an inhaled dose that is distributed over the surface area of the respiratory tract. Studies, in which laboratory animals or human volunteers inhaled CAPs best represent exposures to the general human population.

The *in vivo* and *in vitro* studies reviewed provide indications that the probable mechanisms involved in the respiratory and cardiac effects from high metal exposures include: an inflammatory response mediated by formation of ROS, up-regulation of genes coding for inflammatory cytokines, altered expression of genes involved in cell signaling pathways and maintenance of metals homeostasis.

The fact that doses of metals many orders of magnitude greater than those existing in ambient air were required to produce measurable adverse effects in animals makes it doubtful that metals play any major role in respiratory and cardiovascular effects produced from human exposure to ambient PM. We suggest that future research priorities should focus on testing at more environmentally relevant exposure levels and that any new toxicological studies be written to include dosages in units that can be easily compared to human exposure levels.

**Acknowledgment** The authors would like to thank Dr. Glynis Lough (Battelle), Dr. Debra Kaden (ENVIRON), Dr. Adriana Oller (NiPERA), and members of the Mickey Leland National Urban Air Toxics Research Center (NUATRC) Scientific Advisory Panel for their comprehensive review of this manuscript.

**Declaration of Interest** The authors' affiliations are shown on the cover page. The authors have sole responsibility for the writing and content of the paper. This literature review was supported by a contract from the Mickey Leland National Urban Air Toxics Research Center (NUATRC), and partial funding for this project was provided by the Nickel Producers Environmental Research Association (NiPERA). The views expressed and conclusions drawn are those of the authors.

## References

- Adamson IY, Prieditis H, Hedgecock C, Vincent R (2000) Zinc is the toxic factor in the lung response to an atmospheric particulate sample. *Toxicol Appl Pharmacol* 166(2):111–119
- Adgate JL, Mongin SJ, Pratt GC, Zhang J, Field MP, Ramachandran G (2007) Relationships between personal, indoor, and outdoor exposures to trace elements in PM(2.5). *Sci Total Environ* 386(1–3):21–32
- Alley D, Langley-Turnbaugh S, Gordon N, Wise J, Van EG, Jalbert A (2009) The effect of PM10 on human lung fibroblasts. *Toxicol Ind Health* 25(2):111–120
- Antonini JM, Taylor MD, Leonard SS, Lawryk NJ, Shi X, Clarke RW, Roberts JR (2004) Metal composition and solubility determine lung toxicity induced by residual oil fly ash collected from different sites within a power plant. *Mol Cell Biochem* 255(1–2):257–265
- Aust AE, Ball JC, Hu AA, Lighty JS, Smith KR, Straccia AM, Veranth JM, Young WC (2002) Particle characteristics responsible for effects on human lung epithelial cells. *Res Rep Health Eff Inst* 110:1–65
- Batalha JR, Saldiva PH, Clarke RW, Coull BA, Stearns RC, Lawrence J (2002) Concentrated ambient air particles induce vasoconstriction of small pulmonary arteries in rats. *Environ Health Perspect* 110(12):1191–1197
- Bell ML, Ebisu K, Peng RD, Samet JM, Dominici F (2009) Hospital admissions and chemical composition of fine particle air pollution. *Am J Respir Crit Care Med* 179(12):1115–1120
- Binkova B, Bobak M, Chatterjee A, Chauhan A, Dejmek J, Dockery DW, Kuna-Dibbert B (2004) The effects of air pollution on children's health and development: a review of the evidence. World Health Organization, Geneva

- Burnett RT, Brook J, Dann T, Delocla C, Philips O, Cakmak S, Vincent R, Goldberg MS, Drewski D (2000) Association between particulate- and gas-phase components of urban air pollution and daily mortality in eight Canadian cities. *Inhal Toxicol* 12(Suppl 4):15–39
- Campen MJ, Nolan JP, Schladweiler MC, Kodavanti UP, Evansky PA, Costa DL, Watkinson WP (2001) Cardiovascular and thermoregulatory effects of inhaled PM-associated transition metals: a potential interaction between nickel and vanadium sulfate. *Toxicol Sci* 64(2):243–252
- Campen MJ, Nolan JP, Schladweiler MC, Kodavanti UP, Costa DL, Watkinson WP (2002) Cardiac and thermoregulatory effects of instilled particulate matter-associated transition metals in healthy and cardiopulmonary-compromised rats. *J Toxicol Environ Health A* 65(20):1615–1631
- Carter JD, Ghio AJ, Samet JM, Devlin RB (1997) Cytokine production by human airway epithelial cells after exposure to an air pollution particle is metal-dependent. *Toxicol Appl Pharmacol* 146(2):180–188
- Carty CL, Gehring U, Cyrus J, Bischof W, Heinrich J (2003) Seasonal variability of endotoxin in ambient fine particulate matter. *J Environ Monit* 5(6):953–958
- Chen LC, Lippmann M (2009) Effects of metals within ambient air particulate matter (PM) on human health. *Inhal Toxicol* 21(1):1–31
- Clarke RW, Coull B, Reinisch U, Catalano P, Killingsworth CR, Koutrakis P, Kavouras I, Krishna Murthy GG, Lawrence J, Lovett E, Wolfson JM, Verrier RL (2000) Inhaled concentrated ambient particles are associated with hematologic and bronchoalveolar lavage changes in canines. *Environ Health Perspect* 108(12):1179–1187
- Clayton CA, Perritt RL, Pellizari ED, Thomas KW, Whitmore RW, Wallace LA (1993) Particle Total Exposure Assessment Methodology (PTEAM) Study: distributions of aerosol and elemental concentrations in personal, indoor, and outdoor air samples in a southern California community. *J Expo Ana Environ Epidemiol* 3(2):227–250
- Connell DP, Winter SE, Conrad VB, Kim M, Crist KC (2006) The Steubenville Comprehensive Air Monitoring Program (SCAMP): concentrations and solubilities of PM(2.5) trace elements and their implications for source apportionment and health research. *J Air Waste Manag Assoc* 56(12):1750–1766
- Costa DL, Dreher KL (1997) Bioavailable transition metals in particulate matter mediate cardiopulmonary injury in healthy and compromised animal models. *Environ Health Perspect* 105(Suppl 5):1053–1060
- Dockery DW, Pope CA (1994) Acute respiratory effects of particulate air pollution. *Annu Rev Public Health* 15:107–132
- Dominici F, Peng RD, Ebisu K, Zeger SL, Samet JM, Bell ML (2007) Does the effect of PM10 on mortality depend on PM nickel and vanadium content? A reanalysis of the NMMAPS data. *Environ Health Perspect* 115(12):1701–1703
- Dreher KL, Jaskot RH, Lehmann JR, Richards JH, McGee JK, Ghio AJ, Costa DL (1997) Soluble transition metals mediate residual oil fly ash induced acute lung injury. *J Toxicol Environ Health* 50(3):285–305
- Duvall RM, Norris GA, Dailey LA, Burke JM, McGee JK, Gilmour MI, Gordon T, Devlin RB (2008) Source apportionment of particulate matter in the U.S. and associations with lung inflammatory markers. *Inhal Toxicol* 20(7):671–683
- Dye JA, Adler KB, Richards JH, Dreher KL (1999) Role of soluble metals in oil fly ash-induced airway epithelial injury and cytokine gene expression. *Am J Physiol* 277(3 Pt 1):L498–L510
- Dye JA, Lehmann JR, McGee JK, Winsett DW, Ledbetter AD, Everitt JI, Ghio AJ, Costa DL (2001) Acute pulmonary toxicity of particulate matter filter extracts in rats: coherence with epidemiologic studies in Utah Valley residents. *Environ Health Perspect* 109(Suppl 3):395–403
- Franklin M, Koutrakis P, Schwartz P (2008) The role of particle composition on the association between PM2.5 and mortality. *Epidemiology* 19(5):680–689
- Gavett SH, Haykal-Coates N, Copeland LB, Heinrich J, Gilmour MI (2003) Metal composition of ambient PM2.5 influences severity of allergic airways disease in mice. *Environ Health Perspect* 111(12):1471–1477



- Gerlofs-Nijland ME, Rummelhard M, Boere AJ, Leseman DL, Duffin R, Schins RP, Borm PJA, Sillanpää M, Salonen RO, Cassee FR (2009) Particle induced toxicity in relation to transition metal and polycyclic aromatic hydrocarbon contents. *Environ Sci Technol* 43(13):4729–4736
- Ghio AJ, Richards JH, Dittrich KL, Samet JM (1998) Metal storage and transport proteins increase after exposure of the rat lung to an air pollution particle. *Toxicol Pathol* 26(3):388–394
- Ghio AJ, Carter JD, Dailey LA, Devlin RB, Samet JM (1999a) Respiratory epithelial cells demonstrate lactoferrin receptors that increase after metal exposure. *Am J Physiol* 276(6 Pt 1): L933–L940
- Ghio AJ, Stonehuerner J, Dailey LA, Carter JD (1999b) Metals associated with both the water-soluble and insoluble fractions of an ambient air pollution particle catalyze an oxidative stress. *Inhal Toxicol* 11(1):37–49
- Ghio AJ, Devlin RB (2001) Inflammatory lung injury after bronchial instillation of air pollution particles. *Am J Respir Crit Care Med* 164(4):704–708
- Ghio AJ (2004) Biological effects of Utah Valley ambient air particles in humans: a review. *J Aerosol Med* 17(2):157–164
- Ghio AJ, Piantadosi CA, Wang X, Dailey LA, Stonehuerner JD, Madden MC, Yang F, Dolan KG, Garrick MD, Garrick LM (2005) Divalent metal transporter-1 decreases metal-related injury in the lung. *Am J Physiol Lung Cell Mol Physiol* 289(3):L460–L467
- Gilmour PS, Nyska A, Schladweiler MC, McGee JK, Wallenborn JG, Richards JH (2006) Cardiovascular and blood coagulative effects of pulmonary zinc exposure. *Toxicol Appl Pharmacol* 211(1):41–52
- Götschi T, Hazenkamp-von Arx ME, Heinrich J, Bono R, Burney P, Forsberg B (2005) Elemental composition and reflectance of ambient fine particles at 21 European locations. *Atmos Environ* 39(32):5947–5958
- Graff DW, Cascio WE, Brackhan JA, Devlin RB (2004) Metal particulate matter components affect gene expression and beat frequency of neonatal rat ventricular myocytes. *Environ Health Perspect* 112(7):792–798
- Graham TJ, Schlesinger RB (2007) Health effects of airborne particulate matter: do we know enough to consider regulating specific particle types or sources? *Inhal Toxicol* 19:457–481
- Gutierrez-Castillo ME, Roubicek DA, Cebrian-Garcia ME, De Vizcaya-Ruiz A, Sordo-Cedeno M, Ostrosky-Wegman P (2006) Effect of chemical composition on the induction of DNA damage by urban airborne particulate matter. *Environ Mol Mutagen* 47(3):199–211
- Gutknecht W, Flanagan J, McWilliams A, Jayanty RK, Kellogg R, Rice J, Duda P, Sarver HS, Le M, Kim S, Kim G, Jo Y (2010) Harmonization of uncertainties of X-ray fluorescence data for PM<sub>2.5</sub> air filter analysis. *J Air Waste Manag Assoc* 60(2):184–194
- Hamada K, Goldsmith CA, Suzuki Y, Goldman A, Kobzik L (2002) Airway hyperresponsiveness caused by aerosol exposure to residual oil fly ash leachate in mice. *J Toxicol Environ Health A* 65(18):1351–1365
- Happo MS, Hirvonen MR, Halinen AI, Jalava PI, Pennanen AS, Sillanpää M, Hillarino R, Salonen RO (2008) Chemical compositions responsible for inflammation and tissue damage in the mouse lung by coarse and fine particulate samples from contrasting air pollution in Europe. *Inhal Toxicol* 20(14):1215–1231
- Hirshon JM, Shardell M, Alles S, Powell JL, Squibb K, Ondov J, Blaisdell DJ (2008) Elevated ambient air zinc increases pediatric asthma morbidity. *Environ Health Perspect* 116(6): 826–831
- Hong YC, Hwang SS, Kim JH, Lee KH, Lee HJ, Lee KH, Yu SD, Kim DS (2007) Metals in particulate pollutants affect peak expiratory flow of schoolchildren. *Environ Health Perspect* 115(3):430–434
- Hong YC, Pan XC, Kim SY, Park K, Park EJ, Jin X, Yi SM, Kim YH, Park CH, Song S, Kim H (2010) Asian Dust Storm and pulmonary function of school children in Seoul. *Sci Total Environ* 408(4):754–759
- Huang YC, Ghio AJ, Stonehuerner J, McGee J, Carter JD, Grambow SC, Devlin RB (2003) The role of soluble components in ambient fine particles-induced changes in human lungs and blood. *Inhal Toxicol* 15(4):327–342

- Hyslop NP, White WH (2008) An empirical approach to estimating detection limits using collocated data. *Environ Sci Technol* 42(14):5235–5240
- Hyslop NP, White WH (2009) Estimating precision using duplicate measurements. *J Air Waste Manag Assoc* 59(9):1032–1039
- Jalava PI, Hirvonen MR, Sillanpaa M, Pennanen AS, Happonen MS, Hillamo R, Cassee FR, Gerlofs-Nijland M, Borm PJA, Schins RPF, Janssen NAH, Salonen RO (2009) Associations of urban air particulate composition with inflammatory and cytotoxic responses in RAW 246.7 cell line. *Inhal Toxicol* 21(12):994–1006
- Jaspers I, Samet JM, Erzurum S, Reed W (2000) Vanadium-induced kappaB-dependent transcription depends upon peroxide-induced activation of the p38 mitogen-activated protein kinase. *Am J Respir Cell Mol Biol* 23(1):95–102
- Kadiiska MB, Mason RP, Dreher KL, Costa DL, Ghio AJ (1997) In vivo evidence of free radical formation in the rat lung after exposure to an emission source air pollution particle. *Chem Res Toxicol* 10(10):1104–1108
- Kennedy T, Ghio AJ, Reed W, Samet J, Zagorski J, Quay J, Carter J, Dailey L, Hoidal JR, Devlin RB (1998) Copper-dependent inflammation and nuclear factor-kappaB activation by particulate air pollution. *Am J Respir Cell Mol Biol* 19(3):366–378
- Kim YM, Reed W, Wu W, Bromberg PA, Graves LM, Samet JM (2006) Zn<sup>2+</sup>-induced IL-8 expression involves AP-1, JNK, and ERK activities in human airway epithelial cells. *Am J Physiol Lung Cell Mol Physiol* 290(5):L1028–L1035
- Kinney PL, Chillrud SN, Sax S, Ross JM, Peterson DC, Johnson D (2005) Toxic exposure assessment: a Columbia-Harvard study, The New York City Report. NUATRC Research Report No. 3
- Kinney PL, Chillrud SN, Sax S, Ross JM, Macintosh D, Myatt TA (2008) Toxic exposure assessment: a Columbia-Harvard study, The Los Angeles Report. NUATRC Research Report No. 9
- Klein-Patel ME, Diamond G, Boniotto M, Saad S, Ryan LK (2006) Inhibition of beta-defensin gene expression in airway epithelial cells by low doses of residual oil fly ash is mediated by vanadium. *Toxicol Sci* 92(1):115–125
- Kleinman MT (2000) The health effects of air pollution on children. South Coast Air Quality Management District. Available from: [http://www.aqmd.gov/forstudents/health\\_effects\\_on\\_children.pdf](http://www.aqmd.gov/forstudents/health_effects_on_children.pdf)
- Kodavanti UP, Hauser R, Christiani DC, Meng ZH, McGee J, Ledbetter A, Richard J, Costa DL (1998) Pulmonary responses to oil fly ash particles in the rat differ by virtue of their specific soluble metals. *Toxicol Sci* 43(2):204–212
- Kodavanti UP, Schladweiler MC, Richards JR, Costa DL (2001) Acute lung injury from intratracheal exposure to fugitive residual oil fly ash and its constituent metals in normo- and spontaneously hypertensive rats. *Inhal Toxicol* 13(1):37–54
- Kodavanti UP, Schladweiler MC, Ledbetter AD, McGee JK, Walsh L, Gilmour PS, Highfill JS, Davies D, Pinkerton KE, Richard JH, Crissman K, Andrews D (2005) Consistent pulmonary and systemic responses from inhalation of fine concentrated ambient particles: roles of rat strains used and physicochemical properties. *Environ Health Perspect* 113(11):1561–1568
- Laden F, Neas LM, Dockery DW, Schwartz J (2000) Association of fine particulate matter from different sources with daily mortality in six U.S. cities. *Environ Health Perspect* 108(10):941–947
- Lagorio S, Forastiere F, Pistelli R, Iavarone I, Michelozzi P, Fano V, Marconi A, Ziemacki G, Ostro BD (2006) Air pollution and lung function among susceptible adult subjects: a panel study. *Environ Health* 5(1):11–12
- Lambert AL, Dong W, Selgrade MK, Gilmour MI (2000) Enhanced allergic sensitization by residual oil fly ash particles is mediated by soluble metal constituents. *Toxicol Appl Pharmacol* 165(1):84–93
- Lay JC, Bennett WD, Ghio AJ, Bromberg PA, Costa DL, Kim CS, Koren HS, Devlin RB (1999) Cellular and biochemical response of the human lung after intrapulmonary instillation of ferric oxide particles. *Am J Respir Cell Mol Biol* 20(4):631–642
- Lewis AB, Taylor MD, Roberts JR, Leonard SS, Shi X, Antonini JM (2003) Role of metal-induced reactive oxygen species generation in lung responses caused by residual oil fly ash. *J Biosci* 28(1):13–18

- Lipfert FW, Baty JD, Miller JP, Wyzga RE (2006) PM<sub>2.5</sub> constituents and related air quality variables as predictors of survival in a cohort of U.S. military veterans. *Inhal Toxicol* 18(9): 645–657
- Lippmann M, Chen LC, Gordon T, Ito K, Thurston GD (2013) National Particle Component Toxicity (NPACT) Initiative: Integrated Epidemiologic and Toxicologic Studies of the Health Effects of Particulate Matter Components. Research Report 177. Health Effects Institute, Boston, MA
- Lippmann M, Ito K, Hwang JS, Maciejczyk P, Chen LC (2006) Cardiovascular effects of nickel in ambient air. *Environ Health Perspect* 114(11):1662–1669
- Miller MD, Marty MA, Arcus A, Brown J, Morry D, Sandy M (2002) Differences between children and adults: implications for risk assessment at California EPA. *Int J Toxicol* 21(5): 403–418
- Molinelli AR, Madden MC, McGee JK, Stonehuerner JG, Ghio AJ (2002) Effect of metal removal on the toxicity of airborne particulate matter from the Utah Valley. *Inhal Toxicol* 14(10):1069–1086
- Muggenburg BA, Benson JM, Barr EB, Kubatko J, Tilley LP (2003) Short-term inhalation of particulate transition metals has little effect on the electrocardiograms of dogs having preexisting cardiac abnormalities. *Inhal Toxicol* 15(4):357–371
- Nadadur SS, Kodavanti UP (2002) Altered gene expression profiles of rat lung in response to an emission particulate and its metal constituents. *J Toxicol Environ Health A* 65(18):1333–1350
- Nadadur SS, Haykal-Coates N, Mudipalli A, Costa DL (2009) Endothelial effects of emission source particles: acute toxic response gene expression profiles. *Toxicol In Vitro* 23(1):67–77
- Okeson CD, Riley MR, Riley-Saxton E (2004) In vitro alveolar cytotoxicity of soluble components of airborne particulate matter: effects of serum on toxicity of transition metals. *Toxicol In Vitro* 18(5):673–680
- Ostro B, Feng WY, Broadwin R, Green S, Lipsett M (2007) The effects of components of fine particulate air pollution on mortality in California: results from CALFINE. *Environ Health Perspect* 115(1):13–19
- Ostro BD, Feng WY, Broadwin R, Malig BJ, Green RS, Lipsett MJ (2008) The impact of components of fine particulate matter on cardiovascular mortality in susceptible subpopulations. *Occup Environ Med* 65(11):750–756
- Ostro B, Roth L, Malig B, Marty M (2009) The effects of fine particle components on respiratory hospital admissions in children. *Environ Health Perspect* 117(3):475–480
- Ozkaynak H, Xue J, Spengler J, Wallace L, Pellizzari E, Jenkins P (1996) Personal exposure to airborne particles and metals: results from the Particle TEAM study in Riverside, California. *J Expo Anal Environ Epidemiol* 6(1):57–78
- Patel MM, Hoepner L, Garfinkel R, Chillrud S, Reyes A, Quinn JW, Perera F, Miller RL (2009) Ambient metals, elemental carbon, and wheeze and cough in New York City children through 24 months of age. *Am J Respir Crit Care Med* 180(11):1107–1113
- Pellizzari ED, Clayton CA, Rodes CE, Mason RP, Piper LL, Fort B, Pfeifer G, Lynam D (1999) Particulate matter and manganese exposures in Toronto, Canada. *Atm Environ* 33(5):721–734
- Pope CA III (1989) Respiratory disease associated with community air pollution and a steel mill, Utah Valley. *Am J Public Health* 79(5):623–628
- Pope CA III (1991) Respiratory hospital admissions associated with PM pollution in Utah, Salt Lake and Cache Valleys. *Arch Environ Health* 46(2):90–97
- Pope CA III (1992) Daily mortality and PM<sub>10</sub> pollution in Utah Valley. *Arch Environ Health* 47(3):211–217
- Prieditis H, Adamson IY (2002) Comparative pulmonary toxicity of various soluble metals found in urban particulate dusts. *Exp Lung Res* 28(7):563–576
- Prophete C, Maciejczyk P, Salnikow K, Gould T, Larson T, Koenig J, Jaques P, Sioutas C, Lippmann M, Cohen M (2006) Effects of select PM-associated metals on alveolar macrophage phosphorylated ERK1 and -2 and iNOS expression during ongoing alteration in iron homeostasis. *J Toxicol Environ Health A* 69(10):935–951

- Reff A, Bhawe PV, Simon H, Pace TG, Pouliot GA, Mobley JD, Houyoux M (2009) Emissions inventory of PM<sub>2.5</sub> trace elements across the United States. *Environ Sci Technol* 43(15):5790–5796
- Riley MR, Boesewetter DE, Kim AM, Sirvent FP (2003) Effects of metals Cu, Fe, Ni, V, and Zn on rat lung epithelial cell. *Toxicology* 190(3):171–184
- Rohr AC, Wyzga RE (2012) Attributing health effects to individual particulate matter constituents. *Atmos Environ* 62:130–152
- Roberts JR, Taylor MD, Castranova V, Clarke RW, Antonini JM (2004) Soluble metals associated with residual oil fly ash increase morbidity and lung injury after bacterial infection in rats. *J Toxicol Environ Health A* 67(3):251–263
- Roemer W, Hoek G, Brunekreef B, Clench-Aas J, Forsberg B, Pekkanen J, Schutz A (2000) PM<sub>10</sub> elemental composition and acute respiratory health effects in European children (PEACE project). *Pollution Effects on Asthmatic Children in Europe*. *Eur Respir J* 15(3):553–559
- Saldiva PH, Clarke RW, Coull BA, Stearns RC, Lawrence J, Murthy GG (2002) Lung inflammation induced by concentrated ambient air particles is related to particle composition. *Am J Respir Crit Care Med* 165(12):1610–1617
- Salnikow K, Li X, Lippmann M (2004) Effect of nickel and iron co-exposure on human lung cells. *Toxicol Appl Pharmacol* 196(2):258–265
- Schaumann F, Borm PJ, Herbrich A, Knoch J, Pitz M, Schins RP, Luettig B, Hohlfeld JM, Heinrich J, Krug N (2004) Metal-rich ambient particles (particulate matter 2.5) cause airway inflammation in healthy subjects. *Am J Respir Crit Care Med* 170(8):898–903
- Schins RP, Polat D, Begerow J, Turfeld M, Becker A, Borm PJ (2004a) Platinum levels in nasal lavage fluid as a biomarker for traffic-related exposure and inflammation in children. *Sci Total Environ* 334–335:447–455
- Schins RP, Lightbody JH, Borm PJ, Shi T, Donaldson K, Stone V (2004b) Inflammatory effects of coarse and fine particulate matter in relation to chemical and biological constituents. *Toxicol Appl Pharmacol* 195(1):1–11
- Schlesinger RB (2007) The health impact of common inorganic components of fine particulate matter (PM<sub>2.5</sub>) in ambient air: a critical review 1. *Inhal Toxicol* 19(10):811–832
- Schwartz J, Morris R (1995) Air pollution and hospital admissions for cardiovascular disease in Detroit, MI. *Am J Epidemiol* 142(1):23–35
- Schwartz J (2004) Air pollution and children's health. *Pediatrics* 113(4 Suppl):1037–1043
- Slezakova K, Pereira MC, Alvim-Ferraz MC (2009) Influence of tobacco smoke on the elemental composition of indoor particles of different sizes. *Atmos Environ* 43(3):486–493
- Smith KR, Veranth JM, Hu AA, Lighty JS, Aust AE (2000) Interleukin-8 levels in human lung epithelial cells are increased in response to coal fly ash and vary with the bioavailability of iron as a function of particle size and source of coal. *Chem Res Toxicol* 13(2):118–125
- Sorensen M, Schins RP, Hertel O, Loft S (2005) Transition metals in personal samples of PM<sub>2.5</sub> and oxidative stress in human volunteers. *Cancer Epidemiol Biomarkers Prev* 14(5):1340–1343
- Suh HH, Zanobetti A, Schwartz J, Coull BA (2011) Chemical properties of air pollutants and cause-specific hospital admissions among the elderly in Atlanta, Georgia. *Environ Health Perspect* 119:1421–1428
- Thomas KW, Pellizari ED, Clayton CA, Whitaker DA, Shores RC, Spengler J (1993) Particle Total Exposure Assessment Methodology (PTEAM) 1990 study: method performance and data quality for personal, indoor, and outdoor monitoring. *J Expo Anal Environ Epidemiol* 3(2):203–226
- Turpin BJ, Weisel CP, Morandi M, Colome S, Stock T, Eisenreich S, Buckley B (2007) Relationship of indoor, outdoor, and personal air (RIOPA): part II, Analyses of concentrations of particulate matter species. NUAATRC Research report No. 10
- United States Environmental Protection Agency (2010) Technology transfer network ambient monitoring technology information center – PM<sub>2.5</sub> – Visibility (IMPROVE). Available from: <http://www.epa.gov/ttnamti1/visdata.html>
- United States Environmental Protection Agency (2010) Technology transfer network ambient monitoring technology information center – chemical speciation. Available from: <http://www.epa.gov/ttn/amtic/speciepg.html>

- Urch B, Brook JR, Wasserstein D, Brook RD, Rajagopalan S, Corey P, Silverman F (2004) Relative contributions of PM<sub>2.5</sub> chemical constituents to acute arterial vasoconstriction in humans. *Inhal Toxicol* 16(6–7):345–352
- Vedal S, Campen MJ, McDonald JD, Kaufman JD, Larson TV, Sampson PD, Sheppard CD, Szpiro AA (2013) National Particle Component Toxicity (NPACT) Initiative Report on Cardiovascular Effects. Research Report 178. Health Effects Institute, Boston, MA
- Wallace L, Wang F, Howard-Reed C, Persily A (2008) Contribution of gas and electric stoves to residential ultrafine particle concentrations between 2 and 64 nm: size distributions and emission and coagulation reemission and coagulation rates. *Environ Sci Technol* 42(23):8641–8647
- Wallace L, Williams R (2005) Use of personal-indoor-outdoor sulfur concentrations to estimate the infiltration factor and outdoor exposure factor for individual homes and persons. *Environ Sci Technol* 39(6):1707–1714
- Wallace LA (2000) Correlations of personal exposure to particles with outdoor air measurements: a review of recent studies. *Aerosol Sci Tech* 32(1):15–25
- Wallenborn JG, McGee JK, Schladweiler MC, Ledbetter AD, Kodavanti UP (2007) Systemic translocation of particulate matter-associated metals following a single intratracheal instillation in rats. *Toxicol Sci* 98(1):231–239
- Wallenborn JG, Evansky P, Shannahan JH, Vallanat B, Ledbetter AD, Schladweiler MC, Richards JH, Gottipolu RR, Nyska A, Kadavanti UP (2008) Subchronic inhalation of zinc sulfate induces cardiac changes in healthy rats. *Toxicol Appl Pharmacol* 232(1):69–77
- Wang YZ, Ingram JL, Walters DM, Rice AB, Santos JH, Van Houten B, Bonner JC (2003) Vanadium-induced STAT-1 activation in lung myofibroblasts requires H<sub>2</sub>O<sub>2</sub> and P38 MAP kinase. *Free Radic Biol Med* 35(8):845–855
- Wellenius GA, Coull BA, Godleski JJ, Koutrakis P, Okabe K, Savage ST, Lawrence JE, Krishna Murthy GG, Verrier RL (2003) Inhalation of concentrated ambient air particles exacerbates myocardial ischemia in conscious dogs. *Environ Health Perspect* 111(4):402–408
- Wu W, Wang X, Zhang W, Reed W, Samet JM, Whang YE, Ghio AJ (2003) Zinc-induced PTEN protein degradation through the proteasome pathway in human airway epithelial cells. *J Biol Chem* 278(30):28258–28263
- Zelikoff JT, Schermerhorn KR, Fang K, Cohen MD, Schlesinger RB (2002) A role for associated transition metals in the immunotoxicity of inhaled ambient particulate matter. *Environ Health Perspect* 110(Suppl 5):871–875
- Zhou YM, Zhong CY, Kennedy IM, Pinkerton KE (2003) Pulmonary responses of acute exposure to ultrafine iron particles in healthy adult rats. *Environ Toxicol* 18(4):227–235
- Zhou H, Kobzik L (2007) Effect of concentrated ambient particles on macrophage phagocytosis and killing of *Streptococcus pneumoniae*. *Am J Respir Cell Mol Biol* 36(4):460–465

# Index for Rect Vol. 234

- Abbreviations, chapter 1 (table), **234**: 3-4
- Abbreviations, in chapter 2 (table), **234**: 51
- Air (indoor & outdoor) concentrations, metals (table), **234**: 145
- Air concentrations in U.S., transition metals, **234**: 140
- Air concentrations, target elements & metals (table), **234**: 142-143
- Air concentrations, transition metals (table), **234**: 139
- Air exposure to metals, humans (table), **234**: 157-159
- Air transport, nanoparticles, **234**: 12
- Air-borne particulates, metal contamination, **234**: 136
- Algal toxicity, engineered nanoparticles, **234**: 23
- Alkyldibenzothiophene:alkylphenanthrene ratio, PAH source identification (diags.), **234**: 98, 99
- Analytical approach, PAH source characterization, **234**: 74
- Animal toxicity, engineered nanoparticles, **234**: 24
- Anthropogenic PAHs, formation, **234**: 51
- Applications (major), nanoparticles (table), **234**: 8
- Aquatic systems, PAH distribution, **234**: 73
- Atmospheric release, nanoparticles (table), **234**: 11
- Bacterial toxicity, engineered nanoparticles, **234**: 16
- Benz(a)anthracene:chrysene ratio, PAH source identification (diag.), **234**: 96
- Benz(a)anthracene:chrysene ratio, PAH source identification, **234**: 95
- Benzo[a]pyrene:ghi ratio, PAH source identification (diag.), **234**: 107
- Benzo[e]pyrene:benzo[a]pyrene ratio, PAH source identification (diag.), **234**: 102
- Biogenic form, PAHs, **234**: 72
- Biomass combustion, pyrogenic PAH source, **234**: 68
- Carcinogenic PAHs, motor vehicles, **234**: 66
- Cardiovascular disease, metal exposure, **234**: 150
- Cardiovascular effects, metals, **234**: 135 ff.
- Cardiovascular function effects, metal exposure, **234**: 156
- Cell-line toxic end-points, engineered nanoparticles (diag.), **234**: 32
- Cell-line toxicity, engineered nanoparticles, **234**: 31
- Chemical fingerprinting, PAH profiles, **234**: 78
- Children, metals & chronic respiratory disease, **234**: 149
- Chronic respiratory disease, children, **234**: 149
- Coal combustion patterns, PAHs, **234**: 68
- Concentrated ambient particulates, in vivo exposures, **234**: 171
- Diagenetic form, PAHs, **234**: 72
- Dimethylphenanthrene ratio, PAH source identification, **234**: 88
- DNA damage, engineered nanoparticle toxicity mechanism, **234**: 37
- Earthworms, engineered nanoparticle toxicity, **234**: 26

- Ecosystem transport, engineered nanoparticles (table), **234**: 12
- Effect level summary, in vivo studies with metals (table), **234**: 182-185
- Engineered nanoparticle toxicity mechanism, DNA damage, **234**: 37
- Engineered nanoparticle toxicity mechanism, protein interaction, **234**: 36
- Engineered nanoparticle toxicity, earthworms, **234**: 26
- Engineered nanoparticle toxicity, in vitro cell lines (table), **234**: 33
- Engineered nanoparticle toxicity, invertebrates, **234**: 24
- Engineered nanoparticle toxicity, mollusks & nematodes, **234**: 25
- Engineered nanoparticle toxicity, protozoa, **234**: 24
- Engineered nanoparticle toxicity, to different organisms (table), **234**: 17-20
- Engineered nanoparticle toxicity, to plants (table), **234**: 30
- Engineered nanoparticle toxicity, to plants, **234**: 29
- Engineered nanoparticles, algal toxicity, **234**: 23
- Engineered nanoparticles, antibacterial toxic effects, **234**: 21-23
- Engineered nanoparticles, applications, **234**: 2, 6
- Engineered nanoparticles, cell line toxicity, **234**: 31
- Engineered nanoparticles, cell-line toxic endpoints (diag.), **234**: 32
- Engineered nanoparticles, environmental fate, **234**: 12
- Engineered nanoparticles, environmental life cycle (diag.), **234**: 10
- Engineered nanoparticles, environmental release, **234**: 9
- Engineered nanoparticles, fate & transport in water, **234**: 14
- Engineered nanoparticles, fish toxicity, **234**: 27
- Engineered nanoparticles, mammalian toxicity, **234**: 28
- Engineered nanoparticles, possible toxic mechanism, **234**: 35
- Engineered nanoparticles, release, transport & toxicity, **234**: 1 ff.
- Engineered nanoparticles, soil transport & fate, **234**: 15
- Engineered nanoparticles, toxic endpoints (diag.), **234**: 21
- Engineered nanoparticles, toxicity, **234**: 16
- Engineered nanoparticles, transport facilitation (table), **234**: 12
- Environmental fate, engineered nanoparticles, **234**: 12
- Environmental life cycle, engineered nanoparticles (diag.), **234**: 10
- Environmental release, engineered nanoparticles, **234**: 9
- Environmental release, nanoparticle types (diag.), **234**: 6
- Epidemiology literature, on particulate matter effects, **234**: 138
- Epidemiology studies, critical comments, **234**: 152
- Epidemiology studies, metal effects, **234**: 146
- Epidemiology studies, metal health effects (table), **234**: 147-148
- Fate in air, nanoparticles, **234**: 12
- Fate in soil, engineered nanoparticles, **234**: 16
- Fate in water, engineered nanoparticles, **234**: 14
- Fingerprinting & method detection limit, petroleum products (diag.), **234**: 59
- Fish toxicity, engineered nanoparticles, **234**: 27
- Fluoranthene:pyrene ratio, formation temperature, **234**: 89
- Fluoranthene:pyrene ratio, in petroleum sources (diag.), **234**: 90
- Fluoranthenic ratio, petrogenic-pyrogenic discrimination, **234**: 91
- Fossil fuel combustion, PAH profiles (diags.), **234**: 64
- Fossil fuel pollution index, described, **234**: 113
- Fullerenes, described, **234**: 7
- Health effects of metals, in epidemiology studies (table), **234**: 147-148
- Human exposure studies, metal-contaminated particulates, **234**: 154
- Human exposure to metals, toxicology, **234**: 154
- Human exposure, metals in ambient air (table), **234**: 157-159
- Human exposure, to particulate matter, **234**: 138
- Human health implication, particulate matter exposure, **234**: 137
- Human mortality, metals & cardiovascular disease, **234**: 150
- Human volunteers, metal exposures, **234**: 160
- Humans, metal exposure study insights, **234**: 162
- In vitro cell lines, engineered nanoparticle toxicity, **234**: 33

- In vitro studies with metals, from ambient particulate matter (table), **234**: 194-195
- In vivo exposures, to metals in residual oil fly ash, **234**: 172
- In vivo metal exposures, in concentrated ambient particulates, **234**: 171
- In vivo studies summary, residual oil fly ash (table), **234**: 174-176
- In vivo studies with metals, effect levels summary (table), **234**: 182-185
- In vivo studies, metal effects, **234**: 164
- In vivo studies, metal-contaminated particulate matter, **234**: 167
- In vivo studies, particulate metal concentrations (table), **234**: 165-166
- Indeno[1,2,3-cd]pyrene:benzo[ghi]perylene ratio, pyrolytic source identification (diag.), **234**: 105
- Indoor air concentrations, metals, **234**: 144
- Inflammation indicators, metal exposure in particulates, **234**: 160
- Iron nanoparticles, applications, **234**: 7
- Low molecular weight ratios, PAHs, **234**: 81
- Mammalian toxicity, of engineered nanoparticles, **234**: 28
- Metal concentrations in particulates, in vivo studies (table), **234**: 165-166
- Metal concentrations, in indoor air, **234**: 144
- Metal concentrations, in U.S. air (tables), **234**: 139, 142-143
- Metal concentrations, indoor & outdoor air (table), **234**: 145
- Metal contamination, of air-borne particulates, **234**: 136
- Metal effects, epidemiology studies, **234**: 146
- Metal effects, in vivo studies, **234**: 164
- Metal exposure in air, humans (table), **234**: 157-159
- Metal exposure in particulates, inflammation indicators, **234**: 160
- Metal exposure study insights, humans, **234**: 162
- Metal exposure, cardiovascular disease, **234**: 150
- Metal exposure, cardiovascular effects, **234**: 156
- Metal exposure, pulmonary function effects, **234**: 154
- Metal exposures (in vivo), ambient particulate matter, **234**: 167
- Metal exposures, human volunteers, **234**: 160
- Metal health effects, epidemiology studies (table), **234**: 147-148
- Metal nanoparticles, production & use, **234**: 7
- Metal oxides, as nanoparticles, **234**: 7, 9
- Metal studies (in vitro), from ambient particulate matter (table), **234**: 194-195
- Metal studies (in vitro), toxic effects, **234**: 193
- Metal studies (in vivo), effect level summary (table), **234**: 182-185
- Metal studies (in vivo), toxic effects, **234**: 181-192
- Metal-contaminated particulates, human exposure studies, **234**: 154
- Metals & respiratory disease, children, **234**: 149
- Metals in residual oil fly ash, in vivo studies (table), **234**: 174-176
- Metals, in concentrated ambient particulates, **234**: 171
- Metals, in residual oil fly ash, **234**: 172
- Metals, respiratory & cardiovascular effects, **234**: 135 ff.
- Method detection limit & fingerprinting, petroleum products (diag.), **234**: 59
- Methylalkylated PAHs, vs. parent amounts (diag.), **234**: 85
- Methylfluoranthene ratios, PAH source identification (diag.), **234**: 92
- Methylphenanthrene distribution, PAH source identification, **234**: 86
- Methylphenanthrene:methylanthracene ratio, PAH source tool, **234**: 84
- Methylphenanthrene:phenanthrene ratio, petrogenic vs. pyrogenic pollutants, **234**: 86
- Microbe toxicity, of engineered nanoparticles, **234**: 16
- Molecular indices source characterization, PAHs, **234**: 49 ff.
- Molecular indices, PAHs, **234**: 76
- Molecular weight (low vs. high) ratio, PAH source identification (diags.), **234**: 110, 111
- Mollusca, engineered nanoparticle toxicity, **234**: 25
- Motor vehicles, carcinogenic PAHs, **234**: 66
- Multiple PAH component ratios, source identification, (diag.), **234**: 94
- Nanocrystals, fluorescent semiconductor nanomaterials, **234**: 9
- Nanomaterials, fluorescent semiconductor nanocrystals, **234**: 9
- Nanomaterials, in pollutant remediation, **234**: 11
- Nanomaterials, waste releases, **234**: 2
- Nanoparticle (engineered) toxicity, to different organisms (table), **234**: 17-20
- Nanoparticle interaction, possible effects (diag.), **234**: 37



- Nanoparticle toxicity, possible mechanisms, **234**: 35
- Nanoparticle types released, to environment (diag.), **234**: 6
- Nanoparticle types, described (diag.), **234**: 6
- Nanoparticles (engineered), applications, **234**: 2, 6
- Nanoparticles (engineered), environmental fate, **234**: 12
- Nanoparticles (engineered), release, transport & toxicity, **234**: 1 ff.
- Nanoparticles (engineered), toxic endpoints (diag.), **234**: 21
- Nanoparticles, air transport & fate, **234**: 12
- Nanoparticles, atmospheric release (table), **234**: 11
- Nanoparticles, major applications (table), **234**: 8
- Nanoparticles, metal oxides, **234**: 7
- Nanotechnology, defined, **234**: 2
- Naphthalene indices, PAH source identification, **234**: 81
- Natural nanoparticles, described, **234**: 6
- Nematodes, engineered nanoparticle toxicity, **234**: 25
- Nordtest method, PAH profiling (diag.), **234**: 78
- Oil spill, identification protocol (diag.), **234**: 75
- PAH (poly aromatic hydrocarbon)  
apportionment, by source (table), **234**: 108
- PAH carcinogens, motor vehicles, **234**: 66
- PAH components, petroleum, **234**: 57
- PAH distribution, aquatic systems, **234**: 73
- PAH effects, petrogenic degradation, **234**: 62
- PAH isomer ratios, weathering (diag.), **234**: 103
- PAH patterns, paving materials, **234**: 68
- PAH pollution source,  
methylphenanthrene:phenanthrene ratio, **234**: 86
- PAH profiles, chemical fingerprinting, **234**: 78
- PAH profiles, fossil fuel combustion (diags.), **234**: 64
- PAH profiles, paving materials (diags.), **234**: 70
- PAH profiling, Nordtest method (diag.), **234**: 78
- PAH ratios, value in source identification (table), **234**: 116
- PAH source characterization, analytical approach, **234**: 74
- PAH source characterization, purpose, **234**: 52
- PAH source identification, alkyl dibenzothiophene:alkylphenanthrene ratio (diags.), **234**: 98
- PAH source identification, alkyl dibenzothiophene:alkylphenanthrene (diag.), **234**: 99
- PAH source identification, benz(a)anthracene:chrysene ratio (diag.), **234**: 96
- PAH source identification, benz(a)anthracene:chrysene ratio, **234**: 95
- PAH source identification, benzo[a]pyrene:ghi ratio (diag.), **234**: 107
- PAH source identification, benzo[e]pyrene:benzo[a]pyrene ratio (diag.), **234**: 102
- PAH source identification,  
demethylphenanthrene ratio, **234**: 88
- PAH source identification, methylfluoranthene ratios (diag.), **234**: 92
- PAH source identification, methylphenanthrene distribution, **234**: 86
- PAH source identification, molecular weight (low vs. high; diags.), **234**: 110, 111
- PAH source identification, naphthalene indices, **234**: 81
- PAH source identification, non-isomer ratios, **234**: 106
- PAH source identification, PAH component ratios (diag.), **234**: 94
- PAH source identification, principle component analysis, **234**: 78
- PAH source identification, uncertainties, **234**: 117
- PAH source identification, valued PAH ratios (table), **234**: 116
- PAH source in sediment,  
phenanthrene:anthracene ratio, **234**: 82
- PAH source profiles, petroleum products (diag.), **234**: 58
- PAH source tool, methylphenanthrene:methylanthracene ratio, **234**: 84
- PAH source, biomass combustion, **234**: 68
- PAH sources, pyrogenic index (diag.), **234**: 114
- PAH sum, quantification method, **234**: 81
- PAH weathering, isomer ratios (diag.), **234**: 103
- PAH, four-ringed moieties, **234**: 89
- PAHs (methylalkylated), vs. parent amounts (diag.), **234**: 85
- PAHs (polycyclic aromatic hydrocarbons) (five- & six-ringed), source identification ratios, **234**: 101-106
- PAHs in sediment, principle component analysis (diag.), **234**: 79
- PAHs, and pyrogenic substances, **234**: 65
- PAHs, biogenic vs. diagenetic, **234**: 72
- PAHs, classification, **234**: 52
- PAHs, coal combustion patterns, **234**: 68
- PAHs, described, **234**: 50
- PAHs, differentiating sources (diag.), **234**: 83

- PAHs, low molecular weight ratios, **234**: 81
- PAHs, molecular indices & practical concepts, **234**: 76
- PAHs, molecular indices source characterization, **234**: 49 ff.
- PAHs, most important sources, **234**: 115
- PAHs, natural vs. synthetic, **234**: 50
- PAHs, origin, **234**: 50
- PAHs, physicochemical properties (table), **234**: 53-55
- PAHs, source assignment, **234**: 108
- PAHs, source characterization, **234**: 49 ff.
- PAHs, source profiles, **234**: 56
- PAHs, stormwater transport, **234**: 71
- PAHs, street dust, **234**: 69, 71
- PAHs, toxicity, **234**: 51
- Particulate matter (ambient) in air, characterized, **234**: 136
- Particulate matter contribution, to human health, **234**: 137
- Particulate matter effects, epidemiology literature, **234**: 138
- Particulate matter effects, toxicity literature, **234**: 139
- Particulate matter exposure, metal contamination & effects, **234**: 167
- Particulate matter in air, effects, **234**: 136
- Particulate matter, exposure, **234**: 138
- Particulate matter, metal contamination & effects, **234**: 135 ff.
- Particulate matter, metal-contamination studies (in vitro; table), **234**: 194-195
- Paving materials, PAH patterns, **234**: 69
- Paving materials, PAH profiles (diags.), **234**: 70
- Petrogenic degradation, PAH effects, **234**: 62
- Petrogenic discrimination, fluoranthenic & pyrenic ratios, **234**: 91
- Petrogenic sources, fluoranthene:pyrene ratio (diag.), **234**: 90
- Petrogenic substances, defined, **234**: 56
- Petroleum products, fingerprinting & method detection limit (diag.), **234**: 59
- Petroleum products, PAH source profiles (diag.), **234**: 58
- Petroleum products, weathering effects (diags.), **234**: 61
- Petroleum, PAH components, **234**: 57
- Phenanthrene:anthracene ratio, petrogenic vs. pyrogenic PAH pollution, **234**: 82
- Phenanthrene ratio, source identification (diag.), **234**: 87
- Physicochemical properties, selected PAHs (table), **234**: 53-55
- Plant toxicity, engineered nanoparticles (table), **234**: 30
- Plant toxicity, of engineered nanoparticles, **234**: 29
- Pollutant remediation, nanomaterials, **234**: 11
- Polycyclic aromatic hydrocarbons (PAHs), source characterization, **234**: 49 ff.
- Principle component analysis, PAH in sediment (diag.), **234**: 79
- Principle component analysis, PAH source identification, **234**: 78
- Protein interaction, engineered nanoparticle toxicity mechanism, **234**: 36
- Protozoan toxicity, engineered nanoparticles, **234**: 24
- Pulmonary function effects, metal exposure, **234**: 154
- Pyrogenic discrimination, fluoranthenic & pyrenic ratios, **234**: 91
- Pyrogenic index, described, **234**: 113
- Pyrogenic index, in PAH sources (diag.), **234**: 114
- Pyrogenic PAH source, biomass combustion, **234**: 68
- Pyrogenic PAHs, characterized, **234**: 66
- Pyrogenic sources, fluoranthene:pyrene ratio (diag.), **234**: 90
- Pyrogenic substances, and PAHs, **234**: 65
- Pyrogenic substances, defined, **234**: 65
- Pyrolytic source identification, indeno[1,2,3-cd]pyrene:benzo[ghi]perylene ratio (diag.), **234**: 105
- Reactive oxygen species, engineered nanoparticle toxicity, **234**: 35
- Release, engineered nanoparticles, **234**: 1 ff.
- Residual oil fly ash, in vivo exposures, **234**: 172
- Residual oil fly ash, in vivo studies (table), **234**: 174-176
- Respiratory disease, in children, **234**: 149
- Respiratory effects, ambient particulate matter, **234**: 135 ff.
- Respiratory effects, metals, **234**: 135 ff.
- Retene:chrysene ratios, softwood combustion sources, **234**: 88
- Sediment PAH source, phenanthrene:anthracene ratio, **234**: 82
- Soil fate, engineered nanoparticles, **234**: 16
- Soil transport, engineered nanoparticles, **234**: 15
- Source characterization, PAHs, **234**: 52
- Source profiles of PAHs, petroleum products (diag.), **234**: 58

- Source profiles, PAHs, **234**: 56
- Stormwater transport, PAHs, **234**: 71
- Street dust, PAHs, **234**: 69, 71
- Sulfur PAH source identification, indices & ratios, **234**: 98-101
- Target element concentrations, U.S. air (table), **234**: 142-143
- Toxic effects (in vitro), produced by individual metals, **234**: 193
- Toxic effects (in vivo), produced by individual metals, **234**: 181-192
- Toxic endpoints for engineered nanoparticles, cell lines (diag.), **234**: 32
- Toxic endpoints, of engineered nanoparticles (diag.), **234**: 21
- Toxicity mechanism for engineered nanoparticles, reactive oxygen species, **234**: 35
- Toxicity of engineered nanoparticles, to microbes., **234**: 16
- Toxicity to animals, engineered nanoparticles, **234**: 24
- Toxicity to cell lines, engineered nanoparticles, **234**: 31
- Toxicity to different organisms, engineered nanoparticles (table), **234**: 17-20
- Toxicity to fish, engineered nanoparticles, **234**: 27
- Toxicity to invertebrates, engineered nanoparticles, **234**: 24
- Toxicity to mammals, engineered nanoparticles, **234**: 28
- Toxicity to plants, engineered nanoparticles (table), **234**: 30
- Toxicity to plants, engineered nanoparticles, **234**: 29
- Toxicity, engineered nanoparticles, **234**: 1 ff., 16
- Toxicity, of engineered nanoparticles, to earthworms, **234**: 26
- Toxicity, PAHs, **234**: 52
- Toxicology literature, on particulate matter effects, **234**: 139
- Toxicology, metal exposure in humans, **234**: 154
- Transition metal levels, U.S. air (table), **234**: 139
- Transition metal levels, U.S. air, **234**: 140
- Transport of engineered nanoparticles, influencing factors (table), **234**: 12
- Transport, engineered nanoparticles, **234**: 1 ff., 12
- Water transport & fate, engineered nanoparticles, **234**: 14
- Weathering effects, petroleum products (diags.), **234**: 61